Exploring the function of ZNF804A using human neural stem cells

Deans, Peter James

Awarding institution:
King's College London

EXPLORING THE FUNCTION OF ZNF804A USING HUMAN NEURAL STEM CELLS

P.J. MICHAEL DEANS

INSTITUTE OF PSYCHIATRY, PSYCHOLOGY AND NEUROSCIENCE
KING'S COLLEGE LONDON

THESIS SUBMITTED FOR THE DEGREE OF PHD

2017

ABSTRACT

ZNF804A has recently been identified as a disease candidate gene for several severe neuropsychiatric disorders including bipolar disorder, schizophrenia and autism. Schizophrenia is known to share several clinical, genetic, pathophysiological, neuroanatomical and cognitive features with bipolar disorder, and thus ZNF804A may represent a useful target for investigating the common mechanisms underpinning these diseases. The latest advances in stem cell research have provided a wide variety of cellular models for studying these mechanisms in cultures of human neurons. One of these lines, a conditionally immortalised, cortically derived human neural progenitor cell (NPC) line (CTX0E16), offers a valuable tool for studying ZNF804A in human cortical neurons.

The primary aims of the current investigation were to characterise neurons derived from the CTX0E16 NPC line and to subsequently employ this line in conjunction with other neuronal models in the study of ZNF804A expression, subcellular localisation and biological function, specifically focusing on its potential impact on neuronal morphology. To this end, neuronal cultures differentiated from the CTX0E16 cell line were characterised using a broad set of techniques. These cells were shown to predominately adopt a glutamatergic fate, and demonstrated the morphology, functional responses, synaptic expression and electrophysiological characteristics consistent with immature cortical pyramidal neurons. When examined in human neurons, ZNF804A was shown to be distributed throughout the neuron and demonstrated a novel distribution at putative synapses. ZNF804A was also located within the nucleus of both NPCs and neurons. Interestingly, this pattern changed as NPCs terminally differentiated into excitatory neurons. Moreover, in mature neurons, the presence of ZNF804A within the nucleus was modulated by activity-dependent stimulation. siRNA-mediated knockdown of ZNF804A revealed a role for this protein in early neurite outgrowth, an effect potentially mediated by neuroligin 4x. Knockdown of the rodent homologue, Zfp804A, further revealed a role in the maintenance and plasticity of dendritic spines in mature neurons. Collectively, these data show that the CTX0E16 cell line provides a useful model of human cortical neuron development and disease, and that ZNF804A plays a role in the development, maintenance and plasticity of key aspects of pyramidal neuron morphology. As alterations in these factors are thought to be central to the pathophysiology of schizophrenia and bipolar disorder, it is thus possible that ZNF804A represents a common risk factor that contributes to the cellular disturbances in these diseases.

ACKNOWLEDGEMENTS

I would like to thank first and foremost my supervisor, Deepak. It has been a rather arduous three and a half years completing the work for this thesis, and I sincerely doubt I would have been able to do it without his advice and ever-present encouragement! Deepak is an amazing supervisor and the boost he has consistently given to my morale over the years when experiments have failed or life has gotten the better of me has been crucial. Thank you for all the experiences and opportunities you have provided me with, I know I made the right decision in becoming your first PhD student as a P.I.! I would also like to thank the other members of the lab, both past and present, for all your help and advice as well as all the good times at the Sun and the conferences! Pooja, Kate, Emily, Rodrigo, Carole, Iain, Deep and Nick it has been an absolute privilege working alongside such excellent, admirable and (above all else) fun people! Thanks to the other previous members of James Black Centre and the current members of the Maurice Wohl as well, this really is a fantastic scientific community to be a part of. I would also like to thank Nick Bray for his advice and help with the genetics work – I think I managed to get my head around it in the end! Also thanks to Brenda and Jack for your advice on working with the cells and with PhD questions in general!

I would also like to thank my Mum and Dad for the love and support that got me through this work, as well as other family members and friends both new and absent. Seeing you all has kept my spirits up when work or life has been particularly difficult.

STATEMENT OF WORK COMPLETED

All writing and data presented in this thesis was the result of work completed by P.J. Michael Deans unless stated otherwise in this section. In **Chapter 4**, Dr. Greg Anderson performed the q-PCR and Ca^{2+} imaging experiments and Dr. Ruth Taylor performed the electrophysiological work, with the initial CTX0E16 cultures being set up for this task by P.J. Michael Deans. In **Chapter 5** Rodrigo Rafagnin and Dr. Carole Shum performed the q-PCRs for the CTX0E16 and hiPSC time course experiments respectively, with the initial optimisation of primers for these experiments being carried out by P.J. Michael Deans. Western blots and subcellular fractionation for the ZNF804A antibody experiments were carried out by Pooja Raval, except the peptide pre-incubation experiment and some initial optimisation which was carried out by P.J. Michael Deans. Initial plating, neuralisation and characterisation data on hiPSC lines was carried out by Dr. Carole Shum. Rat primary cortical neuron cultures were prepared and cultured by Pooja Raval and Dr. Katherine Sellers, then fixed, immunostained and imaged by P.J. Michael Deans. Immunostaining and imaging of the mouse cortical tissue section was carried out by Dr. Deepak Srivastava. In **Chapter 6** zinc finger nucleofection and the initial round of dilution cloning was carried out by Dr. Matt Hill and Sanger fluorescent sequencing and CEL-1 assays were conducted by Dr. Nick Bray. Plating and neuralisation of hiPSC lines was conducted by Dr. Carole Shum. Work for the Zfp804A-knockout experiment was carried out by Pooja Raval, Dr. Katherine Sellers and Dr. Deepak Srivastava, with initial siRNA optimisation done by P.J. Michael Deans. Initial work for the cLTP experiment was carried out by Pooja Raval, with subsequent imaging and analysis being undertaken by P.J. Michael Deans.

CONTENTS

ABBREVIATIONS

4-OHT	4-Hydroxytamoxifen
ACC	Anterior Cingulate Cortex
ACSF	Artificial Cerebrospinal Fluid
AEBSF	4- benzenesulfonyl fluoride hydrochloride
APV	(2*R*)-Amino-5-Phosphonovaleric Acid
ASD	Autism Spectrum Disorder
BD	Bipolar Disorder
BSA	Bovine Serum Albumin
DAPI	4',6-diamidino-2-phenylindole
DAPT	N-[N-(3,5-difluorophenacetyl)-l-alanyl]-S-phenylglycine t-butyl ester
DD	Differentiation Day
DIV	Day In Vitro
dlPFC	Dorsolateral Prefrontal Cortex
DMEM	Dulbecco's Modified Eagle's Medium
DPBS	Dulbecco’s Phosphate Buffer Solution
ECL	Enhanced Chemiluminescence
EGF	Epidermal Growth Factor
EPSC	Excitatory Post Synaptic Current
ESC	Embryonic Stem Cell
FA	Formaldehyde
FBS	Fetal Bovine Serum
FGF	Fibroblast Growth Factor
GFP	Green Fluorescent Protein
HBSS	Hanks’ Balanced Salt Solution
HEK	Human Embryonic Kidney
HEPES	4-(2-hydroxyethyl)-1-piperazineethanesulfonic acid
hiPSC	Human Induced Pluripotent Stem Cell
hNPC	Human Neural Progenitor Cell
ICC	Immunocytochemistry
MEF	Mouse Embryonic Fibroblast

MMLV	Moloney Murine Leukemia Virus
N.A.	Normal Aperture
NDM	Neuronal Differentiation Medium
NDS	Normal Donkey Serum
NGS	Normal Goat Serum
NSC	Neural Stem Cell
PBS	Phosphate Buffer Solution
PDL	Poly-D-Lysine
PVDF	Polyvinylidene Fluoride
q-PCR	Quantitative Polymerase Chain Reaction
RMM+++	Reduced Modified Medium supplemented with EGF, FGF and 4-OHT
ROI	Region of Interest
RT	Room Temperature
RT-PCR	Reverse Transcription Polymerase Chain Reaction
SAD	Schizoaffective Disorder
SCZ	Schizophrenia
SD	Standard Deviation
SEM	Standard Error of Mean
shRNA	Short Hairpin RNA
SIM	Structured Illumination Microscopy
siRNA	Small Interfering RNA
SMADi	SMAD inhibitor
TBS-T	Tris-Buffered Saline – Tween20
ZFN	Zinc Finger Nuclease

CHAPTER 1: INTRODUCTION

1.1 FOREWARD

Psychiatric disorders are common and highly debilitating conditions which affect a wide range of cognitive, emotional and behavioural characteristics. These disorders are highly heritable and commonly share clinical features and exhibit co-morbidity with one another. The overlapping clinical features are often accompanied by common environmental and genetic risk factors; alterations in cellular morphology and function; and even similar changes in gross neuroanatomy and functional connectivity, suggesting that some of these diseases share aspects of their etiology (Carroll and Owen, 2009; Kraguljac et al., 2012; Lake and Hurwitz, 2007; Murray et al., 2004; van Os and Kapur, 2009; Peri et al., 2012). Schizophrenia and bipolar disorder have previously been shown to share many of these pathological features and risk factors (Goldstein et al., 2002; Lake and Hurwitz, 2007); understanding how the common etiologies for these disorders contribute to their overlapping clinical presentation is a crucial topic for future research. Previous attempts to tackle this question have relied on multiple approaches, including searching for common genetic risk factors, developing animal models of disease, identifying similar disturbances in neuroanatomy and functional connectivity, assessing comparable cognitive and behavioural phenotypes and investigating cellular pathology and the corresponding mechanisms underlying it (Green, 2006; Nestler and Hyman, 2010; van Os and Kapur, 2009; Rimol et al., 2012; Strakowski et al., 2005). Genetic variants in several genes have now been identified as risk loci for both schizophrenia and bipolar disorder, including *ZNF804A*, *TCF4* and *CACNA1C* (O'Donovan et al., 2009). Recent advances in human stem cell technology have provided a wide array of experimental tools with which common mechanisms contributing to similar neuropsychiatric disorders like bipolar disorder and schizophrenia can be studied (Bray et al., 2012). These cell lines offer an advantage over animal models of such diseases as they permit investigations of human-specific mechanisms of development and disease at the cellular and molecular level. However, stem cell lines require thorough experimental validation prior to being employed in the study of psychiatric diseases, and each stem cell paradigm possesses both strengths and weaknesses in tackling this problem. This chapter will outline these disorders, the common features linking them

including *ZNF804A*, the currently available stem cell models, and the aims of the current investigation as they relate to these topics.

1.2 SCHIZOPHRENIA

Schizophrenia is a severe neuropsychiatric disease which occurs at a lifetime prevalence of around 1% in the general population (McGrath et al., 2008). This disorder is typically diagnosed based on whether a patient's clinical presentation adheres to criteria outlined in the Diagnostic and Statistical Manual of Mental Disorders V (DSM-V) or the 10th International Classification of Diseases (ICD-10) (Jakobsen et al., 2005; Tandon et al., 2013). These features can be broadly separated into three categories: 'positive' symptoms including hallucinations, delusions and thought disorder (also termed as 'psychosis'); 'negative' symptoms including avolition, blunted affect, anhedonia, alogia and asociality; and cognitive impairments, including deficits in attention, memory and executive function (van Os and Kapur, 2009). The onset of schizophrenia typically occurs between the ages of 18 and 25 in men, while in women peak onset occurs around a decade later on average (Canuso and Pandina, 2007). However, there is also growing evidence to support the existence of a prodromal phase 2-4 years prior to the onset of the first positive symptoms, consisting of cognitive deficits, social isolation and affective dysregulation (Cornblatt et al., 2003; Olvet et al., 2010).

The clinical features of schizophrenia are notoriously heterogeneous in their development, presentation and prognosis and thus attempts to establish defining characteristics within this broad diagnosis have often proved challenging (van Os and Kapur, 2009). Given the considerable inter-patient variability in the clinical presentation of schizophrenia, it is perhaps unsurprising that patients with bipolar disorder exhibiting psychotic symptoms are sometimes misdiagnosed as being schizophrenic (McElroy et al., 1996). Attempts to establish a framework through which these disorders may be reliably distinguished remain the subject of considerable debate within the psychiatric and scientific communities (Craddock and Owen, 2005; Lake and Hurwitz, 2007).

1.3 BIPOLAR DISORDER

Bipolar disorder is another severe neuropsychiatric disorder with estimates of lifetime prevalence ranging from 1-3% depending on the diagnostic criteria used (Merikangas and Lamers, 2012; Pini et al., 2005). Unlike schizophrenia, bipolar disorder is primarily defined by the presence of

large alterations in mood, and in the DSM-V classification system can be subdivided into bipolar type I and bipolar type II (Angst, 2013). Bipolar type I patients possess a number of clinical features in common with the positive symptoms of schizophrenia: patients experience periods of mania characterised by greatly elevated or irritable mood which at their apogee may progress to psychotic symptoms – hallucinations, delusions and thought disorder (See **Figure 1.1**). These manic episodes are also accompanied by periods of depression, marked by a decrease in mood, anhedonia, alterations in eating and sleeping habits and decreases in energy, motor activity and self esteem and recurring thoughts of death; in extreme cases these depressive periods may also feature psychotic symptoms (Phillips and Kupfer, 2013). In contrast to this, bipolar type II is characterised clinically by attenuated manic episodes (also known as hypomania), periods of elevated or irritated mood without the development of psychosis; and depressive phases similarly to type I but also without psychotic symptoms (Phillips and Kupfer, 2013).

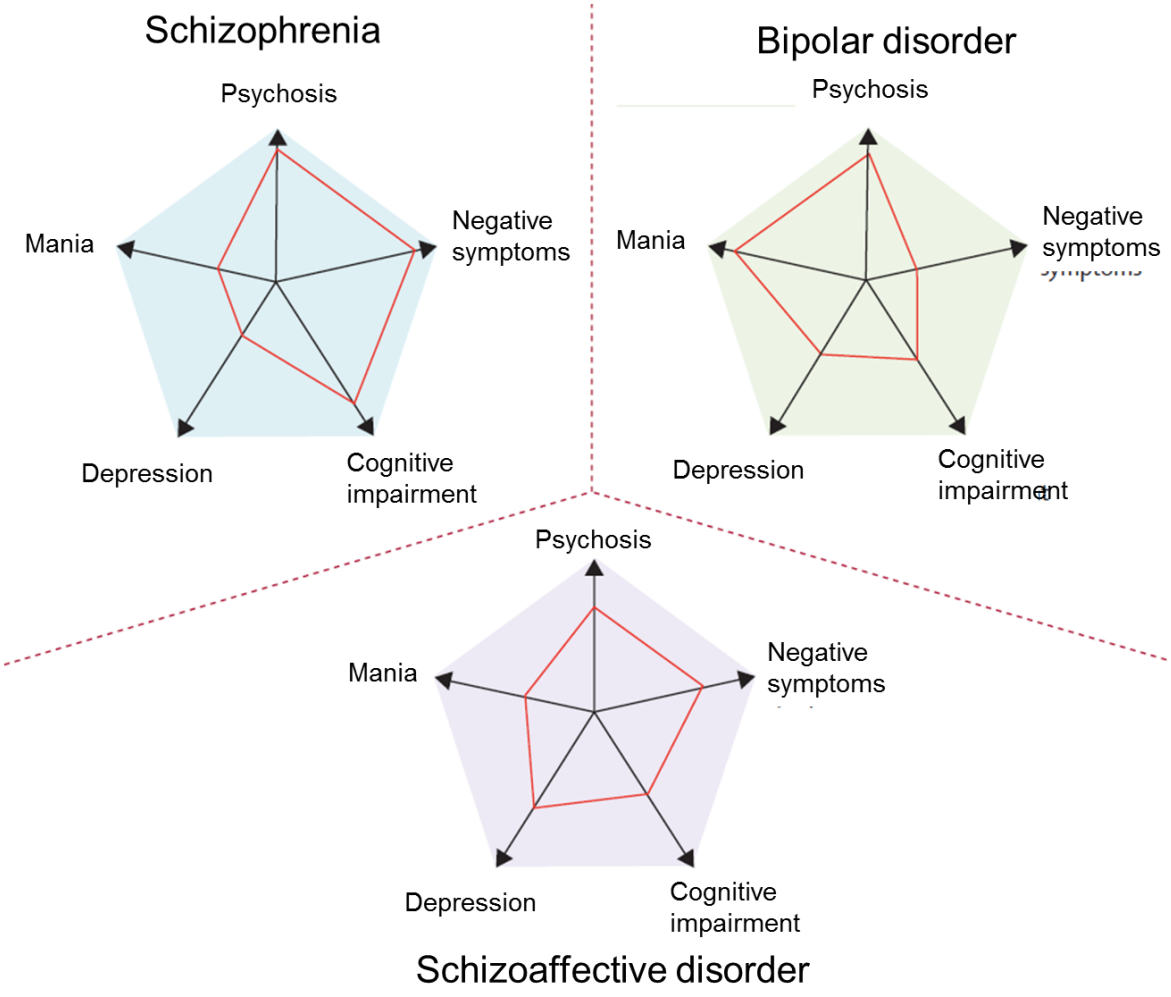

Figure 1.1 (overleaf): Behavioural and cognitive features of prototypical patients diagnosed with schizophrenia, schizoaffective disorder or bipolar disorder. Adapted from van Os and Kapur (2009).

As in schizophrenia, bipolar disorder occurs with roughly equal lifetime prevalence across genders (around 1% and 0.5% for bipolar type I and II respectively) (Diflorio and Jones, 2010). However, the peak age of onset is slightly earlier than in schizophrenia, with both male and female patients typically developing the disorder during the mid teens to mid 20s (Angst et al., 2002). In addition to this, there is also evidence to support the existence of a bipolar prodromal phase with clinical features indistinguishable to the schizophrenia prodrome (Olvet et al., 2010).

Despite the clinical similarities, traditionally schizophrenia and bipolar disorder have been treated as discrete diagnostic categories. However, this dualistic view has come under increasing scrutiny in recent years (see **Figure 1.2**). The DMS-V additionally contains a third diagnostic category, schizoaffective disorder, which encompasses cases that exhibit features of both schizophrenia and bipolar disorder. Furthermore, there is a growing body of clinical, epidemiological, genetic, neurobiological and neuroanatomical evidence supporting diagnostic models which propose a clinical continuum between the previous categories of schizophrenia and bipolar disorder. Specifically, previous research has found similar alterations in brain structure (Ellison-Wright and Bullmore, 2010), metabolism (Kraguljac et al., 2012; Pennington et al., 2008) and neurotransmission (particularly GABAergic, glutamatergic and dopaminergic signalling (Cherlyn et al., 2010; Cousins et al., 2009; Stone et al., 2007; Torrey et al., 2005)); neuropsychological impairments (Schretlen et al., 2007); responses to pharmacological treatment (Post, 1999); and genetic or epidemiological risk factors (Carroll and Owen, 2009) in both disorders. The literature on these similarities is extensive and thus a full outlining of the similarities and differences within each individual category is beyond the scope of this chapter. However, the overlapping genetic features of schizophrenia and bipolar disorder will be briefly outlined due to their particular relevance to the current investigation.

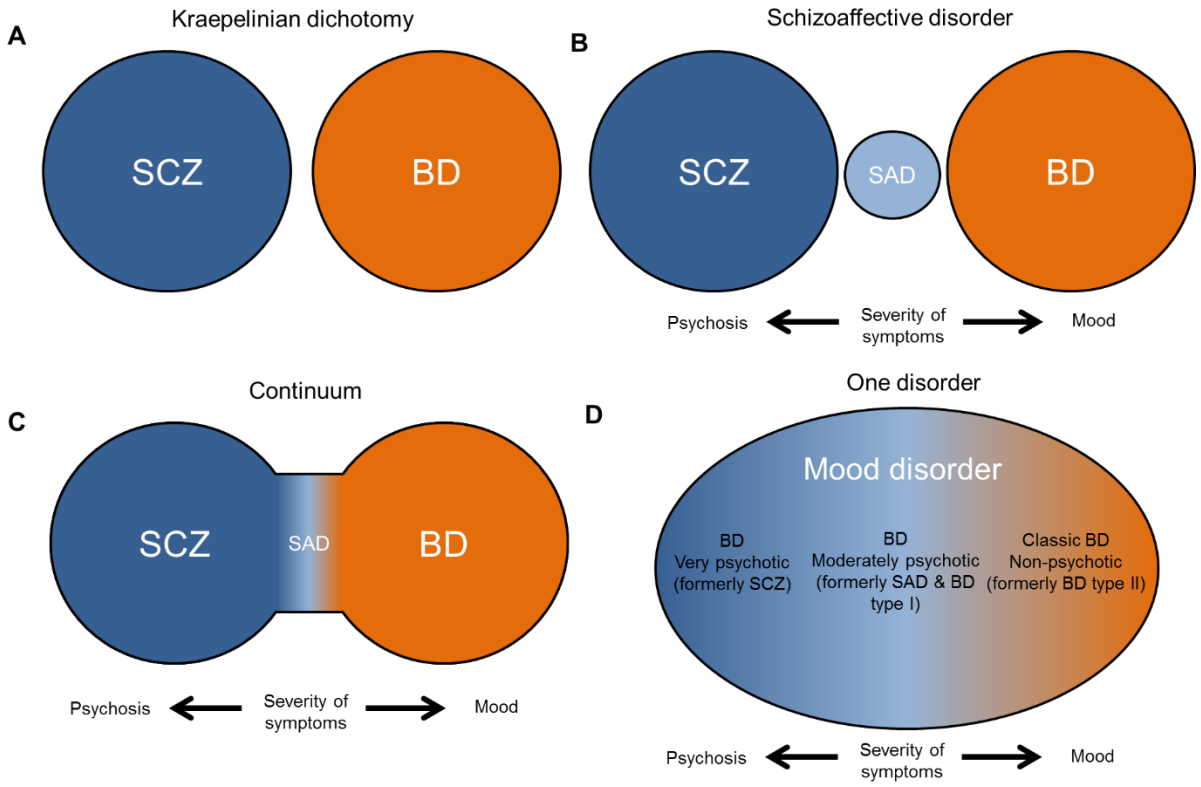

Figure 1.2: Schematic of diagnostic models of psychosis. **A**: The original dichotomy proposed by Emil Kraepelin in the 19th century – two dicrete diagnoses. **B**: The introduction of schizoaffective disorder as a diagnostic category in 1933 – three discrete diagnoses with zones of rarity inbetween. **C**: Psychosis as a continuum (Crow, 1986). **D**: 'One disorder' model proposed by Craddock and Owen, 2005; Lake and Hurwitz, 2007. Figure adapted from Lake and Hurwitz, 2007.

1.4 THE GENETICS OF PSYCHOSIS

In light of the numerous common pathological features of schizophrenia and bipolar disorder, it is perhaps unsurprising that these two diseases have also been linked in a wide variety of epidemiological and genetic studies. The risk of schizophrenia has previously been found to be significantly increased in the offspring of bipolar patients, while the offspring of schizophrenics are likewise significantly more likely to develop mood disorders; offspring of patients with either disorder are also at significantly higher risk of developing the same disorder as their parent (Lichtenstein et al., 2009). Schizophrenia and bipolar disorder are both thought to possess strong genetic components to their etiology, with around 80-85% of the risk of developing these disorders being determined by heritable factors, as estimated by twin studies and meta-analyses (Cardno and Gottesman, 2000; Cardno et al., 1999). Indeed, around 50-70% of this genetic component has been estimated to be shared between the two disorders (Lichtenstein et al., 2009). The genetic architecture of these diseases is highly heterogeneous, with numerous common genetic variants with small effect sizes as well as rare

variants with moderate effects both thought to contribute to their overall risk of developing either disorder.

Early attempts to establish 'risk genes' using candidate gene association studies and genome wide linkage studies focused on finding genetic variants which produced highly penetrant effects, though many of these studies have produced conflicting results and a lack of replication. Despite this, a handful of candidate genes have been linked to both schizophrenia and bipolar disorder including *DISC1*, which codes for a protein involved in neural progenitor cell proliferation, synapse formation, cAMP signalling, neurite outgrowth, neuronal migration and neuronal integration (Hattori et al., 2010; Hayashi-Takagi et al., 2010; Kamiya et al., 2005; Lee et al., 2011; Mao et al., 2009; Millar et al., 2005; St Clair et al., 1990). Further evidence has implicated mutations in the gene coding for Neuregulin-1 (Nrg-1), a protein that plays an important role in neurite outgrowth and also regulates glial cell development, axon myelination and ensheathment and excitatory and inhibitory synaptic plasticity (Georgieva et al., 2008; Stefansson et al., 2002); and mixed findings regarding a polymorphism in the *COMT* gene coding for catechol-O-methyl-transferase, an enzyme responsible for midbrain dopamine catabolism and thus playing a crucial role in dopaminergic neurotransmission (Williams et al., 2007). Despite these findings, candidate gene association studies lack the power required to detect common genetic variants of low effect, and rare variants of moderate effect.

The advent of the first genome-wide association study (GWAS) in 2005 provided a powerful new tool with which novel single nucleotide polymorphisms (SNPs) and copy number variants (CNVs) associated with either disorder could be discovered (Klein et al., 2005). This technique offered a particular advantage over previous methods as it permits detection of rare variants with moderate effects on risk and common variants with low effects on risk of disease development with a degree of confidence not previously possible and without an a priori hypothesis. SNPs have previously been estimated to contribute a substantial portion of the variance in liability for both schizophrenia and bipolar disorder, and the genetic correlation of common SNPs between these two disorders is high. Psychiatric disease-associated SNPs may convey a biological impact in one of several ways. SNPs occurring within the exons of a gene may be synonymous or non-synonymous. Synonymous SNPs are polymorphisms that do not alter the resulting amino acid sequence of the encoded protein, while non-synonymous variants change this sequence with potential consequences in the form of structural and/or functional

alterations of the protein (Cichon et al., 2009). Alterations in the amino acid sequence at binding sites may affect the protein's binding affinity for other molecules, while structural changes arising from SNPs such as altered folding or cleavage may impact the accessibility of these binding sites (Zhang et al., 2014). It is worth noting however that even synonymous SNPs may influence disease by modulating protein folding as well as mRNA structure, stability and splicing, with downstream consequences for the structure, function and level of expression of the resulting proteins (Gandal et al., 2016; Zhang et al., 2014).

In addition to SNPs within coding sequences, the vast majority of SNPs exhibiting genome-wide significance do not directly alter protein structure and occur in noncoding regions, either within introns or between genes. These SNPs may instead impact the transcription or splicing of a given gene via a disruption of regulatory sequences within the genome or by interfering with the binding of transcription factors, splicing factors or microRNAs within promoter and enhancer regions (Zhang et al., 2014). However, noncoding SNPs reaching genome-wide significance may also be indirectly linked to a disease via a non-random association with one or more other genomic variants, known as linkage disequilibrium. The causative variants associated with these SNPs can be subsequently uncovered using *de novo* polymorphism discovery and high density linkage disequilibrium mapping (Williams et al., 2011; Zhang et al., 2014).

Since their inception, GWA studies have uncovered a growing number of susceptibility loci associated with both bipolar disorder and schizophrenia, some of which are highlighted in **Figure 1.3**. These risk loci offer exciting new directions for future research into common mechanisms between these disorders. In particular, the genetic risk factors shared between these disorders appear to suggest a common pathophysiology particularly related to alterations in mechanisms underlying the formation of neural circuits. However, the earliest and best replicated genetic variant discovered via GWAS to be associated with a broad psychosis diagnosis was the T/G rs1344706 SNP, located within intron 2 of the *ZNF804A* gene (O'Donovan et al., 2009). Understanding how the function of ZNF804A relates to the other pathways highlighted by previous genetic studies will thus be critical in further elucidating the link between this protein and each of the three disorders discussed in this chapter.

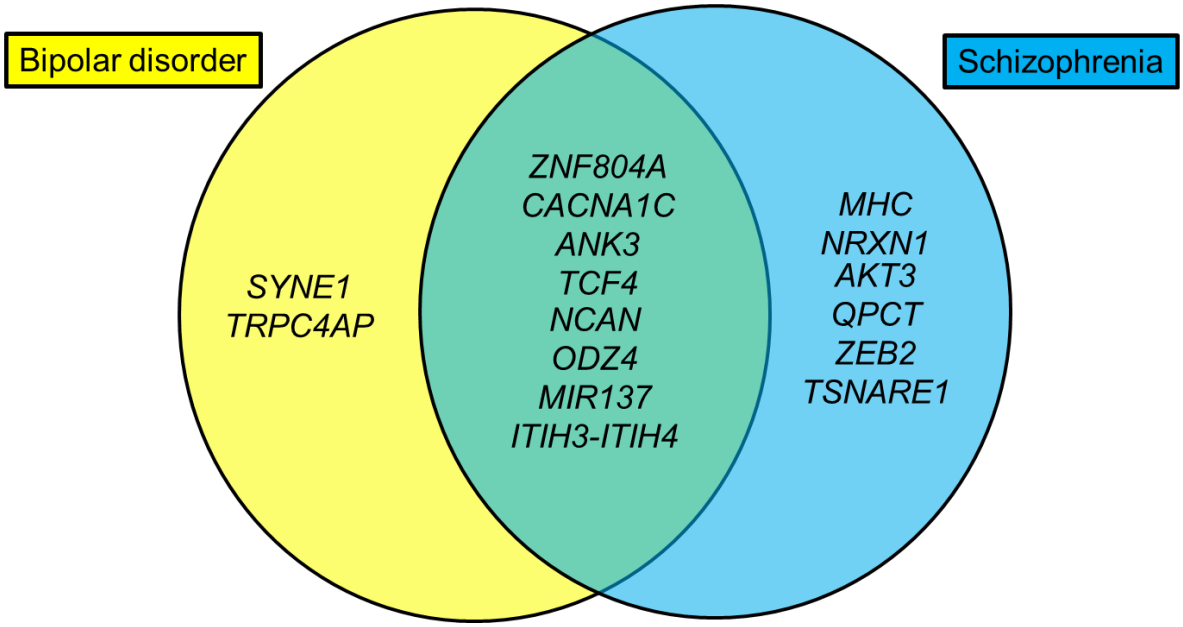

Figure 1.3: Venn diagram of selected GWAS-discovered genes with previously reported links to schizophrenia and/or bipolar disorder. This diagram is not an exhaustive list. (Anitha et al., 2014; Bi et al., 2012; Cross-Disorder Group of the Psychiatric Genomics Consortium, 2013; Ferreira et al., 2008; Green et al., 2013; Ivorra et al., 2014; Jamain et al., 2003; Li et al., 2015; Mühleisen et al., 2012; Need et al., 2009; O'Donovan et al., 2009; Psychiatric GWAS Consortium Bipolar Disorder Working Group, 2011; Ripke et al., 2013; Stefansson et al., 2009; Uchino and Waga, 2013; Weiss et al., 2003; Wright et al., 2013; Xu et al., 2014; Yuan et al., 2012).

1.5 ZNF804A

1.5.1 GENETIC STUDIES

The T allele of the rs1344706 SNP was first discovered to be associated with schizophrenia in a GWAS conducted by O'Donovan et al. in 2008, and this association was strengthened when bipolar disorder was included in the affected cohort, indicating that the variant conferred an increased risk of psychosis in general. Since this initial finding multiple subsequent studies have replicated associations with both schizophrenia and bipolar disorder in multiple cohorts (Riley et al., 2010a; Steinberg et al., 2011; Zaharie et al., 2012), while a 2011 meta-analysis combining data from multiple cohorts to produce a dataset of approximately 60,000 subjects further confirmed this association and found the rs1344706 SNP to provide the strongest association out of multiple markers within the gene (Williams et al., 2011). This initial meta-analysis cohort predominately consisted of European subjects, and initial attempts to replicate these findings among individual Asian cohorts were inconsistent (Chen et al., 2012; Li et al., 2013; Yang et al., 2013; Zhang et al., 2011). However, another recent meta-analysis of GWA studies, this time in a combined Asian cohort of approximately 30,000 subjects, found a smaller but still

significant effect of this variant on psychosis risk (Huang et al., 2016). Both of these meta-analyses have estimated that possession of the T allele of the rs1344706 SNP increases the risk of developing schizophrenia and bipolar disorder by around 10% (odds ratios (ORs) of 1.08 and 1.10 respectively).

Since the initial discovery of a susceptibility locus at rs1344706, several other *ZNF804A* variants have been found to be associated with psychotic disease. The meta-analysis in the combined Asian cohort discovered a further SNP at rs1366842 within exon 4 of the *ZNF804A* gene which contributed a similar increase in risk (OR = 1.095) (Huang et al., 2016). A further SNP at rs7597593 within *ZNF804A* intron 1 was found to be associated with schizophrenia in a 2010 study by Riley et al. studying a European cohort, and a subsequent follow up study combining multiple cohorts found this association was specifically sex modulated, occurring in females (OR = 1.29) but not in males. This SNP has been found to be in moderate linkage disequilibrium with rs1344706, indicating that it was at least partially independent from this locus. A further SNP at rs359895 has been reported as influencing *ZNF804A* promoter activity and found to be associated with schizophrenia in several Han Chinese cohorts (OR = 0.70), though evidence regarding this effect is mixed (Li et al., 2011; Zhang et al., 2015). In addition to the evidence regarding SNPs at the *ZNF804A* locus, a number of rare *ZNF804A* copy number variants have been discovered in psychosis patients, including an entire deletion of the *ZNF804A* gene and a duplication of exon 1, which were not observed in healthy controls and thus were significantly associated with the broad disease category of psychosis (Steinberg et al., 2011). However, other CNV studies have not been able to successfully detect CNVs associated with bipolar disorder or schizophrenia at the *ZNF804A* locus (Stone et al., 2008; Walsh et al., 2008).

Interestingly, variants at the *ZNF804A* locus have also been found to be associated with other psychiatric disorders. Rs1344706 and rs7597593 were both found to be associated with heroin addiction (OR = 1.16 and OR = 1.142 respectively) (Sun et al., 2015); while several CNVs at the *ZNF804A* locus have been found in a group of eight verbally deficient boys with autism (Anitha et al., 2014). Furthermore, a SNP at rs7603001 within *ZNF804A* intron 2 was found to be significantly associated with autism; this association strengthened in families of autistic individuals with verbal deficiencies (Anitha et al., 2014). This association with autism is particularly of note due to the growing body of evidence implicating genetic risk factors, disease mechanisms and pathology common to both autism and schizophrenia (Burbach and Van Der Zwaag, 2009).

As described above, SNPs may be located within coding regions of a gene, directly impacting protein structure, or may instead be found within noncoding regions and impact the expression or splicing of a gene. The rs1344706 SNP, located within intron 2 of the *ZNF804A* gene, has previously been found to influence *ZNF804A* expression in adult and fetal brain and binding affinity for nuclear proteins (Hess and Glatt, 2013). The risk allele of this SNP was previously found to directly reduce expression of the full length *ZNF804A* transcript in second trimester fetal brain tissue (Hill and Bray, 2012), and is also associated indirectly with an increase in allelic expression in the adult frontal, temporal and parietal cortices (Riley et al., 2010a; Williams et al., 2011); this indirect increase in expression is thought to be through additional regulatory variants at the *ZNF804A* locus rather than directly due to the effects of the rs1344706 genotype itself. A subsequent study determined that this effect in the fetal brain was actually due to reductions in the novel $ZNF804A^{E3E4}$ transcript rather than the full length variant.

1.5.2 ZNF804A ISOFORMS AND MOTIFS

The full length *ZNF804A* gene consists of four exons of varying length and numerous alternative splice variants for this gene have been predicted and observed. A recent bioinformatic assessment of the *ZNF804A* gene found a total of eleven predicted *ZNF804A* isoforms using AceView and the Alternative Splicing Gallery, some of which exhibiting truncated or excised exons. Subsequent assessments of expression levels for each of the four *ZNF804A* exons highlighted two potential *ZNF804A* variants, termed variant b and variant c - a 602 amino acid isoform with a truncated 5' end and a 54 amino acid isoform with a truncated 3' end respectively; the latter consisting predominately of exon 2 (Hess and Glatt, 2013).

A recent study conducted in a lymphoblastoid cell line and post-mortem human brain tissue found an alternative exon, termed exon 2.2. This exon was determined to comprise part of a novel mRNA variant consisting of exon 2.2 and exon 2 and predicted to code for a truncated 88 amino acid protein. Interestingly, this novel transcript was found to be differentially expressed in schizophrenia subjects relative to healthy controls (Okada et al., 2012). In addition to this, a study conducted by Tao et al. (2014) discovered a novel *ZNF804A* transcript consisting of exon 3, exon 4 and a new 5' untranslated region within intron 2 close to the rs1344706 SNP, using RNAseq, 5′ RACE, end-to-end PCR, and quantitative reverse transcription PCR. Bioinformatic analysis of the expression pattern of each of the four *ZNF804A* exons in human post-mortem brain tissue has provided additional support

for the existence of this variant, as the 3' exons appeared to be preferentially expressed relative to exon 1 and 2 throughout development and adulthood (Hess et al., 2015).

The full length ZNF804A protein is 1209 amino acids in length and possesses a predicted weight of around 137 kDa (Tao et al., 2014). ZNF804A possesses a predicted Cys2His2 (C2H2) zinc finger domain on exon 2 and is thus a member of the zinc finger protein superfamily, a group of proteins characterised by a common structural motif consisting of a relatively short sequence folded around one or more zinc ions. Zinc finger proteins possess numerous functions and can be further subcategorised according to the particular form of zinc finger motif they possess; classical C2H2 ZNF domains in particular typically possess a repeated 28-30 amino acid with two cysteines and two histidines acting as the conserved chelating region for a single zinc ion (Krishna, 2003). C2H2 ZNF proteins are known to possess multiple functions including mediating protein-protein interactions and binding to specific RNA sequences (Brayer and Segal, 2008; Brown, 2005). However, C2H2 zinc finger domain proteins are perhaps best known for acting as transcription factors, binding to the major groove of DNA sequences through the N-terminus of the alpha helix portion of this motif (Krishna, 2003). In the human brain, zinc finger proteins have been previously found to regulate a wide variety of functions, including synaptic signalling, neurite outgrowth and neuronal proliferation (Aruga et al., 1994; Fenster et al., 2000; Hattori et al., 2007); C2H2 zinc finger proteins have previously been implicated in the pathways underlying neurodevelopmental disease (Bardoni et al., 1999). Thus, the possession of this particular domain may represent a mediator through which the protein functions and thus may indicate how mutations in the *ZNF804A* gene confer an increased risk of developing psychiatric disease in humans.

Interestingly, not all of the predicted or observed ZNF804A isoforms possess the zinc finger binding domain, and thus lack any obvious ability to bind DNA sequences or act as a transcription factor. Specifically, while the full length, variant c and disease-associated exon 2.2 transcripts are predicted to express the C2H2 ZNF domain, the predicted variant b and the putative disease-associated *ZNF804A*^{E3E4} variant lack exon 2 and thus do not possess this motif (Hess and Glatt, 2013; Okada et al., 2012; Tao et al., 2014). Structural analysis of the full length ZNF804A amino acid sequence conducted by Hess et al. (2015) suggested that this protein possessed a predominately disorganised configuration, with around 86% of the full length model displaying random coiling. However, this analysis also revealed that the N-terminal of the full length ZNF804A protein forms a compact structure

consisting of two β-sheets and two α-helices coming into close contact with one another in a manner consistent with a typical C2H2 zinc finger domain, with minor structural deviations consistent with either an artefact of the folding algorithm or an atypical ZNF motif structure. Furthermore, models computed for the variant b and c isoforms suggested that the correct folding of the C2H2 ZNF domain was conserved in the variant c isoform while the variant b isoform (lacking the putative ZNF domain) was around 95% intrinsically disordered.

The full length ZNF804A isoform also possesses two predicted nuclear localisation signals (NLS), on exon 2 and exon 4 of the protein (Hess and Glatt, 2013). NLS are amino acid sequences which mark a given protein for import into the nucleus via a system of nuclear transport (Pemberton and Paschal, 2005). The presence of these signals on the full length ZNF804A protein is particularly of note given the presence of the putative DNA-binding domain on this protein. Thus, these motifs could potentially act in conjunction with the ZNF domain to promote transport of this protein into the cell nucleus where it may act as a transcription factor via the zinc finger motif.

1.5.3 REGIONAL AND TEMPORAL EXPRESSION OF ZNF804A

ZNF804A has been previously found to be expressed within the human brain throughout fetal development and adulthood, peaking at around the third trimester of gestation in the hippocampus, dorsolateral prefrontal cortex and anterior cingulate cortex (Hess and Glatt, 2013; Hill and Bray, 2012). Similarly, in the developing rat brain the rat homologue of *ZNF804A*, *ZFP804A*, reaches peak expression at birth then gradually decreases as the pup matures, with particularly strong expression being seen within the hippocampus (Chang et al., 2015). Furthermore, in cultured rat primary cortical neurons expression of Zfp804A has been found to peak at the 4th day *in vitro* (DIV4); this expression is also enhanced following treatment with glutamate in an NMDA receptor-dependent manner (Chang et al., 2015; Hinna et al., 2015).

In addition to alterations in *ZNF804A* expression during development, *ZNF804A* isoforms have also been found to exhibit differential expression in patients with severe neuropsychiatric illnesses relative to controls. Expression of the novel *ZNF804A*^{E3E4} transcript was significantly reduced in the dorsolateral prefrontal cortex of schizophrenics, but not bipolar patients relative to controls, while the full length transcript was found to be reduced in the bipolar group alone (Tao et al., 2014). Reduced expression of the full length *ZNF804A* transcript has also been observed in the post-mortem anterior

cingulate cortex of autistic individuals relative to controls (Anitha et al., 2014). Taken with the findings of a link between variants at the *ZNF804A* locus and an increased risk of psychotic illnesses, these results suggest the ZNF804A may have an influential role in early brain development which, if disrupted, may contribute to later development of psychiatric diseases like schizophrenia and bipolar disorder.

1.5.4 ZNF804A AND BRAIN STRUCTURE

Since the discovery of a link between variants at *ZNF804A* loci and several neuropsychiatric disorders, multiple studies have attempted to determine whether these variants or otherwise expression of the *ZNF804A* gene are similarly linked to alterations in gross neuroanatomical structures with relevance to these diseases. An initial MRI study conducted by Lencz et al. (2010) in healthy volunteers found that individuals homozygous for the risk allele of the rs1344706 SNP exhibited an increase in total white matter volumes relative to carriers of the other allele, a finding which has since been replicated (Wassink et al., 2012). These individuals further demonstrated grey matter reductions in several cortical regions comprising the 'default mode' network, structures known to exhibit synchronised activity in the absence of a cognitively demanding task (Raichle et al., 2001). Conversely, a further study demonstrated that in schizophrenia patients, possession of both risk alleles was associated with relatively spared grey matter volumes in a number of regions in the hippocampus and neocortex (Donohoe et al., 2011). Despite this, subsequent studies have found mixed success in replicating many of these effects on white matter and grey matter volume in specific regions of the cortex (Nenadic et al., 2015; Wassink et al., 2012).

A number of studies have also attempted to determine the effect of rs1344706 genotype on cortical thinning, a well characterised pathology in schizophrenic brains (Rimol et al., 2012). The first of these utilised a combinatorial MRI/DTI approach to investigate cortical structure in healthy subjects. Individuals homozygous for the risk allele of the rs1344706 SNP were found to exhibit reduced cortical grey matter thickness within several regions including the anterior cingulate cortex (Voineskos et al., 2011). This finding is particularly of note given the grey matter reductions in the anterior cingulate cortex common to both schizophrenia and bipolar disorder (Ellison-Wright and Bullmore, 2010). Following this, a further MRI study found that homozygous risk allele carriers with schizophrenia exhibited greater cortical thickness in the prefrontal or temporal cortex and less pronounced aberrant temporal cortical folding than schizophrenics possessing the non-risk allele, while the reverse was seen in healthy control

homozygotes versus healthy carriers of the non-risk allele (Schultz et al., 2013); similar contrasting effects on cortical thinning depending on diagnostic status could be seen in a subsequent study on a Han Chinese cohort (Wei et al., 2015). However, subsequent research could find no such associations with rs1344706 genotype and cortical thickness regardless of region (Bergmann et al., 2013).

Studies have also assessed the impact of rs1344706 genotype on white matter integrity in patient and control groups, though again results here have been mixed. An MRI-based study of white matter density has found possession of both copies of the risk allele for this SNP to have divergent effects on white matter integrity in the prefrontal lobe of schizophrenic patients and healthy individuals relative to those of non-risk allele carriers (Wei et al., 2012). Carriers of the *ZNF804A* risk allele have also previously been found to possess reduced white matter integrity in a white network of white matter tracts and regions of the parietal and cingulate cortex in several studies of schizophrenic patients and healthy controls, including areas of the 'default mode' network (Ikuta et al., 2014; Kuswanto et al., 2012; Mallas et al., 2016; Zhang et al., 2016). Despite this, not all groups have been able to replicate associations between white matter integrity and rs1344706 genotype (Wei et al., 2013).

Collectively, the literature appears broadly to demonstrate effects of rs1344706 genotype on grey matter volume, cortical thickness and white matter integrity, particularly in regions within the 'default mode' network. Moreover, effects of the homozygous risk-allele genotype appear to diverge within the psychosis and healthy control subgroups. Although evidence is conflicting on some findings, there is also a suggestion that the risk allele is generally associated with potentially pathological changes in a wide range of regions in healthy controls, while in the schizophrenic group possession of this allele is linked to a less pronounced pathology relative to the nonrisk allele.

1.5.5 ZNF804A, FUNCTIONAL CONNECTIVITY AND NEUROCOGNITIVE PHENOTYPES

In conjunction with neuroanatomical effects of variants at the *ZNF804A* locus, there is also a growing body of literature suggesting further alterations in functional connectivity between cortical and subcortical regions, as well as the patterns of activity in individual structures. Possession of the rs1344706 risk allele has previously been found to be associated with altered intra- and inter-hemispheric connectivity within the dorsolateral prefrontal cortex (dlPFC) and increased connectivity between this region, the hippocampus (HC) and the amygdala during a working memory task (Esslinger

et al., 2009, 2011; Paulus et al., 2013; Rasetti et al., 2011; Zhang et al., 2016); increased activation in the right dlPFC during a working memory task (Linden et al., 2013); enhanced PFC-ACC coupling (a phenotype associated with executive function deficits and schizophrenia) (Thurin et al., 2013); and reductions in hippocampal theta waves (thought to co-ordinate PFC-HC activity) (Cousijn et al., 2015). Finally, EEG recordings of healthy subjects during another working memory task found that homozygous risk allele carriers demonstrated an attenuated form of an electroencephalographic endophenotype associated with psychosis (Saville et al., 2015). Taken together, the previous literature indicates that functionally the rs1344706 genotype influences connectivity between and activity within the prefrontal cortex, anterior cingulate cortex and hippocampus –areas known to exhibit pathological alterations in schizophrenia and/or bipolar disorder.

The structural and functional consequences of possession of the rs1344706 risk allele are also accompanied with a number of distinct neurocognitive phenotypes. Homozygous risk allele carriers exhibit impairments in executive control and visuomotor performance in healthy controls, suggesting this SNP may contribute to the cognitive impairment seen in schizophrenia (Balog et al., 2011; Lencz et al., 2010). However, other studies have not found any associations between genotype at this locus and performance in working memory, spatial memory or sustained attention tasks in psychologically healthy individuals (Esslinger et al., 2011; Paulus et al., 2013; Stefanis et al., 2012), indicating that this deficit is limited to visuomotor skills in this group. Disease-associated variants at rs1344706 and rs7597593 were also associated with positive schizotypy-related factors including self-rated paranoia and ideas of reference, behavioural traits related to the positive symptoms of schizophrenia (Stefanis et al., 2012). Interestingly, the effect of the risk allele also extended to cognitive attributes in psychiatric disease. Rs1344706 risk allele homozygotes exhibited poorer decision making than non-risk allele carriers in a study of heroin addicts (Sun et al., 2015), and in patients with schizophrenia possession of the risk allele was associated with more severe psychotic symptoms and impairments in visual memory (Hashimoto et al., 2010; Wassink et al., 2012). However, risk allele also an attenuation of the deficits in working and episodic memory typically seen in schizophrenia (Walters et al., 2010). Finally, schizophrenic carriers of the risk allele at rs1344706 demonstrated positive symptoms that were more resistant to treatment with atypical antipsychotics than those of patients with a non-risk allele (Mössner et al., 2012). Collectively, these studies suggest that the rs1344706 risk allele is preferentially

associated with a schizophrenia subpopulation characterised by a more intense, treatment-resistant positive symptomology, but attenuated cognitive deficits.

1.5.6 CELLULAR AND MOLECULAR STUDIES OF ZNF804A

In contrast to the functional and structural imaging studies of *ZNF804A*, relatively few investigations have attempted to assess the functions of this gene at the cellular and molecular level. The pre-existing literature has focused predominately on a putative role of the ZNF804A protein as a transcription factor in a large variety of *in vitro* paradigms. The first of these studies, conducted by Hill et al. (2012), found that siRNA-mediated silencing of *ZNF804A* expression in a conditionally immortalised, cortically-derived human neural progenitor cell (hNPC) line found resulting alterations in the expression of several genes involved in cell adhesion as well as *C2ORF10* and *STMN3*, a gene known to influence neurite outgrowth, axonal arborisation and dendritic branching. A further investigation has found overexpression of GFP-tagged ZNF804A in rat NPCs to influence expression of the schizophrenia-linked genes *PRSS16*, *COMT*, *DRD2* and *PDE4B* (Girgenti et al., 2012). A further study conducted in HEK cells transfected with a myc-tagged ZNF804A construct found overexpression of this protein to upregulated expression of several genes involved in TGF-β signalling (Umeda-Yano et al., 2013). TGF-β signalling is a cellular pathway known to be involved in several processes including neural development, cellular differentiation, adult neurogenesis and neuroprotection (Ageta et al., 2008; König et al., 2005; Liu and Niswander, 2005); pathological alterations in this pathway have also been implicated in the etiology of schizophrenia (Frydecka et al., 2013).

SNAP25 has also been identified as a potential target of ZNF804A in a study showing a reduction in expression of this protein in neural SH-SY5Y cells following siRNA-mediated knockdown of ZNF804A, as well as a positive correlation between the expression levels of these proteins in SH-SY5Y cultures (Anitha et al., 2014). This protein is a key component of the SNARE complex (Chen and Scheller, 2001), and plays a role in the regulation of exocytosis, growth of axons and dendrites, regulation of dendritic spine density and synaptic plasticity (Antonucci et al., 2013; Fossati et al., 2015; Grosse et al., 1999; Osen-Sand et al., 1993; Tomasoni et al., 2013). In the human brain, SNAP25 levels have been further found to correlate with ZNF804A expression in the anterior cingulate cortex, a key region seen to exhibit pathological changes in structure in schizophrenia, bipolar disorder, some forms of autism and rs1344706 risk allele carriers.

Finally, *ZNF804A* knockdown using an RNA interference technique in hiPSC-derived NPCs was found to alter expression of a wide variety of genes, of which those involved in interferon signalling were particularly enriched among the genes reduced in expression following knockdown. Furthermore, *ZNF804A* knockdown particularly affected the expression of genes mediated by interferon-alpha 2 (IFNA2), a key component of immune response pathways (Chen et al., 2015). This is particularly of note given the vast body of research suggesting that immune responses may in part contribute to the risk of developing schizophrenia (Müller et al., 1999).

Upstream of these effects, a number of mechanisms have been proposed as regulators of *ZNF804A* activity, and further acting as potential mediators of the effect of the rs1344706 SNP on the risk of developing psychosis. Although (as described previously) rs1344706 is unlikely to directly influence *ZNF804A* expression several indirect mechanisms have been suggested, including alterations in pre-mRNA splicing, allele-specific alterations in transcription factor binding efficiency and epigenetic modifications which alter the site's affinity for DNA binding proteins (Hess et al., 2015; Hill et al., 2011; Voineskos et al., 2011). One such proposed epigenetic mechanism is histone 3 lysine 9 trimethylation (H3K9me3), which is specifically enriched at rs1344706 in the fetal and adult cortex (Hess et al., 2015). This alteration is particularly noteworthy as it has been implicated in gene repression and alternate splicing (Saint-André et al., 2011), though the full effect of all the potential epigenetic changes at the rs1344706 locus on *ZNF804A* activity is not yet fully understood.

ZNF804A is known to be a target of miR-137, a non-coding RNA that acts as a regulator of gene expression (Kim et al., 2012). A SNP in the gene for this microRNA has been found to be associated with schizophrenia in a previous GWA study (Ripke et al., 2011). Indeed, expression of miR-137 has recently been found to inversely correlate with *ZNF804A* expression in the primary motor cortex of first trimester fetuses and the ventrolateral and dorsolateral PFC and ACC of adult subjects (Hess et al., 2015). *ZNF804A* expression has also been found to be modulated by treatment with glutamate in and NMDA receptor-dependent mechanism as well as exposure to heat shock (Chang et al., 2015; Lin et al., 2014).

ZNF804A is also predicted to possess binding sites for a number of transcription factors at an intronic region which are implicated in neurodevelopmental processes and schizophrenia-associated pathology as well as cytokine-influenced pathways involved in synaptic plasticity and behaviour (Hess

et al., 2015; J. Chen et al., 2015). Taken together with the literature implicating ZNF804A's involvement in heat shock pathways, NMDA receptor-mediated signalling pathways, TGF-β signalling, IFNA2-mediated gene expression, and expression of multiple psychosis-relevant genes involved in neurotransmission, this suggests that the ZNF804A protein may be a common factor in multiple immune-related and neurotransmission-related pathways underlying psychosis.

Several studies have further attempted to determine the subcellular localisation of both the ZNF804A and Zfp804A proteins, a common method for identifying prospective functions of a given protein. The first study to investigate the localisation of ZNF804A in neural cells found that endogenous and exogenous Zfp804A is expressed predominately within the nucleus of rat NPCs (Girgenti et al., 2012). In rat primary cortical neuron cultures, Zfp804A is initially expressed predominately within the perinuclear cytoplasm, and then during differentiation it is redistributed throughout the neuron, with particularly strong immunostaining being seen in the growth cones of neurites. Finally, in mature rat primary cortical neurons it re-adopts the predominately cytoplasmic distribution, though expression can still be seen along the dendrites and within the nuclei (Hinna et al., 2015).

Further studies have determined that in humans the ZNF804A protein is expressed in layer III pyramidal neurons and interneurons in the temporal and parietal cortex, in granule and purkinje cells in the cerebellum and in fetal neuroblasts during the 19th week of gestation (Bernstein et al., 2014; Tao et al., 2014). Taken together, these studies appear to support a putative role for ZNF804A and Zfp804A as transcription factors due to the localisation of these proteins within the cell nucleus, particularly in NPCs. The data also appears to be suggestive of a potential extra-nuclear role given the prominent cytoplasmic, dendritic and growth cone staining for these proteins in developing and mature neurons in humans and rodents. Despite these interesting findings however, it should be noted that many of these findings are not consistent across studies even using the same anti-ZNF804A antibody, and characterisation of the antibodies used is either limited or missing entirely (Bernstein et al., 2014; Umeda-Yano et al., 2013; Anitha et al., 2014; Tao et al., 2014). Thus, for the purposes of future experiments a thorough characterisation of the currently available anti-ZNF804A antibodies and a subsequent employment of one of these antibodies in the study of subcellular localisation of ZNF804A/Zfp804A in multiple cell lines at various stages of differentiation would be of enormous benefit.

In contrast to the growing number of *in vitro* studies assessing the impact of ZNF804A/Zfp804A manipulation on gene expression, very few investigations have attempted to assess the impact of these proteins on the morphological and functional characteristics of neurons and other neural cell types. A preliminary study conducted in hiPSC-derived NPCs found that knockdown of ZNF804A using RNA interference resulted in a trend towards an increase in proliferation that did not reach significance (Chen et al., 2015). However, no studies have yet attempted to determine whether the alterations in the expression of genes relevant to neurite outgrowth and synapse formation and maintenance following ZNF804A overexpression/knockdown actually impact these parameters. Clearly, this is a critical area for further exploration in future studies in order to link previous work at the genetic and molecular level with that at the neuroanatomical level.

1.6 CELLULAR MODELS OF NEUROPSYCHIATRIC DISEASE

GWA studies have provided an invaluable tool for identifying novel candidate genes which may contribute to psychiatric disease. However, many of the genes marked as potentially contributing to disease pathways underlying psychiatric disease by GWAS have not yet been fully characterised and thus little is currently known about their biological functions. Animal models involving the conditional or unconditional knockout of a given gene offer one method of studying that gene's impact on brain function and development, though such studies are limited by differences in neuronal biology between the commonly used model species and human cells. Neuronal cultures generated from human stem cell sources offer a means of bypassing this issue.

Recent advances in stem cell technology have resulted in an unprecedented variety of experimental paradigms in which neurodevelopmental and neuropsychiatric disease mechanisms can be studied in human neurons. Human neurons can now be generated from several sources, including immortalised lines such as tumour-derived neural cell lines, neural stem cell (NSC) and neural progenitor cell (NPC) lines; as well as patient-derived lines such as induced pluripotent stem cells (iPSCs) and cells taken from the olfactory neuroepithelium.[1] The advantages and disadvantages of these differing platforms will now be discussed in the following section.

[1] It is worth noting that NPC and NSC are terms which are often used interchangeably in the literature. However, typically NSC is used to refer to neural cells which are able to renew themselves indefinitely and differentiate into a variety of neural cell types, while NPC usually refers to cells which only

1.6.1 IMMORTALISED NEURAL STEM CELL LINES

Certain populations of neurons can be obtained directly from human brain tissue during biopsies, surgery, or from post-mortem brains and grown as primary cultures (Gibbons and Dragunow, 2010). However, such sources are limited by ethical and practical considerations, rendering them unsuitable for research purposes in the vast majority of cases. In contrast to this, immortalised stem cell lines offer a method for generating cultures of human neurons from a standardised and continually proliferating source. Tumour-derived lines have long been used in such a manner, though developments in stem cell biology over the past two decades have provided an alternative in the form of immortalised ESC, NSC and NPC lines.

1.6.1.1 TUMOUR-DERIVED CELL LINES

Tumour-derived lines such as the SH-SY5Y line, derived from a metastatic neuroblastoma, can provide a renewable source of cells which display neuronal properties such as neurite outgrowth, synthesis of neurotransmitters, receptor expression and even electrophysiological phenomena such as action potentials after differentiation with retinoic acid (Johansson, 1994). The SH-SY5Y line in particular has been used in a several studies investigating the mechanisms of anti-depressant and anti-psychotic drug activity (Arun et al., 2008; Park et al., 2011; Sanchez-Wandelmer et al., 2009). Due to its ability to express key neuronal proteins this line also represents a useful model for investigating psychiatric disease-associated gene functions and the impact of genetic variants on those functions (Biedler et al., 1978; Bray et al., 2012). However, there remain a number of drawbacks to the use of tumour-derived cell lines in the generation of neuronal cultures. These lines typically have low phenotypic potential and thus the variety of experimental avenues which may be explored using this paradigm is limited. Furthermore, care must be taken to ensure that the SH-SY5Y cells under experimental study adopt the appropriate neuronal characteristics as SH-SY5Y cultures may remain heterogeneous even after differentiation, and neuroblastoma lines in general are predisposed to chromosomal abnormalities (Bray et al., 2012; Encinas et al., 2000). In contrast to this, immortalised

(continued) possess a transient ability to proliferate and which tend to be unipotent or only able to differentiate into a handful of cell types (Seaberg & van der Kooy, 2003). For the purposes of the present discussion, NSC and NPC will be used according the nomenclature applied by the relevant paper being described in a given section.

lines derived from embryonic and fetal brain tissue offer a method for generating multiple neuronal cell types while simultaneously avoiding these pitfalls.

1.6.1.2 EMBRYONIC STEM CELL LINES

Embryonic stem cell (ESC), immortalised neural stem cell (NSC) and neural progenitor cell (NPC) lines offer a means of bypassing several of the limitations of neuroblastoma lines: these cells typically lack the chromosomal abnormalities seen in tumour-derived lines, they are multipotent and thus capable of differentiating into multiple neuronal cell types, and differentiation of neurons from these lines resembles differentiation *in vivo* more closely (Bray et al., 2012). ESCs are obtained from the inner mass of the initial blastocyst and possess the potential to differentiate into all the tissues of the developing fetus (Thomson et al., 1998). The first paper to describe the derivation of these cells from a human blastocyte was conducted by Thomson et al. in 1998; these cells demonstrated continual proliferative capabilities and were shown to form derivatives of all three germ layers including neural epithelium from the ectodermal layer via spontaneous differentiation. However, this method is inefficient in producing neural cells and subsequent techniques have attempted to direct differentiation more specifically towards neural lineages using media supplements such as RA or BMP-inhibitors in adherent cultures, and FGF-2 for cultures in suspension (Dhara and Stice, 2008). Adherent cultures can be grown with or without MEF feeder layers, and progressively generate radial structures resembling a transverse section of the developing neural tube *in vivo*, known as ‘neural rosettes’. These rosettes give rise to nestin-positive neural progenitor cells which can be manually picked and passaged into media containing high levels of FGF-2 and maintained or frozen down into seed stocks (Dhara and Stice, 2008). Depending on the differentiation protocol used, these NPCs can adopt multiple regional characteristics including those consistent with progenitors from the midbrain, spinal cord and forebrain (Johnson et al., 2007; Li et al., 2005; Singh Roy et al., 2005; Yan et al., 2005), and can be further differentiated into neurons, astrocytes and oligodendrocytes (Carpenter et al., 2001; Wilson and Stice, 2006). Additionally, neurons differentiated from these NPCs can demonstrate the hallmarks of functional neurons including neuronal morphology, synaptic protein expression and electrophysiological properties such as action potentials (Johnson et al., 2007). These neurons also develop the characteristics of specific neuronal subpopulations, including midbrain dopaminergic neurons and cortical glutamatergic and GABAergic neurons, though again via specific differentiation protocols (Carpenter et al., 2001; Ma et al., 2012; Zhang, 2006). For example, a combination of retinoic acid and

SHH can push neuroepithelial cells towards a motor neuron identity while SHH and FGF8 drives these cells towards a dopaminergic fate (Singh Roy et al., 2005; Zhang, 2006).

ESCs offer an advantage over tumour-derived cell lines as a model of human neurons in that they faithfully recapitulate the stages of neuronal development during differentiation, from initial neutralisation to terminal differentiation of neurons. Furthermore, they provide greater experimental flexibility in contrast to tumour-derived lines due to the wide variety of cell types which can be generated from a single ESC source (Bray et al., 2012; Gaspard et al., 2008). However, there also exists several drawbacks to their use: strong controversy exists over the source of these cells, and as a result the number of the available lines is relatively limited. Furthermore, there is also a risk of contamination from non-neuronal cells in cultures derived from ESCs, and generation of neuronal cells from ESCs requires a considerable increase in culture times relative to tumour-derived lines, raising the susceptibility of cultures to infection (Jakel et al., 2004). NPC and NSC lines offer a way of avoiding the risks of long term culture by eliminating the initial neutralisation step required with ESCs. Additionally, these lines avoid the risk of contamination with other, non-neural cell types, being directly obtained from the developing fetal brain.

1.6.1.3 NEURAL STEM CELLS AND NEURAL PROGENITOR CELLS

The earliest NSC and NPC lines to be derived from human fetal brain tissue were first described in a series of papers published in the late 1990s. These lines could differentiate into both neurons and astrocytes, though they initially lacked the ability to produce oligodendrocytes (Sah et al., 1997). Subsequent studies have demonstrated full multipotentiality however, both *in vitro* and *in vivo* following grafting experiments (Carpenter et al., 1999a; Flax et al., 1998). The primary samples obtained from fetal brain tissue often contain a mixture of cells, both pluripotent and terminally differentiated cells such as neurons or oligodendrocytes. This mixture will depend on the gestational age of the fetal brain and the region from which the tissue is extracted from, however for the purposes of experimental, therapeutic and screening use it is critical that any NPC and NSC lines arising from these primary samples are homogenous to reduce variability between cultures (Hook et al., 2011). To address this, typically clonal populations are isolated from a single NPC or NSC within the primary sample. However, such clonal lines often lose their ability to proliferate and gradually alter their karyotype following prolonged periods in culture (Villa et al., 2004). To target the former problem, NSC and NPC clonal lines

are commonly conditionally immortalised using the insertion of a transgene into the cell's genome to drive regulated proliferation and thus permit greater control over expansion and differentiation of cultures from the line in question (Pollock et al., 2006) and to counter problems arising from any limited potential for renewal possessed by unedited cells. Despite this, several studies have also demonstrated that certain NSCs are able to proliferate indefinitely in culture in the presence of EGF and FGF2 (Hook et al., 2011; Sun et al., 2008).

NSCs can be derived from embryonic neural tissue following the closure of the neural tube during development, though other populations of NSCs are known to exist in the adult brain in subgranular zone of the dentate gyrus of the hippocampus and the subventricular zone of the lateral ventricles (Fuentealba et al., 2012; Price and Williams, 2001). NPCs subsequently arise from NSCs in later development and possess distinct regional identities determined by their position within the germinal zones of the developing brain, which in turn impacts the genes they express and ultimately the potential cellular fates they can adopt during terminal differentiation (Price and Williams, 2001). NPC lines have previously been generated from a wide variety of fetal tissues, including spinal cord, mesencephalon, dorsal and ventral telencephalon (Cocks et al., 2013; Horowitz et al., 2015; Lin et al., 2015; Pollock et al., 2006; Storch et al., 2001). As isolated hNPCs retain their regional identity these lines produce neurons specific to their origin within the fetal brain. For example, NPCs derived from the mesencephalon can adopt a dopaminergic neuronal identity following differentiation, while those from the ventral telencephalon adopt the features of GABAergic interneurons (Storch et al., 2001; Zhang et al., 2008).

These lines can be employed in similar research to that of SH-SY5Y cells – studying mechanisms of drug action, neuronal development, neuronal function and disease processes – though these lines have also previously been utilised as a therapeutic treatment in an animal model of stroke (Pollock et al., 2006; Stevanato et al., 2009). Previous research has shown NSC and NPC lines to be capable of generating cultures of cells staining positive for markers of neuronal fate and negative for markers of stem cell identity and proliferation. Subsequent to this, neurons expressing markers of distinct regional and functional identity have also been observed, including GABAergic interneurons, glutamatergic cortical neurons, midbrain dopaminaergic neurons (De Filippis et al., 2007; Storch et al., 2001; Zhang et al., 2008), Neurons derived from NPC and NSC lines have also been shown to develop

morphological features consistent with neurons *in vivo*, which are plastic in response to activity-inducing stimuli. Calcium responses have been demonstrated in neurons derived from these lines as a proxy marker of neuronal activity, while the expression of synaptic markers and electrophysiological features consistent with neurons *in vivo* and in other *in vitro* models has also been shown (Cacci et al., 2007; Carpenter et al., 1999a; Cocks et al., 2013; De Filippis et al., 2007; Gaspard et al., 2008; Lin et al., 2015; Nunes et al., 2003; Zhang et al., 2008). Such features place these cell lines in an ideal position to study mechanisms of brain development and disorder at the cellular level. However, there are also several drawbacks to the use of immortalised NSC and NPC lines. As with embryonic cells, there is considerable controversy over the use of embryonic and fetal tissue as a source for experimental lines. In addition to this, neural stem and progenitor cell lines can also be relatively restricted in their neuronal progeny, limiting their experimental flexibility within a single line (Jakel et al., 2004). Moreover, the use of fetal tissue as a source precludes some of their uses in the study of heritable disease-related phenotypes which are only detectable in post-natal individuals, like psychiatric disorders. Patient-derived cell lines provide one method of bypassing some of these difficulties.

1.6.2 PATIENT DERIVED LINES

1.6.2.1 ADULT STEM CELL LINES

Patient-derived stem cell lines offer a valuable tool for investigating the impact of certain genetic variants and genotypes on known clinical syndromes which only emerge following birth, and would otherwise be unpredictable in cell lines derived from fetal tissue. As previously described, olfactory mucosa tissue provides one useful source of NSC and NPC lines. In addition to this, other sources of these lines exist within two key regions in the adult brain: the granular layer of the dentate gyrus and the subventricular zone of the lateral ventricles (Price and Williams, 2001). These cells can be accessed via post-mortem tissue, biopsies and surgical specimens, though NSCs and NPCs derived from these sources are typically limited in their fate specification, are difficult to expand into large populations *in vitro* and also tend to senesce after relatively few passages (Akiyama et al., 2001; Jakel et al., 2004; Schwartz et al., 2003). However, adult stem cells can also be obtained from the olfactory mucosa via biopsies which are considerably less invasive. These cells can be subsequently grown in culture as neurospheres: clustered cultures of NSCs and NPCs undergoing differentiation (Borgmann-Winter et al., 2009). NSCs and NPCs from these cultures can be further differentiated into cells which express a

wide variety of neuronal markers, adopt neuronal morphologies and even express key synaptic proteins and respond to treatment with neurotransmitters (Borgmann-Winter et al., 2009; Wang et al., 2011a). Olfactory neuroepithelium-derived cells have previously been used to show altered cell cycle dynamics in schizophrenia patient-derived cells relative to controls, and demonstrate changes in the expression of genes implicated in axonal guidance (Fan et al., 2012; Matigian et al., 2010).

Olfactory neuroepithelium cell lines offer an advantage over immortalised neural cell lines in that they can be directly obtained from patients known to be diagnosed with a given psychiatric disorder and thus mechanisms and phenotypes differing between psychiatric patient-derived cells and those of healthy controls can be studied. However, like NSCs and NPCs obtained from the dentate gyrus and subventricular zone of the lateral ventricles, neuronal cells derived from such sources are typically limited in their regional and functional identity, and thus other cellular models must be adopted in studies where olfactory neuroepithelium-derived cells are unable to adopt the relevant neuronal identity (Wang et al., 2011a). Additionally, despite being less drastic than the surgery required for biopsies taken from other sources of adult NSCs, biopsies of the olfactory mucosa are still relatively invasive for the subject involved (Roisen et al., 2001). HiPSC lines and other related technologies offer a novel means of circumventing both of these issues.

1.6.2.2 HIPSC LINES

The recent development of iPSC technology has provided a highly flexible new tool for investigating disease and developmental mechanisms in a vast array of neural tissues and cell types that would not be available using olfactory neuroepithelium sources. This technique was first described in a 2006 study by Takahashi & Yamanaka, who reprogrammed dermal fibroblasts from adult mice into pluripotent cells using retroviral transduction of just four transcription factors: Oct3/4, Klf4, Sox2, and c-Myc. Similarly to ESCs, these induced pluripotent stem cells (iPSCs) possessed the ability to differentiate into the cellular identities of all three germ layers, and additionally exhibited similar morphology, proliferative capabilities, gene expression and surface antigens to embryonic stem cells, though some studies have also noted key phenotypic differences in epigenetic modifications and gene expression between these cell types (Puri and Nagy, 2012). Since this initial discovery, integrative and non-integrative iPSC transduction methods have now been successfully applied to a wide range of human somatic cells including dermal fibroblasts, blood cells, amniotic fluid and hair cells, opening the

path to the generation of lines derived from patients with psychiatric diseases (Aasen et al., 2008; C. Li et al., 2009; Loh et al., 2009; Takahashi et al., 2007).

A critical aspect of hiPSC technology as it relates to the study of psychiatric disease is the ability to produce neurons and other neural cell types following the application of directed differentiation protocols. Numerous neuronal cell types can now be generated from hiPSC lines, including basal forebrain cholinergic neurons, spinal motor neurons, pyramidal glutamatergic neurons, GABAergic interneurons and midbrain dopaminergic neurons, as well as astrocytes and oligodendrocytes, though it should be noted that typically such protocols usually result in heterogeneous populations of multiple neuronal cell types (Liu et al., 2013; Ogawa et al., 2011; Ring et al., 2012; Sareen et al., 2013; Shi et al., 2012a; Swistowski et al., 2010). hiPSC-derived neurons have been found to display similar properties to neurons in fetal tissue including expression of neuronal markers, the progressive development of neuronal morphology (including dendritic spines), the expression of a wide variety of key synaptic proteins, functional responses to neurotransmitters and even the generation of action potentials and other key electrophysiological phenomena (Maroof et al., 2013; Nicholas et al., 2013; Pedrosa et al., 2011; Verpelli et al., 2013).

Several studies have employed patient-derived hiPSC lines in the study of disease mechanisms underlying schizophrenia, autism and even bipolar disorder. Neurons generated from schizophrenia patient hiPSCs have previously been found to exhibit reduced neuronal connectivity and alterations in gene expression relative to controls, including reduced expression of *ZNF804A* in two out of four patient lines; these deficits were found to be attenuated following treatment with loxapine, an antipsychotic (Brennand et al., 2011a). Schizophrenic patient hiPSC-derived NPCs have also demonstrated pathological elevations in intracellular zinc and potassium which are reversed by valproate treatment as well as increases in reactive oxygen species (ROS) (Paulsen et al., 2014). Additionally, impairments in synaptic maturation and alterations in mitochondrial function have been seen in schizophrenia patient hiPSC-neurons (Robicsek et al., 2013). For bipolar disorder, hiPSC lines have demonstrated proliferative deficits in bipolar patient NPCs and abnormalities in the expression of genes involved in neurodevelopment and neurogenesis (Madison et al., 2015). Finally, hiPSC-based studies of autism have previously tended to focus on hiPSC lines derived from patients with clinical syndromes characterised by autistic features, including Rett syndrome, Timothy syndrome, Fragile X syndrome,

Prader-Willi/Angelman syndrome and Phelan- McDermid syndrome. It is worth noting that hiPSC-neurons derived from patients within these cohorts have demonstrated variously alterations in synaptic density and calcium signalling; reductions in neurite complexity and electrophysiological dysfunction; and changes in gene expression (Chamberlain et al., 2010; Liu et al., 2012; Marchetto et al., 2010a; Paşca et al., 2011; Shcheglovitov et al., 2013). Although these studies typically use hiPSC lines generated from only a handful of patients and controls, the advent of high-throughput automated techniques in cell culture studies may greatly improve the power of these investigations in the future by exponentially increasing the number of feasible lines in a given study.

As with other patient-derived lines, hiPSCs offer an advantage over immortalised cell lines in modelling late-emerging, genetically heterogeneous diseases such as psychiatric disorders as they permit assessments of neuronal function and development in a system with a genetic background known to ultimately result in disease. Additionally, hiPSC cultures offer similar benefits to ESCs as a model system in that they also recapitulate the cellular stages of human neural development, crucial for studies of brain development or diseases thought to feature early developmental pathology (see **Figure 1.4**). However, caution must be ascribed in attempting to model disease processes which may only occur in the adult human brain (particularly in the case of certain psychiatric and neurological disorders), as iPSC-derived neurons most closely match the gene expression patterns seen in neurons within the developing fetal brain 8-24 weeks post-conception (Brennand et al., 2014). One possible method of sidestepping this problem is to specifically focus studies on mechanisms and signalling pathways in isolation without attempting to model the disease etiology as a whole. Furthermore, iPSCs may also be used to focus instead on early pathological mechanisms which are thought to contribute to later dysfunction in the mature brain.

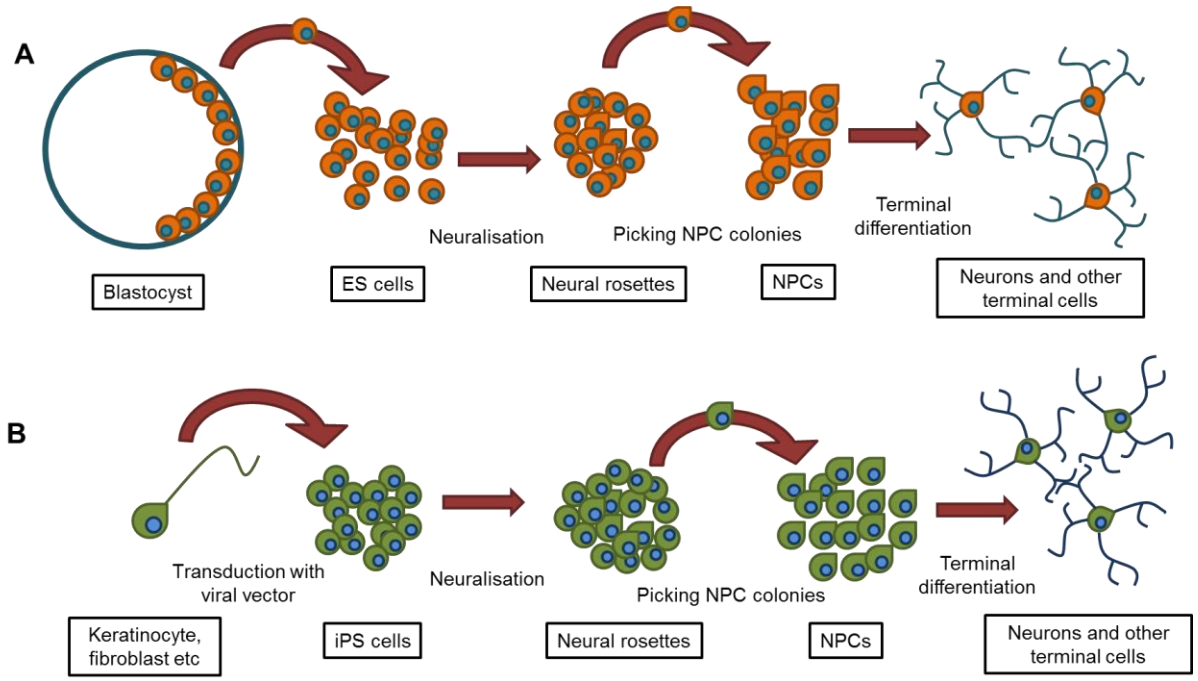

Figure 1.4: Schematic of neuronal differentiation from ESCs (**A**) and iPSCs (**B**). **A**: ES cells are obtained from the inner mass of a blastocyst then expanded in culture. ESCs are neuralised using RA and BMP inhibitors until the formation of neural rosettes. NPCs are picked and expanded. Finally cells are terminally differentiated using a protocol specific to the intended lineage. **B**: IPSCs are transduced from somatic cells using viral vectors or other methods including microRNAs and protein transduction. IPSC cultures are then commonly neutralised using dual SMAD inhibition until the formation of neural rosettes. NPCs are picked from the rosettes and expanded. NPC cultures are then terminally differentiated according to defined protocols.

Despite these advantages, there are several caveats in the use of hiPSC lines which may limit their use in certain forms of experimental inquiry. Genetic lesions associated with particular diseases may impede or halt entirely the process of hiPSC derivation from patient samples due to interference with the reprogramming technique itself – previous attempts to model Fanconi anaemia using hiPSCs reprogrammed from fibroblasts were stymied by the causative mutation for the disorder impacting a DNA repair pathway involved in the reprogramming process (Raya et al., 2009). In addition to this, diseases involving aberrant epigenetic modification of particular genes may not be well suited to study using hiPSCs as typically the reprogramming of somatic cells results in the loss of epigenetic signatures due to chromatin remodelling and competitive growth selection during the expansion of hiPSC colonies (Mertens et al., 2016).

The heterogeneity of hiPSC cultures also poses a challenge for experimental design in several ways. hiPSC lines derived from different somatic tissues within the same individual, or even from the

same tissue but with different reprogramming techniques, have been reported as exhibiting differences in global gene expression, raising the question of whether these cells partially retain elements of their initial identity (Rouhani et al., 2014). However, intra-individual heterogeneity in this regard is still less than inter-individual heterogeneity in gene expression, suggesting that differences between cell lines are predominately driven by genetic differences rather than induction techniques or source tissue and highlighting the priority of using iPSC lines from multiple patients and/or controls rather than within a single individual (Rouhani et al., 2014). The majority of existing techniques for iPSC and neural induction result in diverse cultures populated with multiple cell types, further contributing to the intra- and inter-individual heterogeneity of cell lines. This variability necessitates the generation of multiple lines (typically 3 per patient or control) from multiple individuals in each clinical group in a given study (Brennand et al., 2014). Due to the wide degree of clinical variation typically seen in psychiatric disorders such as schizophrenia, studies focusing on cohorts sharing a clinical phenotype or that are genetically homogenous have been proposed as experimental designs which would bypass the problems caused by the heterogeneity of these diseases (Brennand et al., 2014). However, even limiting an experimental paradigm in this way requires the generation of a large number of patient and control lines, each of which requires culturing and validation for multiple months prior to experimentation. The generation of large quantities of iPSC lines is highly time consuming and expensive, and for the purposes of some studies these may be prohibitive factors. However, recent developments in stem cell technology have produced two new experimental systems which can greatly reduce the time required to generate neuronal cells by reprogramming somatic tissue: induced NPCs (iNPCs) and induced neurons (iNs).

1.6.2.3 INPCS AND INS

Induced neurons were initially reported by Vierbuchen et al. (2010), who found that inducing expression of Ascl1, Brn2 and Myt1l in rodent fibroblasts using lentiviral transduction resulted in the generation of populations of cells expressing markers of neurons, exhibiting action potentials and demonstrating functional synapses. Similar techniques have been subsequently applied to human fibroblasts to generate cultures of glutamatergic and dopaminergic iNs with similar neuronal properties (Pang et al., 2011; Pfisterer et al., 2011). The production of iNPCs from mammalian cells was first demonstrated by Tian et al. (2012), using retroviral induction of just five transgenes (Pou3f2, Nr2e1, Sox2, c-Myc and Bmi1) to convert mouse epidermal fibroblasts. iNPCs have been subsequently derived

from human somatic cells and possess the proliferative, differentiation, self renewal and gene expression properties consistent with NPCs *in vivo* (Ring et al., 2012). These cells can be later used to generate cultures of glutamatergic or dopaminergic neurons which express the neuronal and synaptic markers and electrophysiological properties of functional neurons in the developing mammalian brain (Lim et al., 2015; Ring et al., 2012).

iNs and iNPCs possess several advantages over iPSC models. The time required to generate these lines from somatic cells is greatly reduced in comparison to iPSC reprogramming, thus also reducing cell culture costs and the risk of contamination. In addition to this, iN cultures have been found to retain age-related transcriptomic and functional signatures, raising the possibility that they may be suitable for the study of biological phenomena which only occur in the mature or aged brain. The preservation status of these signatures in iNPCs is currently unknown. iNPCs offer an additional advantage over iN techniques in that they overcome the experimental limitations arising from the restricted numbers of cells arising from iN induction while still retaining the advantage of skipping the iPSC stage and the related problems in culture heterogeneity, inefficiency of differentiation and residual pluripotency (Mertens et al., 2016).

Despite the crucial advantage of reducing culture time relative to iPSC-based paradigms, iNs and iNPCs have several drawbacks. While iPSCs can proliferate indefinitely *in vitro*, iNs are limited by the expandibility of the initial somatic cell cultures and the efficiency of conversion and iNPCs eventually lose their ability to proliferate, ultimately limiting the number of neurons which may be generated using these techniques. Furthermore, while the generation of neurons from iPSCs permits an approximation of the development of neurons from embryonic stem cells *in vivo*, it should be noted that iNPCs and iNs do not go through some of these analogous developmental stages and thus may preclude investigations of disease mechanisms which may occur during neural induction or neuronal maturation (Mertens et al., 2016). Regional patterning of iNPCs has not yet been demonstrated (Brennand et al., 2014) and further refinement of these techniques will be required before they can be employed in studies of all the functional neuron subtypes of the brain. As a result iNPCs have not yet been utilised in studies of psychiatric disease. iN cultures and some iNPC cultures also exhibit mosaicism due to the genetic diversity of the donor tissue, an issue which may increase the variability of differentiated cultures but

may also be useful as a means of modelling the natural genetic diversity seen in mature somatic tissue (Mertens et al., 2016).

1.7 ASSESSMENTS OF SNP FUNCTION USING CELLULAR SYSTEMS

As has been outlined here, human stem cells represent a flexible model system for the study of human disease-relevant genes, and the wide variety of stem cell models now available permits depending on the requirements of the line of experimental inquiry. However, these advances in stem cell technology, coupled with breakthroughs in genome editing techniques, have now additionally produced a means through which individual disease-associated SNPs can be studied in human cells. The generation of hiPSC lines from human patients possessing the disease-associated allele of a GWAS-identified SNP permits detailed evaluations of the impact of this SNP on a wide range of biological attributes, including the binding affinity of transcription factors, splicing factors and/or microRNAs and the transcription and splicing of genes (Merkle and Eggan, 2013). In the case of SNPs occurring outwith the coding regions of the genome, such techniques may also assist in the identification of the candidate gene affected by the SNP which conveys the increased risk of disease. Moreover, as multiple SNPs often occur in linkage disequilibrium with one another, hiPSC lines provide a useful tool for studying haplotypes consisting of several SNPs which are associated with a particular disease (Merkle and Eggan, 2013). The impact of haplotypes or single SNPs on cellular and molecular mechanisms in hiPSC-derived somatic cells may then be further used to identify potential mechanisms linking genetic variants to the associated disorder.

As described in **Section 1.4**, previous GWA studies have found the rs1006737 SNP within an intron of the *CACNA1C* gene (coding for the CaV1.2 voltage gated calcium channel) to be associated with both bipolar disorder and schizophrenia (Green et al., 2010). A subsequent study compared iNs derived from individuals possessing the risk allele for this SNP in comparison to iNs derived from individuals homozygous for the nonrisk allele. Possession of both copies of the risk allele was found to result in a significant increase in *CACNA1C* mRNA relative to heterozygous and homozygous carriers of the nonrisk allele, a finding previously observed in studies of post-mortem brain tissue and suggested to be mediated by multiple cis-elements within the intronic region containing rs1006737 (Yoshimizu et al., 2015). In addition to this, possession of both copies of the risk allele was found to be correlated with

an increase in the density of CaV1.2-mediated currents in these iNs relative to iNs derived from nonrisk allele carriers, indicating that the rs1006737 SNP has downstream functional consequences.

hiPSC lines have also been used to study the impact of disease-associated SNPs on diseases outwith the field of psychiatry. In a study of hiPSC-neurons derived from patients possessing polymorphisms associated with sporadic Alzheimer's disease within the *SORL1* gene exhibited reduced *SORL1* expression and APP processing responses to treatment with BDNF relative to control hiPSC-neurons (Young et al., 2015). Highly penetrant SNPs have similarly been investigated in the case of hiPSC lines derived from patients with Parkinson's disease (PD). In one such study the *LRRK2* mutation G2019S - known to cause an autosomal dominant form of PD – was found to result in deficits in neurite outgrowth and hypersensitivity to treatment with 6-Hydroxydopamine in neurons derived from PD patient hiPSC lines (Reinhardt et al., 2013). These effects were found to be mediated in part by increased ERK phosphorylation and alterations in gene expression in the G2019S lines, highlighting how hiPSCs can ultimately be used as a tool in identifying novel mechanisms underlying disease.

In addition to the use of hiPSC lines derived directly from individuals possessing specific disease-associated polymorphisms, genome editing represents a valuable technique to not only induce these disease-associated polymorphisms in unaffected lines, but also to generate 'rescue' lines whereby the variants known to be associated with disease are 'corrected' in isogenic lines (Wen et al., 2016). In the previously described hiPSC study of the G2019S variant known to cause PD, hiPSC lines carrying the disease-causing mutation were genome edited using zinc finger nucleases to correct this mutation; these genome-edited lines exhibited an amelioration of the disease-related cellular phenotypes seen in hiPSC-neurons derived from PD patient cells. This experimental paradigm permits an assessment of SNP function with much greater specificity than is possible with hiPSC lines alone, as it eliminates the possibility of phenotypic differences between risk allele carrier and noncarrier lines arising from other genomic variation. Recently, a new approach combining both TALENs and the CRISPR/Cas system, termed iCRISPR, has been developed to rapidly and efficiently edit the genome of hiPSC lines (González et al., 2014). This approach permits the generation of biallelic knockout lines and homozygous knockin lines with stage-specific control during differentiation and the potential for double- and triple gene knockouts in a single line. Critically, alterations of single nucleotides can be performed using this technique, thus establishing a highly useful method to study the impact of

individual SNPs - in this study, an Alzheimer's disease-associated SNP located within *APOE* exon 4 was successfully inserted into the genome of hiPSC lines (González et al., 2014).

The functionality of SNPs located within genes coding for microRNAs can also be tested using human stem cell models without the requirement for genome editing. In a study of a SNP at rs147061479 within piR-598, a PIWI-interacting, noncoding RNA linked to glioma formation, immortalised human astrocytes and cells from two human glioma lines were independently transfected with wild type and variant piR-598 mimics (Jacobs et al., 2016). In all cell lines transfection with wild type piR-598 sharply reduced cell proliferation relative to a control RNA, an effect that was ameliorated in the SNP-containing piR-598 transfection condition. Such an experimental system may be useful in future studies of psychiatric disease-associated SNPs located within microRNAs. Moreover, if a particular disease-associated SNP within a given gene is known to be associated with an upregulation or downregulation of that gene's expression, cellular models such as immortalised stem cell lines or hiPSCs may be similarly combined with transfection techniques to either knock down or overexpress the disease-relevant gene as an approximation of the effects of the risk SNP.

Finally, genetic variants linked to a specific disease may exert their effects through non-cell-autonomous pathways which can be investigated through the use of different cell types differentiated through isogenic hiPSC lines. For example, mouse motor neurons carrying the ALS-causing G93A *SOD1* point mutation exhibit cell-autonomous death *in vitro*, but control motor neurons also exhibit non-cell-autonomous apoptosis when co-cultured with astrocytes carrying the disease-causing mutation (Di Giorgio et al., 2007; Nagai et al., 2007); such mechanisms could similarly be explored in hiPSC lines carrying disease-associated SNPs. The combination of hiPSC lines with techniques to produce pure populations of specific cells, such as fluorescence-assisted cell sorting (FACS) (Schöndorf et al., 2014), will in future aid the development of new experimental systems which can be used to identify the cellular populations contributing to the pathology of a particular disease. In the case of pathological alterations of neuronal function, these may even manifest on the level of brain circuitry; purifying distinct populations of hiPSC-derived neuronal cells for co-culture will in future provide a useful method for investigating SNP-associated pathology at specific circuits.

In the context of the current investigation it is particularly worth noting that a conditionally immortalised, cortically derived human NPC line, CTX0E03, has been previously used to study the

impact of ZNF804A on gene expression (Hill et al., 2012). This line expresses a modified c-mycER^{TAM} transgene, which causes these cells to continually proliferate and maintain an NPC identity when cultured in media supplemented with a synthetic drug, 4-hydroxytamoxifen (4-OHT) (Pollock et al., 2006). Recently, a sister cell line to CTX0E03, CTX0E16, has become commercially available and, due to the cortical abnormalities associated with variants at the *ZNF804A* locus, may represent a highly useful model in which key aspects of ZNF804A-mediated cortical dysfunction can be studied at the cellular level. However, this cell line has not yet been thoroughly characterised, and thus it is critical to establish whether NPCs from this line are capable of generating cultures of cells which exhibit all the key hallmarks of mature, functional neurons. Previous characterisation studies of hNSC and hNPC lines have established neuronal identity by assessing a number of attributes including expression of functional and regional neuronal markers; the progressive development of key morphological features of neurons including an axon, dendrites and dendritic spines; the expression of a range of pre- and post-synaptic markers in a manner consistent with *in vivo* observations; functional responses to physiologically-relevant stimuli; electrophysiological properties consistent with mature neurons such as action potentials; and morphological plasticity (Cacci et al., 2007; Carpenter et al., 1999a; Cocks et al., 2013; De Filippis et al., 2007; Gaspard et al., 2008; Lin et al., 2015; Nunes et al., 2003; Zhang et al., 2008). A similar characterisation is thus necessary for the CTX0E16 cell line before it can be used in conjunction with other cellular models to study ZNF804A expression and function.

1.8 AIMS AND HYPOTHESES

In light of the previous literature on neurons generated from immortalised hNSC and hNPC lines**, I hypothesise that cells from the CTX0E16 hNPC line will be capable of differentiating into glutamatergic neurons which exhibit the characteristic phenotypes of functional pyramidal neurons and thus represents an ideal cellular model in which to understand the biological functions of disease risk genes.** With this in mind, the first aim of the present investigation is to characterise the CTX0E16 hNPC line to determine whether a well defined neuralisation protocol that favours the production of glutamatergic neurons from ESCs and other immortalised cells will have similar results in this line. In particular, this study will examine key cellular phenotypes of neurons that have been previously observed in other immortalised ESC, NSC and NPC studies by assessing markers of cell fate, neuronal morphology, functional responses, synaptic expression and electrophysiological characteristics in these cells. These investigations will therefore demonstrate the

CTX0E16 NPC line as a valuable platform from which studies of the mechanisms of human cortical development and disease can be carried out.

Previous research has suggested that ZNF804A acts as a transcription factor that mediates the expression of genes coding for proteins involved in neurite outgrowth and synapse formation and maintenance (Chen et al., 2015; Hill et al., 2011). In addition to this, while early studies suggested this protein was localised to the nucleus, subsequent investigations have demonstrated extra-nuclear expression though the precise distribution of ZNF804A at the subcellular level is currently unresolved (Girgenti et al., 2012; Tao et al., 2014). Finally, expression of ZNF804A is thought to be high during early fetal development and a psychosis-associated genetic variant at the *ZNF804A* locus is known to reduce mRNA expression at this point, suggesting a role for this protein in neural development (Hill and Bray, 2012; Tao et al., 2014). Therefore, **I hypothesise that ZNF80A plays a role in early neural development and is critical in the formation of neuron morphology; that it is expressed outwith the nucleus and along the dendrites of developing and mature cortical neurons; and that it plays a role in the maintenance of dendritic spines.** I aim to investigate these characteristics of ZNF804A using a combinatorial approach integrating multiple cellular models including neurons derived from CTX0E16 NPCs, hiPSCs and rat primary cortical neuron cultures, investigating the expression and localisation of these proteins as well as evaluating the impact of manipulations of ZNF804A on the morphological characteristics of these cells. These experiments will thus provide a more thorough understanding of the functions of this protein and moreover, its potential impact in the etiology of psychiatric disease.

CHAPTER 2: MATERIALS AND METHODS

2.1 CELL CULTURE

2.1.1 PROLIFERATIVE CTX0E16 CELLS

Use of the CTX0E16 cell line was kindly granted by ReNeuron Group plc. (Guildford, UK) under a Material Transfer Agreement. The CTX0E16 cell line is a conditionally immortalised, cortically derived, human neural progenitor cell line. This line was derived from first trimester foetal brain tissue using c-myc^{ER} transgene technology; this transgene was inserted into the genome of the cell line using a pLNCX-2 (Clontech) MMLV retroviral vector. The c-myc^{ER} transgene codes for a protein consisting of a c-myc cell division-promoting region and a modified hormone receptor which responds to binding of a synthetic drug, 4-hydroxytamoxifen (4-OHT) (Pollock et al., 2006). Ectopically expressed within the cell cytoplasm, the monomeric protein undergoes dimerisation upon binding of 4-OHT and subsequently translocates to the nucleus, where the c-myc portion of the protein acts as a transcription factor driving cell proliferation (see **Figure 2.1**).

CTX0E16 hNPCs were maintained in a proliferative state by culturing in Reduced Modified Medium (RMM+++); DMEM:F12 with 15 mM HEPES and sodium bicarbonate (Sigma) supplemented with 0.03% human serum albumin (PAA), 100 μgml^{-1} apo-transferrin (Scipac), 16.2 μgml^{-1} putrescine (Sigma), 5 μgml^{-1} human insulin (Sigma), 60 $ngml^{-1}$ progesterone (Sigma), 2 mM L-glutamine (Sigma) and 40 $ngml^{-1}$ sodium selenite (Sigma)). To maintain proliferation 10 $ngml^{-1}$ human FGF_2 (PeproTec), 20 $ngml^{-1}$ human EGF (PeproTech) and 100 nM 4-OHT (Sigma) were also added to RMM. CTX0E16 hNPCs were seeded onto Poly-D-lysine (PDL, 5 μgcm^{-2}; Sigma) and laminin-coated (1 μgcm^{-2}; Sigma) tissue culture flasks, with full media changes occurring every 2-3 days. Cells were passaged once 70 – 80% confluent using Accutase (Sigma) and maintained for between 25-30 passages; all experiments were carried out using cells from passages 12 to 30.

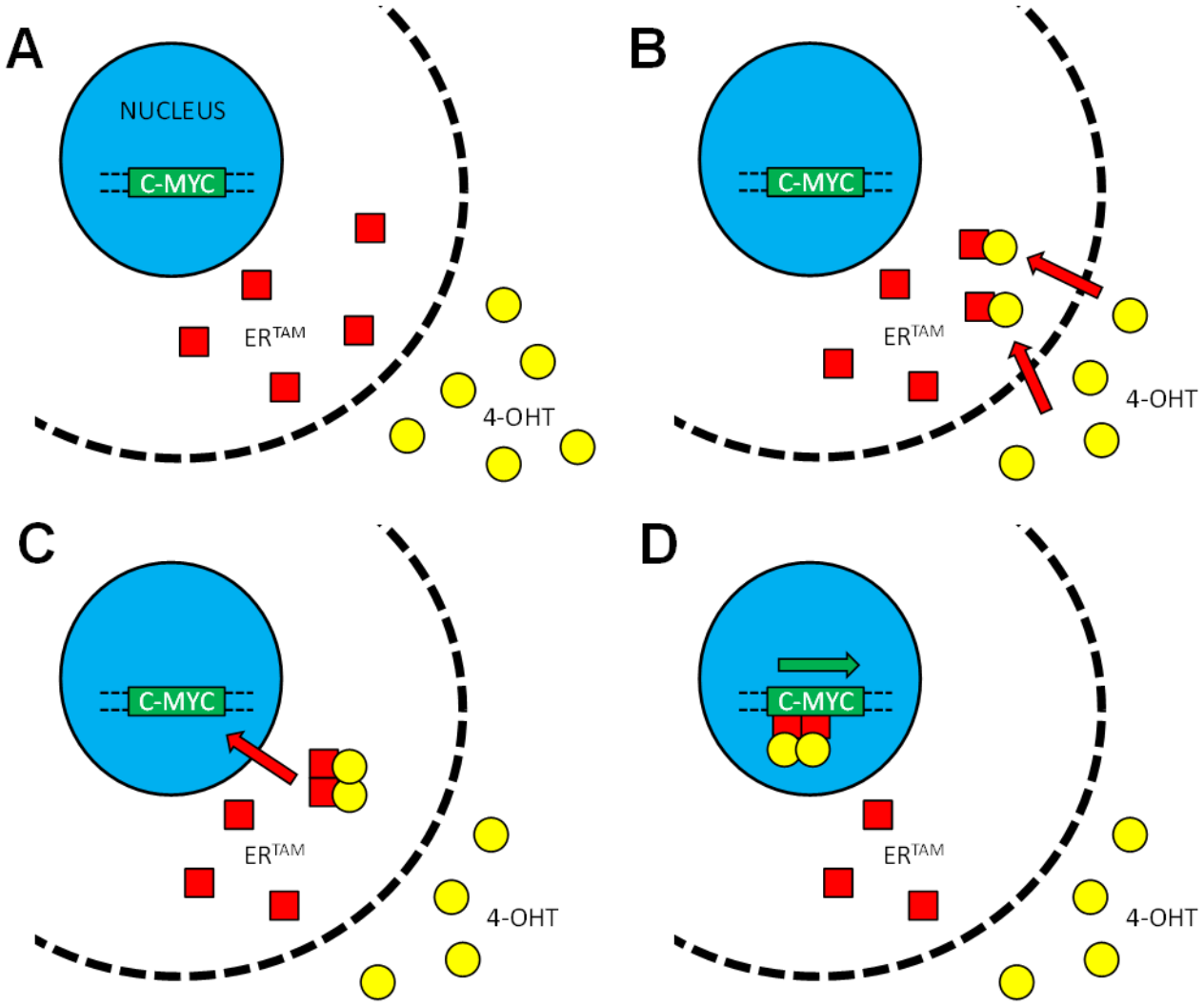

Figure 2.1.1: Schematic of c-myc^{ER} transgene in a CTX0E16 NPC. **A**: The transgene codes for a modified form of the estrogen receptor, which remains in a monomeric form within the cytoplasm when inactive. **B**: 4-OHT diffuses across the cell membrane from the surrounding media, and binds specifically to the monomeric receptor. **C**: Upon binding, the receptor dimerises and translocates to the nucleus. **D**: The dimerised receptor binds to the c-Myc promoter and drives NPC proliferation. Upon removal of 4-OHT from the media, mitosis will cease and the NPC will begin terminal differentiation.

2.1.2 DIFFERENTIATION OF CTX0E16 CELLS

CTX0E16 cultures were maintained under proliferative conditions until 70 – 90% confluent, then washed once with prewarmed RMM+++ and passaged onto Poly-D-lysine (PDL, 5 μgcm^{-2}) and laminin-coated (1 μgcm^{-2}) Nunc tissue culture plastic or No. 1.5 coverglass (The Paul Marienfeld GmbH & Co. KG) at a density of 12,500 cells per ml. Cells were then washed in warm Dulbecco's Phosphate-Buffered Saline (DPBS; Life Technologies) and maintained in Neuronal Differentiation Media (NDM: Neurobasal Medium (Life Technologies) supplemented with 0.03% human serum albumin (PAA), 100 μgml^{-1} apo-

transferrin (Scipac), 16.2 $\mu g ml^{-1}$ putrescine (Sigma), 5 $\mu g ml^{-1}$ human insulin (Sigma), 60 $ng ml^{-1}$ progesterone (Sigma), 2 mM L-glutamine (Sigma), 40 $ng ml^{-1}$ sodium selenite (Sigma) and 1 x B27 serum-free supplement (Life Technologies)). Half medium changes were performed every 2-3 days and cultures were differentiated for up to 61 days (days differentiated (DD) 61).

2.1.3 MOUSE EMBRYONIC FIBROBLASTS

Feeder cultures of Embryomax primary mouse embryo fibroblasts (strain CF1, Millipore) were cultured in MEF media: Advanced DMEM (Sigma) supplemented with Glutamax and Fetal Bovine Serum (FBS) in tissue culture flasks precoated in 0.1% gelatin. Half media changes were performed every 3-4 days and cells were passaged once ~80% confluent with Trypsin to maintain the cultures. MEFs were maintained for up to 5 passages with all experiments being carried out with cells from passages 1-5. In experiments requiring inactivated MEFs, MEF media was aspirated and replaced with fresh media containing 10 $\mu g\ ml^{-1}$ Mitomycin C and incubated for 2 hours at 37°C to arrest mitosis. Flasks of arrested MEFs were washed 3 times with prewarmed PBS before being passaged to generate monolayer support cultures.

2.1.4 HUMAN EMBRYONIC KIDNEY CELLS

Human Embryonic Kidney (HEK293) Cells were cultured in Advanced DMEM supplemented with Glutamax and FBS. HEK293 cells were seeded onto tissue culture flasks, with media changes occurring every 3-4 days. Cells were passaged 70 – 80% confluent using Accutase and maintained for between 10-15 passages; all experiments were carried out using cells from passages 5-20.

2.1.5 HUMAN INDUCED PLURIPOTENT STEM CELLS (HIPSCS)

HiPSCs were generated from keratinocytes of apparently healthy individuals using nonintegrating approaches. Keratinocyte cultures were maintained in Epilife (Invitrogen) supplemented with 10 µM Rock inhibitor (Sigma) on matrigel-coated plastic. 2 $\mu g\ ml^{-1}$ of hexadimethrine bromide was added to the cultures to reduce the charge of the keratinocytes and thus facilitate viral transduction. Cultures were transduced using polycistronic excisable lentiviral vectors expressing the Yamanaka transcription factors (C-MYC, KLF4, OCT4 and SOX-2). Transduced keratinocytes were plated onto monolayers of mitotically arrested MEFs cultured as described previously. These MEF-supported cultures were maintained for 4-5 days and passaged onto fresh MEF monolayers. Epilife media was

gradually replaced with Knock out serum replacement (KOSR) media (ThermoFisher) from day 10 to day 14 of transduction. These cultures were maintained until the emergence of hiPSC colonies, which were picked and transferred to fresh wells containing mTeSR supplemented with 10 µM Rock inhibitor. Full medium changes were performed every day until proceeding to neuralisation at day 16 following transduction.

HiPSCs were differentiated into neurons using an established protocol that favors the generation of cortical forebrain neurons (Cocks et al., 2014; Shum et al., 2015). Neuronal differentiation of hiPSCs was by achieved by the addition of N2- and B27-containing medium supplemented with 5 µg ml^{-1} insulin, 1 mM l-glutamine, 100 µM non-essential amino acids, 100 µM 2-mercaptoethanol and SMAD inhibitors 1 µM Dorsomorphin (Sigma) and 10 µM SB431542 (Cambridge Bioscience). HiPSCs adopted an NPC fate at day 8 of neuralisation, at which point SMAD inhibitors were withdrawn from the culture medium. HiPSC-derived NPCs were continually passaged and maintained in this medium until day 23 of neural induction. Terminal differentiation (day 23) was achieved by culturing plated NPCs with medium containing Neurobasal + B27 and supplemented with 10 µM DAPT for 5 days (day 30); hiPSC-neurons were grown in Neurobasal + B27 medium up to day 35 (see figure 2.1.2 for a schematic of the hiPSC transduction and neuralisation timelines).

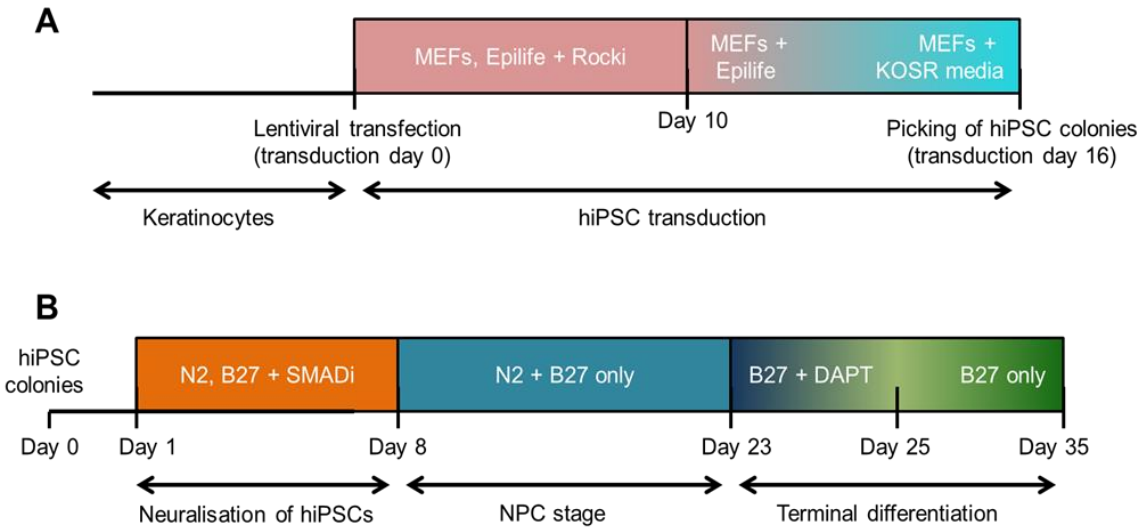

Figure 2.1.2: Schematic of hiPSC transduction and neuralisation timeline. **A**: Days 0-16 of transduction from keratinocyte cultures to hiPSC colonies. **B**: Days 0-35 of hiPSC neuralisation.

2.1.6 RAT PRIMARY CORTICAL NEURONS

Dissociated high-density cultures of primary cortical neurons were prepared from the dissected cortices of E18 Sprague-Dawley rat embryos, plated on glass coverslips coated in PDL (0.2 $mgml^{-1}$) at a density of 3 x 10^5 cells per well and cultured in Neurobasal media (Life Technologies) containing 2% B27 supplement, 1% penicillin/streptomycin and 0.5 mM glutamine. On day in vitro (DIV) 4, 200 µM of APV, an NMDA receptor inhibitor (also known as AP-5) (Tocris) was introduced to the feeding medium until DIV21 in order to reduce cell death arising from excitotoxicity. Half media changes were performed twice a week until fixation.

2.2 GENOME EDITING OF CTX0E16 CELLS

2.2.1 NUCLEOFECTION

A flask of proliferative CTX0E16 cells at 80% confluency was nucleofected using Custom CompoZr Zinc Finger Nucleases (ZFNs) designed to excise the full length ZNF804A gene from the CTX0E16 genome. Cells were initially detached from the flask using acutase before being spun down at 200g for 5 minutes and washed twice with 20ml of prewarmed HBSS. Cells were then resuspended in 400ul of Nucleofection Solution V (Lonza) containing the appropriate supplement according to the manufacturer's instructions. 100 µl of this solution was then added to each of four tubes containing either 2.5 µg of a GFP control plasmid, 5 µl of the supplied ZFN mRNA, 2.5 µg of a 1:1 mix of the two supplied ZFN DNA plasmids or a blank control. These mixtures were transferred to 2 mm electroporation cuvettes and nucleofected on a nucleofector using programme T-030. Immediately following nucleofection these mixtures were transferred to each of four wells in a 6 well Nunc tissue culture plate precoated with PDL and laminin (as described in **Section 2.1.1**) and containing 2ml of prewarmed RMM+++. These were then coldshocked to increase the efficiency of nucleofection (as described in Doyon et al., 2010) by incubation at 30°C for 3 days, changing media at day 1 and day 3 to remove dead cells before returning cells to 37°C. Cultures were then grown as normal until confluent, and during passaging half of cells were retained for continuation of the cell line with the other half being used to assess nucleofection efficiency via CEL-1 assay.

2.2.2 CEL-1 ASSAY

Chromosomal DNA was prepared from the harvested cells by adding Lysis Solution for Blood (Sigma) and incubated at 75°C for 15 minutes. Neutralisation Solution for Blood (Sigma) was added and the solution was mixed to neutralise the lysis buffer. The concentration of the chromosomal DNA in each sample was quantified using a DNA spectrophotometer and an RT-PCR was performed on the samples using the primers provided with the ZFN kit in order to determine the efficiency of the knockout in the nucleofected cells (see RT-PCR section for full protocol).

2.2.3 DILUTION CLONING

To establish a pure population of ZNF804A knockout CTX0E16 cells, the nucleofected cultures were plated on PDL and laminin-coated terasaki plates at a density of 1-5 cells per well. Two hours prior to passaging an apoptosis inhibitor (Y-27632, Cambridge Biosciences) was added to the RMM+++ culture media at a final concentration of 10µM; cells were maintained in this media until confluent. Individual wells were then passaged and plated onto PDL and laminin-coated 24 well Nunc cell culture plates containing a monolayer of mitotically arrested mouse embryonic fibroblasts (MEFs). These individual cultures were subsequently expanded and retested for the efficiency of knockout using the CEL-1 assay.

2.2.4 EXPANDING NUCLEOFECTED POPULATIONS

MEFs were employed to aid the growth of very small populations of CTX0E16 cells (1-5 cells). Flasks of arrested MEFs were washed 3 times with prewarmed PBS, trypsinised and the detached cells were spun down. The cells were then resuspended in fresh MEF media and plated on 24 well Nunc tissue culture plates precoated in 0.1% gelatine at a density of 50,000 cells per well. Whole media changes were performed the following day to RMM+++ supplemented with Y-27632 in preparation for seeding of the nucleofected CTX0E16 populations. Mitotically arrested MEFs do not survive subsequent passages after the initial plating; this permits a pure population of nucleofected CTX0E16 cells to be isolated from the cultures once the initial expansion from a small population of cells is complete.

2.3 TRANSFECTION

2.3.1 LIPOFECTAMINE TRANSFECTION

CTX0E16 cells, HEK293 cells, hiPSC-derived neurons and rat primary cortical neurons were transfected at the desired age using Lipofectamine 2000 (Life Technologies) using a modified form of the manufacturer's protocol, where Optimem was substituted for DMEM (Srivastava et al., 2011). An assay-determined concentration of the desired plasmid was mixed with Lipofectamine 2000 in DMEM pH balanced using HEPES and incubated for 20 minutes in a humidified atmosphere of 95% air/5% CO2 at 37°C with open caps. The DNA:Lipofectamine 2000 mixture was added dropwise to the cells to be transfected, and cells were incubated for 4 hours (CTX0E16 or hiPSC cells) or overnight (HEK293 cells or rat primary cortical neurons) at 37°C, before being transferred to new wells containing fresh media to enhance viability. Transfections were allowed to proceed for 1 or 2 days before either treatment or fixation and subsequent immunocytochemistry.

2.3.2 VIRAL TRANSFECTION

DD28 CTX0E16 neurons were treated with a recombinant AAV vector driving eGFP expression under the control of a CamKII promoter at a concentration of $5.23x10^{10}$ GC/ml (AAV1.CamK110.4.eGFP.WPRE.rBG, Penn Vector Core). Neurons were fixed, immunostained and imaged 7 days later (see **Section 2.7** for immunocytochemistry and imaging protocols).

2.4 SIRNA SILENCING OF ZNF804A AND ZFP804A

2.4.1 N-TER TRANSFECTION

CTX0E16 cells, hiPSC-derived NPCs and rat primary cortical neurons were transfected using the N-TER Nanoparticle siRNA Transfection System. SiRNAs targeting full length ZNF804a mRNA sequence at exon 4 (siRNA#1, Thermo Fisher: HSS150612) and exon 2 (siRNA#2, Thermo Fisher: HSS150613) (see **Table 2.2** and Hill et al., 2011) were used along with Stealth RNAi siRNA negative control med GC duplex (Invitrogen: 465372) that has no significant sequence similarity to human or rat gene sequences. These siRNAs have been previously validated in a sister cell line to the CTX0E16 NPCs, CTX0E03 (Hill et al., 2011). Cells were transfected with both siRNAs (hiPSC-neurons and CTX0E16 neurons) or siRNA#2 only (rat primary cortical neurons) using the N-Ter Nanoparticle siRNA Transfection System (Sigma: N2913) at DD0 (CTX0E16 cells), DD23 (hiPSC-derived neurons) and

DIV21 (rat neurons) in accordance to manufacturer's instructions, along with an N-Ter only blank control condition. Rat primary cortical neurons were SiRNAs in dilution buffer were mixed with N-TER transfection reagent, vortexed, incubated at room temperature in a darkened container for 20 minutes and added to the appropriate culture media. Cells were then washed with prewarmed HBSS or culture media before adding the media containing the siRNA transfection reagents. In the case of CTX0E16 and hiPSC-derived neurons, cells were differentiated for 7 days, with a half media change occurring at day 4. Cells were assessed for transfection efficiency in the fluorescent control condition the day after transfection; all other conditions were fixed or harvested at day 7 of differentiation. In the case of the rat primary cortical neurons, cells remained in the siRNA media for 5 days after which they were processed for western blotting. Rat neurons were transfected with GFP under the control of a synapsin 1 promotor (synGFP) three days after siRNA transfection using Lipofectamine 2000 (see **Section 2.3.1** above), double fixed at day 5 and processed for immunocytochemistry.

2.4.2 TRANSFECTION EFFICIENCY

Transfection efficiency in all three cellular systems was assessed the day following siRNA transfection via live cell imaging using an inverted epifluorescence microscope with a 10x objective and manually performing cell counts of the number of cells expressing the fluorescent oligonucleotide relative to the total number of cells using the multi-point tool in ImageJ, with 3-5 FOV being imaged per well. In each cellular system three independent experiments were carried out, with two technical replicates per biological replicate for each experimental condition.

2.5 COLLECTION OF CELL LYSATES AND WESTERN BLOTTING

2.5.1 CELL LYSATES

To collect protein samples, cells grown on 6 well Nunc plates were washed once with PBS and lysed with 150 µl of lysis buffer (see **Table 2.4**) containing the protease inhibitors 4-(2-Aminoethyl) benzenesulfonyl fluoride hydrochloride (AEBSF), leupeptin, pepstatin A, phosphatase inhibitor cocktail 3 (Sigma), aprotinin and NaF. Protein samples were sonicated and spun at 15,000 rpm at 4°C for 15 minutes to disrupt cell membranes. Supernatants were collected and the protein concentration of each sample was assessed using a BSA protein assay kit (Biorad).

2.5.2 SYNAPTOSOMAL PREPARATIONS

Neurons treated were collected in ice cold RIPA buffer (75 µl/well): 10mM Tris pH 7.2; 150 mM NaCl; 1% Triton x-100; 0.1% SDS; 1% Deoxycholate and 5mM EDTA pH8 containing protease and phosphatase inhibitors. Samples collected were sonicated with 2 pulses every few second for a total of approximately 8 to 10 pulses on ice, left on ice for 30 min and finally centrifuged at 15'000 rpm for 15 min at 4°C**.** Neurons processed for crude synaptosomal preparation were collected at DIV25 in ice cold homogenisation buffer (300 µL/well): 320mM sucrose; 5mM Na4P2O7; 1mM EDTA; 10mM HEPES pH7.4 with freshly added protease and phosphatase inhibitors. Homogenates were centrifuged at 2000 rpm for 5 min at 4°C to obtain the P1 (nuclear) and S1 (extra-nuclear) fractions. 100ul was removed from the S1 fraction and centrifuged at 13,000 rpm for 15 min at 4°C to obtain the P2 (crude synaptosome) and S2 (crude cytosol) fractions. P2 was dissolved in 300 µl homogenisation buffer.

2.5.3 WESTERN BLOTTING

For western blotting, samples (either cell lysates or synaptosomal preparations) were then mixed with 2x lamelli sample buffer in a 1:1 ratio; protein samples were then run on a 4% polyacrylamide gel (Biorad) for one hour at 110 mV to separate proteins according to size via electrophoresis. Proteins were then electrophoretically transferred to a polyvinylidine fluoride (PVDF) membrane at 100 mV for one hour at 4°C. Membranes were stained using Ponceau solution to assess the efficacy of protein transfer, before being washed twice in TBS-T (see **Table 2.4** for composition), blocked for one hour in 5% BSA in TBS-T and incubated with primary antibody (see **Table 2.1**) in 5% BSA TBS-T overnight at 4°C on a rocker (unless otherwise indicated). Membranes were then washed a further 3 times with TBS-T before being incubated with secondary antibody (see **Table 2.1**) in 5% BSA TBS-T for one hour at room temperature then washed in TBS-T a final 3 times. Finally, membranes were incubated in Pierce ECL Western Blotting Substrate (Thermo Scientific) for five minutes and then developed and processed for detection using exposure films in a dark room for varying exposure times. For the purposes of quantification, staining intensities were normalised against a β-Actin staining control to account for variations in overall protein concentration for each sample.

2.6 RNA PREPARATION, CDNA SYNTHESIS, RT-PCR AND Q-PCR

2.6.1 RNA EXTRACTION AND CDNA SYNTHESIS

Proliferative and differentiated CTX0E16 cells and hiPSC-derived neurons were pelleted and lysed using TRIzol reagent (Life Technologies) and total RNA extracted according to the manufacturer's instructions. Each sample was lysed in 500 µl of TRIzol, frozen and stored immediately at -80°C. For RNA extraction, pellets were thawed at RT and left on ice for 5 minutes. 200 µl of 1-bromo-3-chloropropane was added to each sample and the resulting mixture was spun at 20,000 rpm at 4°C for 15 minutes. Supernatants were extracted and added to 500 µl of isopropanol to precipitate the RNA, and spun down as before. RNA pellets were washed twice with 70% ethanol and a final time with 100% ethanol, and dissolved in 20 µl of nuclease-free water. Residual genomic DNA was removed from each replicate using the TURBO DNA-*free*™ Kit (Life Technologies) according to published protocols. RNA concentrations were then measured in the purified samples using a NanoDrop ND1000 spectrophotometer (Thermo Scientific). CDNA was synthesised from 750 ng of total RNA from each extraction using random hexamers and SuperScript III (Life Technologies), according to the manufacturer's instructions.

2.6.2 RT-PCR

To determine the expression of specific genes, primer sequences from previously established amplicons were designed to target all known RefSeq transcripts of genes of interest, sourced from the UCSC Genome Browser website (http://genome.ucsc.edu) (see **Table 2.3**). Primer pairs producing amplicons of 80-120 bp were chosen to ensure compatibility with q-PCR experiments. Reactions were carried out in a total volume of 20 µl containing diluted cDNA, 1 X HOT FIREPol Blend Master Mix (Solis Biodyne) and primers at 200 nM, using a GS4 thermal cycler. Samples were separated and visualised via polyacrylamide gel electrophoresis.

2.6.3 Q-PCR

For quantitative expression analysis, 20 µl cDNA samples from SuperScript III reactions were diluted with a further 100 µl of nuclease-free H_2O. Reactions were carried out in a total volume of 20 µl, containing diluted cDNA, 1× HOT FIREPol® EvaGreen® q-PCR Mix (Solis Biodyne) and primers at 200 nM, using an MJ Research Chromo 4 (Bio-Rad) and MJ Opticon Monitor analytic software (Bio-Rad).

Triplicate q-PCR reactions were performed and averaged to measure each gene in each cDNA sample. For samples taken from siRNA knockdown experiments, normalised q-PCR target gene expression values were compared between siRNA-treated conditions and control conditions. Mean measures of target genes were normalised against a geometric mean determined from 3 control housekeeping genes for each cDNA sample to yield a relative target gene expression value for all samples. The Pfaffl method was used to calculate the relative difference in the normalised expression values of full-length ZNF804A across experimental conditions. In this method, the real time PCR efficiency calculated by the Opticon Monitor analytic software is used to control for any differences in reaction efficiency across samples which may over- or underestimate the relative expression of the target gene (Pfaffl, 2001). Housekeeping genes for CTX0E16 samples were identified as suitable internal controls on the basis of previously conducted whole-genome microarray data of CTX0E16 cells, where they showed the least variability (in terms of standard deviation) across conditions (Anderson et al., 2015). The amplification efficiency of each set of primers was also measured using a standard curve constructed by serial dilution of pooled cDNA from all assayed samples; only primer sets with efficiencies between 1.8 and 2.2 were used in order to ensure reproducibility of results. An efficiency value outside of these parameters indicates either an inefficient amplification reaction, or the amplification of non-specific products. A Kruskall-Wallis test with posthoc Dunn's multiple comparisons test was performed on the normalised q-PCR data for relative expression of the full length ZNF804A transcript using Graphpad Prism.

For assessments of relative gene expression in the CTX0E16 line in **Chapter 4**, the CT values for each gene was measured against a standard curve constructed by serial dilution of pooled cDNA from all assayed samples. A relative value was thus obtained for each of the three triplicate reactions for each cDNA sample. Mean measures of target genes were then normalised against a geometric mean determined from three internal control genes (GAPDH, HPRT1 and RPL13A) for each cDNA sample to yield a relative target gene expression value for all samples. These control genes were identified on the basis of previous whole-genome microarray data of CTX0E16 cells as described above. Normalised q-PCR target gene expression values were compared between proliferative (DD 0) or DD28 CTX0E16 cells. Student's paired t tests were performed on the normalised q-PCR data for expression of each mRNA transcript in DD0 and DD28 cells using Graphpad Prism.

To determine relative expression values of ZNF804A transcripts in each cell line, normalised q-PCR target gene expression values were compared between proliferative (DD0) and DD28 CTX0E16 cells, or between hiPSC-derived NPCS and DD35 hiPSC-neurons. Calculations of relative mRNA expression in these experiments were carried out using the $2^{\wedge -dCT}$ method (Livak and Schmittgen, 2001), as all probes showed similar PCR efficiencies (average efficiency ± SD: 1.95 ± 0.10 for CTX0E16 and 1.87 ± 0.09 for probes for hiPSC-derived cells). dCT was calculated by dividing the difference between the average CT of the target transcripts in each maturation stage by the geometric mean from the best housekeepers for each cell line. A Kruskall-Wallis test with posthoc Dunn's multiple comparisons test was performed on the normalised q-PCR data for relative expression of the full length ZNF804A transcript using Graphpad Prism.

2.7 IMMUNOCYTOCHEMISTRY AND MICROSCOPY

2.7.1 IMMUNOCYTOCHEMISTRY

Prior to fixing, cells were washed once in warm PBS. Cells were then fixed in either 4% formaldehyde/4% sucrose in PBS at room temperature for 10 minutes, or in 4% formaldehyde/4% sucrose in PBS at room temperature for 10 minutes followed by two washes with PBS and incubation with pre-chilled (-20°C) methanol for 10 minutes 4°C. Methanol fixation was used to unmask proteins in lipid rich structures, such as the post-synaptic density (Glynn and McAllister, 2006). Cells were washed a further two times in PBS; where indicated, 50 mM of ammonium hydrochloride was added to the second of these washes to quench autofluorescence. Cells were blocked in PBS containing 2% normal animal serum (NAS; either goat or donkey serum being used depending on the antibody) with 0.1% Triton X-100 (Sigma) for two hours at room temperature. Primary antibodies were added in PBS containing 2% NAS overnight at 4°C, followed by 3 x 15 minute washes in PBS. Cells were then incubated for a further hour in 2% NAS, before incubation with Alexa, 488, 568 or 633 secondary antibody (Life Technologies) diluted in PBS with 2% NAS for one hour at room temperature. Two further washes (15 minutes each) were performed before coverslips were washed once with PBS containing 0.1% DAPI, and then mounted using ProLong antifade reagent (Life Technologies). A list of antibodies used in this study can be found in **Table 2.1**.

2.7.2 IMAGING OF ZFP804A IN MOUSE CORTICAL SECTIONS

For *in vivo* assessment of Zfp804A expression in the mouse cortex, mice were anesthetised with sodium pentobarbital at 50 mg per gram of body weight, and fixed by transcardial perfusion of 4% paraformaldehyde in 0.1 M sodium phosphate buffer (pH 7.4) at postnatal day 28 (P28). Brains were dissected out and sectioned into 50 mm coronal sections and immunostained with DAPI and a mouse anti-bassoon and a rabbit anti-ZNF804A (C2C3) antibody (see **Table 2.1**) as floating sections, before being mounted onto glass slides and covered with glass coverslips. Cells exhibiting Zfp804A staining were imaged by taking 1 mm serial optical sections, 35–45 optical sections per cell, using a Leica confocal microscope with a 40x objective (N.A. 1.3). Following acquisition, images were Z-projected and background subtracted using Metamorph. 3-4 images were taken of each cortical slice.

2.7.2 EPILUORESCENCE AND CONFOCAL MICROSCOPY

For epifluorescent imaging, representative images were taken on a Zeiss Axio Imager Z1, equipped with an ApoTome and an AxioCam MR3 camera running AxioVision 4.7.1 imaging software (Carl Zeiss). Images were acquired using 10x, 20x and 40x objectives (N.A. 0.3, 0.8 and 0.75 respectively). Images of double and triple labelled neurons were also obtained using a Leica SP5 confocal microscope with 40x, 63x or 100x oil-immersion objectives (N.A. 1.25, 1.4 and 1.4 respectively). Images were taken as a Z-series (Z-step = 0.5 µm for 40x images; 0.35 µm for 63x and 100x images). All epifluorescence images were exported to ImageJ (http://imagej.nih.gov/ij/) where maximum intensity projections and background subtracted images were generated (Srivastava et al., 2011). All confocal images were processed using MetaMorph software (Universal Imaging Corporation); Z-projections and background subtraction (via a statistical correction) were generated using a journal. In the green/purple and the green/red color schemes, colocalisation is indicated by white. Images were taken in the linear range, to allow an accurate representation. Some channels are shown individually in grey scale, or were pseudocoloured to emphasise areas of high staining intensity. Scale bars are described for each individual figure panel within figure legends.

2.7.3 STRUCTURED ILLUMINATION MICROSCOPY

SIM imaging was carried out on primary rat cortical neurons transfected with GFP and co-immunostained for ZNF804A (Genetex, C2C3) and either PSD-95 or GluN1. Images were acquired

with a Nikon N-SIM super-resolution microscope. Acquisition was performed in a 3D SIM mode using the 100X N.A. 1.49TIRF objective lens with 13-25 z-steps per stack at a step interval of 0.12 µm. Raw images were acquired on an Andor DU897 EMCCD camera at 512 x 512 pixels (62 nm pixel size in the image). Reconstructed images are displayed with 1024 x 1024 pixels (32 nm pixel size in the image). Image reconstructions were performed with Nikon N-SIM software. Final images, including z-projections and brightness and contrast adjustments were reconstructed in ImageJ and MetaMorph.

2.7.4 ANALYSIS OF CELL IDENTITY MARKERS

Cell counts were performed using images acquired with either a Zeiss Axioimager or Olympus IX70 with a 20x objective (N.A. 0.8), with at least four fields of view (FOV) imaged per biological replicate per condition. Three biological replicates were imaged for each staining condition at each of the time points assessed, with 1-2 technical replicates for each. Z-stacks of 4 slices at 1 µm between each slice were Z-projected and the resulting projections were background subtracted. In all conditions, the DAPI channel was thresholded and regions of interest (ROI) were created around each nucleus and used to assess expression of MAP2 along with the various markers of cell identity via the average intensity of each area in the respective channels. The percentage of cells expressing each marker in each biological replicate was calculated relative to the total number of cells (DAPI positive cells) and the number of MAP2-positive cells. These percentages for each biological replicate were then averaged and the standard errors calculated. All image processing for the quantification of cell counts was performed using ImageJ, and all subsequent analysis of this data was performed using Microsoft Excel.

2.7.5 ANALYSIS OF PUNCTA COLOCALISATION

Z-projected and background subtracted confocal stacks were acquired for DD28 CTX0E16 cultures, DD35 hiPSC-neurons and DIV25 rat primary cortical cultures stained for MAP2, ZNF804A/Zfp804a and the postsynaptic markers PSD-95 or GluN1. For CTX0E16 and hiPSC-derived neurons, images in the ZNF804A and synaptic protein staining channels were thresholded and particle analysis was performed on 50 µm sections of MAP2-positive dendrites. Regions of interest were generated around the subsequent synaptic or ZNF804A-positive puncta, and average staining intensity for all other channels was measured within these regions. For rat primary cortical neurons, dendritic spines along 50 µm sections of dendrite were traced using MetaMorph software. Regions of interest were generated around each spine, and staining intensity of ZNF804A and synaptic markers was

recorded. Expression of a given protein within a region of interest was determined by whether staining intensity was greater than 20% of the maximum staining intensity recorded for all regions; this threshold was determined via qualitative assessment of the staining intensity of puncta deemed to be colocalising with other proteins.

2.7.6 QUANTITATIVE ANALYSIS OF SPINE MORPHOLOGIES AND IMMUNOFLUORESCENCE

Confocal images of double-stained neurons were acquired with a Leica SP-5 confocal microscope using a 63x objective as a z-series as described previously. Two-dimensional maximum projection reconstructions of images were generated and morphometric analysis (spine number, area and breadth) was conducted using MetaMorph software (Srivastava et al., 2011). Morphometric analysis was performed on spines from at least two dendrites (secondary or tertiary branches), totaling 100 µm, from each neuron. Linear density and total gray value of each synaptic protein cluster was measured automatically using MetaMorph (Srivastava et al., 2011). Cultures directly compared were stained simultaneously and imaged with the same acquisition parameters. For each condition, 9-12 neurons from at least 3 separate experiments were used. Experiments were carried out blind to condition and on sister cultures.

2.7.7 RELATIVE EXPRESSION OF ZNF804A

To determine the relative subcellular expression of ZNF804A using immunocytochemistry, DD0 and DD28 CTX0E16 cultures were fixed, immunostained for ZNF804A and βIII-Tubulin and imaged using confocal microscopy with a 63x objective as described previously. 3-5 fields of view per technical replicate were imaged, with 1-2 technical replicates per biological replicate and 3 biological replicates overall being sampled. Regions of interest were traced around DAPI-positive cell nuclei as well as the cytoplasm of each cell used in analysis using ImageJ. Regions of interest were transferred to the ZNF804A staining channel and average staining intensities were measured for each ROI. For each cell, relative expression of ZNF804A in both the nuclear and cytoplasmic regions was normalised to an overall expression value for the whole cell. Values were averaged within each technical replicate and for all technical replicates within each biological replicate. Averages for each subcellular compartment were calculated for both DD0 and DD28 CTX0E16 cells.

2.8 CALCIUM IMAGING

For experiments assessing the responsiveness of CTX0E16 cells to treatment with neurotransmitter ligands, cells were differentiated to DD28 on PDL (5 µg/ml) and laminin- coated (1 µg/cm2) glass coverslips, then incubated with HEPES-buffered physiological saline solution (140 mM NaCl, 5 mM KCl, 2 mM CaCl2,1 mM MgCl2,10mM HEPES and 10 mM glucose, buffered to pH 7.4 using 5 M NaOH) supplemented with 2.5 µM Fura-2AM and 1 mM probenecid (loading buffer) at 37°C for 60 minutes. This solution was then replaced with assay buffer (loading buffer minus Fura-2 AM and probenecid). Images of groups of cells were taken every 2 seconds using fluorescence microscopy with a 10x objective. Fluorescent signal was detected at the 520 nm emission wavelength following excitation at 340 and 380 nm using a microscope-based imaging system (Photon Technology International). Each experiment began with 2 minutes of baseline readings to allow cells to settle before the addition of the neurotransmitter ligand (dopamine, glutamate or acetylcholine; Sigma) at 1 mM, diluted in HEPES-buffered physiological saline solution. Cells were exposed to these compounds for one minute. Image analysis of individual cells by emission intensity ratios from 340 nm/380 nm excitation were performed using ImageMaster software (Photon Technology International).

To investigate spontaneous Ca^{2+} transients in CTX0E16 neurons, cells were differentiated for 42 days on coverslips, then loaded with 2 µM Fluo-4-AM dye (Life Technologies, Paisley, UK) in HEPES-buffered physiological saline solution (140 mM NaCl, 5 mM KCl, 2 mM CaCl2,1 mM MgCl2, 10 mM HEPES, 10 mM glucose and buffered to pH 7.4 using 5 M NaOH) supplemented with 0.02% Pluronic-F27 (Life Technologies) for 15 minutes at 37 °C. This was followed by washing in HEPES-buffered physiological saline solution for a further 15 minutes at 37 °C. Fluo-4 fluorescence was time-lapse-recorded at 1 second intervals with MetaMorph (Molecular Devices) on an Axiovert S100 microscope (Carl Zeiss) equipped with appropriate filter sets (Chroma Technology), with a 40x (N.A. 1.3) PlanNeofluar objective (Carl Zeiss) and a Photometrics Cascade-II 512B EMCCD. KCl (50 mM) and Tetrodotoxin (TTX; 1 µM), were diluted in HEPES-buffer and added to cells to give the final concentration. In all experiments, 10 µM ionomycin was added as a second stimulation for the dye loading control. Offline analysis of the intensity pattern of the Fluo-4 signal was performed in ImageJ. ROI were drawn around the soma of cells with clear dendritic processes. Spontaneous activity was categorised when at least one clear neuronal Ca^{2+} event was detected on an individual soma. Neuronal

calcium events were defined as a sharp transient increase in fluorescence intensity: Fluo-4, ΔF/F0 >5%, with a fast riseand slower decay.

2.9 ELECTROPHYSIOLOGY

Electrophysiological recordings were obtained from CTX0E16 neurons, differentiated for between 29 and 61 days. Patch pipettes (4-7.5 MΩ) were pulled from borosilicate glass capillary tubes using a P97 Flaming/Brown Micropipette Puller (Sutter Instruments). The internal patch solution contained (in mM): 135 KGluconate, 10 KCl, 1 $MgCl_2$, 10 HEPES, 2 Na_2-ATP and 0.4 Na_3-GTP. All recordings were conducted at room temperature. The external recording solution contained (in mM): 139 NaCl, 2.5 KCl, 10 HEPES, 10 Glucose, 2 $CaCl_2$, 1.3 $MgCl_2$. For recordings in older cells (DD55-DD61) electrophysiological recordings were conducted in neuronal differentiation medium. Whole cell voltage clamp recordings were conducted at a holding potential of -70mV in order to monitor predominantly α-amino-3-hydroxy-5-methyl-4-isoxazolepropionic acid (AMPA) receptor mediated spontaneous excitatory post synaptic currents (EPSCs) and at +40 mV to monitor EPSCs mediated by N-methyl-D-aspartate (NMDA) receptors. A stable access resistance was maintained between 20-35 MΩ for the duration of these recordings with no series resistance compensation. In some cases, tight-seal cell-attached recordings were conducted in order to monitor spontaneous action potential firing. In all experiments, corrections were made for liquid junction potentials offline. Data was generated and acquired using an EPC10 amplifier (Heka Instruments) and the software PatchMaster. Data was sampled at 15 kHz and filtered at 3 kHz.

2.10 NEURONAL TREATMENT; CHRONIC NEURONAL DEPOLARISATION

Differentiation day (DD) 13 CTX0E16 neurons were transfected with eGFP using Lipofectamine 2000 as described previously. At DD15, media was replaced with warm experimental media for each of the three experimental conditions: NDM supplemented with pure water, NDM supplemented with 30 mM NaCl as an osmotic control or NDM supplemented with 30 mM KCl. Following 7 hours of exposure to the experimental media cultures were fixed and immunostained. Cells were imaged using a Zeiss fluorescence microscope with a 63x objective (N.A. 1.4) as described previously. Only cells with a neuronal morphology and more than one neurite were imaged for the purpose of assessing neurite length. 3-12 cells were imaged per condition per biological replicate, and 6 experiments were carried

out in total. Images were processed using ImageJ and neurites were traced using the NeuronJ plugin. Imaging and neurite tracing was carried out with the experimenter blinded to experimental condition.

2.11 TREATMENT OF RAT PRIMARY CORTICAL NEURONS WITH CLTP

Rat primary cortical neuron cultures were plated and cultured as described in **Section 2.1.6** until DIV25, then treated with ACSF supplemented with APV or ACSF supplemented with 10 µM glycine, 100mM picrotoxin and 1 µM strychnine (inducing chemical LTP (cLTP)) (Xie et al., 2007) 30 minutes prior to fixation. Cultures were then double fixed in 4% FA and methanol and immunostained for DAPI, Genetex ZNF804A/Zfp804A and PSD-95 as a marker of mature neuronal cells (see **Table 2.1**). PSD-95-positive neurons were imaged using confocal microscopy with a 100x objective to maximise Zfp804A staining quality. Of these image stacks, a single Z-plane which bisects the nuclei of the neurons to be assessed was selected and background subtracted for further analysis. ROI were then drawn around the nuclei and corresponding cytoplasmic regions for each PSD-95-positive neuron in these images and average Zfp804A staining intensity was recorded within each region.

2.12 STATISTICS

For all graphs, bars represent means, and error bars as either standard deviations (S.D.) or standard error mean (S.E.M). To identify differences among means, statistical analyses (Student's unpaired *t*-test, analysis of variance for parametric data, Kruskall-Wallis test for non-parametric data) were performed in either Excel or GraphPad Prism 5. Tukey post hoc analysis was used for multiple comparisons of parametric data, and Dunn's post hoc analysis was used for non-parametric tests.

ANTIBODY	COMPANY	CATALOGUE NO.	DILUTION
chicken α GFP	Abcam	ab13970	1:10000
chicken α MAP2	Abcam	AB104896	1:1000
goat α ZNF804A (D-14)	Santa Cruz	sc-241170	1:200
mouse α Bassoon	Assay Design	SAP7F407	1:300
mouse α CaMKII	Abcam	ab52476	1:500
mouse α GluA2	NeuroMab/Antibody Inc	L21/32	1:500
mouse α GluN1	NeuroMab/Antibody Inc	N308/48	1:500
mouse α GM130	BD Biosciences	610823	1:250
mouse α Nestin	Millipore	MAB5326	1:500
mouse α O4	Sigma	O7139	1:1000
mouse α PSD-95	NeuroMab/Antibody Inc	K28/43	1:1000
mouse α SAP97	NeuroMab/Antibody Inc	K64/15	1:250
mouse α Shank3 (N69/46)	NeuroMab/Antibody Inc	73-109	1:250
mouse α SNAP-25	Synaptic-Systems	111 011	1:1000
mouse α VAMP2	Synaptic-Systems	104 211	1:2000
mouse α VGlut1	Millipore	MAB5502	1:250
mouse α ZNF804A	Millipore	MABN706	1:200
mouse α βIII Tubulin	Millipore	MAB1637	1:1000
rabbit α Ankyrin G	Abcam	ab104896	1:500
rabbit α Calbindin D-28k	SWant	CB-38a	1:20000
rabbit α Calretinin	SWant	7699/4	1:10000
rabbit α Cux1	Santa Cruz	sc-13024	1:500

rabbit α DISC1 (440)	Custom	N/A	1:200
rabbit α Doublecortin	Abcam	ab18723	1:500
rabbit α GABA	Sigma	A2052	1:1000
rabbit α GAD65/67	Millipore	AB1511	1:250
rabbit α Gephyrin	Millipore	AB5725	1:500
rabbit α GluA1	Millipore	AB1504	1:500
rabbit α Glutamate	Sigma	G6642	1:500
rabbit α KI-67	Abcam	ab15580	1:500
rabbit α Neuroligin 3	Santa Cruz	sc-50395	1:250
rabbit α PSD-95	Cell Signalling	25075	1:1000
rabbit α S100β	Dako	M7221	1:500
rabbit α SOX2	Millipore	AB5603	1:100
rabbit α Synapsin-1	Cell Signalling	5297	1:200
rabbit α Tau	Dako	A0024	1:500
rabbit α Tbr1	Abcam	ab31940	1:200
rabbit α VGAT	Millipore	AB5062P	1:300
rabbit α VGlut2	Abcam	ab101756	1:500
rabbit α ZNF804A (C2C3)	Genetex	GTX130124	1:200
rabbit α ZNF804A (C-terminal)	Abcam	ab189630	1:200
rabbit α ZNF804A (N-terminal)	Abcam	ab189630	1:200
rat α CTIP2	Abcam	ab28448	1:500
Milli-Mark™ ChromaPan Neuronal Marker	Millipore	NS420	1:150

Table 2.1: List of antibodies used in immunostaining experiments.

SIRNA ID	ZNF804A SIRNA#	SENSE SEQUENCE
HSS150612	1	CCUAUAGCUGUAAUCCUCUAUGUUU
HSS150613	2	CCAGGAGUUUGACAAUCACAUUAAU

Table 2.2: Sequence of siRNAs against ZNF804A.

	OLIGO SEQUENCE	
	FORWARD (5'-3')	REVERSE (5'-3')
Full length ZNF804A	GAT TTG TCC CCA GTG CTT GT	GCC TCT GGT GGA TGA AAA GA
E3/E4 variant	CAA GCC AAA ATG CGA GAA AAT ATT	CCT TGT CGA GAG GTA AAC ACA ACA
Variant 2.2	GAA TGA GGC AGC ATG CAG TA	TGG GAT CAA AGA CTG GGT TC
HPRT1	TGA CAC TGG CAA AAC AAT GCA	GGT CCT TTT CAC CAG CAA GCT
RPL13A	CCT GGA GGA GAA GAG GAA AGA GA	TTG AGG ACC TCT GTG TAT TTG TC
RPL30	ACA GCA TGC GGA AAA TAC TAC	AAA GGA AAA TTT TGC AGG TTT
SDHA	TGG GAA CAA GAG GGC ATC TG	CCA CCA CTG CAT CAA ATT CAT G
B2M	TAT CCA GCG TAC TCC AAA GA	GAC AAG TCT GAA TGC TCC AC
UBC	ATT TGG GTC GCG GTT CTT G	TGC CTT GAC ATT CTC GAT GGT
GAPDH	ATG GCA AGT TCA AAG GCA CAG TCA	TGG GGG CAT CAG CAG AAG G
GRIN1	AGA TGG CTC TGT CGG TGT G	GTG GGA GTG AAG TGG TCG TT
GRIA2	TTC AGA TGA GAC CCG ACC TC	GCA CAG CTT GCA GTG TTG AT
GRM1	CTA GCT GGC ATC TT	TGA GGC AAT GAT CAC CTG AG

GABRA1	TGG TTA TGA CAA TCG CCT GA	CCG AAA CTG GTG ACG AAG AT
DRD2	ATC TCC TGC CCA CTC CTC TT	TGA CAA TGA AGG GCA CGT AG
CACNA1C	CCT GAG AAT GAG GAC GAA GG	GTT TTC GGT GTT GAC GGA CT
DLG4	TAT CCA GCG TAC TCC AAA GA	GAC AAG TCT GAA TGC TCC AC
CAMK2A	GAG CCA TTC TCA CCA CGA TGC T	TGG TGT TGG TGC TCT CTG AGG A
PPP1R1B	CTA CAC ACC ACC TTC GCT GA	CTG AGG CCT GGT TCT CAT TC
GSK3B	AAA CTA CCA AAT GGG CGA GA	CCG AGC ATG AGG AGG AAT AA
SLC6A4	GTG ATT GGC TAT GCT GTG GA	GGT GTA GGG GAG GAG GAA TG
DLX1	GGA AGG GCT CAG GAG GAA AC	TAG CTT CTT GGT GCG CTG AA
EMX1	CAG GAG AAA CAG GCT AGA CAT AG	CCT GAT TCC CAC CTC TCA ATA C
FOXG1	AGA AGA ACG GCA AGT ACG AGA	TGT TGA GGG ACA GAT TGT GGC
GBX2	GGC AAG GGA AAG ACG AGT CA	GGG TCT TCC TCC TTG TGA GC
ISL1	AAG GAG GAC CGG GCT CTA AT	GGA CTG GCT ACC ATG CTG TT
NKX2.1	GCA AAG AGG ACT CGC TTG TA	AGT GAC AAG TGG GTT ATG TTG A
OTX2	GCA GAG GTC CTA TCC CAT GA	GGT GAT GCA TAG GGG TCA AA
PAX6	TGT CCA ACG GAT GTG TGA GT	TTT CCC AAG CAA AGA TGG AC
TBR1	GTG ATG GGT TTC CCA CTT CT	GGG TGG ATT CTC CTT AGC TAT TT
GAD1	CCA ACA GCC TGG AAG AGA AG	TCG CTG TTT TCA CAG GAA AG

Table 2.3: Primer sequences used in RT- and q-PCR analysis.

SOLUTION	REAGENTS AND CONCENTRATIONS
TBS-T	50 mM Tris, 150 mM NaCl, 0.05% Tween 20
PBS	137mM NaCl, 2.7mM KCl, 10 mM Na2HPO4, 1.8 mM KH2PO4
Lysis Buffer	20mM Tris pH 7.2, 150mM NaCl, 1.0% Triton X-100, 5mM EDTA pH8.
ACSF	125 mM NaCl, 2.5 mM KCl, 26.2 mM NaHCO3,1 mM NaH2PO4, 11 mM Glucose, 5 mM HEPES
Homogenisation buffer	320mM Sucrose, 5mM Sodium pyrophosphate, 1mM EDTA,10mM HEPES pH7.4, 200nM Okadaic Acid, 1mM PMSF, 5mg/ml Aprotinin, 1µg/ml Pepstatin A, 10µg/ml Leupeptin, 1M NaF, 1:100Ser/Thr phosphatase inhibitor cocktail 3

Table 2.4: Composition of solutions.

CHAPTER 3: DIFFERENTIATION OF EXCITATORY CORTICAL NEURONS FROM THE CTX0E16 NPC LINE

3.1 SUMMARY

This chapter describes the characterisation of a conditionally immortalised, cortically derived human NPC line, CTX0E16. CTX0E16 NPCs were assessed for expression of markers of functional and regional identity, as well as the potential to generate neurons following several weeks of differentiation. This chapter also describes the expression of markers of specific neuronal subtype and function in differentiated cultures, and key stages in the development of neuronal morphology in CTX0E16 cells.

3.2 INTRODUCTION

Recent advances in stem cell biology have led to the emergence of several powerful new paradigms for investigating both physiological and pathological processes *in vitro* (Bray et al., 2012). Specifically, the establishment of novel methods for the generation of human neuronal cultures has greatly facilitated our ability to study cellular and molecular mechanisms that may be unique to the human brain. This has provided a particular advantage in research into neuropsychiatric disorders such as schizophrenia, bipolar disorder and autism as these diseases present with several clinical features that can only be observed in humans (Gould and Einat, 2007; Nestler and Hyman, 2010; Powell and Miyakawa, 2006). Several studies have noted alterations in the structure and function of glutamatergic and GABAergic neurons within the prefrontal cortex of patients with these disorders, particularly (Beneyto and Meador-Woodruff, 2008; Harrison, 1999; Howes et al., 2015; Rajkowska et al., 2001; Rao et al., 2012; Stone et al., 2016), a region of the brain that is particularly well developed in humans (Teffer and Semendeferi, 2012). Thus, a system using human cortical neurons may be optimal for modelling the mechanisms underlying these characteristic features. This chapter will focus on the use of hNPCs in particular as a platform for generating neuronal cultures for experimentation.

Recently several clonal hNPC lines have been isolated from first trimester human foetal tissue and conditionally immortalised using retroviral integration of a c-mycER^{TAM} construct (Pollock et al.,

2006; Smith et al., 2011; Stroemer et al., 2009). One such line, CTX0E03, has been generated and subsequently utilised in several studies investigating the efficacy of NPC transplant in treating a rodent-based model of ischaemic stroke (middle cerebral artery occlusion) (Pollock et al., 2006; Smith et al., 2011; Stevanato et al., 2009; Stroemer et al., 2009), as well as in an investigation of the function of ZNF804A, a gene implicated in the pathophysiology of schizophrenia and bipolar disorder (Hill et al., 2011). A sister cell line to CTX0E03, CTX0E16, has been generated from the same first trimester foetus using the same technique, and has been identified as a potential candidate for investigating similar mechanisms of neuropsychiatric disease (Anderson et al., 2015). This cell line is the focus of the present chapter.

In order to determine the suitability of the CTX0E16 hNPCs for use in studying the mechanisms underlying the alterations in neuronal structure and function seen in neuropsychiatric disease, these cultures must first be characterised to establish whether they are capable of generating cells with key neuronal phenotypes. It is thus critical to determine whether these cell cultures can 1) robustly differentiate into glutamatergic neurons *in vitro*; 2) display functional responses to activation of neurotransmitter signalling systems; 3) form putative synapses; and 4) are able to respond to activity-dependent stimulations in the anticipated manner. This chapter will discuss the characterisation of the first of these phenotypes in the CTX0E16 cell line.

Previous studies have established whether comparable cell lines are capable of generating functional neurons by testing for several phenotypes following differentiation. These include determining whether differentiated cells express neuronal markers such as Tau, MAP2 or βIII-Tubulin (Tuj1) and are negative for markers of proliferation (BrdU, ki67) or stem cell identity (Sox2, nestin) (Cacci et al., 2007; Cocks et al., 2013; Donato et al., 2007; Pollock et al., 2006; Zhang et al., 2008). Once positive expression of neuronal markers can be established, markers of regional and functional identity were also assessed. These included determinants of excitatory/inhibitory identity, markers specific to neurons derived from subregions of the central nervous system, and markers of astrocytic and oligodendrocytic identity to determine whether differentiated cultures contained pure or mixed populations of cells (Cacci et al., 2007; Cocks et al., 2013; Donato et al., 2007; Pollock et al., 2006; Zhang et al., 2008). The development of neuronal morphology has also been used as an indicator of cell identity, with the polarisation of the cell, outgrowth of axons and dendrites and establishment of

putative synapses being cited as critical aspects of neuronal differentiation and identifiers of neuronal identity in vitro (Barnes and Polleux, 2009; Dotti et al., 1988; Gaspard et al., 2008; Marchetto et al., 2010; Pollock et al., 2006; Verpelli et al., 2013).

This chapter details a characterisation of the cellular identity of CTX0E16 NPCs and neurons. Proliferative and differentiated (DD28) cultures of CTX0E16 cells were assessed for expression of proliferation, stem cell identity and neuronal identity markers in order to determine whether NPCs adopt a neuronal fate after four weeks of culturing with differentiation media. NPCs and differentiated cells were also assessed for relative expression of glial markers to determine the proportion of differentiated cultures made up by neurons and astrocytes. Following this, cells positive for neuronal markers were further characterised by investigating co-expression of markers of excitatory and inhibitory neurons, superficial- and deep-layer cortical neurons, and various synaptic proteins to determine their regional and functional identity. Finally, cells were qualitatively assessed at several stages throughout differentiation to determine whether they recapitulated critical aspects of the development of cortical neuron morphology, including neurite outgrowth, polarisation of the cell, a pyramidal cell soma, specialisation of dendrites and axons and the establishment of putative synaptic structures.

3.3 RESULTS

3.3.1 OPTIMISATION OF DIFFERENTIATION PROTOCOL FOR CTX0E16 NPCS

Neurons derived from human stem cell sources can typically take several weeks to display the key aspects of neuronal function, such as neuronal morphology, expression of synaptic proteins, and the development of functional synapses (Donato et al., 2007; Verpelli et al., 2013). Thus, it is critical to establish whether pre-existing protocols for the differentiation of CTX0E16 cells are capable of maintaining cultures for several weeks without significant deterioration or cell death.

Modified plating and differentiation protocols were assessed for their viability in producing long term neuronal cultures without excessive proliferation thought to contribute to overcrowding and subsequent culture death. Overcrowding of neuronal cultures also renders evaluation via immunocytochemistry problematic due to the difficulty of resolving individual cells among overconfluent cultures. Thus, cultures generated using several modified forms of this differentiation protocol were assessed for markers of proliferation following 5 days of differentiation in order to develop a differentiation protocol

which minimises the risk of overcrowding and cell death in CTX0E16 cultures. Six culture conditions were assessed for expression of the proliferative marker ki67 and the early neuronal marker MAP2 5 days after exposure to differentiation media (DD5):

1. Cells were plated in RMM+++ and media was switched to NDM three days later.
2. Cells were plated in RMM+++ and media was switched to NDM one day later.
3. Cells were plated in RMM+++ and media was switched to NDM one hour later.
4. Cells were washed in HBSS and plated in NDM as in the original protocol.
5. As condition 4, but with a complete media change one hour after plating.
6. As condition 4, but with a complete media change one day after plating.

(see **Figure 3.3.1**, **A-F**). Of the six conditions assessed, condition 2 was found to have the lowest proportion of ki67-positive cells in comparison to the other five conditions (mean ± SEM: 31.48 ± 2.24% of cells vs 52.71 ± 5.27%, 36.19 ± 2.38%, 40.20 ± 3.43%, 35.06 ± 2.31% and 32.79 ± 1.90% for conditions 1, 3, 4, 5 and 6 respectively). Very little difference was seen in the relative proportion of MAP2-positive cells in each condition (83.84 ± 4.18%, 84.69 ± 4.04%, 85.31 ± 2.09%, 84.12 ± 2.59%, 83.73 ± 2.37% and 85.83 ± 3.02% for conditions 1, 2, 3, 4, 5 and 6 respectively) (see **Figure 3.3.1**, **G**). Condition 2 was also found to produce the lowest density cultures, with an average of 53.00 ± 5.60 cells per FOV compared to 56.00 ± 8.90, 101.25 ± 10.37, 85.75 ± 6.92, 64.38 ± 4.02 and 63.29 ± 5.78 cells per FOV for conditions 1, 3, 4, 5 and 6 respectively (see **Figure 3.3.1**, **H**). Taken together, these findings suggest that differentiation protocol 2 is the most optimal condition to generate long term cultures of differentiating CTX0E16 cells. The lower density of the cultures at DD5 in this condition indicates that these cultures will be easier to assess via experimental methods using immunofluorescence techniques at later stages of differentiation. The lower proportion of ki67-positive cells indicates that cells cultured using this protocol exit the mitotic cycle sooner than those cultured under other conditions; this suggests that these cultures are less likely to become overcrowded at later time points. As a further measure to reduce cell density in mature cultures of CTX0E16 cells, all subsequent experiments were plated at a quarter of the initial density used (12,500 cells per well of a 24 well plate). This did not appear to negatively impact long term culture viability.

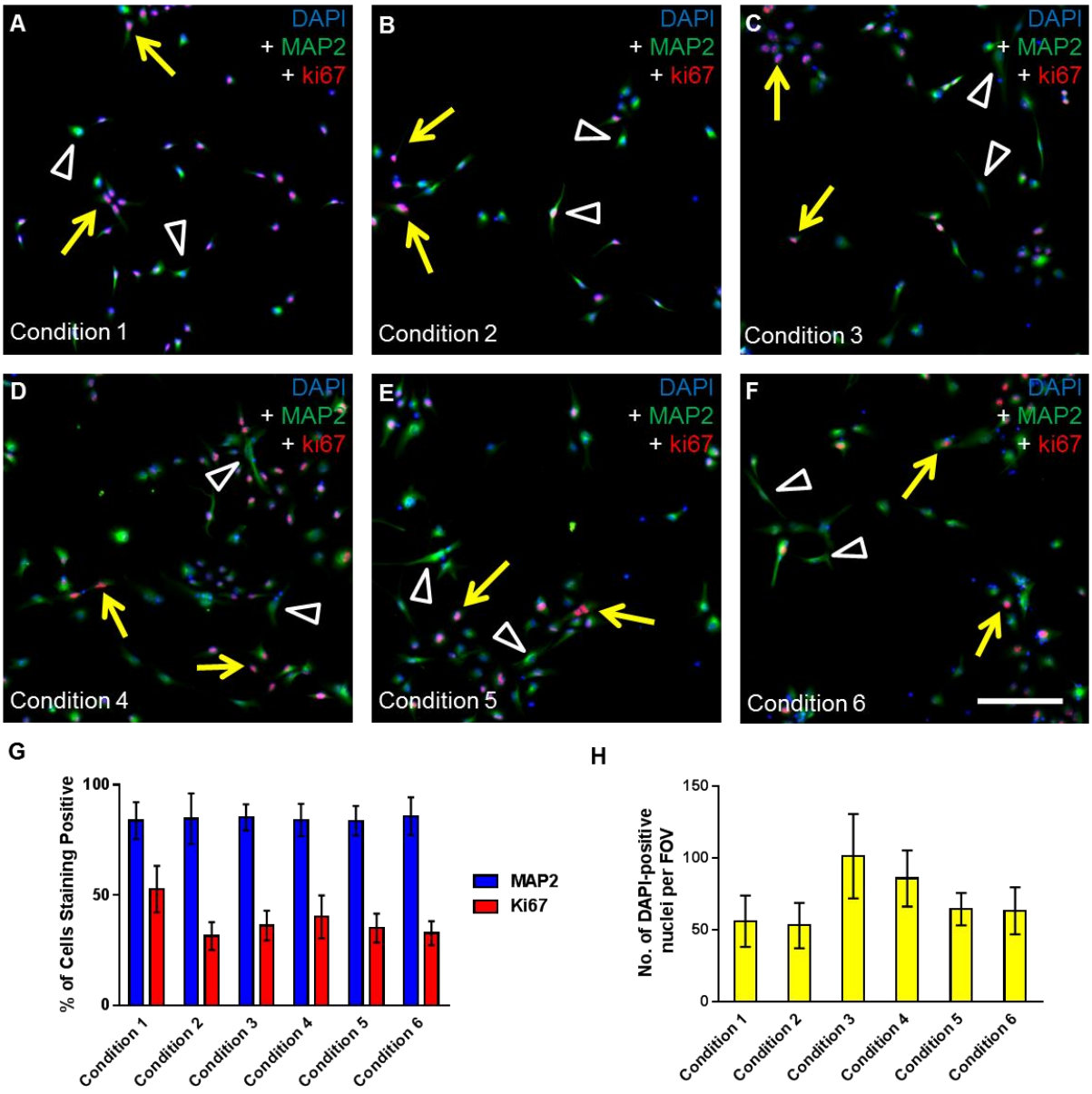

Figure 3.3.1: Optimisation of CTX0E16 plating protocol. **A-F**: CTX0E16 cells were plated according to one of six different plating conditions as detailed in **Section 3.3.1**, differentiated for 5 days and stained for DAPI, MAP2 and ki67. Yellow arrows indicate ki67-positive cells, white arrowheads indicate MAP2-positive cells. **G**: Quantification of proportion of CTX0E16 cells staining positive for each marker in each plating condition. Condition 2 resulted in the lowest proportion of ki67-positive cells after 5 days of differentiation. **H**: Average number of DAPI-positive nuclei per FOV in each plating condition. Condition 2 resulted in the lowest cell density after five days of differentiation. Scale bar = 20 µm, bar graphs show mean ± SD.

3.3.2 CHARACTERISATION OF DIFFERENTIATION IN THE CTX0E16 CELL LINE

Following the initial establishment of optimal conditions for prolonged culturing of the cell line, a characterisation of markers of cellular identity was carried out on cultures of proliferative (DD0) and

differentiated (DD5 or DD28) CTX0E16 cells. Previous studies have focused on the downregulation of proliferative and stem cell markers and the upregulation of postmitotic neuronal and astrocytic markers as a means of assessing the efficiency of differentiation of neurons from proliferative hNPC lines (Cacci et al., 2007; Donato et al., 2007; Zhang et al., 2008). To investigate this in the CTX0E16 cell line, proliferative (DD0) and differentiated (DD28) CTX0E16 cells were fixed and immunostained for DAPI, the NPC marker Nestin, the astrocytic marker S100β and the neuronal markers MAP2 and Tau. DD0 and DD5 CTX0E16 cells were additionally stained for the proliferative marker ki67, to determine whether proliferation is rapidly reduced following the switch to differentiation media. These cultures were assessed for expression of each marker according to the method detailed in **Section 2.7.4**. In DD0 cultures, 91.41 ± 5.22% of cells were positive for the proliferative marker ki67 while only 52.82 ± 3.28% of cells were ki67 positive by DD5; analysis of this data with a Student's unpaired t test revealed this difference to be significant ($p<0.001$) (see **Figure 3.3.2**, **A, B & K**). Thus, CTX0E16 proliferation is rapidly reduced following the introduction of differentiation media.

Analysis of expression of the neural progenitor cell marker nestin in DD0 and DD28 CTX0E16 cultures indicated that 39.04 ± 9.54% of proliferative cells and 63.75 ± 5.58% of differentiated cells were positive for this marker (see **Figure 3.3.2**, **C, D** & **L**). This finding was surprising in that it seemed to imply that a greater proportion of cells in the differentiated cultures were positive for a marker of neural stem cell identity. However, further assessment of the pictures taken of nestin staining in these cultures suggested that analysis using nuclear regions of interest is susceptible to an overestimation of the number of nestin-postive cells in later stage cultures due to 1) the higher density of the cultures and 2) large processes from nestin-positive cells overlapping nestin-negative cells. This would compound an underestimation of the number of nestin-positive cells in proliferative cultures due to nestin staining being primarily localised to non-nuclear regions of the CTX0E16 NPCs (see **Figure 3.3.2**, **C & D**).

S100β-positive cells accounted for only a subset of both proliferative and differentiated CTX0E16 cultures, with 2.77 ± 0.38% of DD0 cultures and 8.46 ± 2.08 of DD28 cultures staining positive for the marker (see **Figure 3.3.2**, **E, F** & **L**). Analysis of this data with a Student's unpaired t test did not find this difference to be significant ($p>0.05$). This finding suggests that only a small subset of cells in proliferative and differentiated cultures are astrocytes.

MAP2-positive cells accounted for 2.92 ± 0.24% of the DD0 cultures and by DD28 this had increased to 68.21 ± 6.66% of all cells; this increase was also reflected in the number of Tau-positive cells, with 8.05 ± 1.07% of DD0 cells increasing to 65.28 ± 5.61% of DD28 cells staining positive for Tau. Analysis of this data with two Student's unpaired t tests did found both of these differences to be significant ($p<0.001$, see **Figure 3.3.2**, **G**-**L**). Taken together, these data indicate that neuronal cells make up the majority of CTX0E16 cultures by day 28 of differentiation.

Taken together, these findings suggest that CTX0E16 NPCs represent a robust source from which cultures of neurons can be continually differentiated, with the majority of cells ceasing proliferation soon after being switched to differentiation media. Interestingly, a small subset of these differentiated cultures is comprised of astrocytes; attempts at varying culture conditions for the cell line to attempt to minimise or increase the proportion of astrocytes in differentiated cultures may be a fascinating avenue for future research.

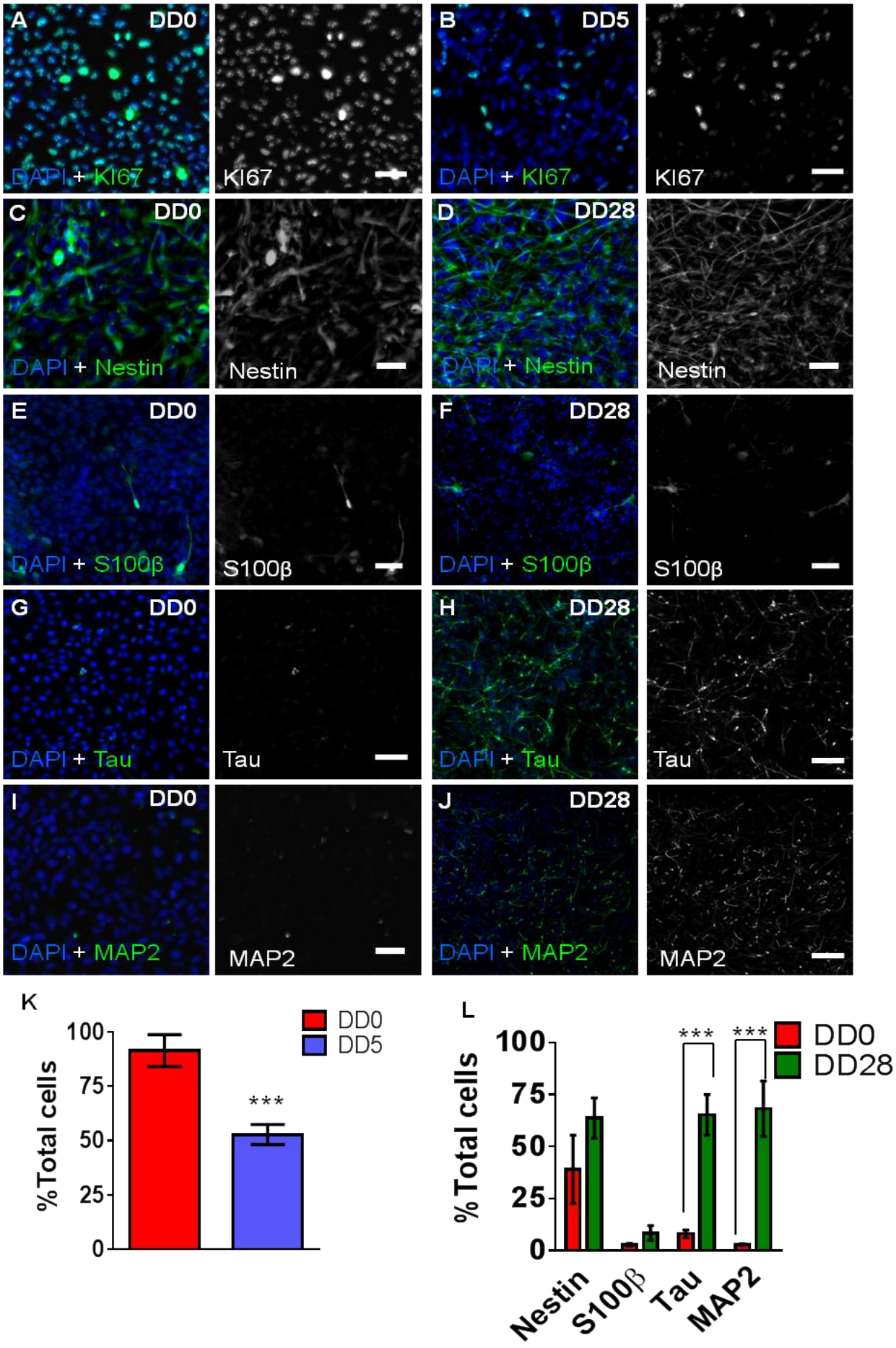
A
DD0
DAPI + KI67
KI67
B
DD5
DAPI + KI67
KI67
C
DD0
DAPI + Nestin
Nestin
D
DD28
DAPI + Nestin
Nestin
E
DD0
DAPI + S100β
S100β
F
DD28
DAPI + S100β
S100β
G
DD0
DAPI + Tau
Tau
H
DD28
DAPI + Tau
Tau
I
DD0
DAPI + MAP2
MAP2
J
DD28
DAPI + MAP2
MAP2
K
% Total cells
100
75
50
25
0
DD0
DD5
***
L
% Total cells
100
75
50
25
0
***
***
DD0
DD28
Nestin
S100β
Tau
MAP2

Figure 3.3.2 (overleaf): Differentiation of CTX0E16 cells. **A-J**: Representative images of immunostaining for the proliferative marker ki67 (**A & B**), the neural stem cell marker Nestin (**C & D**), the astrocytic marker S100β (**E & F**), and the neuronal markers Tau (**G & H**) and MAP2 (**I & J**) in proliferative (**left columns**) and differentiated (**right columns**) CTX0E16 cultures. **K**: Quantification of the number of ki67-positive cells as a percentage of total cells; n = approximately 1,500 cells from three independent experiments carried out in triplicate; error bars represent SD; ***p <0.001 (Student's unpaired t test). **L**: Number of proliferative (DD 0) or differentiated (DD 28) cells positive for Nestin, S100β, Tau or MAP2; N = approximately 1,500 cells from three independent experiments carried out in triplicate; error bars represent SD; ***p <0.001 (unpaired t tests).

3.3.3 CHARACTERISATION OF NEURONAL SUBTYPES AND FUNCTIONAL MARKERS IN DIFFERENTIATED CTX0E16 CULTURES

Following the preliminary finding that a majority of CTX0E16 cells are neuronal in four-week-differentiated cultures, a similar investigation was undertaken into the functional and regional identity of these neurons. Previous characterisations of human NPC lines have assessed the relative expression of excitatory and inhibitory markers, as well as various neurotransmitters, cortical region markers and markers of various synaptic proteins to determine whether these cell lines are suitable models of specific neuronal subtypes (Cacci et al., 2007; Donato et al., 2007; Verpelli et al., 2013; Zhang et al., 2008). As the CTX0E16 cell line has been cortically-derived and proposed as a platform to conduct studies of mechanisms of glutamatergic dysfunction in neuropsychiatric disease (Anderson et al., 2015), it is therefore critical to establish whether the neurons generated from this cell line have a specific cortical identity, whether they are glutamatergic and whether they produce excitatory synapses. DD28 CTX0E16 cultures were and immunostained for DAPI, MAP2 and one of several neuronal subtype markers. These included the excitatory, glutamatergic markers VGlut1 and CaMKIIα and the inhibitory, GABAergic markers Calretinin, Calbindin-D28k, VGAT and GAD65/67 (see **Table 3.3.5** for a list of these markers and their biological functions). 75.25 ± 8.74% of DD28 CTX0E16 neurons were found to also co-express the glutamatergic neuron marker VGlut1, while 67.09 ± 10.15% of these neurons co-expressed CaMKIIα (see **Figure 3.3.3**, **A, B & G**). Both of these markers exhibited a punctate pattern of staining in both the cell bodies and along neurites of MAP2-positive neurons (see **Figure 3.3.3**, **A & B**) suggesting the presence of functional excitatory synapses (Herzog et al., 2006). In contrast to this, only 44.58 ± 11.09% of neurons expressed VGAT and 39.30 ± 11.51% of neurons were positive for GAD65/67 (see **Figure 3.3.3**, **C, D & G**). Moreover, only a fraction of the neuronal population of DD28 CTX0E16 cultures expressed calretinin or calbindin (1.03 ± 0.18% and 2.13 ± 0.40% of neurons

respectively; see **Figure 3.3.3**, **E-G**). However, the distribution of calretinin and calbindin in these neurons reflects the pattern of localisation seen in previous research (DeFelipe, 1997; Rogers, 1992). VGAT and GAD65/67 were expressed in a punctate pattern around the cell soma of MAP2-positive neurons, consistent with previous studies (Schwab et al., 2013). Taken together, these data indicate that CTX0E16 cultures predominately produce excitatory, glutamatergic neurons following 28 days of differentiation while a subset of these neurons are GABAergic interneurons.

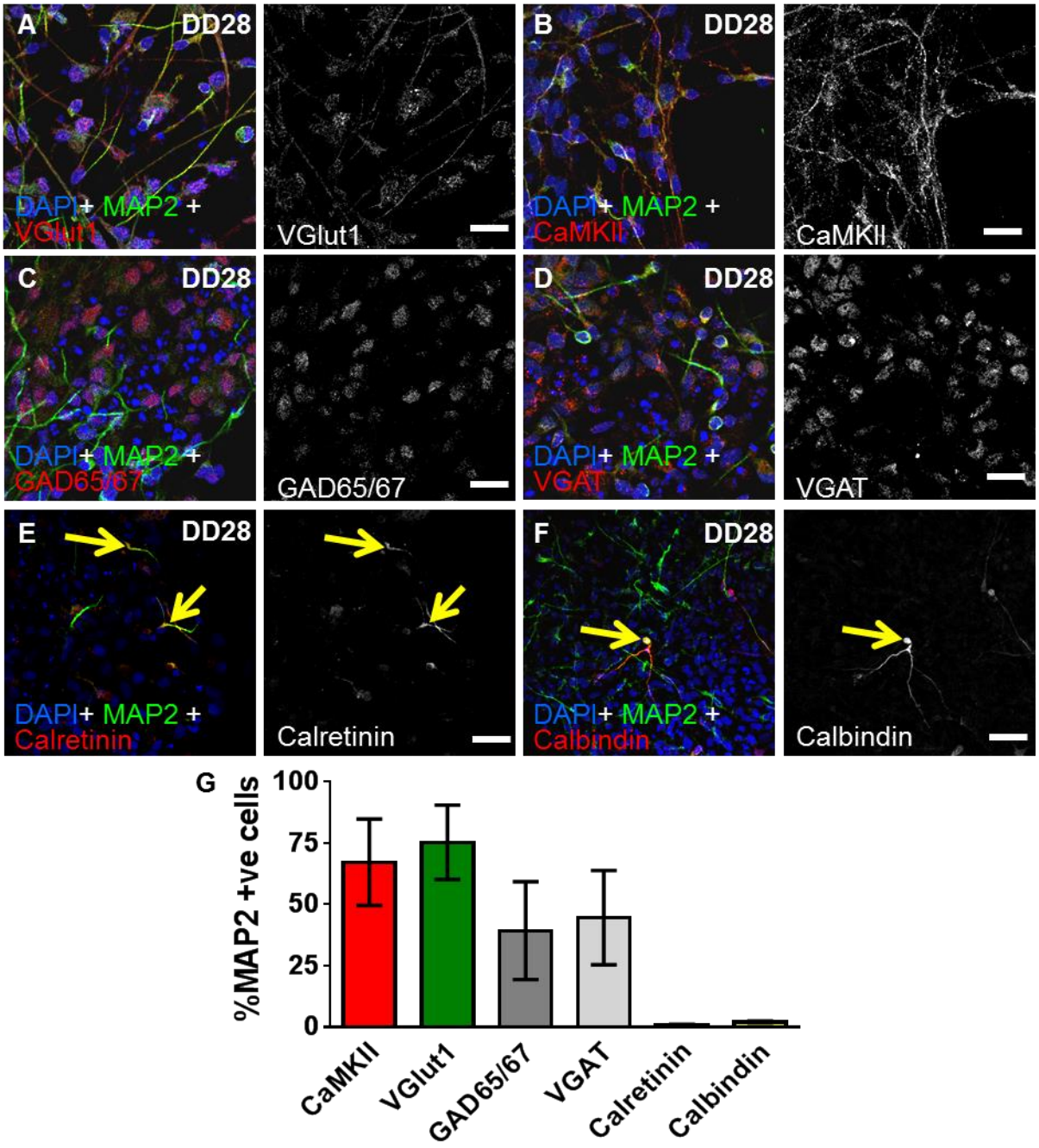

Figure 3.3.3 (overleaf): Differentiation of CTX0E16 cells generates glutamatergic and GABAergic neurons. **A-F**: Representative images of differentiated (DD28) CTX0E16 neurons stained with the neuronal marker MAP2 and the glutamatergic markers VGlut1 (**A**) and CaMKII (**B**) and the GABAergic interneuron markers GAD65/67 (**C**), VGAT (**D**), Calretinin (**E**) and Calbindin (**F**). Yellow arrows indicate neurons staining positive for these markers. **G**: Quantification of **A-F** revealed that over 65 % of MAP2-positive neurons also expressed VGlut1 or CaMKIIα, whereas less than 45 % of MAP2-neurons were also positive for either GAD65/67 or VGAT, and less than 10% of MAP2-positive neurons were positive for Calretinin or Calbindin; n = approximately 1,500 cells per condition from three independent experiments carried out in triplicate; error bars represent SD. Scale bars = 20 µm.

triplicate; error bars represent SD; ***p <0.001 (unpaired t tests).

3.3.4 EXPRESSION OF REGIONAL MARKERS IN CTX0E16 CULTURES

The expression of both GABAergic and glutamatergic markers in differentiated cultures of CTX0E16 cells was perhaps surprising given that in the human brain these neurons typically originate from different regions of the developing telencephalon: glutamatergic neurons in the cortex are generated by progenitors located within the ventricular zone of the dorsal telencephalon (Hansen et al., 2010; Stiles and Jernigan, 2010) while GABAergic cortical neurons derive from ventral telencephalic regions known as the medial, lateral and caudal ganglionic eminences (Ma et al., 2013; Radonjić et al., 2014). Although the CTX0E16 cell line is reported to be a clonal population, the heterogeneity of neurons within the differentiated cultures may be indicative of a mixed population of progenitors derived from both dorsal and ventral regions of the developing telencephalon. Thus, to identify the lineage of the CTX0E16 line RNA samples were taken from proliferative (DD0) and differentiated (DD28) cultures and assessed for expression of several regional NPC and neuronal markers using semi-quantitative RT-PCR. The markers included genes expressed in the dorsal telencephalon during development: *EMX1*, *OTX2* and *PAX6*; genes expressed in the ventral telencephalon: *DLX1*, *NKX2.1* and *GBX2*; and neuronal markers: *FOXG1*, *TBR1*, *GAD1* and *ISL1* (see **Table 3.3.4** for a list of these markers and their biological functions). Interestingly, markers of both dorsal and ventral telencephalic identity could be detected in proliferative and differentiated CTX0E16 cultures, suggesting that the CTX0E16 line may indeed be comprised of a mixed population of progenitors with different regional identities (see **Figure 3.3.4**, **A** & **B**). Moreover, markers of both GABAergic and glutamatergic cortical neuron identity were detected in differentiated CTX0E16 cultures, further supporting the possibility of multiple lineages being present within the CTX0E16 line (**Figure 3.3.4**, **A** & **B**). Semi-quantitative analysis of the normalised

RT-PCR bands for each gene of interest suggested that relative expression of dorsal telencephalon markers increased in differentiated CTX0E16 cultures relative to proliferative cultures; Student's t tests with posthoc Bonferonni-Sidak correction for multiple comparisons revealed that these increases in expression were significant ($p<0.05$).

EMX1 and *TBR1* were not found to be significantly upregulated following several weeks of differentiation, an unexpected result given that typically these genes are highly expressed in terminally differentiated cortical projection neurons. However, semi-quantitative analysis of RT-PCR results may not be sensitive enough to detect changes in expression across multiple time points; such techniques are typically better suited to determine the presence rather than level of expression of a given gene. To more accurately evaluate the pattern of expression of these two genes in CTX0E16 NPCs and neurons, RNA samples were again taken from DD0 and DD28 CTX0E16 cultures and assessed via q-PCR to determine whether expression of these genes was significantly altered following several weeks of differentiation. q-PCR analysis revealed a significant increase in the dorsal forebrain marker EMX1, and the cortical marker TBR1 28 days after differentiation (**Figure 3.3.4**, **C**), indicating that a significant proportion of CTX0E16 NPCs were differentiating into neurons with a cortical identity.

Following this initial assessment of regional marker expression, a previously-conducted microarray of proliferative (DD0) and differentiated (DD28) CTX0E16 RNA samples was re-analysed to confirm the findings of the RT-PCR and to expand the number of markers assessed as a means of better identifying the putative regional identity of CTX0E16 progenitors. To improve the reliability of analysis, data for probes which did not detect expression of a given gene in all samples were removed from the overall dataset. Student's t tests were conducted on the data for each individual gene to determine whether expression had significantly altered following several weeks of differentiation, with subsequent FDR correction to account for multiple comparisons. Not all of the regional markers assessed using RT-PCR could be observed in the microarray data; this may be due to one or more of the biological replicates exhibiting insufficient expression at a given time point.

Of the genes present in both analyses, *PAX6* exhibited a significant increase in expression after four weeks of differentiation (FDR-corrected $p<0.05$), reflecting the trend seen in the RT-PCR data (**Figure 3.3.4**, **D**). *DLX5* exhibited a significant increase in expression following four weeks of differentiation (FDR-corrected $p<0.05$) as assessed by microarray, reflecting the previous findings via

RT-PCR. *NKX2.1* showed no significant changes in expression after differentiation, in contrast to the RT-PCR data which demonstrated a significant increase in expression in the neuronal cultures relative to CTX0E16 NPCs. *FOXG1* expression did not differ in differentiated cultures as compared to NPC cultures, similarly to the findings of the RT-PCR. Surprisingly, *ISL1* expression decreased significantly in the differentiated CTX0E16 cultures relative to the NPC stage (FDR-corrected $p<0.05$), in contrast to the RT-PCR data which did not demonstrate any significant alterations in expression. Finally, *GAD1* expression significantly increased in CTX0E16 cultures after four weeks of differentiation, as assessed by microarray (FDR-corrected $p<0.05$); again this was in contrast to the RT-PCR data, which did not detect any significant changes in expression. Overall, despite some discrepancies in the findings of the microarray relative to semi-quantitative analysis of RT-PCR data, both investigations found expression of dorsally- and ventrally expressed telencephalic markers, as well as markers of excitatory and inhibitory cortical neurons. This further supports the conclusion that the CTX0E16 cell line represents a heterogenous population of NPCs comprised of both dorsal and ventral telencephalic progenitors.

The expression of several other markers of regional and functional identity was further explored in the microarray dataset (see **Table 3.3.4** for a list of these markers and their biological functions) (**Figure 3.3.4**, **D**). Differentiation of CTX0E16 cells for several weeks was accompanied with a significant upregulation of *DCX*, a marker of newborn cortical neurons, and *GFAP*, expressed in neural progenitor cells and astrocytes (FDR-corrected $p<0.05$ for both genes). This upregulation was accompanied with a concommittant downregulation of the proliferative marker *MKI67* and the neural stem cell marker *NES* (FDR-corrected $p<0.05$ for both genes). Surprisingly, the neural progenitor marker *SOX2* was found to significantly increase expression in CTX0E16 cultures after four weeks of differentiation (FDR-corrected $p<0.05$). Expression of *SP8*, a marker of cortical interneurons, was found to be significantly upregulated in differentiated CTX0E16 cultures relative to CTX0E16 NPCs (FDR-corrected $p<0.05$). Other genes expressed in cortical interneurons including *MASH1* and *CTIP1* were similarly upregulated after four weeks of differentiation (FDR-corrected $p<0.05$ for both genes). *BRN2*, a gene expressed in upper layer neurons of the cortex, was further found to be significantly upregulated in CTX0E16 neuronal cultures relative to the NPC stage (FDR-corrected $p<0.05$), though this was not similarly seen with *CUX1* expression, another marker of upper layer cortical neurons. Overall, these additional markers support the findings of **Section 3.3.2** and the previous RT-PCR, indicating that not only do CTX0E16 cultures lose their stem cell identity and differentiate into mixed cultures of neuronal

and non-neuronal cells, but also that this NPC line is comprised of a mixed population of NPCs from both the dorsal and ventral telencephalon.

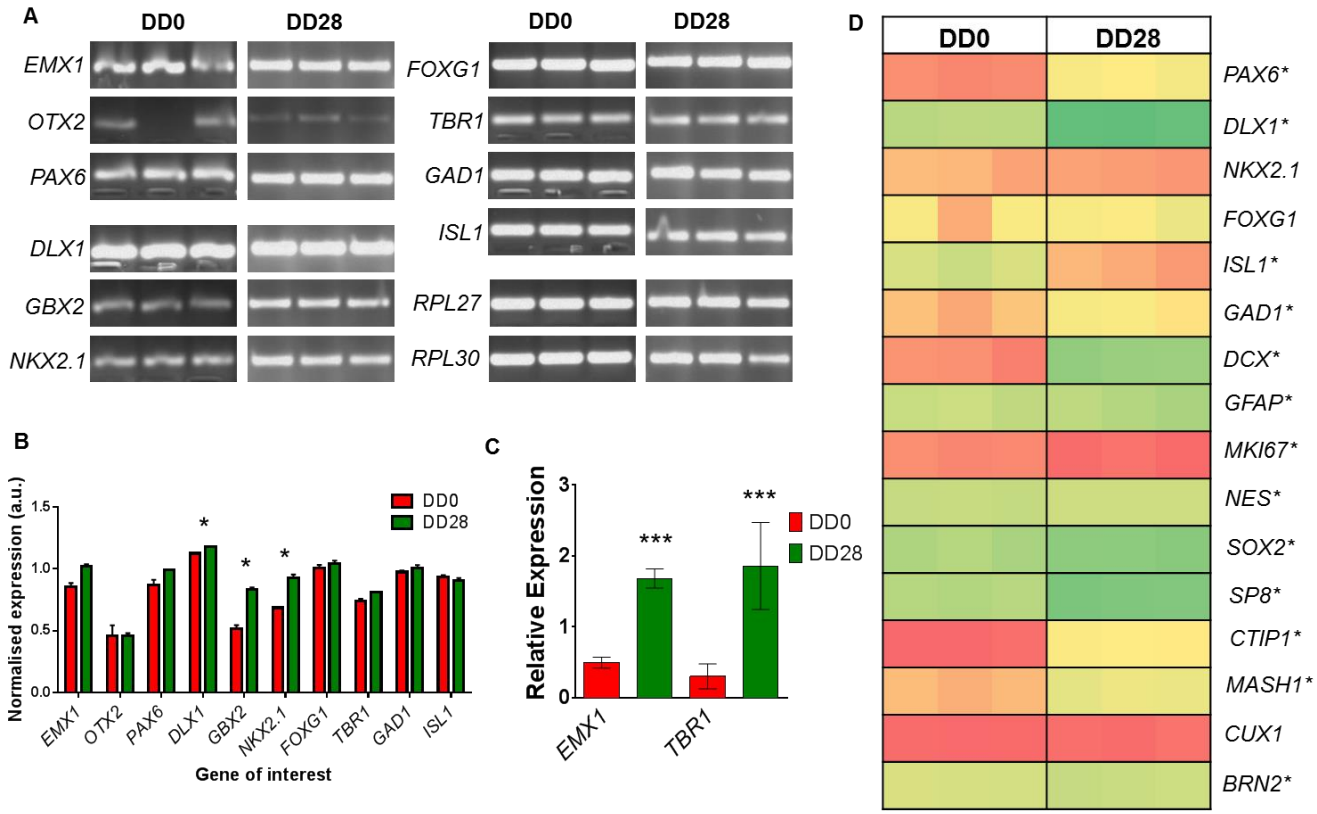

Figure 3.3.4: Expression of markers of regional identity in proliferative and differentiated CTX0E16 cultures. **A**: RT-PCR of markers expressed in defined regions of the developing forebrain, including the dorsally-expressed telencephalic markers *EMX1*, *OTX2* and *PAX6*, the ventrally-expressed telencephalic markers *DLX1*, *GBX2* and *NKX2.1* and the neuronally-expressed genes *FOXG1*, *TBR1*, *GAD1* and *ISL1*. Expression of all markers was seen in both proliferative and differentiated CTX0E16 cultures. **B**: Quantification of RT-PCR bands seen in **A**, with the mean intensity of each band normalised to intensity values for two housekeeping genes obtained from the same RNA sample. N = 3 biological replicates per time point; error bars represent SD; *p<0.05, Student's t test. **C**: Quantitative PCR (q-PCR) analysis revealed an increase in the expression of dorsal forebrain marker, *EMX1* and cortical neuron marker *TBR1* in DD 28 CTX0E16 neurons compared to DD 0 cells; n = 4 independent experiments carried out in triplicate; error bars represent SD; ***p <0.001 (Student's unpaired t test). **D**: Heat map of relative expression of selected markers derived from a microarray of samples taken from proliferative (DD0) and differentiated (DD28) CTX0E16 cultures. Green = higher relative expression, red = lower relative expression. N = 3 biological replicates per time point, *FDR-corrected p<0.05, Student's unpaired t test. Previous microarray data was generated by Rodrigo R. Duarte and analysed by P.J. Michael Deans.

3.3.5 DIFFERENTIATION OF CTX0E16 CULTURES PREDOMINATELY PRODUCES CORTICAL NEURONS WITH A LOWER CORTICAL LAYER IDENTITY

The upregulation of *BRN2* expression in differentiated CTX0E16 cultures is suggestive of the production of upper layer cortical neurons (Shi et al., 2012b). To further investigate whether CTX0E16 cultures produced neurons with layer-specific identities, DD28 CTX0E16 cultures were immunostained for markers expressed in both deep and superficial cortical layer neurons: Tbr1, Cux1 and Ctip2 (see **Table 3.3.4** for a list of these markers and their biological functions). Analysis of regional neuronal markers in the DD28 neurons determined that 41.58 ± 6.45% of MAP2-positive cells costained for the marker of deep-layer cortical neurons, Ctip2. In contrast to this, only 3.57 ± 1.32% of MAP2-positive neurons were also positive for Cux1, a marker of upper-layer cortical neurons (Molyneaux et al., 2007) (See **Figure 3.2.5**, **D**), reflecting the low expression of *CUX1* seen in the previous microarray. Assessment of the pattern of staining with these markers indicated that expression was restricted to the nucleus of CTX0E16 cells, consistent with previous in vivo studies (Shi et al., 2012a) (see **Figure 3.2.5**, **A & B**). 77.82 ± 12.23% of MAP2-positive cells were also positive for Tbr1 staining, another marker of deep-layer cortical neurons (Molyneaux et al., 2007) (see **Figure 3.2.5**, **D**). However, further qualitative assessment of images of Tbr1-stained cultures indicated that this finding may have been due to non-specific binding of the Tbr1 antibody, as the pattern of Tbr1 staining did not match that observed in previous studies (Shi et al., 2012a). The Tbr1 protein acts as a transcription factor, and thus expression of this protein would typically be restricted to the nuclei of positive neurons. However, the antibody used in the present study appeared to stain nuclei, cytoplasm and neurites evenly, indicating that analysis using this antibody may not be reliable (see **Figure 3.2.5**, **C**). Despite this, the data obtained using the Ctip2 and Cux1 antibodies indicates that the majority of neurons differentiated from the CTX0E16 cell line have a deep cortical layer identity, with a subset adopting a superficial-layer fate.

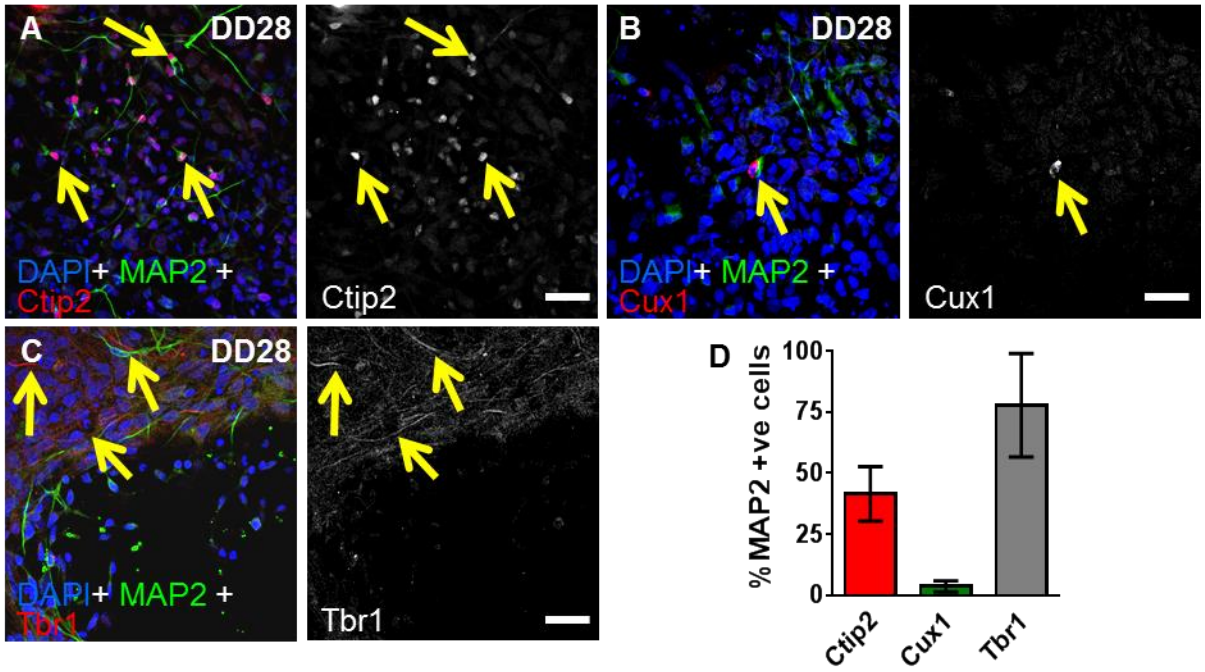

Figure 3.3.5: Differentiation of CTX0E16 cultures predominately produces cortical neurons with a lower cortical layer identity. **A-C**: Representative images of differentiated CTX0E16 cultures stained for the neuronal marker MAP2 and the deep layer cortical neuron markers Ctip2 (**A**) and Tbr1 (**C**) and the upper layer cortical neuron marker Cux1 (**B**). Yellow arrows indicate neurons staining positive for these markers. **D**: Quantification revealed that 41.6 % of MAP2-positive neurons expressed Ctip2, whereas less than 10 % of MAP2-labelled neurons were positive for Cux1. Note: although ~75% of MAP2-positive neurons appeared to also costain for Tbr1, closer assessment of the immunostaining images revealed non-specific staining in the neurites of CTX0E16 cells (**C**, yellow arrows). N = approximately 1,500 cells per condition from three independent experiments carried out in triplicate; error bars represent SD. Scale bars = 20 µm.

3.3.6 EXPRESSION OF EXCITATORY SYNAPTIC MARKERS IN CTX0E16 NEURONS

In light of the evidence indicating that differentiated CTX0E16 cultures generated excitatory cortical neurons, the expression of excitatory synaptic proteins was assessed in these cells to determine whether they produce key components of glutamatergic synapses, a hallmark of mature excitatory neurons. DD28 CTX0E16 cultures were immunostained for the postsynaptic proteins PSD-95, SAP97, GluN1 and GluA2 (see **Table 3.3.4**). Analysis of synaptic protein immunostaining revealed that PSD-95 and SAP97 expression occurred in 50.30 ± 8.46% and 55.59 ± 8.22% of DD28 MAP2 positive cells respectively (see **Figure 3.3.6**, **E**). However, further assessment of the pattern of SAP97 staining in high magnification confocal images revealed that this staining was non-specific, indicating that the findings for this marker were not reliable (**Figure 3.3.6**, **B**). The glutamatergic receptor subunit proteins

GluN1 and GluA2 were expressed in 49.33 ± 8.51% and 37.95 ± 8.61% of neurons in DD28 CTX0E16 cultures respectively. PSD-95, GluN1 and GluA2 exhibited punctate staining within the cell bodies and along the MAP2-positive dendrites of CTX0E16 neurons, reflecting the pattern of localisation seen in previous research (see **Figure 3.3.6**, **C-E**). These data indicate that even after only 28 days of differentiation, CTX0E16 neurons are already expressing key components of the glutamatergic postsynaptic density, in addition to the presynaptic glutamatergic protein VGlut1 and GABAergic proteins GAD65/67 and VGAT, described previously.

Taken together, these data demonstrate that CTX0E16 cultures predominately produce excitatory, glutamatergic neurons expressing both pre- and post-synaptic components of excitatory synapses, with a subset of neurons adopting a GABAergic interneuron identity. Generally, neurons also expressed the deep-layer cortical marker Ctip2, reflecting the relatively immature stage of cortical development these neurons would correspond to.

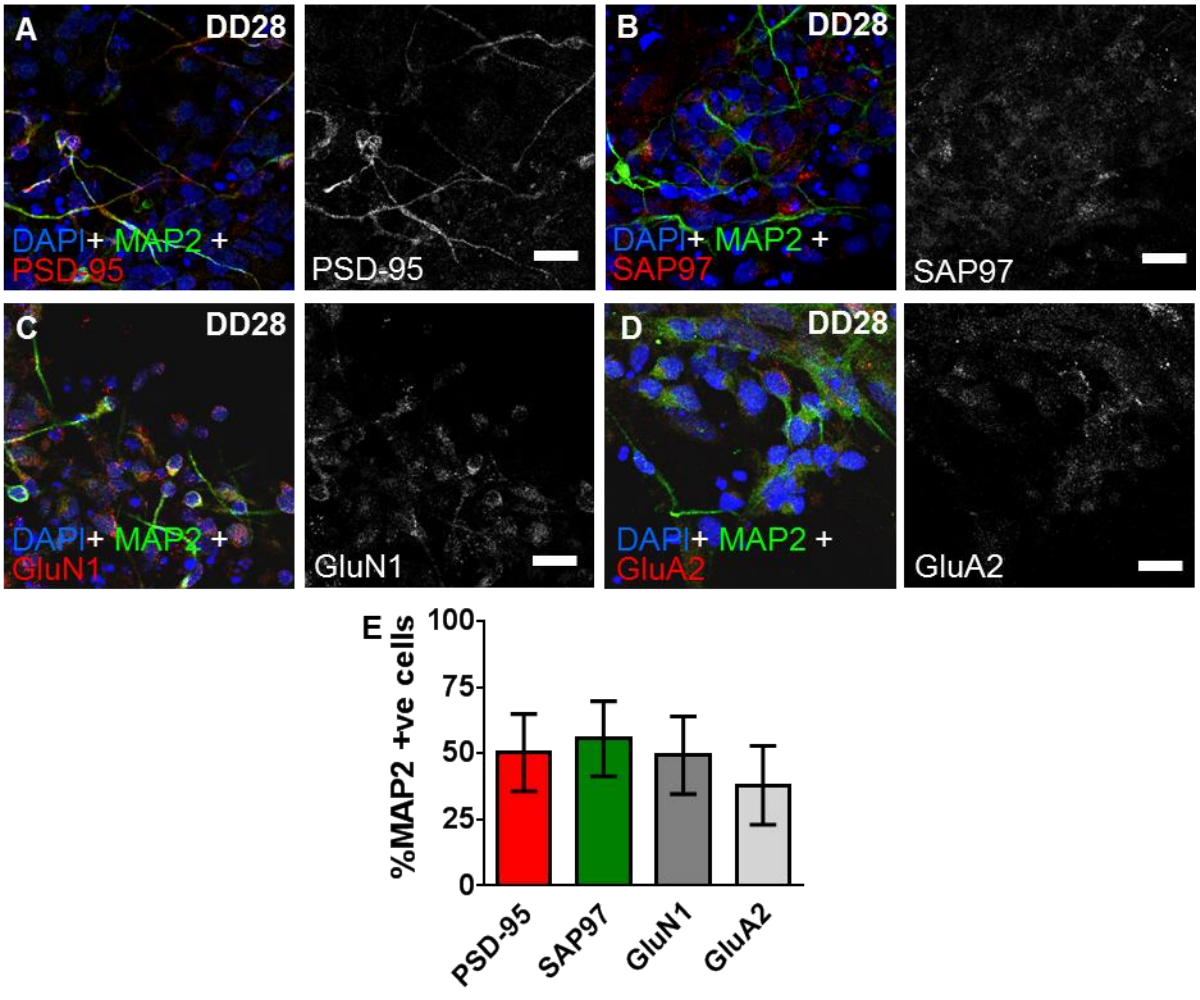

Figure 3.3.6 (overleaf): Differentiated (DD28) CTX0E16 cells express postsynaptic markers and glutamatergic receptor proteins. **A-D**: Representative images of differentiated CTX0E16 cultures stained for the neuronal marker MAP2 and the postsynaptic density proteins PSD-95 (**A**) and SAP97 (**B**) and the glutamatergic receptor proteins GluN1 (**C**) and GluA2 (**D**). Note: SAP97 immunostaining appeared to be non-specific and so quantification with this marker is unlikely to be representative of actual expression levels. **E**: Quantification revealed that ~50 % of MAP2-positive neurons expressed the synaptic markers PSD-95, GluN1 or GluA2. N = approximately 1,500 cells per condition from three independent experiments carried out in triplicate; error bars represent SD. Scale bars = 20 µm.

3.3.7 DEVELOPMENT OF NEURONAL MORPHOLOGY IN DIFFERENTIATING CTX0E16 CULTURES

Following these promising early results, an investigation was then conducted into whether CTX0E16 cells recapitulate key stages in the development of neuronal morphology during differentiation. Previous *in vitro* studies have found that primary rodent neuronal cultures are capable of generating unipolar neurons, with distinct primary and secondary dendrites akin to the apical and basal dendrites seen *in vivo* (Dotti et al., 1988; Horton et al., 2005; Threadgill et al., 1997). The development of a polarised neuronal morphology *in vitro* can be subdivided into four phases: the initial outgrowth of several processes; the specification of an axonal process; the specification of the other processes into dendrites; and the maturation of both axon and dendrites and subsequent synaptogenesis (Dotti et al., 1988; Fukata et al., 2002). This section will detail the investigation of the progressive development of key stages of neuronal morphology in CTX0E16 cells during differentiation.

To investigate the development of early development of neuronal morphological characteristics, DD0, DD2 and DD4 CTX0E16 cultures were immunostained for the marker of immature neurons and hNPCs, βIII-Tubulin (Tuj1). To assess later-stage neuronal morphology, CTX0E16 cultures were also transfected at DD13, DD18 and DD33 with a CMV-driven pEGFP construct. A qualitative examination of the transfected cells at each time point revealed that DD15 CTX0E16 cells were capable of developing the triangular somatic morphology consistent with that of cortical pyramidal neurons *in vivo* (see **Figure 3.2.7**, **D**) (Dichter, 1978; Kriegstein and Dichter, 1983). These cells also possessed neurites with multiple branch points at this stage. By DD20 neurites with distinct dendritic and axonal characteristics could be observed (**Figure 3.2.7**, **E**); a single long, thin process with a relatively uniform diameter extending from the soma (consistent with axonal morphology) and multiple shorter tapering processes reminiscent of early-stage dendrites (Fukata et al., 2002). Typically one of these dendrites

would extend from the apex of the cell soma much further than the others, similar to the polarisation of apical and basal dendrites seen on cortical pyramidal neurons *in vivo* (McAllister, 2000). By DD35 these dendrites had developed complex arbors and even some small filopodial protrusions protruding from the dendritic shaft, similar to the morphology of immature dendritic spines *in vivo* and *in vitro* (García-López et al., 2010; Irwin et al., 2001) (see **Figure 3.2.7**, **F-H**).

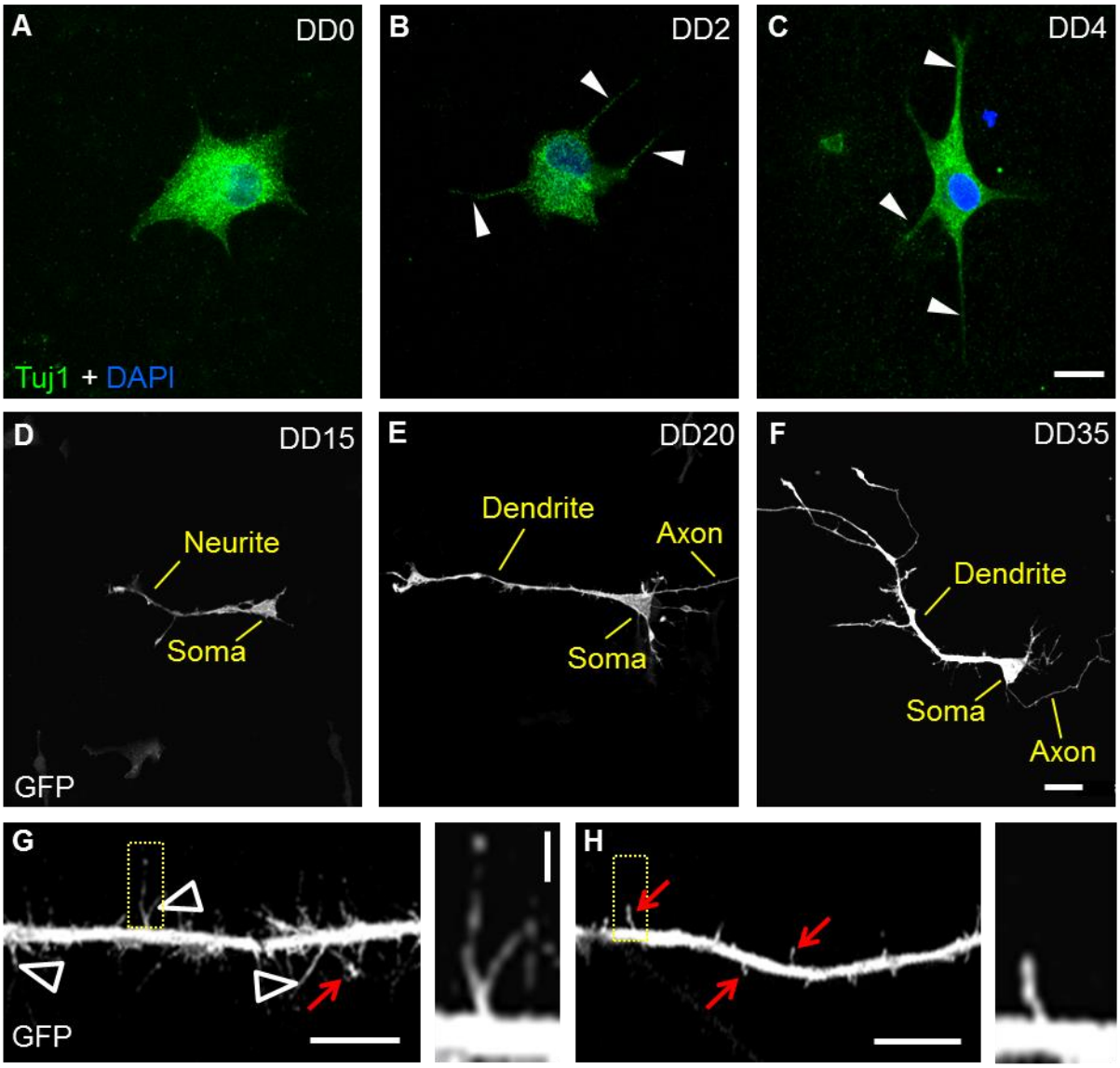

Figure 3.3.7: Differentiated CTX0E16 neurons display morphological features of pyramidal neurons. **A-C**: Generation of small neurites in βIII Tubulin (Tuj1)-positive CTX0E16 cells after 2 or 4 days of differentiation. **D-F**: Expression of green fluorescent protein (GFP) in young CTX0E16 neurons, reveals the development of neuronal morphology; at DD15, neurite processes extend from the cell's soma (**D**). By DD20, a single long and thin process can be seen emerging from the cell soma with a thicker single process also emerging from the opposite side. Note the pyramidal shape of the cell soma. **F**: By DD35, the dendritic process displays some level of arborisation; additional smaller processes protruding from the cell soma are also evident. **G & H**: Representative confocal images of a distal dendrite of GFP-

expressing CTX0E16 neurons (DD35). Examination of dendrites revealed the presence of filopodia (white arrow heads) and dendritic spine-like structures (red arrows), indicative of ongoing synaptogenesis. Yellow boxes indicate region used in high magnification in inset. Scale bars = 20 µm (**A-F**), 5 µm (**G & H**) & 1 µm (**G & H, inset**).

Taken together, these observations suggest that cells from the CTX0E16 line are capable of developing several key features of cortical neuron morphology after several weeks of differentiation. Crucially, these cells also develop filopodial protrusions consistent with early dendritic spine morphology, suggesting that CTX0E16 neurons may be capable of producing functional synapses. This avenue of inquiry is expanded on and discussed in **Chapter 4**.

3.3.8 POLARISATION OF SUBCELLULAR STRUCTURES IN CTX0E16 NEURONS

Following the initial findings of a polarised morphology in GFP-transfected CTX0E16 cultures, an investigation was conducted into the polarisation of the trans-Golgi apparatus in differentiated CTX0E16 neurons, another hallmark of the development of cortical neuron morphology *in vivo* and *in vitro* (Horton et al., 2006, 2005). Typically the trans-Golgi network localises to the apical dendrite of pyramidal neurons *in vivo* (Horton et al., 2005; Srivastava et al., 2012); interestingly, this phenomenon is also recapitulated in the primary dendrites of primary neuronal cultures (Jones et al., 2014; Srivastava et al., 2012). To confirm whether this polarisation also occurred in differentiated CTX0E16 neurons, DD35 CTX0E16 cultures were immunostained for the dendritic marker MAP2 and the cis-Golgi network protein GM130. The majority (83.89±4.55%) of MAP2-positive cells were found to have GM130 staining within the cell soma (see **Figure 3.2.8**, **A**). Notably, in the majority (81.96±4.96%) of these cells this staining was oriented towards a single MAP2-positive dendrite, typically the longest of the dendrites, consistent with a polarised neuronal morphology. Moreover, GM130 staining occasionally extended into this dendrite, consistent with the formation of primary dendrites and secretory networks seen in functional neurons *in vivo* and *in vitro* (**Figure 3.2.8**, **B**) (Horton et al., 2005). These findings further indicate that after several weeks of differentiation, CTX0E16 cultures are capable of generating neurons with a polarised morphology consistent with that of cortical pyramidal neurons in vivo.

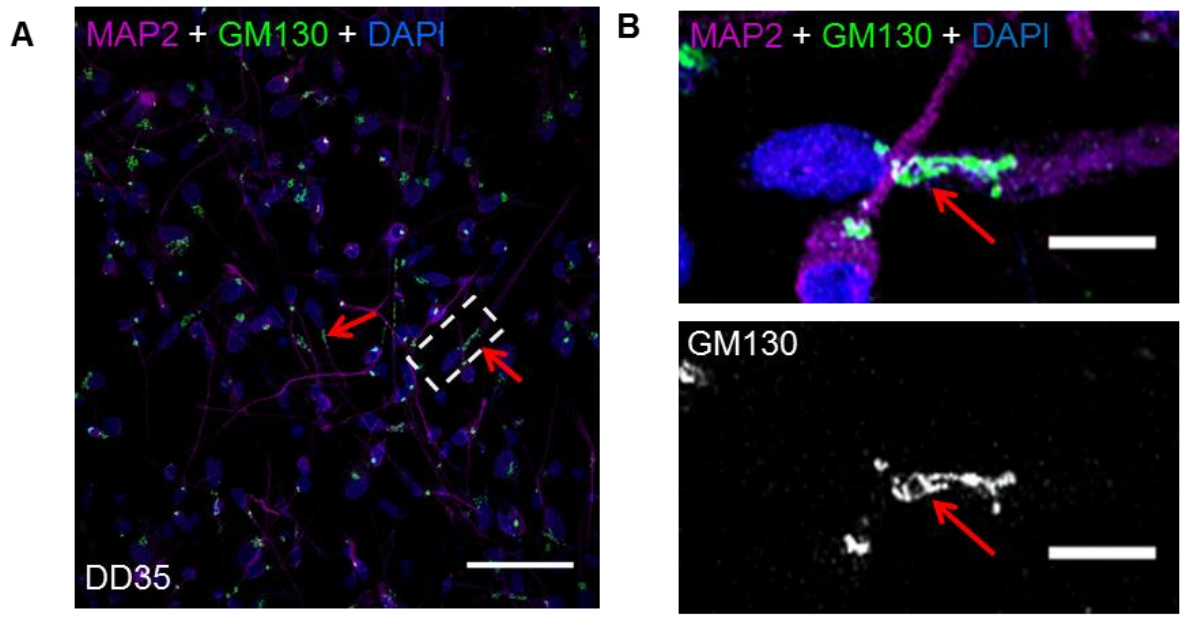

Figure 3.3.8: Differentiated CTX0E16 neurons exhibit polarisation of intracellular organelles. **A**: Double immunostaining of DD 35 CTX0E16 neurons for the trans-Golgi marker, GM130 and MAP2. In MAP2-positive neurons, GM130 is clearly seen orientated towards a single, typically the longest, dendrite (red arrows). This indicates the primary dendrite, and the formation of a polarised morphology). **B**: High-magnification images reveal that the Golgi-network is present along the primary dendrites (red arrow). Scale bars = 20 µm (**A**) & 5 µm (**B**).

3.4 DISCUSSION

This chapter has provided data on the optimisation of several protocols using the CTX0E16 cell line, and subsequently has shown the application of these protocols in the characterisation of the cell line at various time points during differentiation, via assessments of the expression of markers of cellular identity and synaptic proteins and an evaluation of the progressive development of key aspects of neuronal morphology. Taken together, these experiments have demonstrated that differentiation of the CTX0E16 cell line successfully produces pyramidal glutamatergic neurons and GABAergic interneurons, and these cells recapitulate the critical phases in the development of neuronal morphology that may be further studied in the context of neuropsychiatric disease-relevant mechanisms at the cellular level.

As a significant number of the experiments in this body of work involved the use of the CTX0E16 cell line, it was crucial to establish the optimal culture conditions to differentiate these NPCs for long periods of time without excessive cell density or cell death impacting the viability of this line as a tool for studying cellular phenomena. To this end, the optimisation of transfection and immunocytochemistry protocols was also of critical importance as a large proportion of the subsequent experiments in this

thesis rely on both of these techniques to investigate the cell line in later chapters. The successful application of transfection protocols to neurons of the CTX0E16 line proved highly valuable in the assessment of CTX0E16 morphology in this chapter, and this protocol may be a useful method for assessing the function of psychiatric disease-associated proteins via overexpression in further experiments.

Evidence has been presented indicating that CTX0E16 NPCs are multipotent, being capable of differentiating into mixed cultures primarily consisting of glutamatergic and GABAergic neurons, but also possessing a subset of astrocytes. The heterogeneity of differentiated CTX0E16 cultures was particularly interesting given that this line is reportedly derived from just a single NPC and therefore ostensibly a clonal population. During the development of the human forebrain glutamatergic neurons are generated by neural progenitors located within the ventricular zone of the pallium and migrate radially to form the cortical plate. In contrast to this, GABAergic interneurons are derived from separate populations of progenitors located within the subpallium: the medial, lateral and caudal ganglionic eminences as well as the preoptic area (Hansen et al., 2013; Ma et al., 2013). Newborn interneurons migrate along tangential routes into the neocortex, then switch to radial migration as they move to specific layers of the developing cortex (Ma et al., 2013). Each of these progenitor populations expresses a distinct set of regional markers; thus the putative lineage of NPCs from the CTX0E16 line may be determined on the basis of whether or not these cultures express dorsal or ventral telencephalic markers, and subsequently whether differentiated CTX0E16 neurons express markers of the neuronal populations known to arise from specific regions of the developing telencephalon.

Surprisingly, proliferative CTX0E16 cultures were shown to express not only markers seen in dorsal telencephalon progenitors such as *EMX1*, *OTX2* and *PAX6*, they were also demonstrated to express ventral markers including *NKX2.1*, *GBX2* and *DLX1*. Moreover, differentiated CTX0E16 cultures also simultaneously expressed *ISL1*, a marker typically expressed in lateral ganglionic eminence progenitors and striatal projection neurons (Stenman et al., 2003); and *TBR1*, expressed in cortical projection neurons (Englund et al., 2005). These findings were further reflected in data collated from a microarray of proliferative and differentiated (DD28) CTX0E16 cultures showing expression of markers of both the dorsal and ventral telencephalon, including several additional markers not included in the RT-PCR experiment. Taken together, these data suggest that rather than being a clonal

population derived from a single cell from a specific region of the developing telencephalon, the CTX0E16 line may instead be comprised of a mixed population of both dorsal and ventral telencephalic progenitors, which later differentiate into glutamatergic and GABAergic cortical neurons respectively. However, the simultaneous expression of dorsal and ventral telencephalic markers in a reportedly clonal line may also be an artefact of an *in vitro* culture system wherein these progenitors are not subjected to the influence of the same extracellular milieu as would be seen in human telencephalic development *in vivo*. Moreover, the simultaneous expression of markers indicative of multiple regional NPC identities may also be a consequence of the reprogramming process whereby the CTX0E16 cell line is conditionally immortalised following integration of the c-mycER^{TAM} transgene into the host genome.

Neural progenitor cells in the developing human forebrain can be further sub-divided into separate classes with distinct temporal and functional properties. Neuroepithelial progenitors are the first of these populations in the cerebral cortex, and give rise to radial glial cells (RGCs), a class of progenitors which subsequently produces all the excitatory neurons of the cortex (Otani et al., 2016). RGCs can produce neurons either directly via mitosis or indirectly via the generation of one of two further classes of progenitor cells: intermediate/basal progenitor cells (IPCs) or outer radial glial cells (oRGCs) (Otani et al., 2016). Each of these classes of progenitor can be distinguished from each other via the expression of distinct combinations of transcription factors, their morphology, their localisation within the developing cortical plate and the presence or absence of inter kinetic nuclear migration (IKNM) during mitosis. RGCs are found within the ventricular zone of the developing primate cortex, express neural stem cell and astroglial markers, exhibit both apical and basal processes and, unlike IPCs and oRGCs, display IKNM during mitosis (Ladran et al., 2013). IPCs are found primarily (but not exclusively) within the inner subventricular zone of the developing cortex, are typically *PAX6*-and *TBR2*-positive and typically exhibit no apical or basal processes (Betizeau et al., 2013; Englund et al., 2005; Otani et al., 2016). In contrast to this, oRGCs are found within the outer subventricular zone of the developing cortex, are typically *PAX6*-positive but *TBR2*-negative and can be further subclassified according to the exhibition of apical and/or basal processes (Betizeau et al., 2013). oRGCs have previously been suggested to contribute to the differences in cortical size between humans and other primates (Betizeau et al., 2013; Otani et al., 2016), and thus may be of particular interest in the study of cortical mechanisms underlying human psychiatric diseases. However, the identification of each of the above NPC populations in CTX0E16 cultures is problematic for several reasons: as the CTX0E16

cultures do not form neural rosettes, as in the case of 2D hiPSC cultures undergoing neuralisation, it is not possible to establish NPC identity via an assessment of localisation to a particular region of the cortex or any other analogous structure. Moreover, the lack of polarity in the NPC cultures may preclude the identification of directional processes in the CTX0E16 cells as an indicator of NPC subtypes. Finally, although *TBR2* and *PAX6* expression can be used generally to distinguish between IPC and oRGC populations *in vivo* and in polarised cultures, these markers are not specific enough to determine the identity of progenitor populations in non-polarised cultures *in vitro* (Betizeau et al., 2013; Otani et al., 2016; Shi et al., 2012a). In addition to this, analysis of the CTX0E16 microarray in **Section 3.3.4** did not produce any data on *TBR2* expression in this line. Future investigations utilising the CTX0E16 cell line may therefore benefit from the identification of markers specific to the oRGC and IPC populations.

Among the glutamatergic neurons within the differentiated CTX0E16 cultures, VGlut1 was observed in the cell soma of a large proportion of these cells. Although typically VGlut1 is not found in the cell soma of excitatory neurons, instead being limited to the presynaptic bouton (Herzog et al., 2006; Real et al., 2006), previous studies have found VGlut2 to be expressed within the cytoplasm of immature mouse neurons derived from embryonic stem cells and *in vivo* (Illes et al., 2009; Real et al., 2006). One possible explanation for this may be that the somatic localisation is due to an accumulation of synaptic proteins during early development and immediately prior to axogenesis and synaptogenesis. Thus, the presence of VGlut2 within the cell body of immature neurons may have arisen from the accumulation of synaptic proteins which are to be subsequently transported into the developing axon to facilitate synaptogenesis. This may also be the reason for the somatic localisation of VGlut1 seen in the relatively immature CTX0E16 neurons used in the present investigation.

Interestingly, MAP2-positive neurons in the differentiated CTX0E16 cultures were found to predominately express Ctip2, a marker expressed in deep layer neurons (Shi et al., 2012b). In contrast to this, the upper layer marker Cux1 was not found to be expressed at high levels in DD28 CTX0E16 neurons via ICC and microarray, though surprisingly expression of *BRN2*, another marker of upper layer neurons, was found to be upregulated after several weeks of differentiation in this microarray. A previous investigation conducted by Gaspard et al. (2008) using neural progenitor cells generated from mouse ESCs found that neurons expressing markers of specific cortical layers differentiated sequentially from these NPCs in a manner that mimicked the stages of cortical development *in vivo*.

Neurons expressing markers of deep cortical layers differentiated first, with superficial-layer markers being expressed by neurons that differentiated from the NPCs at a later time point. This has also been demonstrated in neurons differentiated from human iPSC lines (Paşca et al., 2011; Shi et al., 2012b). Given the relatively early developmental time point being assessed in the CTX0E16 cell line, neurons generated from these NPCs at later stages of differentiation may therefore preferentially express markers of upper layer neurons such as Cux1 rather than the lower layer markers seen in the present experiment, though time constraints precluded this experiment during the confines of the current study. If the sequential generation of cortical neurons with distinct layer-specific expression profiles is demonstrated in the CTX0E16 line in future experiments then this will indicate that these cells provide a useful model of the mechanisms of cortical development, similarly to ESC and iPSC methods but bypassing the ethical concerns and lengthy transduction process associated with these paradigms respectively (Brennand et al., 2014; Jakel et al., 2004). However, despite these interesting results it should be noted that Ctip2 expression has also been previously observed in GABAergic interneurons of the striatum, which in the human brain are derived from neural progenitors within the lateral ganglionic eminence of the ventral telencephalon (Arlotta et al., 2008). Given that CTX0E16 NPCs were found to express markers of the lateral ganglionic eminence (see **Section 3.3.4**), and that a relatively large proportion of differentiated CTX0E16 cells also express GABAergic markers, this may alternately account for why the number of Ctip2-positive neurons is comparatively high.

The development of key aspects of neuronal morphology during differentiation was also assessed using several experimental paradigms. Ultimately, CTX0E16 cultures were shown to be capable of generating cells which recapitulated several key phases in the establishment of neuronal morphology, including the initial outgrowth of several neurites, the specialisation of a single axon and multiple dendrites, an increase in dendritic arbour complexity and even the development of filopodia reminiscent of immature dendritic spines, further supporting the evidence suggesting that cells from the CTX0E16 cell line may be capable of generating functional synapses. Early neurite outgrowth is a critical stage in the development of neuronal morphology, and a wide range of proteins implicated in psychiatric disease are known to influence this process including Shank3 and Disc1 (Durand et al., 2012; Hattori et al., 2010). The early stages of CTX0E16 differentiation may therefore be a useful target for genetic and molecular manipulations in order to determine the role of other psychiatric disease-associated proteins in modulating this crucial developmental process. This experimental paradigm is

further explored in **Chapter 6**, where the impact of the siRNA-mediated knockdown of a protein linked to autism, schizophrenia and bipolar disorder, ZNF804A, on early neurite outgrowth in CTX0E16 neurons is assessed.

Dendritic spines are the primary site of excitatory glutamatergic neurotransmission within the mammalian forebrain. Alterations in the number and morphology of these spines within certain regions of the cortex are known to feature in autism spectrum disorders, bipolar disorder and schizophrenia (Hutsler and Zhang, 2010; Konopaske et al., 2014; Marchetto et al., 2010a; Sweet et al., 2009a), These changes are thought to underlie the altered connectivity demonstrated in these disorders, and ultimately may be a significant component of their overall etiology (Penzes et al., 2011). The demonstration of putative dendritic spines in neurons differentiated from the CTX0E16 line suggests that this line may be of use in studies of the genetic and molecular underpinnings of this spine pathology. However, the relative paucity of spines in DD35 CTX0E16 neurons currently precludes their use in such experiments at this developmental stage, and further differentiation may be required before spines are expressed in sufficient numbers to permit quantification. However, the punctate staining of several excitatory and inhibitory synaptic proteins seen along the MAP2-positive neurons in this study suggests that immature synapses may yet still be present on these neurons, and assessments of puncta density may therefore be a useful approximate marker of synapses in the CTX0E16 line in future studies. Dendritic spines have previously been demonstrated in neurons derived from human ESC and iPSC sources (Espuny-Camacho et al., 2013; Marchetto et al., 2010b), though neurons derived from these cells typically require multiple months of differentiation before the first of these spines appear. Clearly, optimisation of differentiation protocols for these lines and CTX0E16 cells to promote more rapid spinogenesis will be a critical area for further study in order to maximise their potential in future investigations of the cellular pathology underlying neuropsychiatric diseases.

Taken together, these data suggest that CTX0E16 cultures offer a useful platform for generating cultures of excitatory cortical neurons from a human source. This cell line provides a reliable method of continually generating mixed cultures comprised predominately of glutamateric and GABAergic cortical neurons and therefore may be of considerable use in studies of excitatory and inhibitory dysfunction underlying severe psychiatric disease. However, further work is first required to

determine whether these neurons are capable of producing physiological responses to chemical and pharmacological stimuli, as well as generating functional synapses, key hallmarks of neuronal identity.

To address these issues, **Chapter 4** will focus on characterising the functional responses to a variety of chemical stimuli in neurons from the CTX0E16 cell line, as well as the development of critical features of synaptic structure and function in these cells. This chapter will also discuss the relevance of these findings in relation to the study of psychiatric disease pathology, specifically that of schizophrenia and bipolar disorder.

MARKER	CELL TYPE LABELLED	FUNCTION
VGlut1	Canonical glutamatergic neurons; excitatory synapses	Vesicular glutamate transporter 1; key component of glutamatergic neurotransmission apparatus.
CaMKIIα	Excitatory pyramidal neurons	Ca^{2+}/calmodulin-dependent protein kinase II; key component of several intracellular signalling cascades and involved in long term potentiation.
VGAT	Inhibitory GABAergic and glycinergic neurons; inhibitory synapses	Vesicular GABA transporter; key component of GABAergic neurotransmission apparatus.
GAD65/67	GABAergic interneurons	Glutamate decarboxylase; responsible for synthesis of GABA in inhibitory interneurons.
Calretinin	Cortical interneurons	Calcium binding protein involved in calcium signalling.
Calbindin-D28k	Cortical interneurons	Calcium binding protein involved in calcium signalling.
Tbr1	Deep layer cortical neurons	Transcription factor involved in the regulation of neuron differentiation and migration.
Cux1	Superficial layer cortical neurons	DNA binding protein involved in the regulation of gene expression, morphogenesis and differentiation.
Ctip2	Deep layer cortical neurons	Regulates neuronal differentiation.
PSD-95	Post-synaptic density marker of neurons	Post-synaptic density scaffolding protein 95; core component of synapses

SAP97	Post-synaptic density marker of neurons	Synapse-associated protein 97; involved in neurotransmitter receptor trafficking in neurons.
GluN1	Glutamatergic synapses in neurons.	NMDA receptor subunit 1; key component of glutamatergic neurotransmission.
GluA2	Glutamatergic synapses in neurons.	AMPA receptor subunit 2; key component of glutamatergic neurotransmission.
Emx1	Cortical neurons and dorsal telencephalon progenitor cells	Transcription factor regulating telencephalic development.
Foxg1	Telencephalic progenitor cells and neurons	Transcription factor regulating telencephalic development.
Otx2	Neural progenitor cells in the forebrain and midbrain	Transcription factor regulating patterning of the forebrain/midbrain during development.
Pax6	Neural progenitor cells in the dorsal forebrain	Transcription factor involved in several developmental processes in the CNS.
Gad1	Cortical interneurons	Enzyme involved in the production of GABA from glutamate.
Dlx1	Lateral ganglionic eminence progenitor cells	Transcription factor regulating interneuron differentiation.
Isl1	Lateral ganglionic eminence progenitors and early striatal projection neurons	Transcription factor regulating cholinergic neuron identity
Nkx2.1	Progenitor cells within the medial ganglionic eminence	Transcription factor involved in ventral telencephalic patterning.

Dcx	Newborn cortical neurons	Microtubule-associated protein involved in cytoskeletal stabilisation during early neuronal maturation.
GFAP	Neural progenitor cells and astrocytes	Intermediate filament protein regulating cell shape.
Gbx2	Progenitor cells in the hindbrain	Transcription factor involved in hindbrain development.
Nestin	Neural stem cells	Intermediate filament protein regulating cytoskeletal remodelling.
MASH1	Cortical interneurons	Transcription factor involved in medial and lateral ganglionic eminence patterning and differentiation.
SP8	Cortical interneurons from the lateral and caudal ganglionic eminences	Transcription factor regulating patterning of the telencephalon.
Brn2	Upper layer neurons of the cortex	Transcription factor involved in the production of neocortical neurons.

Table 3.3.4: List of markers of functional and regional neuron identity and their key functions.

CHAPTER 4: DEVELOPMENT OF SYNAPSES AND FUNCTIONAL CHARACTERISTICS IN CTX0E16 NEURONS

4.1 SUMMARY

This chapter details the further functional characterisation of differentiated neurons from the CTX0E16 cell line, in particular the development of functional synapses and physiological attributes consistent with mature neurons *in vivo*. The expression of numerous synaptic proteins, including several which have been strongly implicated in the pathological mechanisms underlying neuropsychiatric disorders, is shown in differentiated CTX0E16 neurons. The pattern of synaptic protein expression in these neurons was consistent with previous findings showing that neurons diiferentiated from the CTX0E16 line adopt a predominately glutamatergic fate. This chapter also describes spontaneous and evoked physiological phenomena in CTX0E16 neurons: these cells are found to exhibit morphological plasticity in response to prolonged depolarisation, adopt functional Ca^{2+} responses to several neurotransmitters, exhibit spontaneous fluctuations in intracellular Ca^{2+} concentrations and produce key electrophysiological events including action potentials.

4.2 INTRODUCTION

The characterisation of neural lineages and the development of neuronal morphology in the CTX0E16 cell line in the previous chapter provided a valuable insight into the composition and function of CTX0E16 cultures, both during proliferation and after several weeks of differentiation. However, in order to determine whether differentiated CTX0E16 cells adopt the features of mature, cortical neurons it is critical to establish whether these cells develop functional synapses as well as the specific electrophysiological properties and responses to physiologically relevant stimuli consistent with those observed in previous *in vivo* research and in neuronal cultures derived from comparable cell lines.

The generation of synapses is a critical step in the differentiation of neurons during the development of the cerebral cortex (Huttenlocher and Dabholkar, 1997). The formation of synapses involves the recruitment and functional integration of a wide variety of scaffolding, intracellular signaling

and neurotransmitter receptor proteins at the presynaptic bouton and postsynaptic density (Tada and Sheng, 2006). The expression of synaptic proteins in a discrete “punctate” immunostaining pattern has been commonly used as a marker of putative synapses in previous *in vitro* and *in vivo* studies (Johnson et al., 2007; Pinches and Cline, 1998; Silver and Stryker, 1999; Washbourne et al., 2004; Woolfrey et al., 2009). Research into the properties of neurons differentiated from cortically-derived hNPCs have attempted to investigate the expression of synaptic proteins as markers of neuronal subtypes, including those corresponding to specific regions of the brain; or as markers of specific categories of synapses (Carpenter et al., 1999b; Lin et al., 2015; Zhang et al., 2008).

A characterisation of the expression and distribution of synaptic proteins in neurons derived from the CTX0E16 hNPC line will similarly be a critical experiment to assess neuronal identity and functionality in this line as well as highlighting the suitability of the cell line as a platform for investigating synaptogenesis and synaptic mechanisms in human neurons. As several proteins expressed at the synapse have been implicated in disease pathways in neuropsychiatric disorders (Penzes et al., 2011), establishing whether these proteins are expressed in the CTX0E16 cell line would be an important step in ascertaining the suitability of the CTX0E16 cell line in studies of neuropsychiatric disease mechanisms at the cellular and molecular level.

Morphological plasticity in response to neuronal activity or depolarising stimuli is another well characterised feature of mature neurons *in vitro*; neurite outgrowth and growth cone assays in particular have been used in a number of studies to assess this plasticity (Cohan and Kater, 1970; Fields et al., 1990; Krey et al., 2013; Schilling et al., 1991). Assessing this phenomenon in the CTX0E16 cell line would ideally require an experimental paradigm which has previously been successfully employed in a comparable human cell line.

Calcium responses have previously been used in numerous studies as a proxy marker of neuronal activity in response to treatment with neurotransmitters and depolarising stimuli (Nunes et al., 2003; Zhang et al., 2008). Calcium imaging can also be used as a means of investigating oscillations in intracellular calcium concentration in neurons. These oscillations are reflective of calcium influx via voltage-gated calcium channels following spontaneous neuronal activity and are a hallmark of functional, mature neurons (Cocks et al., 2013; Murphy et al., 1992). This method of assessing neuronal activity has been employed in previous studies of neuronal cultures differentiated from immortalised

human NPC lines (Cocks et al., 2013), and may therefore provide additional valuable information about the functional properties of differentiated CTX0E16 neurons. However, an electrophysiological assessment is likely to produce a more direct and detailed profile of these properties. Several facets of the electrophysiological makeup of the mature neuron have been used in previous studies as an indicator of neuronal and synaptic maturity in neuronal cultures generated from hNPC, hES and hiPSC lines, specifically postsynaptic currents, action potentials and the development of a mature resting potential (Gaspard et al., 2008; Johnson et al., 2007; Nunes et al., 2003; Paşca et al., 2011; Pedrosa et al., 2011). Taken together, an assessment of these features in CTX0E16 neurons would provide critical information on whether these cells are able to replicate key neuronal phenomena necessary for their regular functioning *in vivo*.

This chapter describes the further characterisation of neuronal cultures generated from the CTX0E16 cell line, in particular focusing on the development of synapses, electrophysiological characteristics and functional responses to neuronal activity-inducing stimuli. To investigate the development of synapses, DD28 CTX0E16 neurons were qualitatively assessed for the expression of a wide variety of inhibitory and excitatory synaptic proteins (as well as several neuropsychiatric disease-relevant proteins) in discrete puncta consistent with synaptic immunostaining *in vivo*. Colocalisation of pre- and postsynaptic protein puncta was also assessed in these neurons as a putative marker of fully formed synapses. Expression of several genes coding for key synaptic and intracellular signalling proteins was also quantified in proliferative and differentiated CTX0E16 cultures via q-PCR. morphological plasticity of differentiating CTX0E16 cells in response to depolarising stimuli was Intracellular fluctuations in calcium concentration in response to treatment with activity-inducing or –blocking stimuli as well as spontaneous calcium oscillations were also assessed in differentiated cultures as a means of determining whether CTX0E16 neurons exhibited Finally, the electrophysiological characteristics of CTX0E16 neurons were assessed at several time points of differentiation. Taken together, these lines of inquiry provided a more thorough understanding of the neuronal cells generated from the hNPC line, the synaptic and electrophysiological properties of these neurons, and ultimately showed that this cell line provides an ideal platform from which to launch investigations into the development and dysfunction of human cortical neurons.

4.3 RESULTS

4.3.1 DIFFERENTIATED CTX0E16 NEURONS EXPRESS KEY PRESYNAPTIC AND POSTSYNAPTIC PROTEINS

Glutamatergic synapses comprise the majority of inter-neuronal connections between pyramidal cells in the mammalian forebrain (Robinson, 1998). A key feature of mature, functional glutamatergic neurons is the presence of pre- and post-synaptic structures containing a wide range of key synapse-specific proteins including neurotransmitter receptor proteins (McAllister, 2007). Previous studies have utilised the expression of synaptic proteins as a marker of neuronal maturity *in vitro*. However, in cultures derived from hNPCs characterisation of synaptic protein expression has historically been superficial or entirely lacking from characterisation studies (Carpenter et al., 1999b; Lin et al., 2015; Zhang et al., 2008). Thus, a thorough assessment of synaptic protein expression in the CTX0E16 cell line would provide valuable insights into the characteristics of the synapses generated during differentiation, and subsequently would produce a useful platform from which to launch investigations into synaptic mechanisms in human neurons.

CTX0E16 cell cultures were differentiated up to DD35 then immunostained for the dendritic marker MAP2 as well as markers of the presynaptic and postsynaptic components of excitatory and inhibitory synapses. These included the postsynaptic density scaffolding protein PSD-95, excitatory postsynaptic markers such as the AMPA receptor subunits GluA1 and GluA2, the NMDA receptor subunit GluN1, the inhibitory postsynaptic marker gephyrin, the excitatory presynaptic markers Synapsin, bassoon and VGlut1 and the inhibitory presynaptic markers GAD65/67 and VGAT. Cultures were qualitatively assessed for the presence of punctate staining, a key characteristic of immunostaining for synaptic proteins in mature cortical neurons. Interestingly, discrete puncta could be observed along MAP2-positive dendrites for all synaptic proteins investigated in the DD35 neurons. The postsynaptic density protein PSD-95, the NMDA receptor subunit GluN1, and the AMPA receptor subunits GluA1 and GluA2 could all be found in discrete points along the dendrites of CTX0E16 neurons, strongly suggesting the presence of the postsynaptic densities of excitatory synapses (see **Figure 4.3.1, A-D**). Furthermore, gephyrin, a scaffolding protein typically present at the postsynaptic densities of inhibitory synapses, was also found along MAP2-positive dendrites in a pattern consistent with the established literature (Budreck and Scheiffele, 2007) (**Figure 4.3.1, E**).

In addition to this, several presynaptic proteins could be observed in punctate structures along MAP2-positive CTX0E16 dendrites, including excitatory markers such as the active zone protein bassoon and the vesicular proteins Synapsin and VGlut1 (**Figure 4.3.1**, **F-H**). Furthermore, inhibitory markers including the vesicular GABA transporter VGAT and the enzyme responsible for the production of GABA at inhibitory synapses, GAD65/67, were also observed, suggesting the potential for expression of functional GABAergic synapses in differentiated CTX0E16 cultures (**Figure 4.3.1**, **I & J**). Although these proteins would not typically be present within dendrites the juxtaposition with MAP2-positive processes is likely to be reflective of the close proximity of these presynaptic structures to the post-synaptic densities located on the adjacent dendrites. These findings are altogether highly suggestive of the development of both excitatory and inhibitory synapses in CTX0E16 neurons.

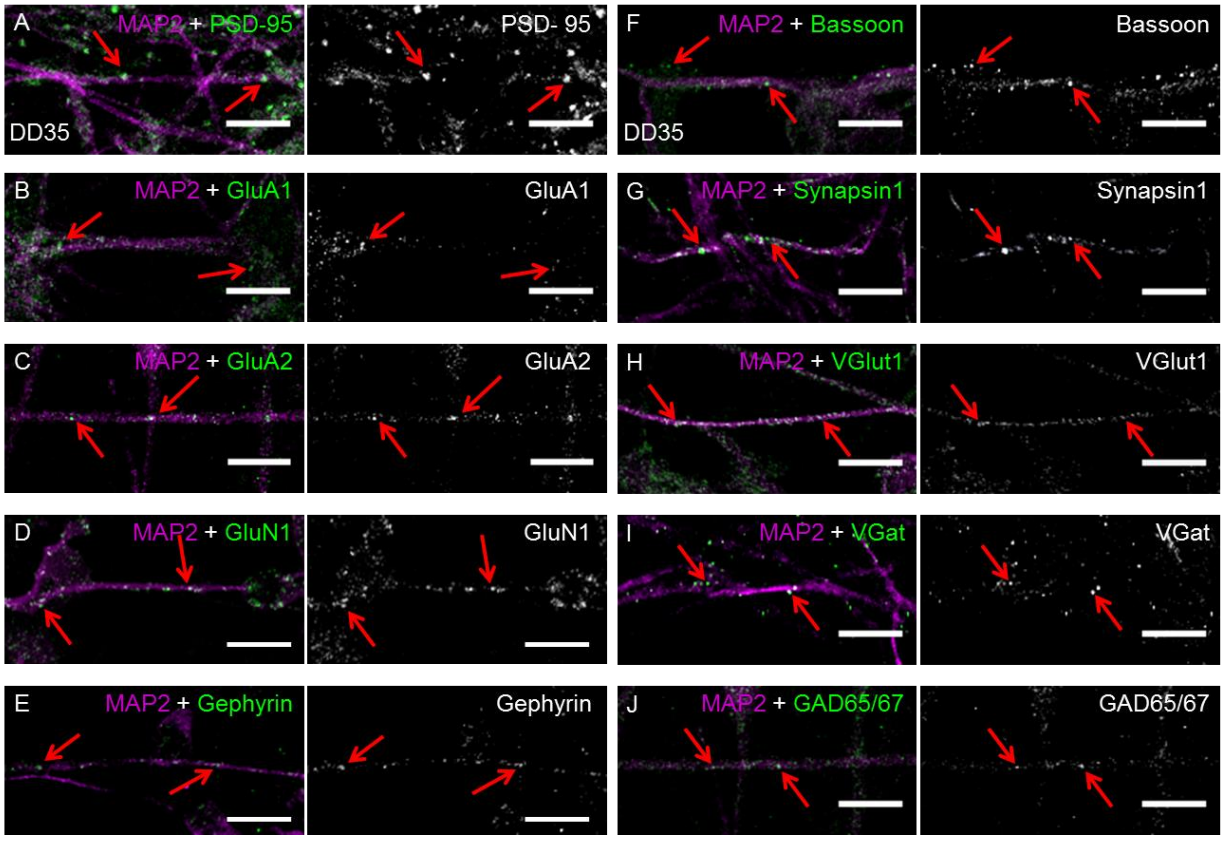

Figure 4.3.1: CTX0E16 neurons express key pre- and post-synaptic proteins. **A-E**: DD35 CTX0E16 neurons express puncta for the post-synaptic proteins PSD-95 (**A**), GluA1 (**B**), GluA2 (**C**), GluN1 (**D**) and gephyrin (**E**) along MAP2-positive dendrites (red arrows). **F-J**: CTX0E16 neurons also expressed the excitatory pre-synaptic proteins bassoon (**F**), synapsin1 (**G**) and VGlut1 (**H**) and the inhibitory pre-synaptic proteins VGAT (**I**) and GAD65/67 (**J**) in punctate structures juxtaposed along MAP2-positive dendrites. Scale bars = 5 µm.

In addition to these qualitative findings, PSD-95 and GluN1 were chosen as markers of putative synapses for the purposes of quantification due to the consistent high quality of the staining observed in the previous images. These images were assessed for synaptic density along MAP2-positive dendrites to determine whether CTX0E16 neurons produce comparable synaptic densities to those observed for other *in vitro* systems and *in vivo*. DD35 CTX0E16 neurons were found to express PSD-95 puncta along their dendrites at an average density of 3.38 ± 0.32 per 10 µm, while GluN1 was expressed at a comparable density of 3.07 ± 0.41 puncta per 10 µm of dendrite (see **Figure 4.3.2**, **A**).

Taken together, these data indicate that not only do DD35 CTX0E16 neurons express a wide variety of excitatory and inhibitory, pre- and postsynaptic proteins in a pattern reminiscent of synaptic structures seen in previous studies in human and rat neurons *in vitro* (Brennand et al., 2011b; Ippolito and Eroglu, 2010). Furthermore, analysis of the density of synaptic puncta along MAP2-positive dendrites in DD35 CTX0E16 neurons suggested that synapses were expressed in these neurons at a comparable level to that seen in immature rat primary cortical neurons and neurons derived from human iPSC lines, suggesting that the CTX0E16 cell line may provide a useful platform for studying the early development of synapses in human neurons.

4.3.2 PRE- AND POST-SYNAPTIC PROTEINS COLOCALISE ALONG DENDRITES IN CTX0E16 NEURONS

A key feature of functional, mature synapses is the presence of highly specialised pre- and postsynaptic structures at sites directly adjacent to one another (McAllister, 2007). Following the previous findings of putative dendritic spines and punctate staining for a wide variety of key presynaptic proteins, DD35 CTX0E16 neurons were further assessed to determine whether the postsynaptic density marker PSD-95 colocalised with markers of excitatory and inhibitory presynaptic boutons. Although PSD-95 is typically used as a marker of excitatory synapses, previous research has found PSD-95 to also localise to the postsynaptic densities of a subset of inhibitory synapses (Fattorini et al., 2009). DD35 CTX0E16 neurons were double fixed as described previously and immunostained for MAP2, PSD-95 and one of three presynaptic markers: the excitatory markers Synapsin and VGlut1 and the inhibitory synapse marker VGAT. Immunostained cultures were imaged using confocal microscopy with a 63x oil immersion objective, and images were background subtracted and Z-projected as described previously. Qualitative assessment of the dendrites of MAP2-positive CTX0E16 neurons revealed that postsynaptic PSD-95 puncta could be observed directly juxtaposed with puncta staining positive for

both excitatory (Synapsin, VGlut1) and inhibitory (VGAT) presynaptic markers. Taken together with the previous findings in **Section 3.3.8** of the appearance of dendritic spine-like structures along the dendrites of DD35 CTX0E16 neurons, these results indicate that CTX0E16 neurons are capable of producing key structural features of mature excitatory and inhibitory synapses after five weeks of differentiation.

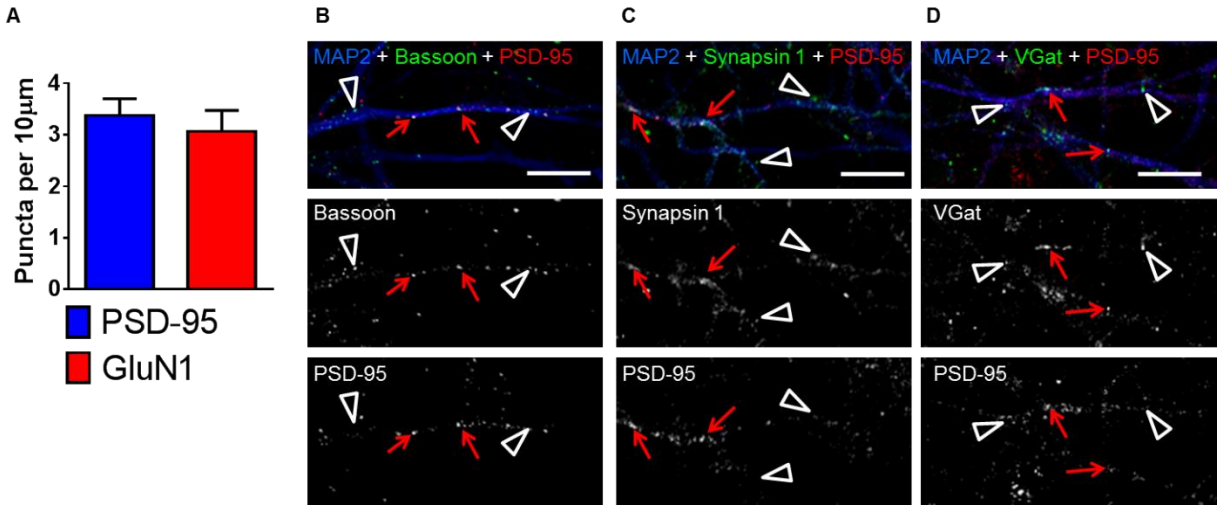

Figure 4.3.2: Synaptic density and hallmarks of putative synapses in differentiated CTX0E16 neurons. **A:** Quantification of PSD-95 and GluN1 puncta density in DD35 CTX0E16 neurons (puncta per 10 µm: PSD-95, 3.4±0.32; GluN1, 3.1±0.4). **B-D**: Representative confocal images of DD35 CTX0E16 neurons immunostained for MAP2, PSD-95 and either bassoon (**B**), synapsin 1 (**C**) or VGAT (**D**). As previously seen, all synaptic proteins display punctate distribution along MAP2-positive dendrites. In addition, a subset of PSD-95 puncta colocalised with all three pre-synaptic proteins (**red arrows**), indicating the presence of putative synapses; colocalisation is indicated in white. Not all presynaptic puncta colocalised with PSD-95 (**white open arrowheads**), suggesting that synaptogenesis was ongoing. Scale bars = 5 µm.

4.3.3 DIFFERENTIATED CTX0E16 NEURONS EXPRESS PROTEINS IMPLICATED IN NEUROPSYCHIATRIC DISEASE MECHANISMS

Synaptic structures are a common convergence point for pathways involved in the pathophysiology of several neuropsychiatric diseases (Penzes et al., 2011). Autism, schizophrenia and bipolar disorder all feature distinct pathological changes in synaptic structure and function (Bourgeron, 2009; Eastwood and Harrison, 2001), and a number of synaptic proteins have been implicated in the mechanisms underlying these complex diseases. To determine whether the CTX0E16 cell line would be a useful platform from which to conduct experiments investigating these mechanisms, the expression of several disease-related synaptic proteins was qualitatively expressed in CTX0E16 neurons. These

included Disc1, a postsynaptic density protein implicated in the pathophysiology of schizophrenia, bipolar disorder and depression; Shank3, a postsynaptic scaffolding protein thought to be involved in mechanisms underlying ASD and schizophrenia; and Neuroligin 3 (NL3), a postsynaptic adhesion protein associated with autism (Bourgeron, 2009; Craddock et al., 2005). DD35 or DD30 CTX0E16 cultures were immunostained for MAP2 in addition to the synaptic proteins Disc1, Shank3 and NL3. Images for each disease-associated protein were assessed for the presence of discrete synaptic puncta along MAP2-positive dendrites of CTX0E16 neurons (see **Figure 4.3.3**, **A-C**). For each protein, punctate staining could be observed along the MAP2-positive dendrites of CTX0E16 neurons at DD35, in a manner consistent with previous research (Budreck and Scheiffele, 2007; Durand et al., 2012; Wang et al., 2011b). These observations suggest that the CTX0E16 cell line may be a useful platform from which to launch investigations into the functions of several key neuropsychiatric disease-associated proteins - and how they relate to synaptic mechanisms – in human neurons.

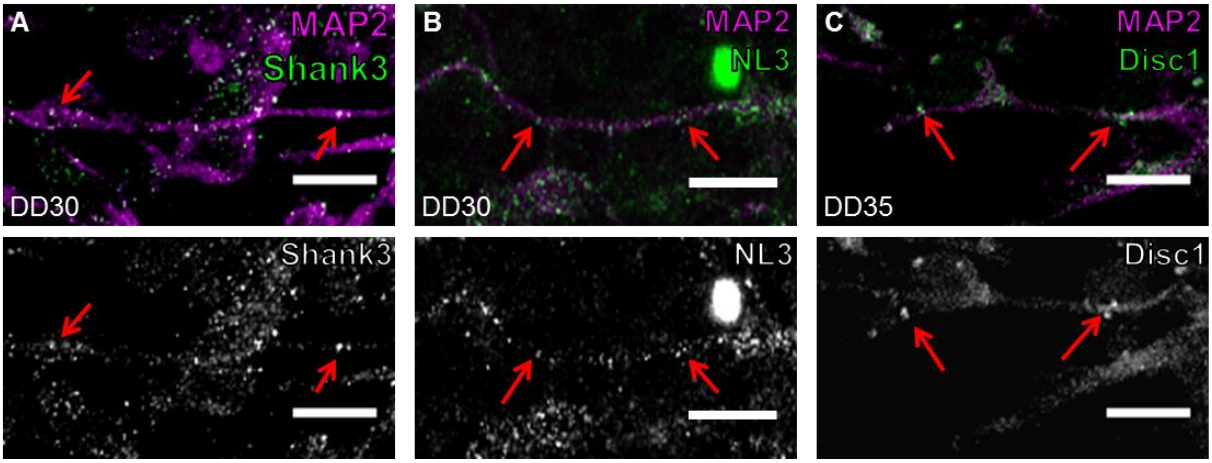

Figure 4.3.3: Differentiated CTX0E16 neurons express synaptic proteins associated with neurodevelopmental disease**. A-C:** Representative confocal images of DD30 and DD35 CTX0E16 neurons immunostained for MAP2 and endogenous Shank3 **(A)**, neuroligin 3 (NL3) **(B)** or Disc1 **(C).** Puncta were observed along MAP2-positive dendrites of CTX0E16 neurons in a manner consistent with previous research (**red arrows**). Scale bars = 5 µm.

4.3.4 EXPRESSION OF KEY SYNAPTIC AND SIGNALING PROTEINS IS UPREGULATED DURING DIFFERENTIATION OF THE CTX0E16 CELL LINE

The development of putative synaptic structures and expression of key synaptic proteins observed in differentiated CTX0E16 neurons suggested that these cells bear the hallmarks of mature neurons. To further investigate whether cells from the CTX0E16 line upregulated a range of key neuronal genes during differentiation, q-PCRs were performed on RNA samples from both proliferative

and DD28 CTX0E16 cultures. Mean measures of several key genes involved in intracellular signaling pathways (*PPP1R1B*, *GSK3B* and *SLC6A4*), neurotransmitter receptors (*GRIN1*, *GRIA2*, *GRM5*, *GABRA1* and *DRD2*) and other synaptic proteins (*CACNA1C*, *DLG4* and *CAMK2A*) were normalised against a geometric mean of three housekeeping genes (*GAPDH*, *HPRT1* and *RPL13A*) and compared across the two differentiation time points using an unpaired Student's t test with a posthoc correction for multiple comparisons (see **Table 4.3.4** for a summary of the assessed genes). Expression of the NMDA receptor subunit gene *GRIN1*, the AMPA receptor subunit gene *GRIA2*, the metabotropic glutamate receptor subunit gene *GRM5*, the GABA receptor subunit gene *GABRA1* and the dopamine receptor gene *DRD2* was significantly upregulated in differentiated CTX0E16 cultures relative to proliferative cells (see **Figure 4.3.4**, **A**). This increase in GABAergic and glutamatergic receptor expression is consistent with the neural lineages observed in differentiated cultures in **Section 3.2.5**. Furthermore, expression of the synaptic genes *DLG4* and *CAMK2A* as well as the calcium channel subunit gene *CACNA1C* increased significantly following 4 weeks of differentiation. This is consistent with the emergence of synaptic structures and expression of synaptic protein puncta observed in **Sections 4.3.1** and **4.3.2**. Finally, expression of the signaling protein gene *PPP1R1B* was significantly reduced in DD28 CTX0E16 neurons in comparison to proliferative cells, while *GSK3B* and *SLC6A4* expression was upregulated in the differentiated cultures in comparison to the hNPC cultures. Taken together, these data indicate that CTX0E16 hNPCs express a wide range of neurotransmitter receptor subunits, intracellular signaling proteins and other synaptic proteins which are upregulated after several weeks of differentiation. These findings also mirror the predominately glutamatergic identity of differentiated neurons observed in **Section 3.3.3**.

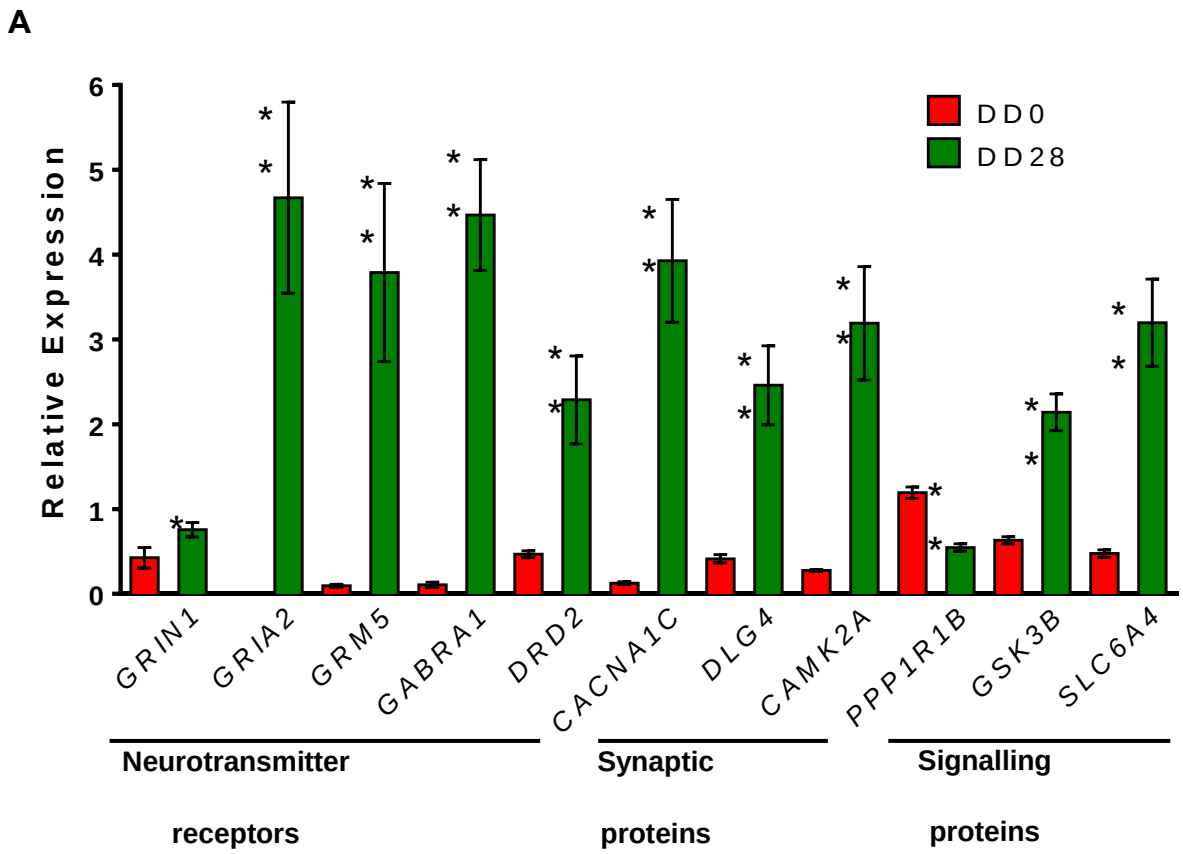

Figure 4.3.4: Upregulation of genes involved in neuronal function in CTX0E16 cultures after four weeks of differentiation. **A**: Expression of a subset of neurotransmitter receptors, synaptic and signalling proteins is increased in DD28 CTX0E16 neurons in comparison to proliferative (DD0) CTX0E16 hNPCs shown by quantitative PCR (q-PCR); n = 4 independent experiments carried out in triplicate; error bars represent SD; **p <0.01; ***p <0.001 (Student's unpaired t test). This work was carried out by Dr. Greg Anderson.

4.3.5 IMMATURE CTX0E16 NEURONS EXHIBIT MORPHOLOGICAL PLASTICITY IN RESPONSE TO PROLONGED DEPOLARISATION

As demonstrated in **Section 3.3.8** in the CTX0E16 cell line and in previous studies, the morphology of a neuron and functional identity of outgrowing neurites (both axonal and dendritic) is progressively established early on in development. The extension and arborisation of dendritic and axonal processes is highly regulated and critical to the formation of neural circuits and synaptic connections as well as the processing of synaptic inputs. During development neuronal morphology is highly plastic and susceptible to manipulation in response to a wide range of physiological and pathological mechanisms. Neuronal activity can act as an important regulator of neuronal development and has also been established as a mediator of dendritic and axonal outgrowth and arborisation.

Crucially, the impact of neuronal activity on neurite extension and retraction hinges on several factors including the maturity of the neurons studied, the species and brain region from which the neurons are derived, the intracellular calcium concentration induced by the neuronal activity and the duration of depolarisation. Typically, short bursts of neuronal activity appear to arrest or even reverse neurite outgrowth in neuronal cultures (Cohan and Kater, 1970; Fields et al., 1990; Schilling et al., 1991). However, prolonged depolarisation of neuronal cultures appears to enhance neurite outgrowth via a calcium-dependent process. Interestingly, a previous study conducted by Krey et al. (2013) found that prolonged depolarisation of hiPSC-derived neurons resulted in a significant increase in neurite length via a calcium-dependent mechanism. To determine whether CTX0E16 neurons exhibited comparable morphological plasticity at an early stage of differentiation in response to prolonged depolarisation, DD13 CTX0E16 cultures were transfected with a CMV-driven pEGFP plasmid as described previously. Cultures were treated with one of three conditions for 7 hours: control NDM media, an osmotic control consisting of NDM supplemented with 30 mM NaCl and depolarisation media consisting of NDM supplemented with 30 mM KCl. A one way ANOVA with Tukey post-hoc analysis for multiple comparisons was performed on neurite tracing data for each of the three conditions; this revealed that neuronal cells from cultures treated with 30 mM KCl for 7 hours were found to possess significantly longer neurites than those of the two control culture conditions (average neurite length (μm): control, 20.46 ± 1.76 μm; 30 mM NaCl, 21.03 ± 1.20 μm; 30 mM KCl, 31.95 ± 6.02 μm; n = 12−22 cells, ANOVA, $p < 0.05$) (see **Figure 4.3.5**, **A** & **B**). This finding indicates that DD15 CTX0E16 neuronal cells are capable of exhibiting morphological plasticity in response to prolonged depolarisation in a manner consistent with previous studies (Krey et al., 2013), indicating that they display the functional characteristics of developing synaptic networks *in vivo*.

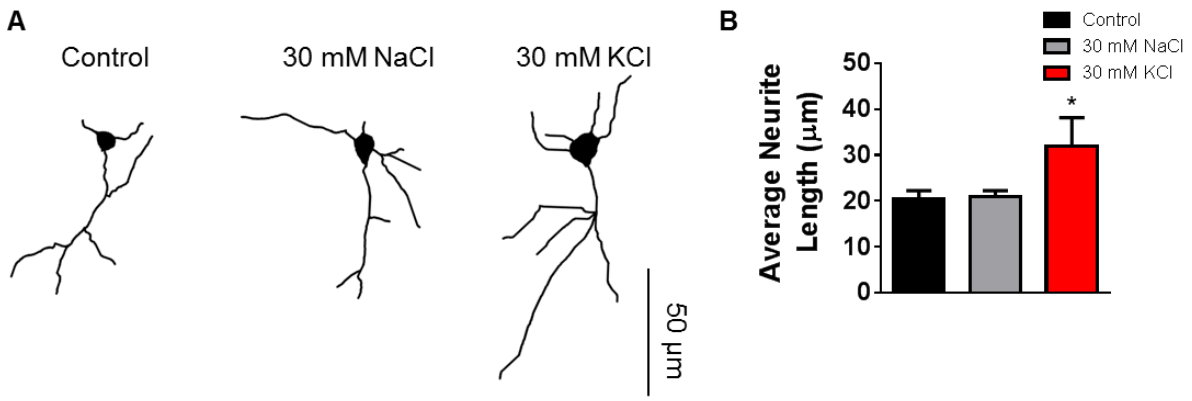

Figure 4.3.5: Differentiated CTX0E16 neurons exhibit morphological plasticity in response to activity-dependent stimulation. **A**: Representative binary images of GFP-expressing CTX0E16 neurons (DD 15) following treatment with control conditions (vehicle or osmotic control (30 nM NaCl)) or activity-dependent stimulation with 30 nM KCl for 7 hours. **B**: Measurement of average neurite length in response to stimulation demonstrates that activity-dependent stimulation results in an increase in average neurite length; n = 14–22 neurons from 3–5 independent experiments carried out in triplicate; error bars represent SEM; *p <0.05 (one way analysis of variance with Tukey post hoc analysis). Scale bar = 50 µm.

4.3.6 DIFFERENTIATED CTX0E16 CELLS EXHIBIT ELECTROPHYSIOLOGICAL CHARACTERISTICS OF FUNCTIONAL NEURONS

Based on the immunostaining data in **Sections 3.3.3**, **3.3.6**, **4.2.1** and **4.2.2**, and the data on morphological plasticity in **Section 4.3.5**, CTX0E16 neurons exhibit the structural characteristics of functional synapses and express a wide range of signaling, scaffolding and neurotransmitter receptor proteins, and these cells respond to depolarising stimuli by exhibiting morphological plasticity, indicating that they also possess key ion channels even at an early stage of differentiation. To determine whether these proteins are functionally integrated in CTX0E16 neurons and subsequently, whether these cells possess physiological characteristics consistent with mature, functional neurons, the electrophysiological properties of CTX0E16 neurons were assessed using current and voltage clamp recordings via whole cell patch clamps at several time points during differentiation. CTX0E16 cultures were differentiated up to DD61, with voltage clamp recordings being carried out at DD33, DD36 and DD50 to record NMDA receptor-mediated spontaneous excitatory postsynaptic currents (EPSCs), AMPA receptor-mediated EPSCs and action potentials respectively. Current clamp recordings of cell resting membrane potentials took place at DD29, DD33 and DD61. Resting potentials of CTX0E16 neurons were initially depolarised and steadily became more negative at later stages of differentiation (DD29: −31.3 mV, n = 6; DD33: −51.25 mV, n = 4; DD61: −56.4 mV, n = 3) (see **Figure 4.3.6**, **A**); this

is highly consistent with previous studies indicating that neuronal resting membrane potentials are typically less polarised but highly variable in immature neurons and gradually become more polarised but less variable over the time course of differentiation (Johnson et al., 2007; Magnuson et al., 1995; Vierbuchen et al., 2010).

One of the key stages in the development of mature, functional neurons both *in vivo* and *in vitro* is the attainment of action potential generation, a crucial form of cell-cell communication within the brain (Khazipov and Luhmann, 2006; Luhmann et al., 2000; Nunes et al., 2003). To determine whether cells from differentiated CTX0E16 cultures reproduce this critical event, CTX0E16 neurons were assessed at several time points from DD33 to DD61 via cell-attached voltage clamp recordings. Action potentials only became apparent in CTX0E16 cultures from DD50 onwards, while burst firing of CTX0E16 neurons did not develop over the time course investigated in the current experiment (**Figure 4.3.6**, **B**). Another hallmark of functional synapses is the generation of spontaneous EPSCs (via excitatory synapses) and IPSCs (via inhibitory synapses). To determine whether CTX0E16 neurons possessed the ability to produce spontaneous EPSCs and IPSCs, differentiated CTX0E16 cultures (DD33-35) were monitored using cell-attached voltage clamp recordings. AMPA receptor-mediated EPSCs were recorded using a holding potential of -70mV; a holding potential of +40mV was used to record NMDA receptor mediated EPSCs; and GABA-mediated IPSCs were recorded using a holding potential of +0mV. Whole-cell voltage clamp recordings revealed that after around five weeks of differentiation a subset of neurons in CTX0E16 cultures exhibited spontaneous EPSCs, mediated by both AMPA and NMDA receptors (**Figure 4.3.6**, **C** & **D**). These findings are consistent with the results seen in **Sections 3.2.5** and **4.3.1**, where the expression of multiple markers of glutamatergic neurons and excitatory synaptic structures were observed in a majority of differentiated CTX0E16 neurons. However, spontaneous IPSCs could not be detected in CTX0E16 cultures at this stage of differentiation, indicating that these cells had not yet develped functional inhibitory synapses. Taken together, these data indicate that CTX0E16 neurons develop key physiological characteristics that progressively grow more consistent with those of mature, functional neurons over the course of several weeks of differentiation.

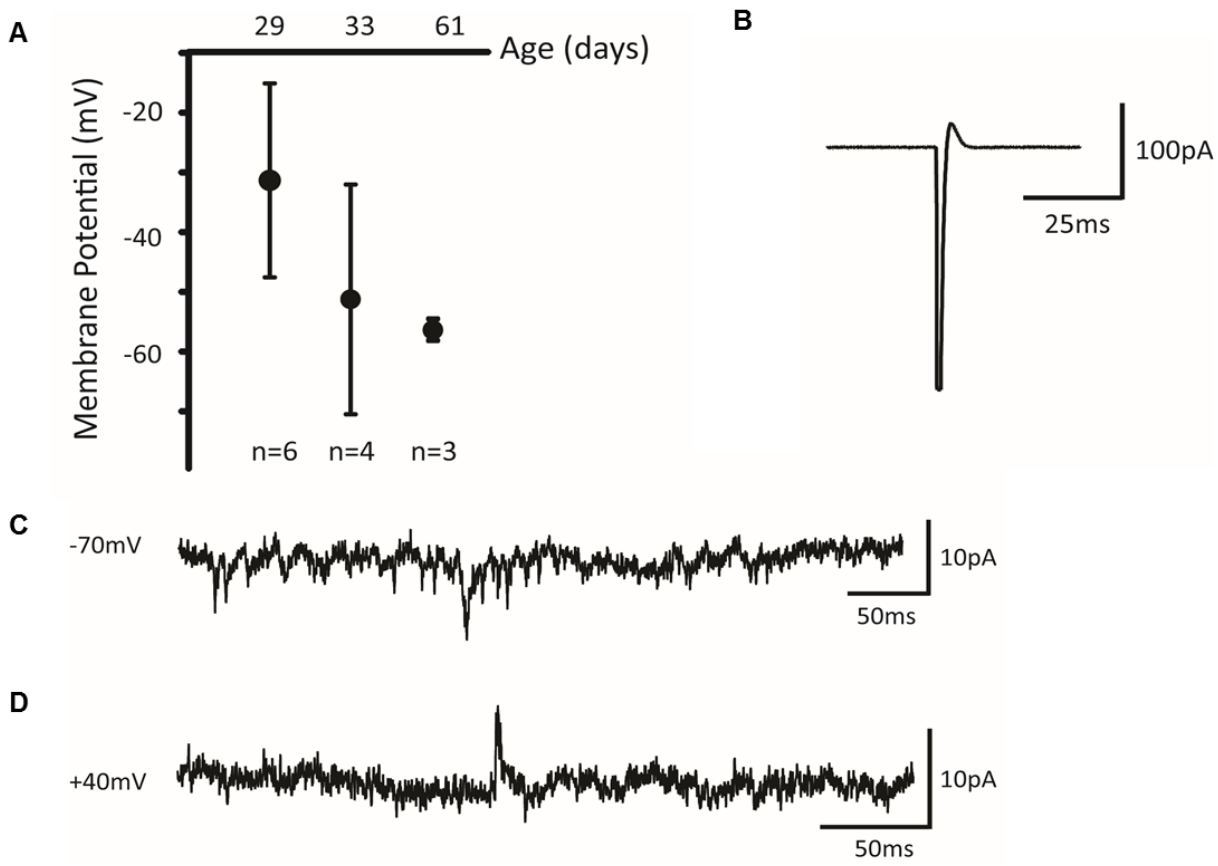

Figure 4.3.6: Development of electrophysiological properties in differentiated CTX0E16 neurons. **A**: Resting membrane potential (in mV) recorded using current clamp progressively becomes more negative throughout differentiation of CTX0E16 neurons (DD29−DD61); error bars represent SD. **B**: Representative action potential recorded in voltage clamp using the cell attached configuration, recorded in DD50 CTX0E16 neurons. **C:** Representative voltage clamp recording at a holding potential of −70 mV in DD36 CTX0E16 neurons. The downward deflections indicate the presence of AMPA receptor-mediated spontaneous excitatory postsynaptic currents (EPSCs). **D**: Example of a spontaneous N-methyl-D-aspartate (NMDA) receptor-mediated EPSC recorded in voltage clamp at +40 mV from DD33 CTX0E16 neurons; n=3–6 cells from at least three independent coverslips. This work was conducted by Dr. Ruth Taylor.

4.3.7 CTX0E16 NEURONS DISPLAY FLUCTUATIONS IN INTRACELLULAR CALCIUM CONCENTRATIONS IN RESPONSE TO PHYSIOLOGICAL STIMULI

Calcium imaging was used to investigate whether differentiated CTX0E16 neurons displayed physiological responses to several key neurotransmitters and exhibited oscillations in intracellular [Ca^{2+}] due to neuronal activity. DD28 CTX0E16 cultures were loaded with Fura-2 AM ratiometric dye, an

intracellular calcium indicator, and then treated with 1 mM glutamate, acetylcholine or dopamine in HEPES-buffered physiological saline solution for 1 minute. Successful loading of cultures with this dye was demonstrated by fluorescent emissions from CTX0E16 cells at 520 nm following excitation at 380 nm as described in **Section 2.8** of the materials and methods chapter (see **Figure 4.3.7**, **A**). DD28 CTX0E16 cells exposed to the glutamate condition exhibited both rapid, strong responses and slower, less pronounced responses after treatment (**Figure 4.3.7**, **B**). The former of these responses is likely to be brought about via fast-activation of AMPA or NMDA receptors, while the lower magnitude responses are likely to be mediated by metabotropic glutamate receptors. Approximately 80% of CTX0E16 cells were found to increase intracellular Ca^{2+} concentrations following treatment with glutamate, though these responses were typically modest: just over 30% of cells produced a response of 20% above baseline and less than 20% producing a response of 50% above baseline; the average increase in intracellular Ca^{2+} for all cells was approximately 20% above the baseline level (**Figure 4.3.7**, **E** & **F**).

Treatment with acetylcholine produced potent responses in nearly all CTX0E16 cells assessed. More than 60% of cells produced responses of 20% above baseline, while 40% of cells produced responses of 50% above baseline; the average response for all cells was nearly 50% above baseline, a finding that was more than double than that found for glutamate and an order of magnitude greater than the average response to treatment with dopamine (**Figure 4.3.7**, **C, E** & **F**). Assessment of individual traces indicated that predominately these responses consisted of a rapid yet sustained increase in intracellular Ca^{2+}, though a subset of cells showed a slower increase in the magnitude of the response.

In contrast to the responses to glutamate and acetylcholine treatment, dopamine-mediated responses were considerably smaller and exhibited a more gradual or delayed increase in intracellular Ca^{2+} (**Figure 4.3.7**, **D**). This is consistent with previous research showing that the physiological actions of dopamine on neuronal signalling and intracellular calcium are exerted through metabotropic receptors (Beaulieu and Gainetdinov, 2011). Less than 40% of total cells exhibited Ca^{2+} responses that were greater than 5% above baseline, and less than 3% of total cells exhibited responses that exceeded a level 20% above baseline (**Figure 4.3.7**, **E** & **F**).

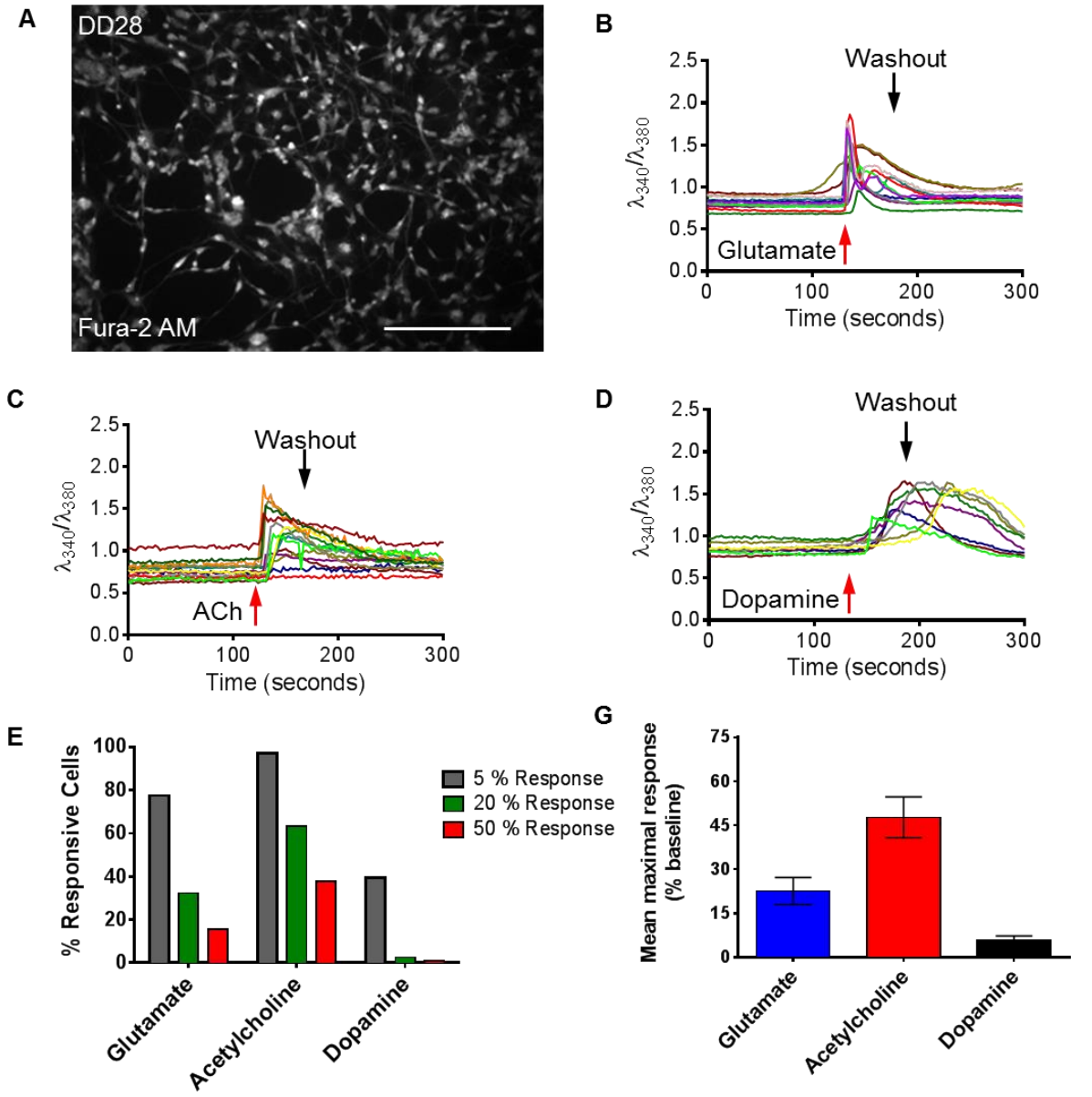

Figure 4.3.7: CTX0E16 cultures generate neurons that respond to treatment with neurotransmitters. **A**: Representative image of neurons loaded with Fura-2 AM used for single cell Ca2+ imaging. **B-F**: Representative traces of intracellular Ca2+ in response to various neurotransmitter receptor ligands. **E**: Number (%) of total cells generating 5%, 20% or 50% responses following treatment with neurotransmitter ligands; n = 3 independent experiments carried out in triplicate (600 cells in total). **F**: Mean maximal response produced by DD28 CTX0E16 neurons following application of neurotransmitter ligands; n = 3 independent experiments carried out in triplicate (600 cells in total); error bars represent SD. Scale bar for **A** = 50 µm. This work was conducted by Dr. Greg Anderson.

4.3.8 CTX0E16 NEURONS DISPLAY SPONTANEOUS CALCIUM OSCILLATIONS

Another feature of the early maturation of neuronal cells is the development of spontaneous rhythmic fluctuations in the intracellular concentration of Ca^{2+} in response to neuronal activity (Spitzer, 2002). To determine whether CTX0E16 cells exhibited these Ca^{2+} oscillations, DD28 and DD42 CTX0E16 cultures were assessed using single cell Ca^{2+} imaging with Fluo-4, another fluorescent Ca^{2+} indicator. Fluo-4 fluorescence in individual cells was time lapse recorded using epifluorescent microscopy with a temporal resolution of 1 image per second (see **Figure 4.3.8**, **A**). Spontaneous activity was defined as the presence of a sharp transient increase in fluorescence intensity with a rapid rise and slow decay in the soma of CTX0E16 cells with clear dendritic processes (see **Section 2.8** for the full protocol). No spontaneous oscillations in intracellular Ca^{2+} concentrations could be detected in DD28 CTX0E16 cultures. In DD42 cultures however, Ca^{2+} oscillations could be detected in 38.0 ± 6.89% of CTX0E16 neurons, indicating that by this stage of differentiation CTX0E16 cells exhibit physiological events consistent with functionally active neurons *in vivo* (**Figure 4.3.8**, **B**).

To determine whether intracellular Ca^{2+} concentrations in CTX0E16 neurons could also be manipulated through treatment with depolarising or activity-blocking stimuli, DD42 CTX0E16 cultures were loaded with Fluo-4 dye, treated with 50 mM KCl or 1 µM TTX and imaged as described previously. Application of KCl resulted in a marked influx of Ca^{2+} in 79.1 ± 4.2% of DD42 CTX0E16 neurons, indicating the presence of voltage-gated Ca^{2+} channels (**Figure 4.3.8, C**). Treatment with TTX, a voltage-gated sodium channel blocker, halted spontaneous Ca^{2+} transients in DD42 CTX0E16 cultures, indicating that these transients were mediated by neuronal activity via voltage-gated sodium channels (**Figure 4.3.8**, **D**). Taken together, these data demonstrate that not only do differentiated CTX0E16 neurons respond to several key neurotransmitters, but they also exhibit spontaneous and evoked fluctuations in the intracellular concentration of calcium that were blocked by the addition of TTX, further indicating the presence of functional synapses in differentiated CTX0E16 cells.

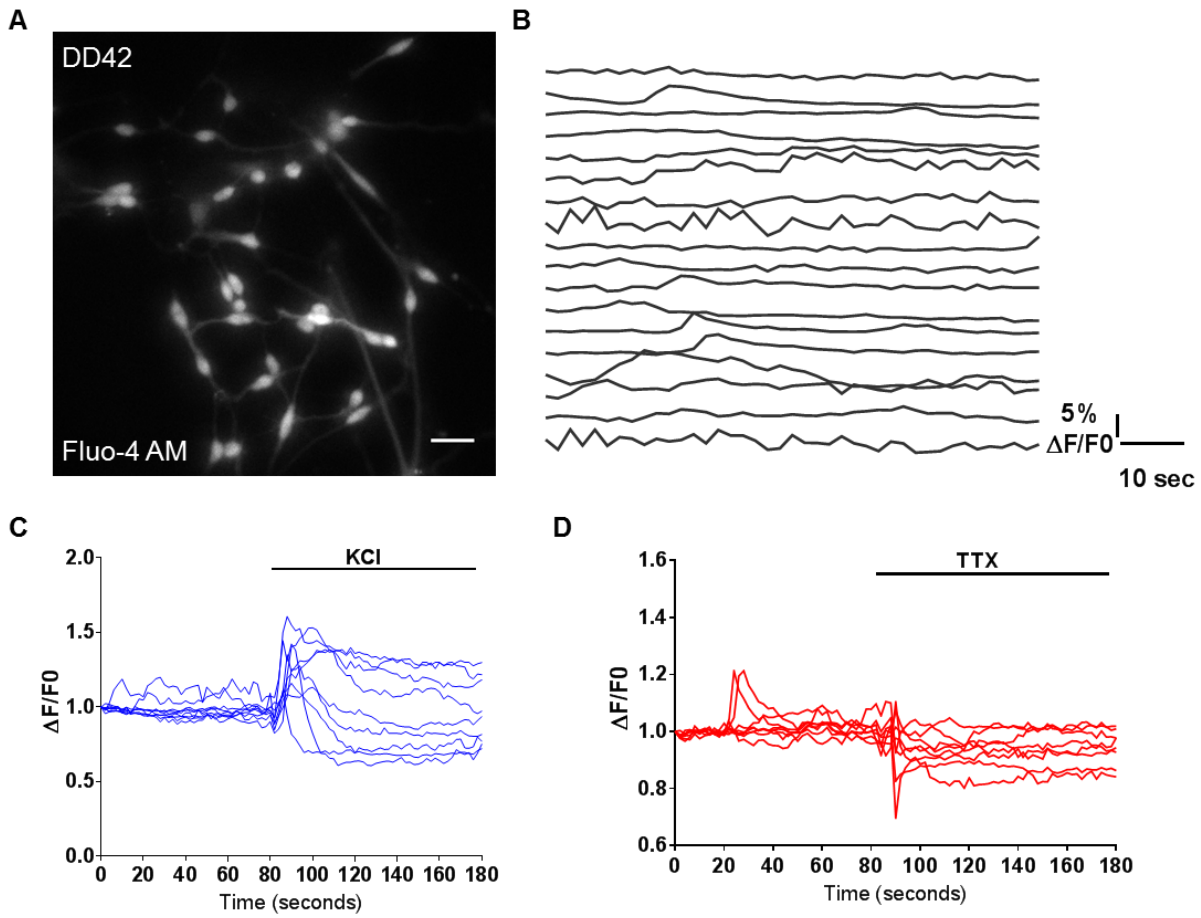

Figure 4.3.8: Development of spontaneous calcium oscillations in CTX0E16 neurons. **A**: Representative image of DD42 CTX0E16 neurons loaded with Fluo-4 AM and used for single cell Ca^{2+} imaging. **B**: Representative time series of 18 neurons displaying spontaneous Ca^{2+} transients. Spontaneous activity was classified as a somatic calcium event greater than 5% ΔF/F0. 38.0 ± 6.89% of DD42 CTX0E16 cells displayed spontaneous activity over an 80-second period of imaging (n = 155 cells from 14 coverslips). **C** & **D**: Representative traces of intracellular Ca^{2+} in response to 50 mM KCl (**C**) or 1 μM tetrodotoxin (TTX) (**D**). Scale bar for **A** = 10 μm. This work was conducted by Dr. Greg Anderson.

4.4 DISCUSSION

This chapter has provided data on the development of putative excitatory and inhibitory synapses in neurons from the CTX0E16 cell line, outlining the broad variety of presynaptic and postsynaptic proteins, including several disease-relevant proteins, expressed in these cells. This chapter has also shown the relative density of these synaptic puncta along the MAP2-positive dendrites of these cells, and the upregulation of genes involved in neurotransmission and intracellular signaling after several weeks of differentiation in the CTX0E16 cell line. Morphological plasticity during early neurite outgrowth is described Data is also presented on the spontaneous and activity-induced fluctuations in intracellular calcium concentrations observed in differentiated CTX0E16 cultures.

The broad range of excitatory and inhibitory synaptic proteins expressed by differentiated CTX0E16 neurons at DD35 indicate that even at this relatively early stage the development of functional synapses is well underway. Synaptic proteins were found to be expressed in discrete puncta reminiscent of synaptic immunostaining *in vivo*. Furthermore, both excitatory and inhibitory presynaptic proteins were found to colocalise with the postsynaptic density protein PSD-95, suggestive of mature, functional synapses with both pre- and postsynaptic structures. Although PSD-95 is predominately localised to excitatory synapses, it has also been found to localise to a subset of inhibitory synapses. Furthermore, VGAT and VGlut1 have been found to colocalise at a subset of synapses, permitting selective release of both glutamate and GABA as a potential preventative measure against systemic overexcitability (Fattorini et al., 2009; Zander et al., 2010). Supporting this, spontaneous excitatory postsynaptic currents observed at a similar time point (DD33 and DD36 for ionotropic NMDA and AMPA receptor-mediated currents respectively), but inhibitory postsynaptic currents could not be observed at all during the time course assayed in the present study. This suggests that the immunostaining of synaptic puncta in DD35 CTX0E16 neurons is representative of functional excitatory synapses with both NMDA- and AMPA-receptor mediated EPSCs. Furthermore, the lack of spontaneous GABA receptor-mediated IPSCs in these neurons may be a result of multiple factors, including the relative paucity of GABAergic neurons in the differentiated cultures, the early stage of differentiation of these cells relative to foetal brain development *in vivo* and the possibility that at this early stage of differentiation GABAergic synapses in these neurons are excitatory (Cherubini et al., 1991). Previous research has found that GABA acts as an excitatory neurotransmitter early on in development, and later switches to an inhibitory neurotransmitter due to a shift in the cross-membrane chloride ion gradient

(Taketo and Yoshioka, 2000). It is therefore possible that there are functional excitatory GABAergic synapses in these cultures that will adopt an inhibitory role later in differentiation.

CTX0E16 neurons also express several synaptic proteins which have been implicated in severe neuropsychiatric illness in discrete puncta along MAP2-positive dendrites in a manner consistent with previous studies (Budreck and Scheiffele, 2007; Durand et al., 2012; Wang et al., 2011b), including Disc1, Shank3 and Neuroligin 3. Prior research has found a balanced chromosomal translocation disrupting the gene coding for Disc1 to segregate with severe mental illness in a large Scottish pedigree (Millar et al., 2000); subsequent studies have reported that mutations in the DISC1 gene were associated with schizophrenia-relevant endophenotypes and there is evidence to suggest rare DISC1 variants are associated with both schizophrenia and bipolar disorder (Callicott et al., 2005; Kamiya et al., 2005; Saetre et al., 2008; Serretti and Mandelli, 2008). Mechanistic studies have found the Disc1 protein to be involved in a wide range of cellular mechanisms including the regulation of cell adhesion, neurite outgrowth, dendritic spine morphology and synaptic activity (Hattori et al., 2007, 2010; Hayashi-Takagi et al., 2010; Wang et al., 2011b). The SHANK3 gene codes for a scaffolding protein that is recruited to the postsynaptic density early on in synaptic maturation and has been found to regulate dendritic spine density and morphology and metabotropic glutamate receptor-mediated signaling (Durand et al., 2012; Roussignol et al., 2005; Sheng and Kim, 2000; Verpelli et al., 2011). Mutations in this gene have been associated with an increased risk of developing autism spectrum disorder (ASD) and schizophrenia (Durand et al., 2007; Gauthier et al., 2010). Neuroligin 3, a cell adhesion protein at glutamatergic and GABAergic synapses, has been found to play a role in the regulation of inhibitory neurotransmission (Budreck and Scheiffele, 2007; Südhof, 2008); mutations in NLGN3, the gene coding for the neuroligin 3 protein, have also been found to be associated with an increased risk of ASD (Südhof, 2008). The findings of the current investigation indicate that the CTX0E16 cell line may provide a useful platform for studying disease-relevant mechanisms involving these proteins in human cortical neurons without the considerable delays and expense associated with performing similar experiments in hiPSC lines.

The alterations in expression of several genes observed in the CTX0E16 cell line during differentiation offered an interesting insight into the changing profile of these cells over time. Several of these genes have been implicated in the pathological mechanisms underlying neuropsychiatric

diseases, further lending justification to the future use of the CTX0E16 cell line as a platform from which to conduct investigations into the pathways contributing to these disorders. Mutations in the dopamine receptor gene DRD2 have been associated with schizophrenia (Kukreti et al., 2006); the D2 receptor this gene codes for is a target of several antipsychotic drugs employed in the treatment of this disorder (Howes and Kapur, 2009). Surprisingly, PPP1R1B expression was found to be downregulated over the same time period. The PPP1R1B gene codes for a dopamine and cAMP-regulated neuronal phophoprotein (DARPP-32), regulating the activity of both protein phosphatase 1 and PKA and acting as an integrator of information from multiple neurotransmitters and other signaling pathways at dopaminoreceptive neurons (Blom et al., 2013; Svenningsson et al., 2004). There is some evidence also implicating this protein in mechanisms underlying schizophrenia – expression of this protein has previously been found to be reduced in the prefrontal cortex of schizophrenic patients (Albert et al., 2002). The downregulation observed in the current study may be a result of a relative lack of specific subtypes of dopaminergic synapses which typically express this protein. Mutations in CACNA1C have been found to be associated with an increased risk of developing bipolar disorder and schizophrenia (Green et al., 2010). In addition to this, a specific point mutation in an alternatively spliced exon of CACNA1C causes Timothy syndrome, a heritable disorder characterised by cardiac arrhythmia, hypoglycemia, global delay in development and, in over 60% of patients, autism (Paşca et al., 2011). CACNA1C has also been found to mediate morphological plasticity in response to prolonged depolarisation in neurons derived from hiPSCs (Krey et al., 2013).

CTX0E16 cells also exhibit morphological plasticity during early neurite outgrowth in response to prolonged depolarisation. This experiment was adapted from a comparable protocol conducted by Krey et al. (2013), which showed a similar increase in neurite outgrowth following depolarisation in early-stage hiPSC-neurons. This paper went on to apply the same protocol to neurons differentiated from hiPSCs derived from Timothy syndrome patient kerinocytes, finding a reversal of the neurite-extension phenotype observed in neurons derived from control lines. The findings of the current study suggest that this paradigm may be similarly employed to study disease mechanisms affecting morphological plasticity in the CTX0E16 cell line in future experiments.

A large proportion of cells in DD28 CTX0E16 cultures exhibited increases in intracellular calcium in response to treatment with glutamate, consistent with the previous findings on the neuronal

lineages and synaptic proteins expressed in these cultures seen in **Section 3.3.5** & **4.3.1**. However, responses were typically modest, with less than 20% of cells producing a response more than 50% above baseline. This may be due to multiple factors including the presence of non-neuronal cells in the cultures, glutamatergic receptor expression not yet being sufficient to result in a pronounced increase in calcium and glutamate binding to multiple receptor types with contradictory effects on intracellular calcium concentration. The calcium responses observed in these cultures followed patterns consistent with both ionotropic (AMPA, NMDA and kainate) and metabotropic glutamate receptors. Group 1 metabotropic glutamate receptors influence intracellular calcium concentrations via slower, indirect pathways: mediating Ca^{2+} release from internal stores and modulating the activity of voltage-gated calcium channels (Pin and Duvoisin, 1995). In contrast to this, ionotropic glutamate receptors typically mediate a rapid rise in intracellular calcium as Ca^{2+} ions flow into the cell through the constitutive cation-permeable channel following ligand binding. AMPA receptors are typically only permeable to sodium and potassium, though AMPA receptors lacking the GluA2 subunit will also permit Ca^{2+} ions to pass through (Black, 2005; Hume et al., 1991). NMDA receptors are highly permeable to calcium while the permeability of kainate receptors to calcium depends on the configuration of two transmembrane segments within the channel, TM1 and TM2 (Huettner, 2003; Petrie et al., 2000). Thus, the modest Ca^{2+} responses observed following glutamate treatment may also reflect specific ionotropic receptor subunit compositions at this stage of differentiation.

Calcium responses to acetylcholine were virtually ubiquitous and tended to be more profound than those observed for glutamate. Although cholinergic receptors have not been extensively investigated in the present study, several subtypes of nicotinic receptor are expressed within the cerebral cortex; the permeability of these ligand-gated ion channels to calcium is dependent on the composition of their subunits (Shen and Yakel, 2009; Wallace and Bertrand, 2013). Metabotropic cholinergic receptors in the cortex also mediate increases in intracellular calcium via release from internal stores (Porter et al., 2002; Rathouz et al., 1995), though these receptors are unlikely to be responsible for the calcium responses to acetylcholine treatment seen in the current study as the increase in the calcium signal was rapid and therefore more consistent with calcium influx via ionotropic receptors.

Dopamine receptors have previously been found to regulate intracellular calcium concentration via mediating calcium release from internal stores (Lezcano and Bergson, 2002). Intracellular increases in calcium in response to treatment with dopamine were relatively low in comparison to both glutamate and acetylcholine, with only a minority of DD28 CTX0E16 cells exhibiting a response and less than 5% of cells producing an increase in the calcium signal greater than 50% above baseline. Although the present investigation has indicated that CTX0E16 neurons are predominately glutamatergic or GABAergic, q-PCR analysis of proliferative and differentiated CTX0E16 cultures has indicated that the metabotropic dopamine receptor subunit DRD2 is greatly upregulated following several weeks of differentiation, indicating that a minority of MAP2-positive neurons may in fact be dopaminergic. This is perhaps unsurprising as typically only a fraction of cortical neurons express the dopaminergic marker tyrosine hydroxylase, with the majority of dopaminergic afferents originating from various regions within the midbrain (Gaspar et al., 1987).

Treatment of differentiated CTX0E16 cells with KCl also resulted in marked increases in intracellular calcium. A high external concentration of KCl acts as a depolarising stimulus in neuronal cultures as the cell membrane is highly permeable to potassium ions at rest and so K^+ ions will flow into the lower concentration of the intracellular environment. The subsequent increase in calcium is due to voltage gated calcium channels opening as a result of the depolarisation of the cell (Simms and Zamponi, 2014). This result indicates that CTX0E16 neurons express voltage gated calcium channels by DD42 and is consistent with the upregulation of CACNA1C expression observed in differentiated cultures relative to proliferative cells seen in **Section 4.3.4**. Spontaneous calcium oscillations, a marker of activity in mature neurons, were also found to occur in DD42 CTX0E16 cultures. These transient fluctuations in intracellular calcium were blocked by treatment with TTX, confirming that they were mediated by neuronal activity as predicted.

Spontaneous action potentials could only be observed in CTX0E16 cultures after 50 days of differentiation. This provided a more direct confirmation of the previous findings via calcium imaging in younger cultures. Several previous studies assessing these electrophysiological characteristics in neurons derived from other human cell lines were able to observe this phenomenon at an earlier time point of differentiation (De Filippis et al., 2007; Gaspard et al., 2008; Nunes et al., 2003). There are several factors which may contribute to a shortening of the duration of differentiation required before

CTX0E16 cells produce functional synapses and neuronal activity. Co-cultures of MEFs have previously been found to aid the rapid differentiation and viability of human neuronal cultures *in vitro* (Ghasemi-Dehkordi et al., 2015). Additionally, although differentiated CTX0E16 cultures were found to contain small populations of s100β-positive astrocytes, this proportion may not provide the optimal conditions for synapse formation and function. Previous studies have found astrocytes to play a critical role in synaptogenesis and in the regular function of synaptic transmission at the tripartite synapse – synaptics connections consisting of the three way partnership of the presynaptic bouton, postsynaptic density and the surrounding astrocytic elements (Faissner et al., 2010; Swanson et al., 1999). In addition to this, *in vitro* investigations have also determined that co-culturing neurons with astrocytes increases the efficiency of synaptic transmission and accelerates the onset of synaptic current development (Johnson et al., 2007). Thus, optimising the balance of astrocytes or other glial cells via co-cultures with the neuronal component of CTX0E16 cultures may accelerate the onset of synaptogenesis and mature functional characteristics. Finally, supplements for the culture media which promote differentiation (or the use of alternate differentiation media compositions entirely) may further reduce culture times when generating mature neurons. Retinoic acid promotes neuronal differentiation of pluripotent stem cells *in vitro*, while forskolin has also been previously used to potentiate neuronal differentiation from both hNSC and hNPC lines (Cacci et al., 2007; Wang et al., 2004). Furthermore, a new neuronal medium, BrainPhys, has recently been designed to promote rapid neuronal differentiation of human IPSC lines (Bardy et al., 2015). This medium has been found to improve the proportion of synaptically active cells in these cultures relative to differentiation media based on DMEM or neurobasal. Thus, the application of neuronal differentiation-promoting media or supplements to culturing protocols for CTX0E16 cells may provide a useful method for reducing differentiation times.

Finally, the progressive development of an increasingly polarised resting membrane potential in neurons from differentiated CTX0E16 cultures not only reflects the increasing maturity of these cells but also closely matches the alterations in membrane potential seen during differentiation in other human cell lines and *in vivo* (Johnson et al., 2007; Magnuson et al., 1995; Vierbuchen et al., 2010).

In conclusion, this chapter has shown that CTX0E16 cells are capable of developing functional excitatory synapses containing a wide host of neurotransmitter receptors, intracellular signaling proteins, scaffolding proteins and vesicular proteins as well as several proteins relevant to

neuropsychiatric disease. Differentiated CTX0E16 neurons were also shown to develop several key electrophysiological characteristics and functional responses in a manner consistent with mature glutamatergic neurons. These findings, taken together with the conclusions of the previous chapter, indicate that the CTX0E16 cell line offers a useful platform from which to launch investigations into developmental and disease-relevant mechanisms and pathways in human glutamatergic neurons. Future modifications of the differentiation protocol may yield a more rapid attainment of mature, functional properties in these neurons and thus improve their use as an experimental model.

In light of these findings, **Chapter 5** will detail the employment of this cell line in conjunction with hiPSC-derived neurons and primary rat cortical neurons in a study of the expression and subcellular localisation of a protein implicated in schizophrenia and bipolar disorder, ZNF804A. This chapter will also discuss these experiments in the context of previous research into the potential functions of this protein.

GENE	PROTEIN	FUNCTION
GRIN1	Glutamate receptor subunit zeta-1	Subunit of glutamatergic NMDA receptor; involved in excitatory neurotransmission
GRIA2	Glutamate receptor 2	Codes for several glutamatergic AMPA and kainate receptor subunits; involved in excitatory neurotransmission
GRM5	Metabotropic glutamate receptor 5	G protein coupled glutamate receptor; involved in excitatory neurotransmission
GABRA1	Gamma-aminobutyric acid receptor subunit alpha-1	GABA-A receptor subunit involved in inhibitory neurotransmission
DRD2	Dopamine receptor D_2	Key component of dopaminergic neurotransmission
CACNA1C	Calcium channel, voltage-dependent, L type, alpha 1C subunit	Voltage dependent calcium channel; regulates intracellular calcium concentration
DLG4	Post-synaptic density protein PSD-95	Core component acting as a protein scaffold at the postsynaptic density
CAMK2A	Calcium/calmodulin-dependent protein kinase type II alpha chain	Serine/threonine protein kinase that mediates long term potentiation and other aspects of neuronal plasticity
PPP1R1B	Protein phosphatase 1 regulatory subunit 1B	Involved in secondary signalling pathways in dopaminergic neurotransmission
GSK3B	Glycogen synthase kinase 3	Serine/threonine protein kinase involved in the regulation of neuronal differentiation
SLC6A4	Solute carrier family 6, member 4	Serotonin transporter; key component of the serotonergic neurotransmission system

Table 4.3.4: Summary of neurotransmitter receptor, cell signalling and synaptic protein genes.

CHAPTER 5: EXPRESSION AND SUBCELLULAR LOCALISATION OF ZNF804A

5.1 SUMMARY

This chapter details the characterisation of the expression of a protein implicated as a risk candidate for schizophrenia and bipolar disorder. This involved an assessment of ZNF804A expression at the mRNA level in multiple human cell lines, the identification and validation of the optimal candidate for immunostaining for the ZNF804A protein out of several commercially available anti-ZNF804A antibodies and the subsequent optimisation of ICC protocols utilising this antibody. This chapter also describes the characterisation of ZNF804A protein expression and subcellular localisation in several *in vitro* paradigms including neurons derived from hNPC and hiPSC lines as well as primary rat cortical neurons. Finally, this chapter discusses these findings in the context of the pre-existing literature.

5.2 INTRODUCTION

ZNF804A was first identified as a schizophrenia risk candidate gene in a GWAS conducted by O'Donovan et al. (2008), which discovered an association with a SNP at rs1344706 within an intronic region of the *ZNF804A* gene. This association grew stronger when bipolar disorder was included in the affected phenotype, suggesting a broader link to psychosis in general. An initial study assessing the impact of the risk allele of the rs1344706 SNP on ZNF804A expression in the human brain found a reduction in the expression of the full length ZNF804A transcript in second trimester fetal tissue (Hill and Bray, 2012). However, a subsequent study found evidence to suggest that this reduction was in fact limited to a novel variant lacking the first two exons of the full length transcript, termed ZNF804A$^{E3/E4}$ (Tao et al., 2014).

ZNF804A belongs to the ZNF (zinc finger) family, a class of proteins characterised by the presence of a domain consisting of a small motif folded around one or more zinc ions (Laity et al., 2001). These ZNF proteins are well known for their ability to bind DNA and act as transcription factors, however ZNF motifs have also been found to mediate a wide variety of functions including the regulation of protein-protein interactions, protein-lipid interactions and acting as RNA-binding molecules (Laity et al.,

2001). In the brain, ZNF proteins have been previously found to be involved in several processes including neurogenesis (Aruga et al., 1994), neurite outgrowth (Hattori et al., 2007) and synaptic function (Fenster et al., 2000).

Several studies have also attempted to identify the role of ZNF804A and its rodent homologue Zfp804A at the cellular and molecular level. Knockdown of ZNF804A has been found to affect expression of several genes involved in neurite outgrowth, axonal and dendritic arborisation and cell adhesion (Hill et al., 2012); schizophrenia-associated genes (Girgenti et al., 2012); genes involved in the cytokine signalling pathway (Chen et al., 2015); and genes involved in TGF-β signalling (Umeda-Yano et al., 2013). However, despite these findings providing a valuable insight into ZNF804A and Zfp804A's potential role as a transcription factor, there is still currently a lack of reliable data on fundamental characteristics of this protein including its localisation due to a lack of well-validated antibodies.

Assessments of the regional, cellular and subcellular localisation of a protein can provide a valuable insight into that protein's potential functions. Prior research into the subcellular localisation of ZNF804A and the rodent homologue, Zfp804A, has yielded mixed results, a problem potentially compounded by the frequent lack of thorough antibody characterisation and differences in the neuronal models studied in these papers. ZNF804A and Zfp804A expression has been reported variously as nuclear in rat neural progenitor cells (Girgenti et al., 2012), within the cytoplasm and nuclei of human cortical pyramidal neurons (Bernstein et al., 2014; Tao et al., 2014) and from perinuclear regions to a wide distribution with particularly strong expression in growth cones during differentiation of cultured rodent neuronal cells (Chang et al., 2015). Future research will thus greatly benefit from a more thorough characterisation of the subcellular localisation of these proteins with a well-validated antibody across several cellular models.

This chapter presents a study of the subcellular and sub-structural localisation of this protein in several neuronal cell lines from both human and rodent sources. Following a thorough validation of a candidate anti-ZNF804A antibody, the subcellular expression of ZNF804A and Zfp804A is described in NPCs and neurons from the CTX0E16 cell line and hiPSC sources, as well as subcellular and sub-synaptic localisation in rat primary cortical neurons. The expression of several ZNF804A transcripts and protein

isoforms in these cell lines is also demonstrated. Finally, this chapter discusses the ramifications of this work in the context of the findings of previous research.

5.3 RESULTS

5.3.1 CHARACTERISATION OF ZNF804A TRANSCRIPT EXPRESSION IN THE CTX0E16 CELL LINE

Several splice variants of *ZNF804A* have been identified in previous studies, including the full length transcript; the disease-relevant E3/E4 variant which lacks exon 1 and 2 (which codes for the C2H2 zinc finger domain) and contains a 5' untranslated region; variant b which lacks the first two exons and one of the putative nuclear localisation signals; variant c which is composed almost entirely of exon 2; and variant 2.2, consisting of exon 2 and a novel exon termed exon 2.2 (see **Figure 5.3.1, A**) (Hess and Glatt, 2013; Okada et al., 2012; Tao et al., 2014). To assess whether several key transcripts were expressed in CTX0E16 cells throughout early differentiation, CTX0E16 cultures were differentiated up to DD10 and lysed, processed and RNA extracted at DD0, DD2, DD4, DD6, DD8 and DD10. RNA samples were then assessed for expression of *ZNF804A* exon 4 (present in *ZNF804A* variant b and E3/E4 as well as full-length *ZNF804A* transcripts) via RT-PCR with *GAPDH* as an expression control; experiments were carried out in triplicate. Expression of $ZNF804A^{E3/E4}$ and $ZNF804A^{exon2.2}$ was also assessed using transcript-specific primers. All three transcripts could be detected in proliferative CTX0E16 cells and throughout early differentiation (see **Figure 5.3.1, B**).

As individual transcripts of ZNF804A possess differential sequences which may omit key domains in the final translated ZNF804A protein, including the zinc finger region and putative nuclear localisation signals, these variants may have also differential functions in neurons. In light of the preliminary finding of multiple *ZNF804A* transcripts being expressed throughout early differentiation of CTX0E16 cells, proliferative and differentiated (DD28) CTX0E16 cells were quantitatively analysed using q-PCR to determine whether the relative expression of each of these transcripts altered as these cells adopted a more mature neuronal fate. RNA samples from DD0 and DD28 CTX0E16 cultures were analysed using q-PCR to assess expression of $ZNF804A^{exon4}$, $ZNF804A^{E3/E4}$ and $ZNF804A^{exon2.2}$. Expression values for each transcript were normalised to a geometric mean of the expression values of three housekeeping genes (*GAPDH*, *HPRT1* and *RPL13A*) using the $2^{\wedge\text{-dCT}}$ method (Livak and Schmittgen, 2001) $ZNF804A^{exon4}$ was found to be the most abundant transcript in both proliferative and

differentiated CTX0E16 cells (see **Figure 5.3.1, C**). Interestingly, a Kruskall-Wallis test of the expression data with a Dunn's posthoc multiple comparisons test revealed that expression of this transcript was significantly reduced in DD28 cells relative to CTX0E16 hNPCs (relative expression to 3 decimal places: 0.012±0.003 vs 0.021±0.002, p<0.001). No significant differences in expression between DD28 and DD0 cells could be detected for *ZNF804A*$^{exon2.2}$ (0.007±0.001 vs 0.009±0.000 for DD28 and DD0 cells respectively, p>0.05) or *ZNF804A*$^{E3/E4}$, which was barely detectable at both time points (0.001±0.000 vs 0.001±0.000 for DD28 and DD0 cells respectively, p>0.05). Overall, these findings indicate that the expression profile of these variants alters after several weeks of differentiation; this may have implications for differential functions of each of these transcripts throughout development. Previous studies have found a psychosis-associated SNP to reduce expression of the full length and E3/E4 transcripts of ZNF804A in a time-restricted manner in the fetal brain (Hill and Bray, 2012; Tao et al., 2014); identifying the roles these variants play in the developing brain as their expression profile alters may help identify the pathways they mediate which potentially underlie neuropsychiatric disease.

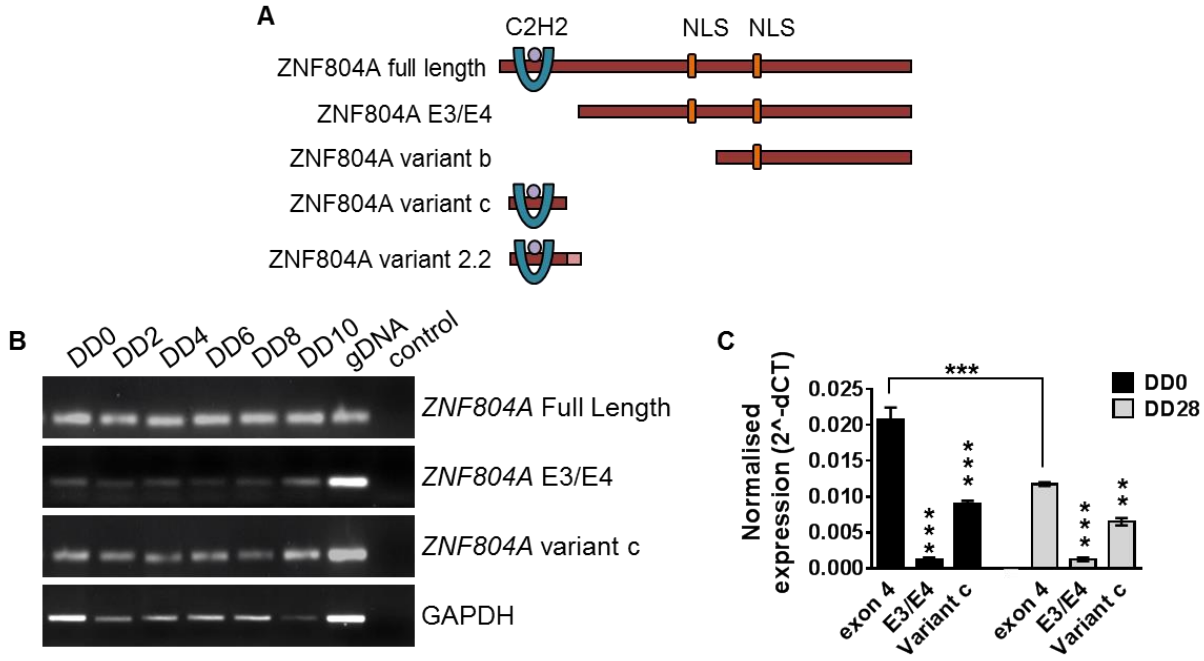

Figure 5.3.1: Expression of ZNF804A mRNA transcripts in the CTX0E16 cell line**. A:** Schematic of domain structure in known and predicted ZNF804A variants. B: RT-PCR of mRNA for *ZNF804A*^{exon4}, $^{E3/E4}$ and $^{exon\ 2.2}$ transcripts in proliferative and early-stage differentiated cells derived from the CTX0E16 cells. **C**: q-PCR of mRNA samples for *ZNF804A*^{exon4}, $^{E3/E4}$ and $^{exon\ 2.2}$ transcripts in proliferative and early-stage differentiated cells derived from the CTX0E16 line. Results show relative expression values normalised to three housekeeping genes (n = 3 independent experiments; **p<0.01; ***p<0.001). q-PCR was performed by Rodrigo Rafagnin using primers optimised by P.J. Michael Deans.

5.3.2 SELECTION OF A CANDIDATE ANTIBODY FOR THE INVESTIGATION OF ZNF804A EXPRESSION

As described in **Section 5.2**, previous studies assessing the expression of the ZNF804A and Zfp804A proteins in human and rat cells have typically lacked a thorough validation of the antibodies used for western blotting, immunocytochemistry and immunohistochemistry. Thus, the selection and validation of a suitable antibody targeted to these proteins is crucial prior to any further investigations into the pattern of expression. Two independent antibodies were assessed for their ability to successfully detect the full length ZNF804A protein via western blotting; these results were subsequently validated using siRNA-mediated knockdown of the ZNF804A protein. Additionally, the specificity of each of these candidate antibodies to their corresponding antigens was further determined in a peptide preabsorption experiment. The candidate antibodies included the previously described goat anti-ZNF804A D-14 Santa Cruz antibody, which recognises an epitope within an internal region of the ZNF804A protein; and a rabbit anti-ZNF804A Genetex antibody (C2C3) targeted to an epitope on the C-terminal of the protein. Human neuronal cells are predicted to express several variants of ZNF804A with differing molecular weights based on amino acid sequences derived from the NCBI record: the full length protein (1209 a.a., ~137 kDa), the E3/E4 variant (1074 a.a., ~125 kDa), variant b (602 a.a., ~68 kDa) and variant 2.2 (88 a.a., ~9 kDa). One method of providing supporting evidence for the validity of an antibody targeted to a particular protein is to assess whether it can specifically detect protein bands corresponding to the predicted weights of the known isoforms. DD30 CTX0E16 lysates were probed for ZNF804A expression using each of the two antibodies. Western blotting revealed that the Genetex C2C3 antibody detected a major protein band at ~135 kDa, as well as minor protein bands at >100 kDa, ~75 kDa, ~60 kDa and ~40 kDa. The ~135 kDa protein band is the mass predicted to be encoded by full length ZNF804A, and the >100 and 75 kDa bands are small enough to be encoded by the E3/E4 and variant b ZNF804A isoforms. It is also worth noting that only low E3/E4 transcript expression seen via q-PCR is similarly reflected by the low expression of the protein band matching this isoform's predicted mass. In contrast to this, the Santa Cruz antibody detected a major protein band at ~40 kDa, as well as minor protein bands at ~300 kDa, ~250 kDa, ~200 kDa, ~135 kDa, ~85 kDa, ~60 kDa and ~45 kDa (see **Figure 5.3.2, A**). This is of particular interest as in previous studies this antibody had only been found to detect a single band at around 135 kDa, with no additional bands corresponding to other isoforms or putative non-specific staining being seen in rat NPCs or postmortem human tissue. Taken

together, these initial findings suggest that the Genetex anti-ZNF804A antibody may represent a more specific probe for ZNF804A than the previously used Santa Cruz antibody.

siRNA-mediated knockdown of protein expression represents a useful method of verifying whether specific protein bands detected by a given antibody represent a true protein signal. To determine whether the protein bands seen in **Figure 3.3.2, A** would be reduced by knockdown of ZNF804A expression (an indicator of antibody specificity), DD7 CTX0E16 cultures were treated with two siRNAs targeting exon 2 and exon 4 of *ZNF804A*. These siRNAs have previously been validated via microarray and Q-PCR in a sister cell line of CTX0E16, CTX0E03 (Hill et al., 2012). siRNA-treated cultures were subsequently lysed and processed for either western blotting with both the Genetex and Santa Cruz antibodies, or for Q-PCR. An additional fluorescent oligonucleotide control condition was included as a measure of transfection efficiency using the N-Ter tranfection reagent; assessment of oligonucleotide uptake in CTX0E16 cells via live epifluorescence imaging revealed a transfection rate of 86.08±1.43% (see **Figure 6.3.5**, **A**). Knockdown of *ZNF804A*^{exon4} at the mRNA level was confirmed using q-PCR followed by subsequent analysis using the 2^2dCT method, normalising values for the *ZNF804A* transcript to three previously validated internal control genes (*RPL13A*, *RPL30* and *HPRT1*), then expressing the values for each condition relative to the scramble siRNA control as described in **Section 2.6.3**. Of these experimental replicates, relative expression of *ZNF804A*^{exon4} was (in arbitrary units) 1.02±0.09 for the blank control; 1.00±0.00 for the scramble control; 0.56±0.17 for siRNA 1; and 0.62±0.08 for siRNA 2 (see **Figure 6.3.6**, **A**). A Kruskall Wallis test of these data with posthoc Dunn's multiple comparisons testing revealed that there was an overall significant effect of experimental condition ($p<0.01$) with the reductions in expression of *ZNF804A*^{exon4} in the knockdown conditions relative to the scramble siRNA control condition being close to significant at the $p=0.05$ level ($p=0.068$ and $p=0.051$ respectively). Analysis of *ZNF804A*^{exon4} expression by Q-PCR revealed that both siRNA 1 and 2 reduced ZNF804A mRNA by ~40%.

To determine whether knockdown of ZNF804A could also be detected using each of the ZNF804A antibodies. For analysis of western blots, average intensities of bands mapping to known ZNF804A isoforms were normalised to a β-Actin control and expressed relative to the corresponding bands in the scramble siRNA condition. Normalised intensity values for bands corresponding to the predicted sizes of the full length (~135 kDa), E3/E4 (>100kDa) and variant b (~80kDa) ZNF804A

isoforms were all significantly reduced in siRNA-treated samples relative to untreated and scramble siRNA treated controls in western blots stained with the Genetex C2C3 antibody 40-50% reduction in protein levels for bands corresponding to predicted sizes for full length, E3/E4 and variant b isoforms of the ZNF804A protein, while two additional bands not corresponding to any known ZNF804A isoforms were not reduced (see **Figure 5.3.2** in **Chapter 5**, **G** & **H**). A two way ANOVA with a posthoc Bonferroni multiple comparisons test revealed a highly significant effect of experimental condition ($p<0.001$) and the reductions of all three isoforms in the ZNF804A knockdown conditions to be highly significant ($p<0.01$). (**Figure 5.3.2, G** & **H**). However, two additional bands at around 40 and 50 kDa could also be seen in these blots which did not diminish in siRNA-tread conditions, suggesting possible non-specific staining. Additionally, in a western blot of the siRNA-treated cultures probed with the Santa Cruz D-14 antibody major bands seen at ~135, 100 and 80 kDa were reduced in the siRNA 1 and 2 conditions indicating that this antibody is specific for ZNF804A; however, the presence of numerous additional protein bands not seen in the C2C3 antibody-stained western blots suggests that the Santa Cruz D-14 antibody may not be as specific as C2C3 (**Figure 5.3.2, I**). Taken together, these findings indicate that despite the presence of apparent non-specific bands in western blots of CTX0E16 lysates probed with the Genetex C2C3 antibody, this antibody appeared to provide a more accurate determinant of ZNF804A expression than the widely used D-14 Santa Cruz antibody.

Peptide blocking experiments offer a further method for assessing the specificity of a particular antibody to its corresponding antigen. Previous research has found preincubation with a peptide for the Santa Cruz anti-ZNF804A antibody to abolish detection of the full length ZNF804A isoform protein band via western blotting. To assess the specificity of both antibodies for their respective antigens, and to determine the efficacy of these antibodies in ICC experiments, DD0 CTX0E16 cultures were immunostained for DAPI and either the Santa Cruz D-14 or the Genetex C2C3 ZNF804A antibody. Antibodies were either preincubated with their corresponding peptide or a blank control solution. Interestingly, peptide preincubation was not found to abolish immunostaining with the Santa Cruz antibody in DD0 CTX0E16 hNPCs as had been seen in western blotting experiments in previous research (see **Figure 5.3.6, A** & **B**). In contrast to this, peptide preabsorption of the Genetex antibody almost completely abolished the strong immunostaining in the DD0 CTX0E16 hNPCs. These results demonstrate that the Santa Cruz D-14 antibody does not exclusively target its intended epitope, while the Genetex C2C3 antibody appears to specifically bind to its corresponding peptide.

Overall, the evidence presented here indicates that of the two antibodies assessed in the present investigation, the Genetex C2C3 antibody appears to produce the greatest specificity of staining in both western blotting and ICC. However, additional validation of this antibody is required prior to further use in investigations of ZNF804A's expression and distribution in neurons. In particular, the detection of both endogenous and exogenous ZNF804A protein must be confirmed in folded (ICC) and denatured (western blotting) conformations. Finally, it may also be of use to determine whether the Genetex C2C3 antibody also successfully and specifically detects the rodent homologue of ZNF804A, Zfp804A.

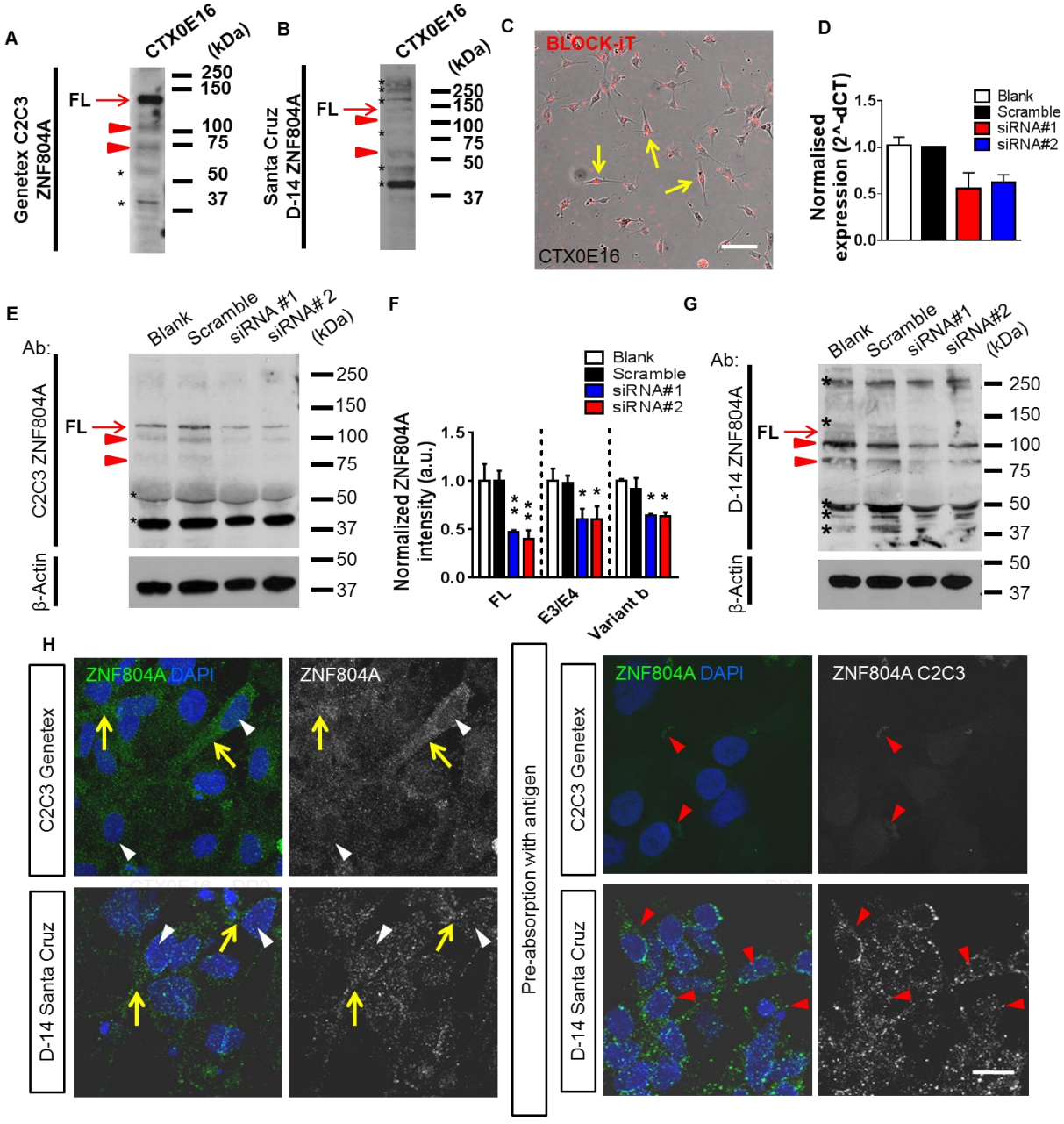

Figure 5.3.2 (overleaf): Selection of a candidate anti-ZNF804A antibody. **A & B**: Western blotting of DD30 CTX0E16 lysates with C2C3 Genetex **(A)** and D-14 Santa Cruz **(B)** antibodies targeted to the ZNF804A protein. Red arrows denote bands corresponding to the predicted full length ZNF804A isoform; red arrowheads indicate bands corresponding to the predicted weights of other ZNF804A isoforms; asterisks indicate bands not corresponding to any known ZNF804A variants. **C**: siRNA treatment experiments: representative image of fluorescent oligonucleotide control condition assessing efficiency of N-Ter siRNA transfection. 86.08±1.43% of CTX0E16 cells were transfected with BLOCK-iT red fluorescent oligo 1 day post transfection. Yellow arrows indicate transfected cells. **D**: Q-PCR of mRNA for ZNF804A^{exon4} transcripts following 7 day siRNA treatment in DD7 CTX0E16-neurons. **E & F**: Western blot of ZNF804A and quantification of knockdown following 7 day siRNA treatment in DD7 CTX0E16 cells using Genetex C2C3 anti-ZNF804A antibody. Expression of all three protein isoforms was significantly reduced; asterisks indicate nonspecific bands (n = 3 independent experiments *p<0.05; **p<0.01). **G**: Western blot of ZNF804A following 7 day siRNA treatment in DD7 CTX0E16 cells using the Santa Cruz D-14 anti-ZNF804A antibody. **H**: Representative confocal imaging of DD0 CTX0E16 cells immunostained with the Genetex C2C3 or the Santa Cruz D-14 ZNF804A antibody with or without pre-incubation using the corresponding antigenic peptide. Yellow arrows indicate immunoreactive staining within the cytoplasm of CTX0E16 cells, white arrowheads highlights staining within cell nuclei and red arrow heads indicate possible non-specific staining. Note the pre-absorption with antigen abolished the granular staining produced by the ZNF804A C2C3 antibody alone, while staining using the Santa Cruz D-14 antibody was not abolished by antigen pre-absorption. Scale bars = 50 µm (**C**) and 10 µm (**H**). Western blots for **A, B, E & G** were conducted by Pooja Raval.

5.3.3 FURTHER VALIDATION OF A CANDIDATE ZNF804A ANTIBODY – WESTERN BLOTTING

Following the selection of the Genetex C2C3 antibody as a candidate for further validation, the protein bands seen in **Figure 5.3.2** were further investigated using peptide pre-absorption and immunoprecipitation to determine whether they represented true binding of the antibody to the corresponding antigen on the unfolded ZNF804A protein. DD30 CTX0E16 lysates were immunoprecipitated with the C2C3 antibody, and probed with this antibody with or without peptide preabsorption. Preincubation of the C2C3 antibody with antigenic peptide prevented immunoprecipitation of the ~135, ~100 and 75 kDa proteins, demonstrating that binding to the protein was specific; a possible band at 40 kDa could potentially be seen, but due to signal from the IgG band the presence of this protein in the pre-immune condition could not be confirmed. These results were further investigated in rat primary cortical neurons to determine whether the C2C3 antibody also detected Zfp804A, the rodent homologue of ZNF804A. In whole cell lysate derived from DIV25 primary rat cortical neurons, western blotting using the C2C3 antibody revealed a single major protein band at

~140 kDa; this mass is higher than the predicted weight of Zfp804A, but could be due to post-translational modifications. Immunoprecipitation with C2C3 as well as pre-immune and IgG control experiments further support that the ~140 kDa protein was specifically being bound to by the C2C3 antibody.

The specificity of a given antibody for a target protein can also be determined using the overexpression of a tagged protein construct in a cell line which does not express the endogenous protein; thus detection of this protein using the antibody can subsequently verified using an additional antibody targeted to the exogenous protein's tag. As hEK293 cells have previously been demonstrated not to express the endogenous ZNF804A protein in detectable quantities (Girgenti et al., 2012), hEK293 cultures were transfected using a myc-tagged ZNF804A construct and lysed two days later for subsequent western blotting. Probing of western blots with an anti-myc antibody revealed a major protein band at ~135 kDa, consistent with the predicted mass of the tagged ZNF804A protein. Interestingly, additional bands could be detected at lower weights, which may be indicative of protein degradation. Probing of the same lysates with the Genetex C2C3 ZNF804A antibody also detected proteins that corresponded to those detected by the myc antibody, demonstrating that the C2C3 antibody specifically detects full length ZNF804A.

In a final set of control experiments, a polyclonal population of SH-SY5Y cells stably expressing full length human ZNF804A with an N-terminally fused halo tag (halo-ZNF804A) was assessed for expression of the tagged full length ZNF804A protein using both fluorescence imaging of the HaloTag^{R}TMRDirect^{TM} ligand and probing using the Genetex C2C3 antibody. Pure wild type and polyclonal halo-ZNF804A SH-SY5Y cultures were lysed for subsequent western blotting. Importantly, a single band at >150 kDA was detected by the HaloTag^{R}TMRDirect^{TM} ligand in the halo-ZNF804A condition, a size consistent with a fusion of the halo tag and full length ZNF804A (halo tag = 33 kDa, ZNF804A = 135 kDa, total predicted weight of fusion protein = 168 kDa). A protein band of the corresponding weight was also detected by the Genetex C2C3 antibody in the halo-ZNF804A condition, but not wildtype conditions. It should be noted that additional bands of ~140 kDa and lower could be detected in both wildtype and halo-ZNF804A conditions. It is likely that these bands represent the endogenous protein expressed by these cells; however, it is also possible that these may be non-

specific bands. Collectively, these data indicate that the C2C3 antibody specifically detects full length ZNF804A/Zfp804A, but that some minor non-specific band of low mass are also detected.

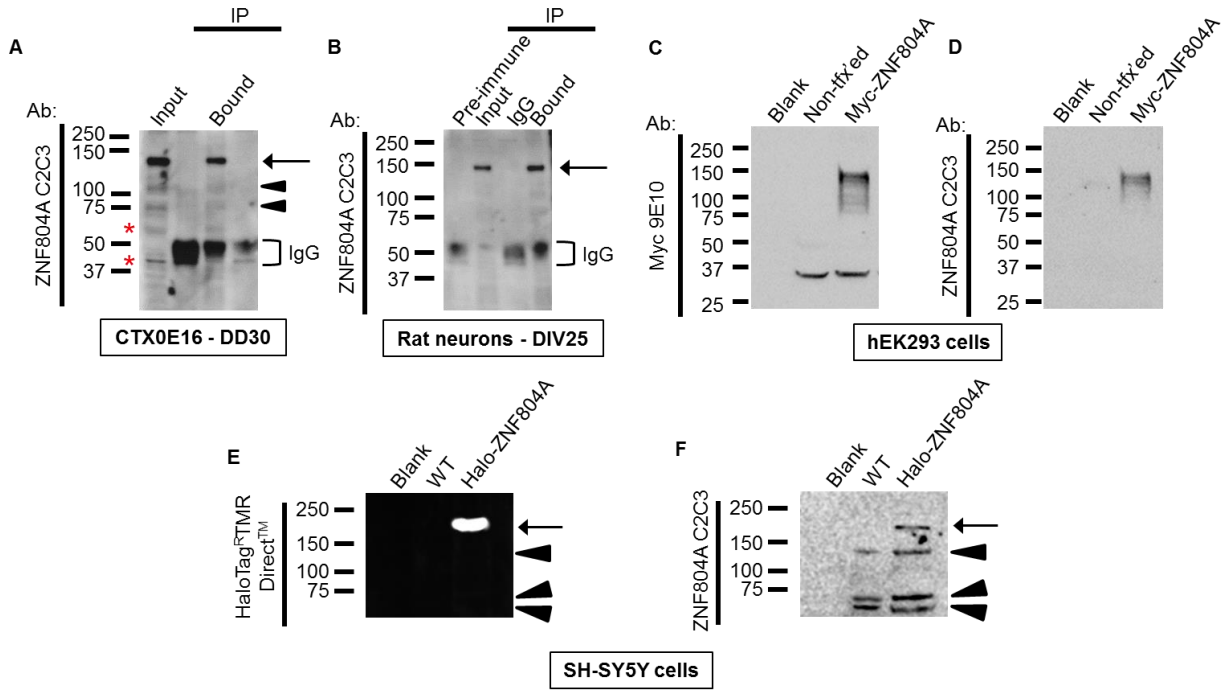

Figure 5.3.3: Further validation of a candidate ZNF804A antibody using western blotting. **A**: Western blot of DD30 CTX0E16 cell lysates immunoprecipitated with the C2C3 antibody, and probed using this antibody with or without pre-incubation with 10 µg of antigenic peptide. Black arrow denotes band corresponding to the predicted mass of the full length ZNF804A protein; black arrow heads denote minor bands potentially corresponding to other known or predicted ZNF804A protein isoforms. Red asterisks denote non- specific bands. **B**: Western blot of DIV25 rat primary cortical neuron lysates immunoprecipitated with the C2C3 antibody and probed using this antibody with or without pre-incubation with 10 µg of antigenic peptide. Black arrow denotes band corresponding to the predicted mass of the full length Zfp804A protein. **C**: Western blot of hEK293 cell lysates untransfected or transfected with a myc-tagged ZNF804A construct and probed with an anti-myc antibody; note the presence of additional smaller bands potentially indicating degradation of the overexpressed protein. **D**: Western blot shown in **C** but probed with the C2C3 anti-ZNF804A antibody; C2C3 specifically detects myc-ZNF804A. **E** & **F**: Western blot of wild-type and Halo-ZNF804A- expressing SH-SY5Y cell lysates probed with HaloTag^{R}TMRDirect^{TM} ligand (**E**) and C2C3 (**F**) antibody. A single band >150 kDa was highlighted by the HaloTag ligand in Halo- ZNF804A cells, confirming presence of exogenous Halo-ZNF804A. An identical band could also be observed in Halo-ZNF804A-expressing, but not wildtype, SH-SY5Y cultures (black arrow) probed using the C2C3 antibody. In addition, several smaller proteins bands could be detected by the C2C3 antibody in both wildtype and Halo-ZNF804A SH-SY5Y cell lysates, further indicating expression of endogenous protein (black arrow heads). Western blots were carried out by Pooja Raval on lysates prepared by P.J. Michael Deans.

5.3.4 FURTHER VALIDATION OF A CANDIDATE ZNF804A ANTIBODY – ICC

Antibodies which successfully detect a given protein via western blotting techniques may not similarly detect the same protein in experiments using immunocytochemistry (ICC), as alterations in the folded protein structure relative to the denatured form may potentially impact the binding of antibodies to a given epitope. Therefore, any validation of an antibody for future use in ICC requires similar evidence that it may also bind specifically to the protein in its folded configuration. In western blotting, the Genetex C2C3 antibody was previously shown to detect a protein band corresponding to the predicted weight of the full length ZNF804A protein fused with the HaloTag^{R}TMRDirect^{TM} ligand; this band was also detected by the fluorescence signal from the ligand itself. To confirm this observation via ICC, a mixed population of halo-ZNF804A and wild type SH-SY5Y cells was immunostained using the Genetex C2C3 ZNF804A antibody. Here, ZNF804A immunofluorescence as detected by the Genetex C2C3 antibody could be seen to overlap with the halo signal, indicating that the ZNF804A antibody successfully detects the halo-tagged protein in SH-SY5Y cells. Non-transfected cells were also positive for ZNF804A, albeit at a lower level; this may be endogenous expression of the ZNF804A protein in wildtype SH-SY5Y cells as indicated by the previous western blotting experiment.

In light of the finding that the Genetex C2C3 antibody could also detect exogenous ZNF804A tagged with a reporter molecule, hEK299 cultures were again utilised to determine whether the expression of exogenous ZNF804A tagged with a reporter molecule in a non-expressing cell line could be detected using the Genetex C2C3 antibody via ICC. hEK293 cultures were transfected with a GFP-tagged human ZNF804A construct and double immunostained with GFP and Genetex C2C3 ZNF804A antibodies. GFP-ZNF804A could be observed within the cell nucleus as well within the cytoplasm; the protein was also found to accumulate at the plasma membrane of the cells. Examination of the C2C3 ZNF804A channel revealed that it almost entirely overlapped with the GFP fluorescent signal. This can be readily seen in the colocalisation image, which highlights where the GFP and C2C3 channels overlap. Taken together with the findings of the halo-ZNF804A SH-SY5Y cell line and western blotting experiments, these data indicate that the Genetex C2C3 antibody specifically detects exogenous and endogenous ZNF804A and so is suitable for a wide variety of experimental paradigms.

Finally, the specificity of the Genetex C2C3 ZNF804A signal in CTX0E16 cells was also demonstrated in an ICC evaluation of Genetex immunostaining in both DD7 CTX0E16 cells treated with the previously described siRNAs. Here, analysis of ZNF804A immunostaining in cell soma revealed that ZNF804A staining intensity was reduced by around 30-40% in cultures treated with the two anti-ZNF804A siRNAs relative to the two control conditions (see **Figure 3.3.4**, **C & D**). A one way ANOVA of this data with a posthoc Bonferroni multiple comparisons test revealed a main effect of treatment condition ($p<0.01$) and that the reduction in staining intensity seen in siRNA 1 and 2 treated cultures relative to the scramble control condition was also significant ($p<0.05$ for both comparisons), thus providing further support to the validity of the C2C3 antibody as a probe for ZNF804A. (see **Figure 5.3.4, C & D**). Overall, these results indicate that siRNA-mediated knockdown of ZNF804A can be detected using the Genetex C2C3 antibody via ICC, further indicating that the signal detected by this antibody represents true staining of the protein.

Taken together, the evidence presented in **Section 5.3.3** and **Section 5.3.4** strongly supports the validity of the Genetex C2C3 antibody as a specific probe for the full length ZNF804A protein, both via western blotting and ICC. This antibody also detects transgenic expression of this protein while fused to several reporter molecules, and further specifically detects the rodent homologue of ZNF804A, Zfp804A. Subsequent experiments will thus employ this antibody in a further characterisation of the pattern of ZNF804A expression in CTX0E16 NPCs and neurons as well as neurons derived from hiPSCs and rodent sources.

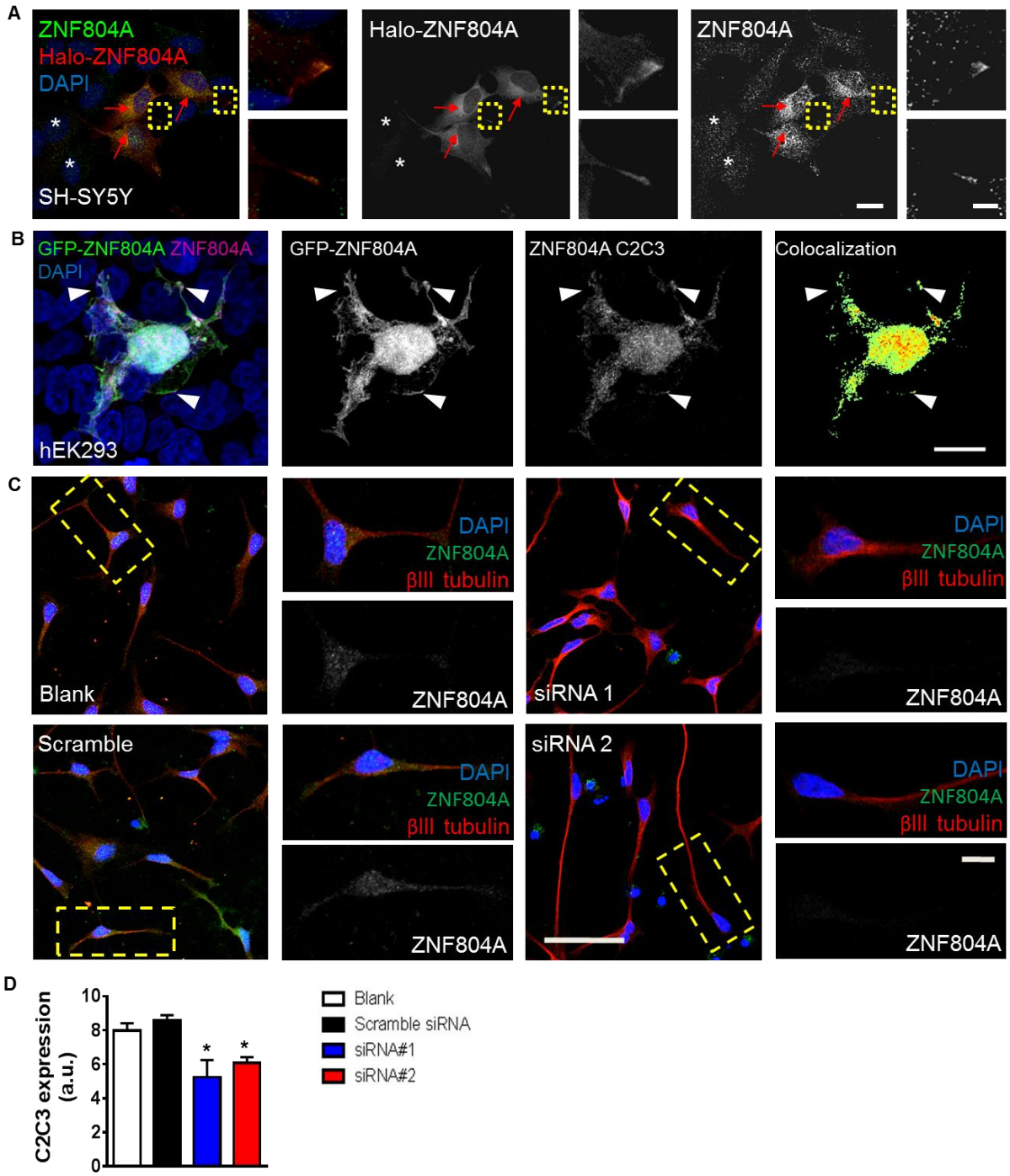

Figure 5.3.4: Further validation of a candidate ZNF804A antibody via immunocytochemistry. **A**: Representative confocal image of fixed SH-SY5Y cells overexpressing Halo-ZNF804A. Cells were triple labelled with the HaloTag^{R}TMRDirect^{TM} ligand, Genetex C2C3 antibody, and DAPI. Halo-ZNF804A was observed within the cell nuclei, cytosol and processes (magnified images). Moreover, C2C3 immunofluorescence was strongest in Halo positive cells (red arrow); magnified images demonstrates overlap of C2C3 staining with HaloTag ligand signal. C2C3 immunofluorescence could also be observed in non- transfected cells (asterisks), suggesting that wildtype SH-SY5Y cells express ZNF804A at significant levels. **B**: Confocal image of hEK293 cell transfected with a GFP-tagged ZNF804A construct and doubled immunostained with GFP and Genetex C2C3 ZNF804A antibodies.

Figure 5.3.4, continued: White arrowheads highlights ZNF804A expression within cellular processes, and indicates overlapping GFP and ZNF804A immunostaining. Note the colocalisation of GFP and ZNF804A staining as shown in the final panel. **C**: Representative confocal images of DD7 CTX0E16 cultures treated with a blank control condition (no transfection), a scramble siRNA or one of two siRNAs targeting the full length ZNF804A transcript for 7 days and immunostained for ZNF804A using the Genetex C2C3 antibody in addition to βIII tubulin as a marker of neuronal cells. **D**: Quantification of ZNF804A staining as seen in **C**. siRNA treatment of CTX0E16 cells significantly reduced C2C3 staining intensity in confocal images relative to control or scramble siRNA conditions (n = 3 independent experiments *p<0.05). Scale bars = 10 µm (**A & B**), 50 µm (**C1**) and 5 µm (**C2**).

5.3.5 SUBCELLULAR LOCALISATION OF ZNF804A IN CTX0E16 NPCS AND NEURONS

ZNF804A has been previously suggested to act as a transcription factor and thus would be expected to be expressed within the nuclei of neuronal cells (Girgenti et al., 2012). An assessment of the subcellular localisation of this protein may therefore provide valuable information on its potential roles within neurons, particularly if it is found outwith the cell nucleus. Following the promising early findings of ZNF804A transcript expression in proliferative CTX0E16 cells, the Genetex C2C3 ZNF804A antibody was employed using ICC to assess the subcellular localisation the endogenous ZNF804A protein in human NPCs from the CTX0E16 cell line, while overexpression of a ZNF804A construct tagged with GFP was used to independently confirm this pattern of localisation. DD0 hNPCs were either left untransfected or were transfected with a GFP-tagged ZNF804A construct then immunostained for DAPI, MAP2, GFP and ZNF804A, using the Genetex C2C3 antibody. Interestingly, granular ZNF804A immunostaining could be detected not only in the cell nucleus of CTX0E16 hNPCs (as highlighted by co-localisation with DAPI staining), but also could be seen within the cytoplasm of these cells (see **Figure 5.3.5, A**). This was further confirmed in CTX0E16 hNPCs overexpressing the GFP-tagged ZNF804A construct, with GFP signal being observed in the nuclei, cytoplasm and even within filopodia of transfected cells (**Figure 5.3.5, B**).

The localisation of ZNF804A was further explored in neurons derived from the CTX0E16 line, to determine whether the subcellular pattern of expression of this protein is altered following several weeks of differentiation. DD28 CTX0E16 neuronal cultures were stained with DAPI, MAP2 and the Genetex C2C3 ZNF804A antibody. Assessment of ZNF804A staining with the C2C3 antibody in DD28 MAP2-positive CTX0E16 neurons revealed that ZNF804A was distributed throughout nuclear and cytoplasmic compartments in a distinct punctate manner (see **Figure 5.3.5, C** & **E**). Interestingly,

ZNF804A immunostaining appeared to be predominately cytoplasmic, with greater staining intensity being found in MAP2-positive but DAPI-negative regions of the neurons relative to nuclear staining (see **Figure 5.3.5, C** & **E**). Furthermore, the ZNF804A-positive puncta were surprisingly found to be present along MAP2-positive dendrites in a manner reminiscent of staining for synaptic proteins *in vivo* and *in vitro*. Transfection of DD28 CTX0E16 cultures with a reporter-tagged ZNF804A construct was not possible due to cell death and a lack of transfection efficiency. However, early stage (DD7) CTX0E16 cultures were successfully transfected with a c-myc-tagged ZNF804A construct and immunostained for the early neuronal marker βIII-tubulin and c-myc. A qualitative assessment of the pattern of myc immunostaining in myc-ZNF804A-positive cells indicated that exogenous expression of the tagged ZNF804A construct similarly displayed somatic expression, as well as expression of puncta within the developing neurites even at this early stage of differentiation (see **Figure 5.3.5, D**).

As the endogenous ZNF804A protein appeared to exhibit differential staining in DD0 NPCs and DD28 neurons, the average staining intensity of this protein in cytoplasmic and nuclear compartments at both time points was measured to determine whether there was a significant alteration in protein distribution after several weeks of differentiation. As expected, quantification of relative ZNF804A expression in each compartment revealed that in DD0 cultures, ZNF804A was predominately localised to the nuclei of CTX0E16 hNPCs, while in DD28 cultures this localisation had become inverted, with ZNF804A expression being seen prominently in cytoplasmic regions while nuclear expression was more muted in comparison (see **Figure 5.3.5, E**). Student's t tests performed on these data revealed that inter-compartmental differences in ZNF804A staining at each time point were significant (nuclear vs cytoplasmic expression, arbitrary units: 62.8±2.6 vs 37.2±2.6 (DD0) and 38.7±2.6 vs 61.3±2.6 (DD28); 3 independent experiments for each time point, $p<0.05$ and $p<0.01$ for DD0 and DD28 cultures respectively). Overall, these findings suggest that in human NPCs ZNF804A is expressed predominately within the nucleus and thus may primarily function within this compartment, while in differentiated neurons this protein is mostly expressed outside the neuronal nuclei.

In addition to this, the density of ZNF804A-positive puncta in distal MAP2-positive dendrites was quantified in the immunostained DD28 CTX0E16 cultures. Interestingly, DD28 CTX0E16 neurons were found to express ZNF804A-positive puncta at a density of 2.6±0.4 puncta per 10 µm (see **Figure 5.3.6, C**); this is comparable to the previous findings of synaptic protein puncta density detailed in

Section 4.3.1. Given the similar pattern and density of ZNF804A staining to that previously seen for synaptic proteins in CTX0E16 neurons, it may be possible that this staining in fact represents a synaptic distribution. This possibility is further explored in **Section 5.3.6**.

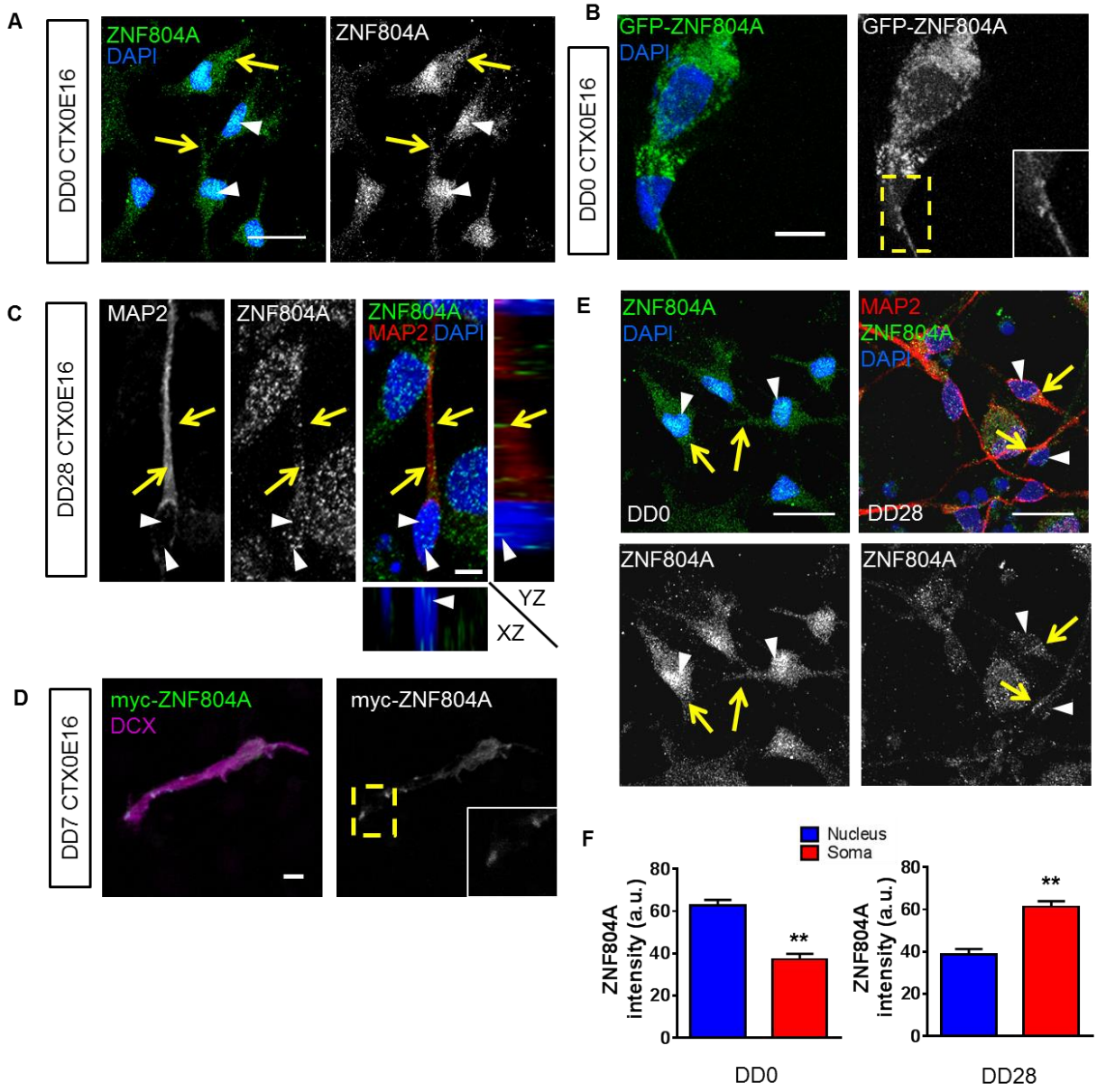

Figure 5.3.5: Expression of ZNF804A in CTX0E16 hNPCs and immature neurons. **A**: Distribution of endogenous ZNF804A in proliferative (DD0) CTX0E16 cells as determined by C2C3 Genetex. ZNF804A immunoreactive puncta were observed within the nucleus (white arrow heads), soma and in neurite-like protrusions (yellow arrows). **B**: Localisation of exogenously expressed GFP-ZNF804A in DD0 CTX0E16. This protein was found to localise to cell nuclei, cytosol and processes (inset). **C**: In DD28 CTX0E16 neurons ZNF804A was localised to the nucleus (white arrowheads) and along microtubule-associated protein 2 (MAP2)-positive dendrites (yellow arrows) using the GeneTex anti-ZNF804A antibody. Orthogonal projections confirm ZNF804A presence at nuclear and extranuclear sites. **D**: Exogenous expression of myc-ZNF804A in DD7 CTX0E16-neurons, resulted in the protein

localising to punctate structures along doublecortin (DCX) positive neurites and at growth cones. Yellow dash box highlights magnified images (inset) of neurite processes demonstrating localisation of myc-ZNF804A at growth cones. **E**: Distribution of endogenous ZNF804A in proliferative (DD0) and differentiated (DD28) CTX0E16 cells as determined by immunocytochemical analysis using C2C3 antibody. ZNF804A immunoreactive puncta were observed within the nucleus (white arrowheads), soma, and in neurite-like protrusions (yellow arrows). **F**: Quantification of relative staining intensity of ZNF804A in nuclei and cytoplasm of DD0 and DD28 CTX0E16 cells (n = 3 independent experiments; **p<0.01). Scale bars = 20 µm (**A** & **E**), 10 µm (**B**) and 5 µm (**C** & **D**).

5.3.6 ZNF804A IS PRESENT ALONG DENDRITES AND CO-LOCALISES WITH SYNAPTIC PROTEINS IN CTX0E16 NEURONS

The expression of ZNF804A along the distal portions of MAP2-positive dendrites in a punctate manner echoes the immunostaining pattern characteristic of synaptic proteins in mature neurons, suggesting that this protein may be present at synapses. Indeed, several other zinc finger proteins have previously been found to localise to and regulate mechanisms at synapses. These include piccolo and bassoon, involved in the regulation of neurotransmitter release at glutamatergic and GABAergic synapses (Fenster et al., 2000; Waites et al., 2013), Makorin ring zinc finger protein 1 (MKRN1), a regulator of synaptic local translation (Miroci et al., 2012); and RIM proteins which interact with a number of key proteins at the active zone (Mittelstaedt et al., 2010). In light of this fascinating initial finding and with the previous findings of synaptic protein expression in CTX0E16 neurons (see **Section 4.3.1**), DD28 CTX0E16 neurons were immunostained for DAPI, MAP2, Genetex-ZNF804A and either PSD-95 or GluN1 to determine whether these puncta co-localise with markers of putative excitatory synapses, suggestive of a post-synaptic localisation. Additionally, a subset of these cultures was transfected with a recombinant AAV vector driving eGFP expression under the control of a CamKII promoter as described in **Section 2.3.2** and immunostained for C2C3 ZNF804A, DAPI and GFP to determine whether ZNF804A could also be found at putative dendritic spines in human neurons. Surprisingly, ZNF804A puncta were found to co-localise with a subset of both PSD-95 and GluN1 puncta, with ~44% of ZNF804A ROI staining positive for PSD-95 while approximately 40% of ZNF804A puncta co-expressed GluN1 (puncta per 10 µm: ZNF804A, 2.8±0.38; PSD-95, 3.4±0.32; GluN1, 3.1±0.4; ZNF804A & PSD-95, 1.5±0.14; ZNF804A & GluN1, 1.2±0.17) (see **Figure 5.3.8, A**-**C**). Moreover, only a fraction of these synaptic puncta were themselves positive for ZNF804A staining, indicating that this protein may only possess a role at a subset of excitatory synapses in glutamatergic neurons. Interestingly, ZNF804A puncta could also be seen in the putative dendritic spines of CaMKII-positive

CTX0E16 neurons, further indicating a post-synaptic presence of this protein (**Figure 5.3.7, D**). These findings suggest that in addition to being distributed along MAP2-positive dendrites, a subset of ZNF804A also localises to the post-synaptic densities of glutamatergic synapses.

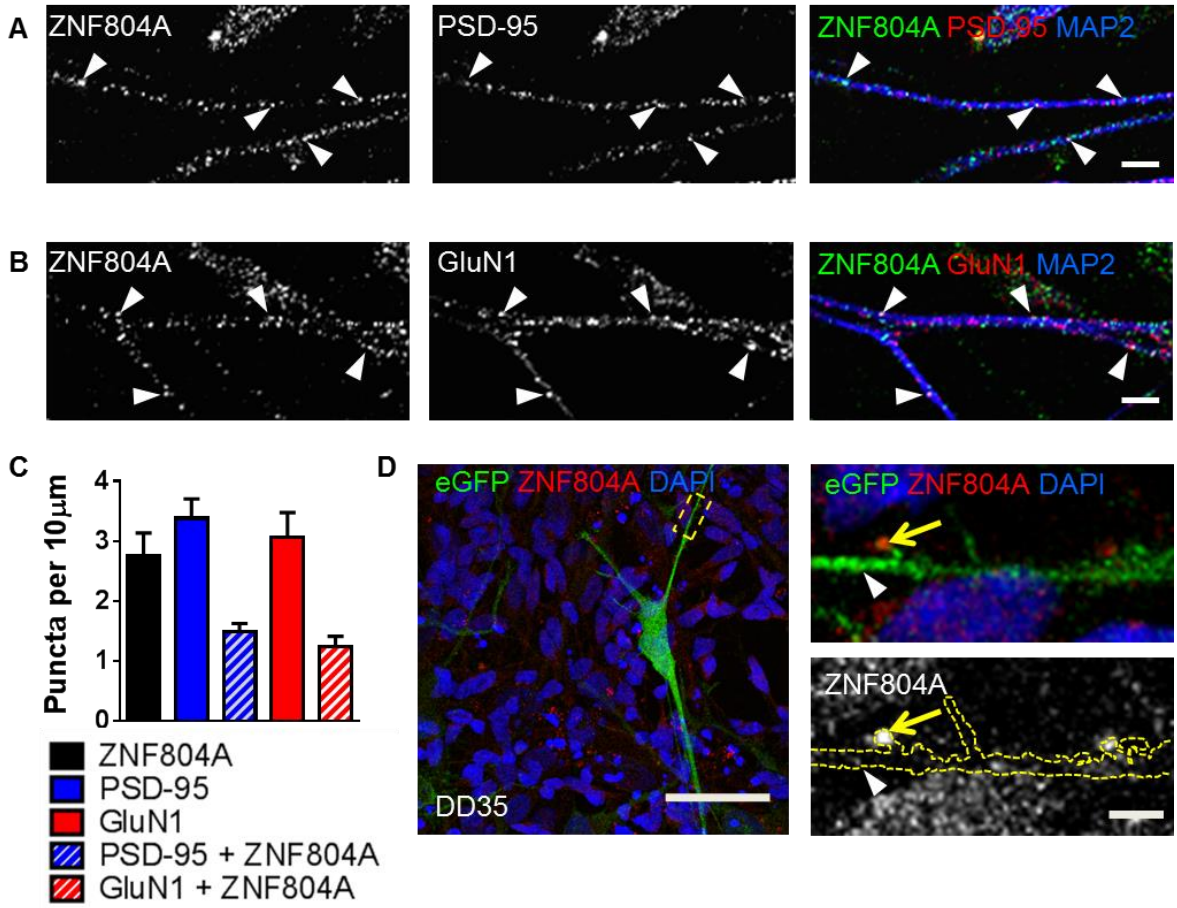

Figure 5.3.8: ZNF804A localises to putative synapses in DD28 CTX0E16 neurons. **A & B**: ZNF804A is present along distal dendrites of DD28 CTX0E16 neurons, where a sub-set of puncta co-localise with putative synaptic markers. White arrow heads indicate co-localisation of ZNF804A with PSD-95 **(A)** or the NMDA receptor subunit, GluN1 **(B)**. **C**: Quantification of ZNF804A, PSD-95, GluN1 and co-localised puncta density in DD28 CTX0E16 neurons (puncta per 10 µm: ZNF804A, 2.8±0.38; PSD-95, 3.4±0.32; GluN1, 3.1±0.4; ZNF804A + PSD-95, 1.5±0.14; ZNF804A + GluN1, 1.2±0.17; n = 17 neurons from 3 independent experiments). **D**: ZNF804A puncta were present within the heads of dendritic spines of DD35 CTX0E16 neurons transfected with peGFP. Yellow arrows indicate ZNF804A puncta within the heads of dendritic spines, white arrow heads indicate puncta within the dendritic shaft. Scale bars = 5 µm **(A, B & D, inset)**, 50 µm **(D)**.

5.3.7 SUBCELLULAR DISTRIBUTION OF ZNF804A IN HIPSC-DERIVED NEURONS

The CTX0E16 cell line offered a useful model through which the subcellular localisation of ZNF804A could be characterised in both human neural progenitors and differentiated neurons. However, as this cell line is derived from the neuroepithelium of a single fetus, it is important to verify these novel findings in neurons generated from multiple sources. hiPSCs offer a powerful new system to assess the impact of genetic variation on specific cellular phenotypes, particularly within the context of diseases with a genetic component contributing to their overall risk. In addition to the benefit of a confirmation of the phenotype seen in CTX0E16 cells, experiments studying ZNF804A in hiPSC-neurons also offer a “proof of concept” for potential future investigations into the impact of patient-relevant mutations in the ZNF804A gene on expression and subcellular localisation of this protein. hiPSCs were derived from keratinocytes of three apparently healthy individuals via lentiviral transduction. These lines were differentiated for five weeks using a protocol which favours the robust generation of forebrain excitatory neurons (Shum et al., 2015). A prior in-house characterisation of these cell lines revealed that early hiPSC differentiation resulted in a homogenous population of neural precursor cells that stained positive for the neural stem cell markers nestin and Sox2, followed by the formation of nestin and ZO-1-positive neural rosettes (see **Figure 5.3.9, A** & **B**). Upon addition of the NOTCH inhibitor DAPT these cells underwent terminal differentiation, producing Tbr1-positive neurons, indicative of a deep cortical layer identity (**Figure 5.3.9, C**). These neurons also expressed VGlut1, indicating the adoption of an excitatory, glutamatergic fate (**Figure 5.3.7, D**).

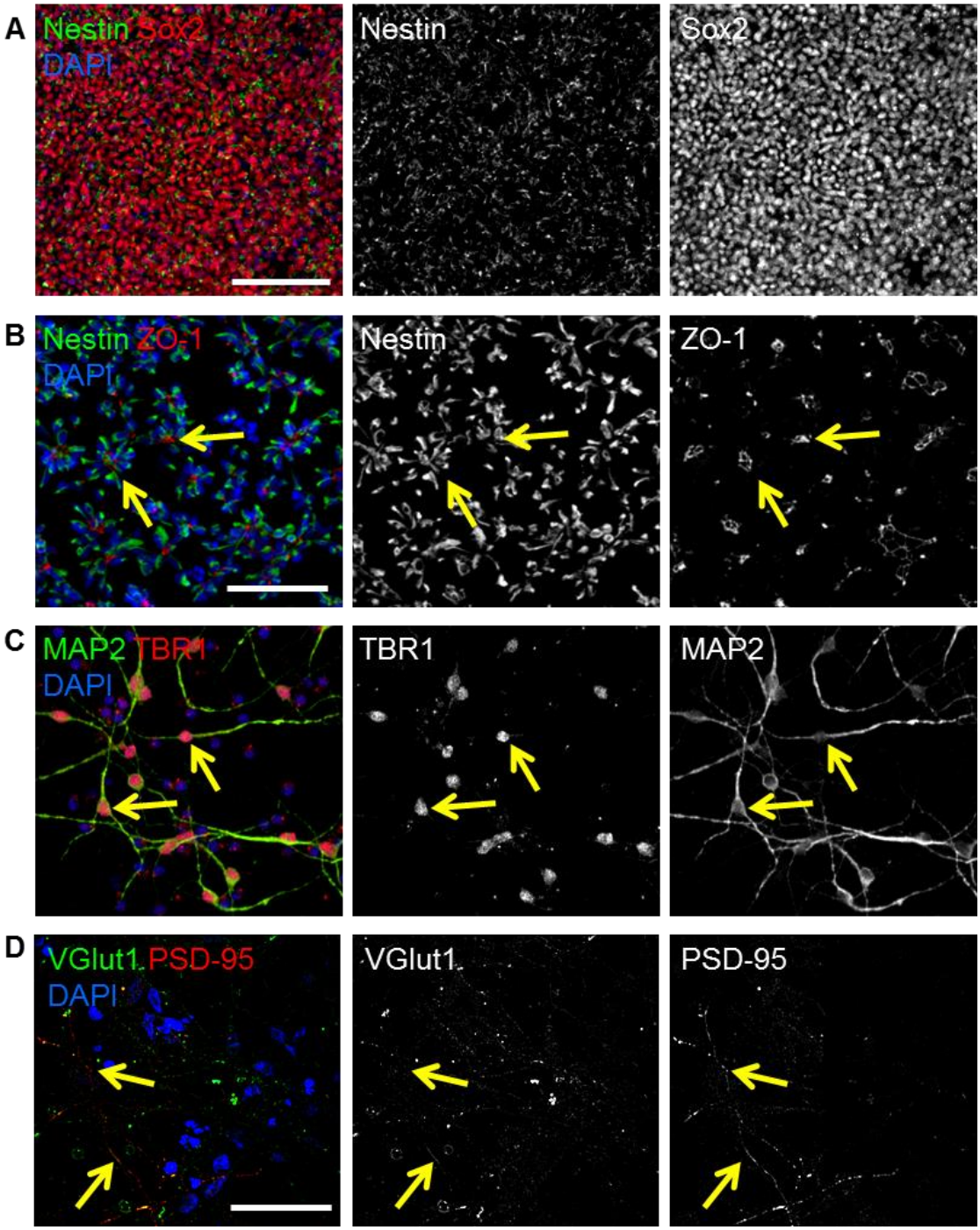

Figure 5.3.9: Derivation of neurons from hiPSCs. **A**: Following 8 days of neuralisation, a population of early neuroepithelial cells was formed as determined by positive staining for nestin and SOX2. **B**: Subsequent generation of neural progenitor cells (NPCs) was determined by formation of neural rosettes. Apical lumen of rosettes were positive for ZO-1 with nestin positive cells forming a radial structure surrounding the lumen (yellow arrows). **C** & **D**: Terminal differentiation of NPCs resulted in the generation of projecting glutamatergic neurons which stained positive for TBR1 **(C,** yellow arrows**)** and VGlut1 **(D**, yellow arrows**)**. Scale bars = 100 µm **(A** & **B)**; 50 µm **(C)** or 20 µm **(D)**. This work was conducted by Dr. Carole Shum.

ZNF804A transcript expression was again assessed via q-PCR and quantified using the ΔΔCT method in hiPSCs and DD30 hiPSC-derived neurons from three independent experiments in each cell line (see **Figure 5.3.10, A**). *ZNF804A^{exon4}* was found to be the most abundant transcript in both hiPSCs and hiPSC-neurons, though surprisingly this expression was significantly upregulated in the neuronal cells relative to the hiPSCs (relative expression in arbitrary units: 0.270±0.066 vs 0.016±0.007 for hiPSC-neurons and hiPSCs respectively; $p<0.05$). Although at first this may appear to contradict the downregulation of the *ZNF804A^{exon4}* following differentiation of CTX0E16 cells, it may be possible that the relatively high expression of this variant in hNPCs may represent a transient increase as these cells adopt a neural progenitor cell identity, followed by a modest downregulation as these cells terminally differentiate. *ZNF804A$^{E3/E4}$* expression was also found to be significantly increased in hiPSC-neurons in comparison to hiPSCs (0.061±0.015 vs 0.007±0.003 respectively; $p<0.05$); while *ZNF804A$^{2.2}$* was also significantly upregulated following several weeks of terminal differentiation though this variant was only expressed at very low levels at both stages of development (0.002±0.001 vs 0.001±0.001 for hiPSC-neurons and hiPSCs respectively; $p<0.05$). Taken together, these data support the findings of the previous q-PCR of CTX0E16 mRNA samples, indicating that expression of *ZNF804A^{exon4}* is upregulated as neuronal cells differentiate.

With this initial finding in mind, hiPSC-derived neurons were assessed via immunocytochemistry to determine whether these cells also recapitulate the extranuclear distribution and putative synaptic localisation seen in differentiated CTX0E16 neurons. DD35 hiPSC-neurons were immunostained for DAPI, MAP2, Genetex-ZNF804A and either PSD-95 or GluN1. As in CTX0E16 neurons, MAP2-positive hiPSC-derived neurons were found to exhibit both nuclear and extranuclear distributions of ZNF804A, including within the cell soma and along MAP2-positive dendrites (see **Figure 5.3.10, B**). In addition, discrete ZNF804A-positive puncta could be observed along the distal portions of these dendrites, consistent with the previous findings in differentiated CTX0E16 neurons (**Figure 5.3.7, C**). Crucially, approximately 39% of these ZNF804A puncta were found to co-localise with PSD-95, while ~45% of ZNF804A puncta co-localised with GluN1, a degree of co-localisation which was comparable to that seen in CTX0E16 neurons (puncta per 10 µm: ZNF804A, 2.46±0.36; PSD-95, 3.18±0.30; GluN1, 2.61±0.32; PSD-95 & ZNF804A, 1.21±0.12; GluN1 & ZNF804A, 1.01±0.15) (**Figure 5.3.7, D**). This further supports the interpretation that a subset of ZNF804A protein expressed along dendrites is localised to putative synapses. Additionally, as only a fraction of GluN1 and PSD-95 puncta

co-localised with ZNF804A, this may represent a subpopulation of glutamatergic synapses with a distinct functional identity. Collectively, these findings indicate that hiPSC-neurons will provide a useful paradigm for studying alterations in *ZNF804A* expression resulting from disease relevant mutations in this gene, in lines derived from patient subgroups and apparently healthy controls.

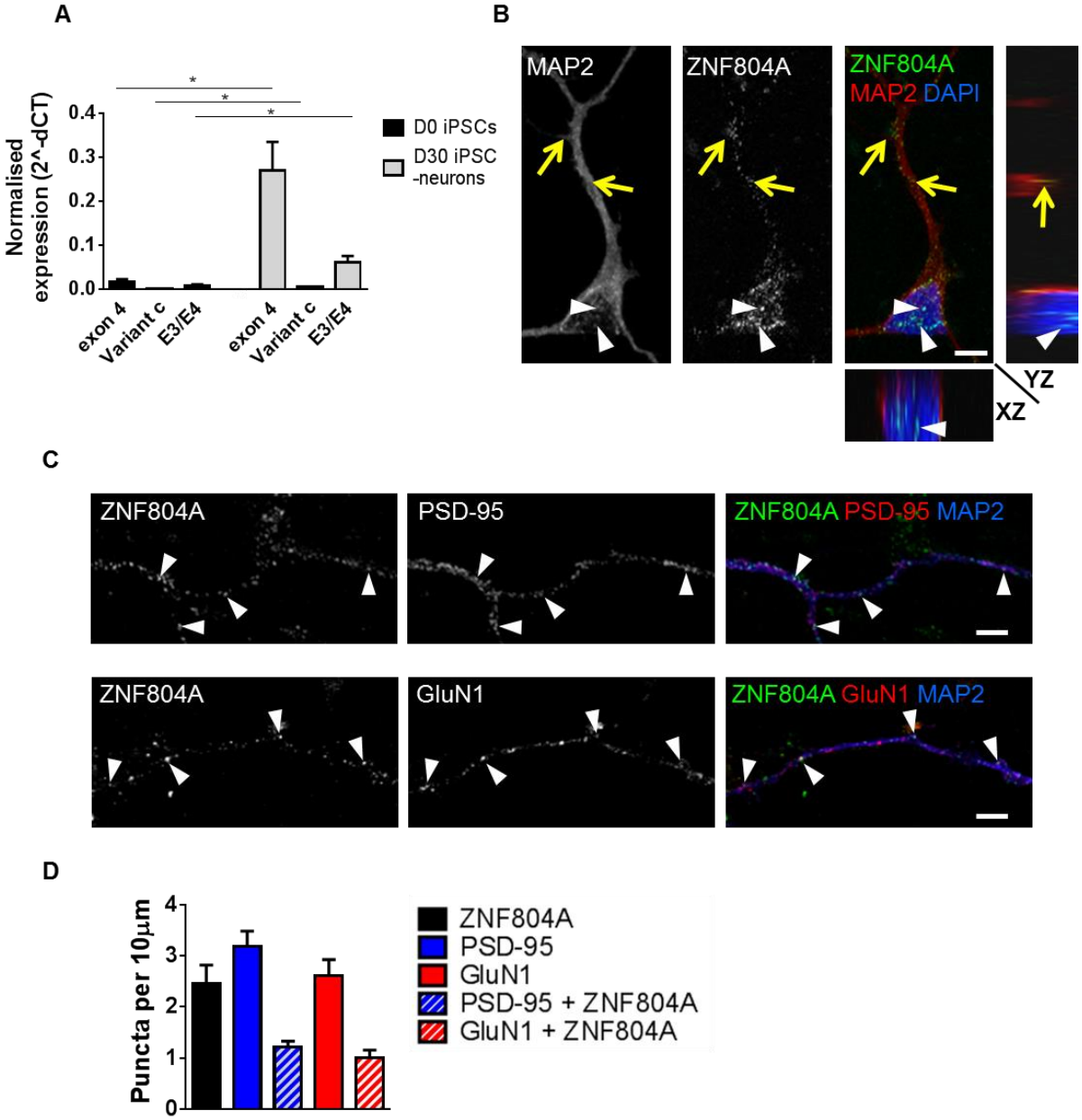

Figure 5.3.10: ZNF804A localises to the cytosol and putative synapses in hiPSC-neurons. **A**: q-PCR of mRNA for ZNF804A exon 4, E3/E4 and variant c transcripts in hiPSCs and immature neuronal cells derived from three separate hiPSC lines (n = 3 independent experiments from 3 individual lines; *p<0.05). **B**: In 35 day old neurons differentiated from hiPSCs, ZNF804A puncta were observed in the nucleus (white arrow heads) and along dendrites (yellow arrows) in XY, XZ and YZ planes. **C**: ZNF804A puncta are also found along distal MAP2 positive dendrites. Co-staining with PSD-95 or GluN1 reveals

Figure 5.3.10, continued: that a fraction of ZNF804A puncta co-localise with either synaptic protein. **D**: Quantification of ZNF804A, PSD-95, GluN1 and co-localised puncta in hiPSC-neurons (puncta per 10 µm: ZNF804A, 2.5±0.36; PSD-95, 3.2±0.3; GluN1, 2.6±0.32; ZNF804A + PSD-95, 1.2±0.11; ZNF804A + GluN1, 1.0±0.15; n = 16 neurons from 3 independent experiments). Scale bars = 5 µm **(B** & **C)**.

5.3.8 SUBCELLULAR LOCALISATION OF ZFP804A IN RAT PRIMARY CORTICAL NEURONS

The description of ZNF804A localisation within various subcellular compartments in CTX0E16 and hiPSC-derived neurons provided a valuable insight into the potential extranuclear functions of this protein. As ZNF804A was found to co-localise with key post-synaptic density proteins in both of these cellular models, an interesting further avenue of inquiry would be to investigate whether ZNF804A was expressed within dendritic spines, where the post-synaptic densities of excitatory synapses typically occur in the mammalian forebrain. However, despite CTX0E16 neurons being capable of developing putative dendritic spines (see **Section 3.3.8**) and previous research establishing that under certain protocols hiPSC-derived neurons are also capable of attaining spinogenesis (Marchetto et al., 2010a), these paradigms were impractical for assessing the distribution of ZNF804A in spines as the majority of synapses in these young developing neurons occur on the dendritic shaft rather than on spines. Thus, CTX0E16-neuron spines were too sparse to permit a meaningful analysis of protein expression and hiPSC-neuron spines typically require multiple months of culturing before they attain spinogenesis (Ricciardi et al., 2012; Verpelli et al., 2013). To address this, GFP-transfected rat primary cortical neurons were instead employed to determine whether the pattern of ZNF804A expression observed in CTX0E16- and hiPSC-neurons was conserved in neurons derived from another mammalian species and additionally to find whether the rat homologue Zfp804A was also located within the dendritic spines of these neurons.

Cultures of primary rat cortical neurons were transfected with Synapsin-driven GFP at DIV23 and immunostained at DIV25 for GFP or MAP2, Genetex-ZNF804A and DAPI. Qualitative assessment of the GFP-transfected and MAP2-positive pyramidal neurons revealed that Zfp804A was again localised within both the cell nuclei and the cytoplasm of the cell soma in a distinct punctate staining pattern (see **Figure 5.3.11, A** & **B**). Furthermore, Zfp804A puncta could also be observed within proximal and distal dendrites, consistent with the findings seen in neurons derived from human cell lines (see **Figure 5.3.11, C** & **D**). Critically, Zfp804A staining could also be observed within dendritic spines,

with 44.5±5.9% of spines expressing this protein (**Figure 5.3.11, D**). As spine morphology is thought to be closely related to synaptic function, Zfp804A-positive and –negative spines were categorised according to size, length and width. An evaluation of the size distributions of both Zfp804A-positive and Zfp804A negative spines found that the majority of dendritic spines containing Zfp804A had a total spine area of less than 1.0 μm^2 (>70%) (**Figure 5.3.11, E**). Unpaired Student's t tests were performed on spine length, width and area data to determine whether any differences between the two spine populations were significant. No significant differences could be found between the average lengths, widths or areas of Zfp804A-positive and negative spines ($p>0.05$; mean ± SEM of Zfp804A-positive vs Zfp804A negative spines: 1.30±0.08 µm vs 1.38±0.05 µm; 1.47±0.09 µm vs 1.60±0.06 µm; and 0.97±0.07 μm^2 vs 1.04±0.09 μm^2 for spine length, width and area respectively) (**Figure 5.3.11, F**-**H**). A subset of Zfp804A-positive puncta could also be observed along putative axons of GFP-positive pyramidal neurons, suggesting that this protein may also be part of pre-synaptic or axonal structures (**Figure 5.3.11, I**).

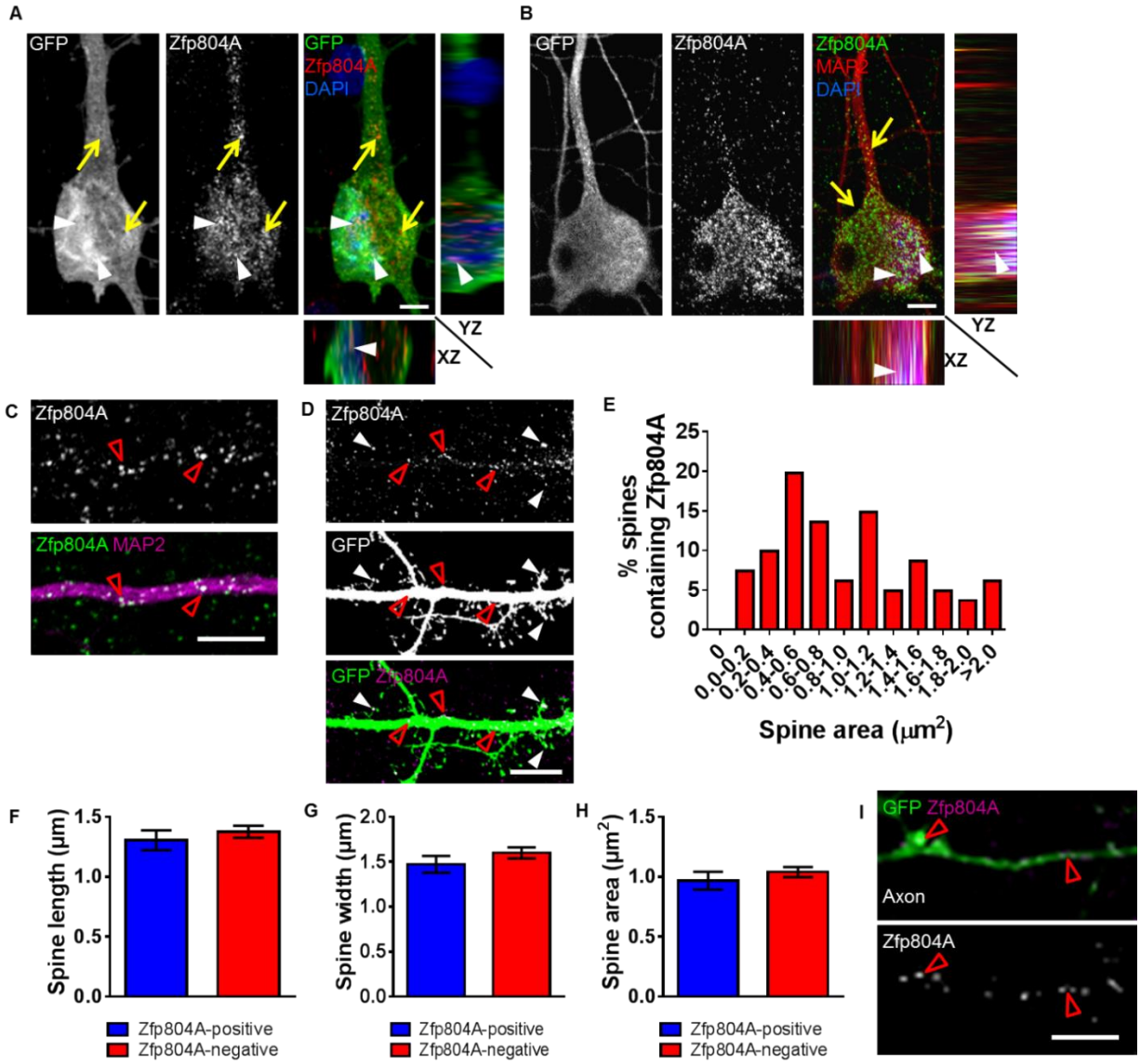

Figure 5.3.11: Zfp804A is present at synapses in mature primary cortical neurons. **A**: Representative confocal image, including orthogonal views in the XZ and YZ planes, of a 25 days *in vitro* (DIV25) rat primary cortical neuron transfected with eGFP and immunostained for endogenous Zfp804A (rodent homologue of ZNF804A). Expression of Zfp804A within the cell nucleus is indicated with white arrow heads, while expression of Zfp804A within the cell soma and in proximal dendrites is indicated by yellow arrows. **A**: Endogenous Zfp804A is present in the nucleus and somato-dendritic compartments in MAP2-positive cortical neurons. Zfp804A was observed within the nucleus (white arrow heads) and as punctate structures along dendrites (yellow arrows). **B**: Representative confocal image, with orthogonal views, of MAP2-positive DIV25 rat primary cortical neuron co-stained for Zfp804A. Expression of Zfp804A within the cell nucleus is indicated with white arrow heads, while expression of Zfp804A within the cell soma and in proximal dendrites is indicated by yellow arrows. **C**: Zfp804A **Figure 5.3.11, continued**: -puncta are also found along distal MAP2 positive dendrites (open red arrow heads). **D**: Zfp804A localised to the dendritic shaft (open red arrow heads) and dendritic spines (white arrow heads) in the dendrites of mature primary cortical neurons. **E**: Histogram of the areas of spines that contain

Figure 5.3.11, continued: Zfp804A. A larger proportion of spines that contained Zfp804A had small-to-medium area (<1 µm^2), while fewer large spines (>1 µm^2) contained Zfp804A signal. **F**-**H**: Quantification of morphological characteristics in Zfp804A-positive and Zfp804A-negative spines. No significant differences could be found for these characteristics in either population. **I**: Examination of endogenous ZNF804A distribution in DIV 25 cortical neurons revealed that a small amount of protein was present in axon processes (open red arrow heads). Scale bars = 5 µm (**A**-**D**, **I**).

To further confirm this observed synaptic distribution, synaptosomal preparations were generated from DIV25 rat primary cortical neuron cultures and analysed via western blot using the Genetex anti-ZNF804A antibody alongside the whole cell lysates. Consistent with the immunocytochemistry data, a band at the expected ~137kDa size could be observed in the whole cell lysates and in crude synaptic lysates, further supporting a synaptic localisation of Zfp804A (**Figure 5.3.12**, **A**). Additionally, multiple weaker bands not corresponding to any known ZNF804A isoforms could also be seen in these samples; these may have arisen from rat-human differences in the expressed variants. Overall, these observations indicate that in mature cortical neurons Zfp804A is present along the dendritic shaft and in pre- and post-synaptic structures, consistent with the findings in human cell lines.

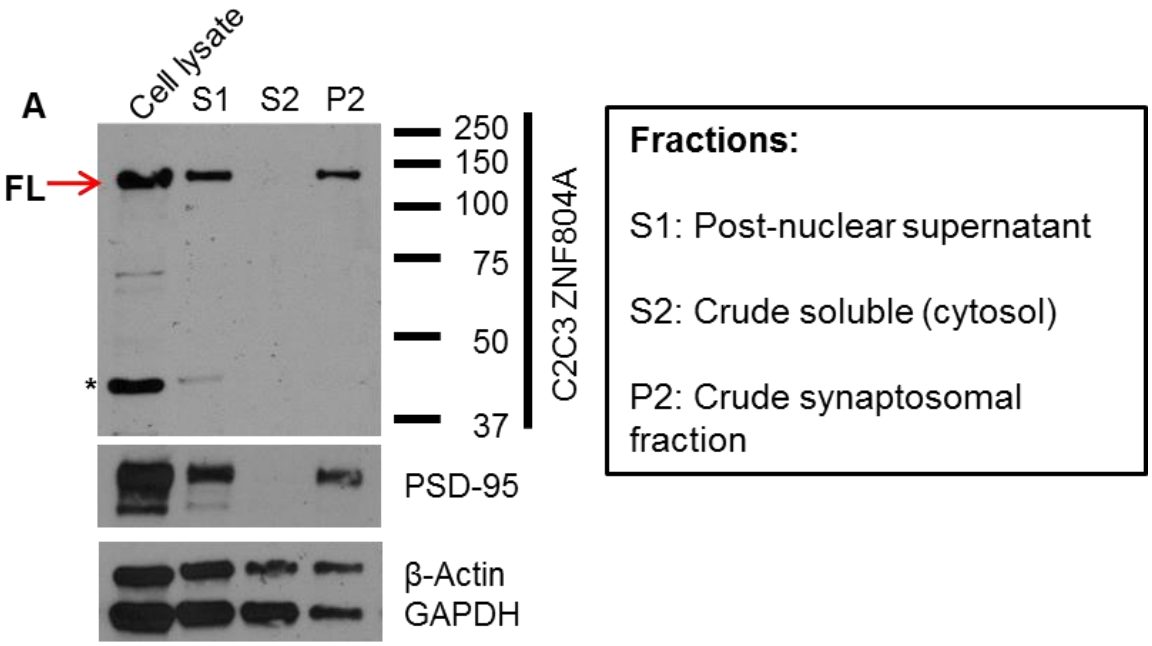

Figure 5.3.12: Western blot of lysates and subcellular fractions of DIV25 rat primary cortical neurons. **A**: Subcellular fractionation of DIV25 rat primary cortical neurons. Note the full length protein band at the predicted size of 137 kDa within the crude synaptosomal fraction.

Interestingly, a subset of pyramidal neurons exhibited Zfp804A staining with a greatly increased intensity in contrast to the majority of the other Zfp804A-positive neurons (hereafter described as “classical” or “type I” neurons; **Figure 5.3.13**, **A** & **B**). Brightly stained neurons could be further categorised into those expressing Zfp804A in punctate structures (hereafter described as “type II” neurons; see **Figure 5.3.13, C**) and other brightly-stained neurons expressing Zfp804A in distinct elongated “log” structures structures (hereafter described as “type III” neurons; see **Figure 5.3.13, D**), located within the cell nuclei and within dendro-somatic compartments. Although this discovery was made relatively late in the present investigation and therefore precluding any further investigation into this phenomenon, an interesting avenue of inquiry in future research would be to determine whether each of these neuronal subtypes is limited to specific classes or regional identities of neuron. Furthermore, as in type II and type III neurons the Zfp804A puncta and “logs” could be observed along the dendrites of these cells similarly to classical Zfp804A-positive neurons, it may be possible that these structures correspond to differing categories of synapse.

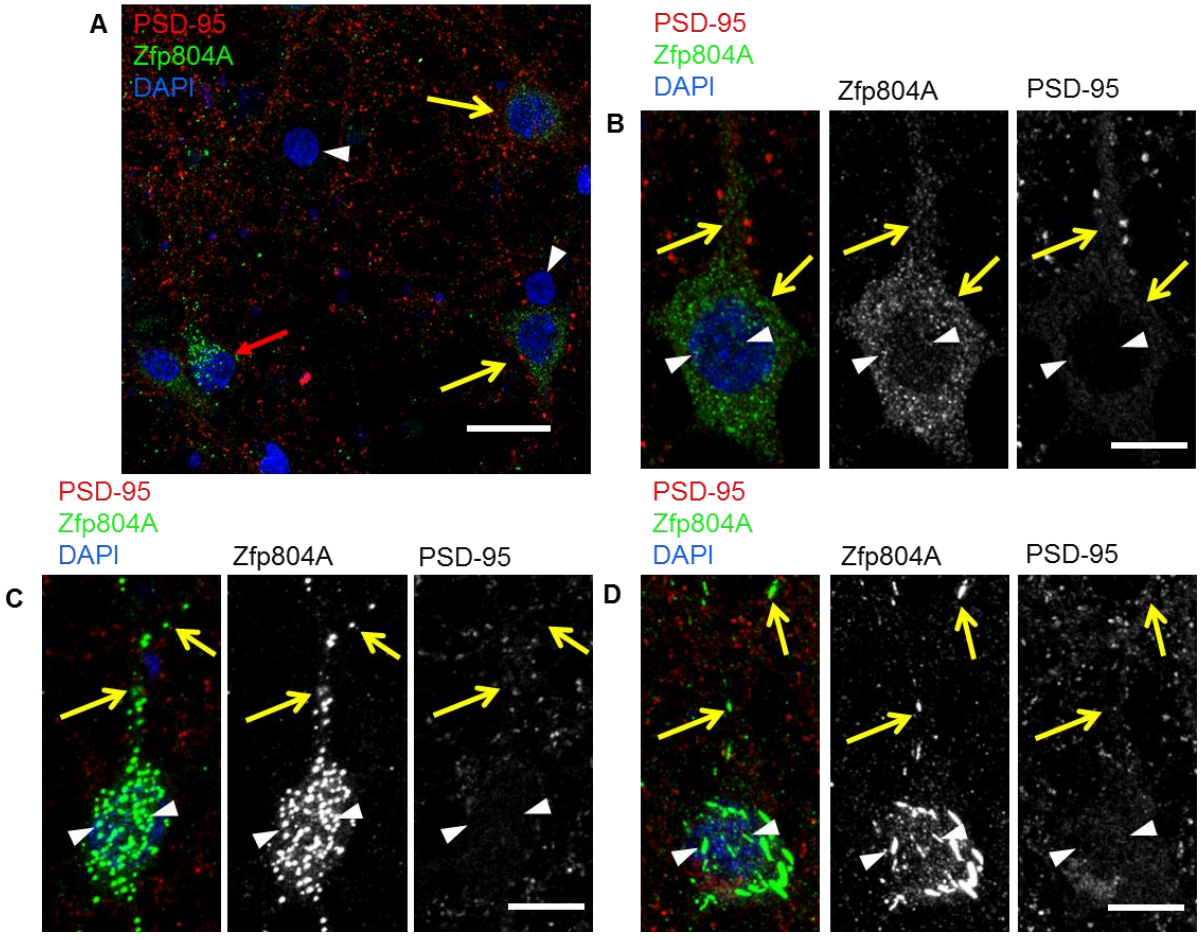

Figure 5.3.13, overleaf: Subtypes of Zfp804A staining. **A**: In DIV25 primary rat cortical cultures, Zfp804A-positive cells adopt differential patterns of localisation. A minority of Zfp804A-positive cells adopt a particularly strong Zfp804A staining pattern (red arrow) in contrast to the subdued staining of the "classical" Zfp804A-positive neuron (yellow arrows). Zfp804A-negative cells (white arrowheads) are also shown. **B**-**D**: Representative confocal images of each of the three Zfp804A expression subtypes. **B**: A "classical" or "type I" Zfp804A-positive neuron. **C**: A "bright puncta" or "type II" Zfp804A-positive neuron. **D**: A "bright log" or "type III" Zfp804A-positive neuron. White arrowheads highlight nuclear staining, yellow arrows indicate staining along putative neurites. Scale bars = 20 µm (**A**) & 10 µm (**B**-**D**).

5.3.9 SUBSYNAPTIC LOCALISATION OF ZFP804A

Recent research into synaptic protein localisation has resulted in a growing recognition that these proteins are organised into sub-synaptic domains (Smith et al., 2014; Willig and Barrantes, 2014). Although confocal imaging of Zfp804A in GFP-transfected neurons provided some useful information about the general expression of this protein in spines, the limit of resolution possible with this imaging technique (~200nm) precludes any characterisation of protein localisation at the sub-synaptic level. To address this limitation, GFP-transfected rat primary cortical neurons immunostained as described previously were instead imaged using structured illumination microscopy (SIM), a superresolution imaging technique which utilises an algorithm based on the diffraction of light through a rotating grid to enhance the resolution of standard confocal microscopy (Gustafsson, 2000). SIM imaging revealed that this protein was present within nanoscopic structures along the dendritic shaft and in spines see (see **Figure 5.3.14, A**). Furthermore, SIM imaging confirmed putative axonal expression of this protein in discrete nanoscale structures (**Figure 5.3.14, B**). In contrast to the results of confocal imaging which indicated Zfp804A was distributed throughout the dendritic spine head and neck (**Figure 5.3.14, C)**, SIM imaging revealed Zfp804A clustered in domains within spine heads; intensity profiles of Zfp804A staining throughout the spine confirmed this enrichment in spine heads (**Figure 5.3.13, D**). Zfp804A-positive nanodomains could also be observed along dendrites and surprisingly, specific localisation of the protein could be seen at the base of a subpopulation of dendritic spines.

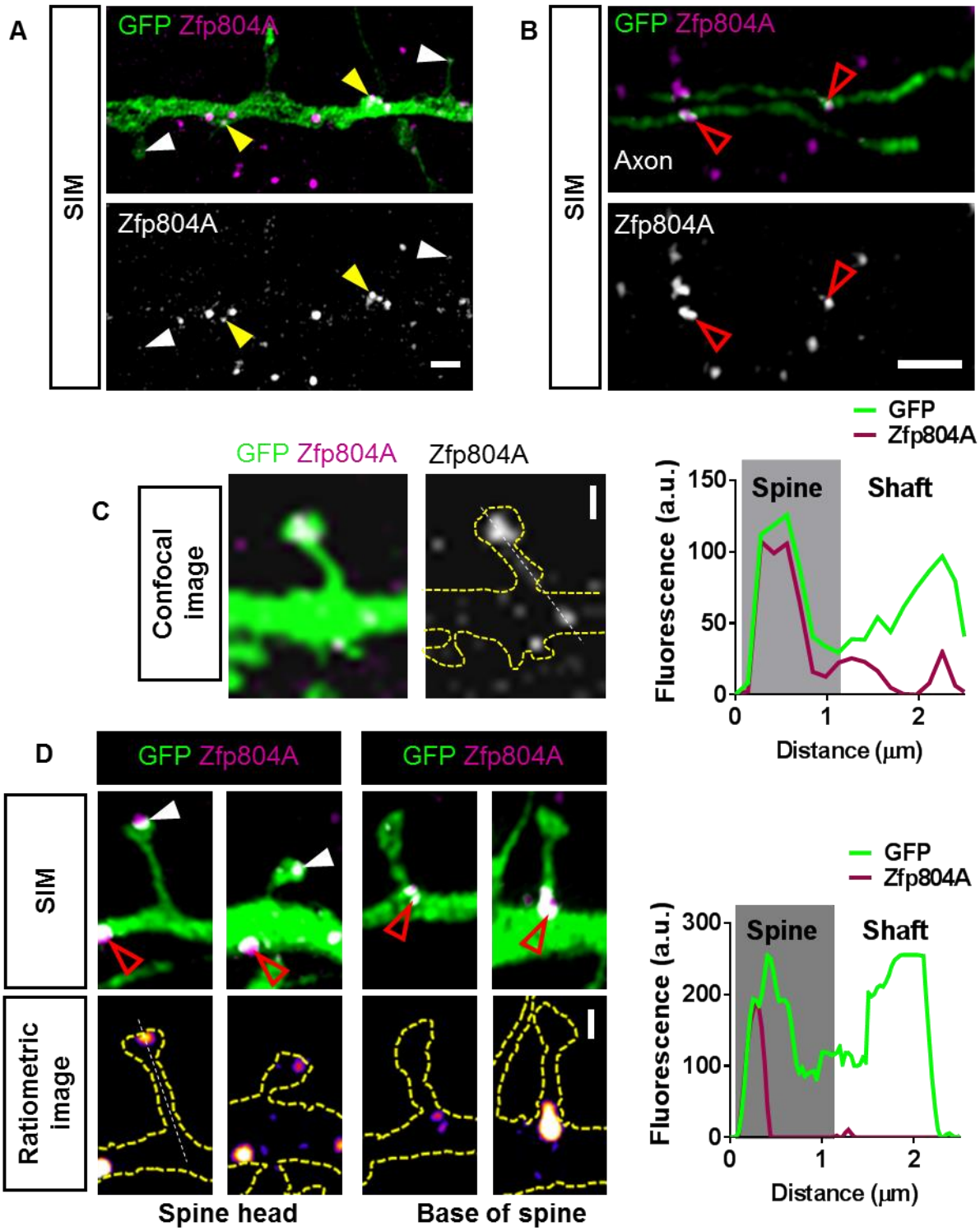

Figure 5.3.13: Sub-structural localisation of Zfp804A in primary rat cortical neurons. **A**: Superresolution SIM images of Zfp804A sub-cellular localisation in GFP expressing primary rat cortical neurons (DIV 25). Zfp804A is present in spine heads (white arrow heads) and along the dendrite (yellow arrow heads). **B**: SIM image of axon from GFP-expressing neuron reveals that Zfp804A is present in small puncta along axons (red open arrow heads). **C**: High magnification confocal image of dendritic spine in **Figure 5.3.11**, **D**. A line scan through the spine and shaft shows greater Zfp804A fluorescence intensity in the head compared to the shaft. **D**: Superresolution SIM images of Zfp804A subsynaptic localisation

Figure 5.3.13, continued: in primary cortical neurons. Zfp804A is present in spine heads (white arrow heads) and along the dendrite (red open arrow heads). Outline of neuronal **Figure 5.3.13, continued: -**morphology is indicated by yellow dashed lines. Zfp804A signal could also be detected at the base of (red open arrow heads). A line scan through the spine and shaft shows that spines is present within the heads of spines. Scale bars = 5 µm **(A** & **B)**, 1 µm **(C)** and 500 nm **(D)**.

5.3.10 ORGANISATION OF ZFP804A WITHIN THE GLUTAMATERGIC SYNAPSE

The post-synaptic density of excitatory synapses contains a wide array of proteins arranged in highly organised subsynaptic structures. Previous ultrastructural studies have shown that PSD-95 and GluN1 are both core components of the post-synaptic density of glutamatergic synapses (Gerrow et al., 2006; Kim and Sheng, 2004). To determine the co-localisation rate of Zfp804A with these proteins in spines, and additionally to determine how Zfp804A integrates into the post-synaptic density relative to these proteins, GFP-transfected DIV25 rat primary cortical neurons were immunostained for GFP, Genetex-ZNF804A and either PSD-95 or GluN1 and imaged using confocal and SIM microscopy as described in **Section 5.3.10**. Similarly to previous results in CTX0E16 and hiPSC-neurons, Zfp804A puncta were found to co-localise with a subset of synaptic puncta in dendritic spines (**Figure 5.3.14, A**). Confocal images of these proteins in dendritic spines revealed that approximately 53.8±6.9% of PSD-95-positive spines also expressed Zfp804A. In contrast to this, 89.9±2.5% of GluN1-positive spines exhibited Zfp804A (**Figure 5.3.14, B**). This suggests that in the dendritic spines of mature cortical neurons, Zfp804A may preferentially segregate to synapses containing ionotropic NMDA receptors at this stage of development. An additional attempt at confirmation of this pattern of immunostaining *in vivo* was carried out in adult mouse cortical sections. Sections were immunostained for the nuclear marker DAPI, Genetex-ZNF804A/Zfp804A and the excitatory pre-synaptic marker bassoon. Interestingly, in these sections Zfp804A retained the punctate staining pattern seen *in vitro*, with a subset of ZNF804A-positive puncta being juxtaposed or co-localising with the pre-synaptic marker bassoon, again indicating a synaptic localisation of this protein (**Figure 5.3.14, C** & **D**). Taken together, these findings indicate that Zfp804A co-localises with several key synaptic proteins in discrete puncta *in vitro* and *in vivo*, and thus may be a component of excitatory synapses.

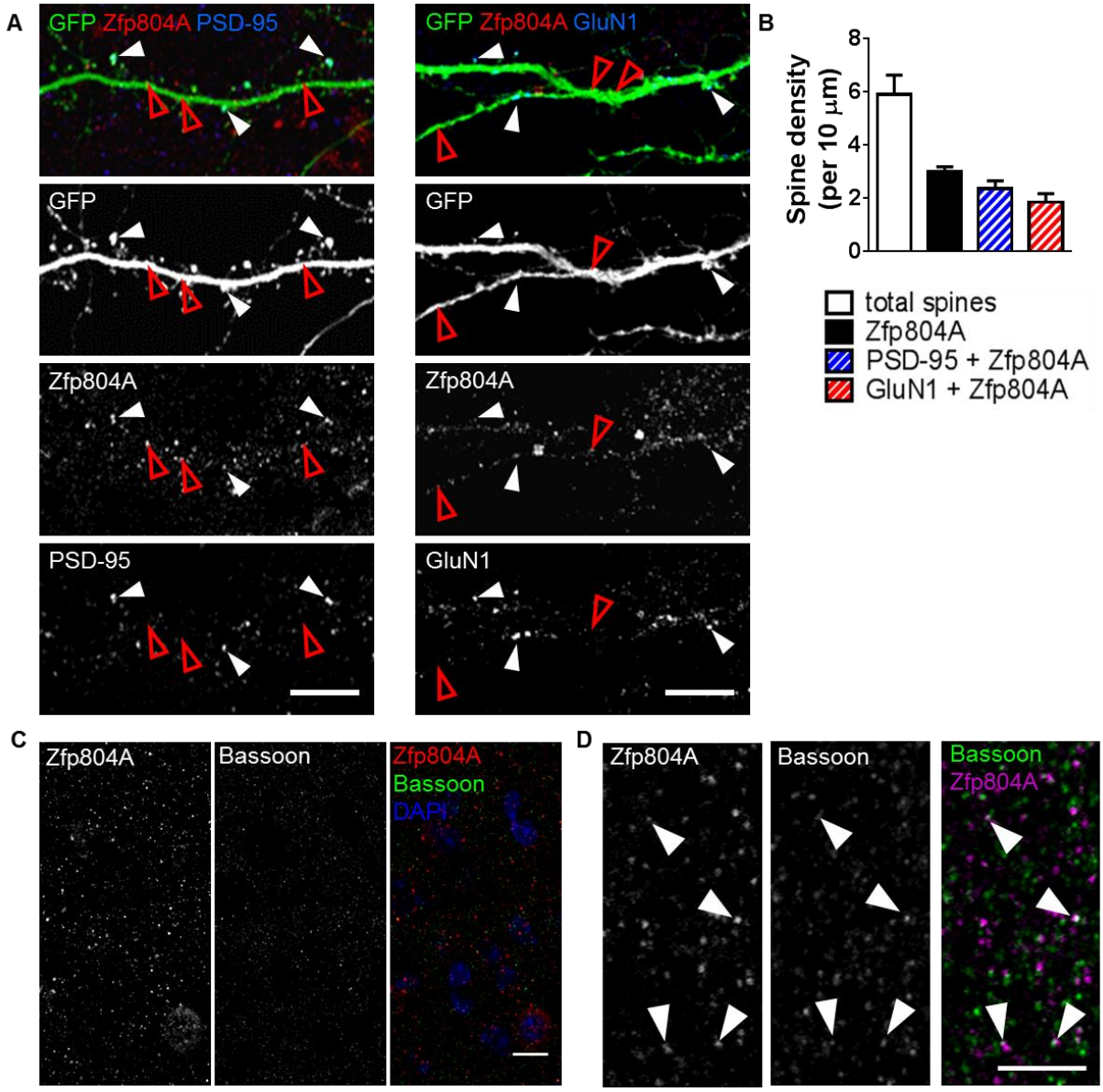

Figure 5.3.14: Endogenous Zfp804A localises to putative excitatory synapses in cortical rodent neurons *in vitro* and *in vivo*. **A**: Representative confocal image of GFP-expressing cortical neurons co-stained for Zfp804A and either PSD-95 or GluN1. This revealed that a fraction of Zfp804A puncta co-localise with PSD-95 and GluN1 in spines (white arrows heads). Open red arrow heads label Zfp804A puncta not co-localised. **B**: Quantification of Zfp804A, PSD-95, GluN1 and co-localised puncta in dendritic spines (spines per 10 µm: total, 5.9±0.68; Zfp804A, 2.9±0.17; Zfp804A + PSD-95, 2.34±0.32; Zfp804A + GluN1, 1.8±0.23). **C** & **D**: Representative confocal images of mouse cortical sections stained for Zfp804A and the pre-synaptic excitatory marker bassoon. White arrowheads indicate areas of co-localisation highlighted in white. Scale bars = 5 µm **(A, C** & **D)**.

Qualitative assessment of the substructural organisation of these proteins via SIM imaging revealed that Zfp804A adopted a non-uniform distribution within spine heads; this domain was found to partially co-localise with a surrounding PSD-95-positive region (**Figure 5.3.15, A**). Linescans across

Zfp804A and PSD-95-positive regions in spine heads further supported a partial co-localisation of these proteins, while a qualitative assessment of expression within the spine head across the Z-plane confirmed that this was not an artifact of Z-projecting multiple planes of a three dimensional structure into a two dimensional image (**Figure 5.3.15, C**). SIM imaging of Zfp804A-positive spines co-stained for GluN1 revealed that this protein also partially co-localised with Zfp804A; intensity profiles of these puncta confirmed this partial overlap, while an evaluation of the Z-plane of these spines again determined that this was not an artifact of the Z-projection of the image (**Figure 5.3.15, B** & **D**). Taken as a whole, these findings indicate that in a majority of spines expressing the core glutamatergic post-synaptic density components PSD-95 or GluN1, Zfp804A is co-expressed with either protein. In addition to this, within dendritic spine heads Zfp804A appears to be predominately localised to the perisynaptic region. Moreover, a small proportion of this protein may potentially be present within the post-synaptic density, raising the possibility that a subset of Zfp804A forms complexes with synaptic proteins.

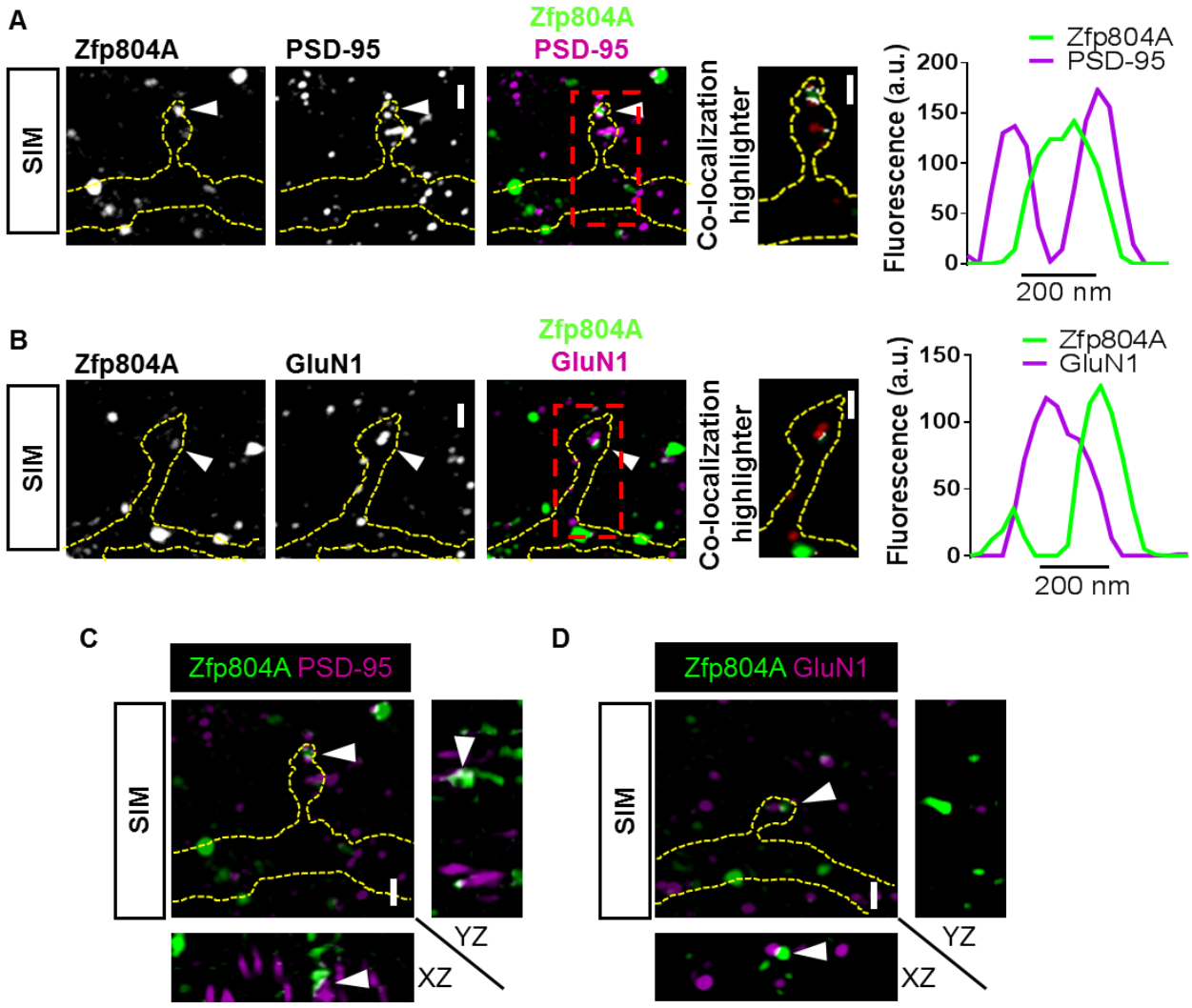

Figure 5.3.15: Subsynaptic distribution of Zfp804A in mature rat primary cortical neurons. **A** & **B**: High magnification SIM image of co-localised ZNF804A and PSD-95 (**A**) or GluN1 (**B**) puncta (indicated with white triangles) within GFP-transfected dendritic spines (outline of spine indicated with yellow dashed lines): co-localisation is indicated by white overlap. Intensity profiles of co-localised ZNF804A and either PSD-95 or GluN1 within spine heads demonstrates partial co-localisation of the puncta. **C** & **D**: High magnification SIM image of co-localised Zfp804A and PSD-95 (**C**) or GluN1 (**D**) puncta (indicated with red triangles) within GFP-transfected dendritic spines (outline of spine indicated with yellow dashed lines), including orthogonal views in the XZ and YZ planes. Co-localisation is indicated by white overlap. Scale bars = 500 nm (**A**-**D**).

5.4 DISCUSSION

This chapter has presented evidence validating a candidate anti-ZNF804A antibody for use in studies of ZNF804A protein expression and localisation. It has also demonstrated the expression of several transcript variants of the *ZNF804A* gene in neurons derived from several human stem cell lines, and has described how expression of these variants alters during terminal differentiation. In addition to this, it has demonstrated the subcellular distribution of ZNF804A and Zfp804A proteins in several neuronal models, surprisingly finding that these proteins are expressed outwith neuronal nuclei, along axons and dendrites and even within putative synapses. Finally, this chapter has demonstrated that Zfp804A can be found in distinct nanodomains highly integrated within the architecture of the post-synaptic density using super-resolution imaging.

Expression of *ZNF804A* transcripts in hNPC and hiPSC-derived cultures was found to vary as these cells were terminally differentiated. Previous research has found expression of *ZNF804A* to be expressed throughout the lifespan, though expression of both $ZNF804A^{E3/E4}$ and $ZNF804A^{FL}$ is particularly high during fetal development (Tao et al., 2014). In addition to this, $ZNF804A^{E3/E4}$ has been found to be expressed at a higher level than $ZNF804A^{FL}$ at this stage. This is in contrast to the findings of this thesis, where $ZNF804A^{E3E4}$ expression was found to be much lower than $ZNF804A^{exon4}$ in both CTX0E16 neurons and hiPSC-neurons at a comparable stage of development to the second trimester fetal brain. However, it should be noted that this may be due to the predicted b variant of *ZNF804A* also being detected by the $ZNF804A^{exon4}$ primers used in this experiment. In rats, expression of the rodent homologue Zfp804A peaks at around postnatal day 21 in the dentate gyrus and CA1 of the hippocampus, and expression within the lower layers of the cortex was found to be highest at postnatal day 1, though the possibility remains that expression could be even higher prenatally. Although there are limitations in the comparison of developmental stages in rodents to those of the human fetus (Bayer et al., 1993; Clancy et al., 2008), it is worth noting that should the pattern of high but Zfp804A transcript expression within the lower layers of the postnatal rodent cortex may be comparable to the developmental stage assessed in the fetal brain. These investigations were both past the estimated stage of neuronal proliferation during neurodevelopment in their respective species (Bayer et al., 1993). However, the possibility remains that expression of these transcripts may be even higher in neural progenitor cells, as seen in the current investigation. Indeed, if the trend of a progressive postnatal decrease in deep layer cortical Zfp804A expression is extrapolated to prenatal NPCs, this would predict

an even higher expression in these multipotent cells. When CTX0E16 expression data is taken in conjunction with that taken from hiPSC lines it suggests that peak expression of the full length transcript occurs once cells have adopted a neural identity, but that expression decreases as these cells terminally differentiate.

Surprisingly, in contrast to the findings of Tao et al. (2014) the current study found *ZNF804A*$^{E3/E4}$ to be expressed at a much lower level than *ZNF804A*^{exon4} variant in all cell types assessed. However, it must be stressed that the relative maturity of the neurons assessed in the present investigation may not yet match that of the fetal tissue assessed by Tao et al, and it is possible that the E3/E4 variant may be upregulated further later on in differentiation. Other explanations for this divergence in results include differences between the cohort from which the hiPSC lines are derived and the cohort assessed in the Tao paper, artefacts arising from the use of *in vitro* systems and the predominately glutamatergic identity of the CTX0E16 cultures in contrast to the more diverse environment of the whole brain slices used by Tao.

In western blots of DD7 and DD20 CTX0E16 cells, bands corresponding to the full length, E3/E4 and variant b isoforms could be seen after probing with the Genetex C2C3 anti-ZNF804A antibody, with two additional bands which did not match to any known ZNF804A isoforms. Interestingly, the E3/E4 protein isoform has never been detected before via western blotting; this has previously been postulated to be a result of post-translational modifications of this variant increasing its molecular weight and thus merging its predicted band with that of the full length protein (Tao et al., 2014). The presence of additional bands within these western blots may be suggestive of non-specific binding. As these bands did not respond to siRNA treatment it is unlikely that they correspond to ZNF804A isoforms containing exon 2 or exon 4, though the possibility remains that they may correspond to an as yet unknown ZNF804A variant. Although the current investigation presents considerable evidence to justify the use of the C2C3 antibody as a probe for the full length ZNF804A protein – through western blotting, immunoprecipitation, ICC, peptide blocking and detection of exogenous protein – future research will benefit from with use of transcript-specific constructs and ZNF804A knockout lines to verify whether the additional bands detected by this antibody represent other ZNF804A isoforms. This would in turn permit an evaluation of the specific functions of each individual *ZNF804A* isoform.

The present investigation found ZNF804A and Zfp804A to not only be expressed within both nuclear and extranuclear regions in NPCs and neurons derived from multiple sources. The expression of ZNF804A/Zfp804A within multiple cellular compartments is likely to be consistent with multiple functions within NPCs and mature neurons. In NPCs ZNF804A is seen predominately within the nucleus, consistent with previous work by Girgenti et al. (2012), who found expression of Zfp804A to be predominately located within the nucleus of rat neural progenitor cells. This nuclear expression is comparatively reduced in mature neurons, reflecting the predominately cytoplasmic but partially nuclear immunostaining described by Tao et al. (2014) and Bernstein et al. (2014) in layer III pyramidal neurons of the adult inferior parietal cortex and temporal cortex. The full length ZNF804A protein contains a C2H2 zinc finger domain, a motif known to mediate DNA-binding in several other proteins (Najafabadi et al., 2015). Moreover, previous research has found ZNF804A to regulate expression of a wide range of genes involved in cell adhesion, neurite outgrowth (Hill et al., 2012), TGF-β signalling (Umeda-Yano et al., 2013), synaptic function (Girgenti et al., 2012) and interferon signalling (Chen et al., 2015). The nuclear expression demonstrated in the current investigation and previous studies is therefore likely to be consistent with a role as a transcription factor.

In addition to the nuclear expression demonstrated in the present investigation, ZNF804A was found to co-localise with synaptic proteins in multiple human cell lines, and Zfp804A was found in nanodomains highly integrated within the post-synaptic densities of dendritic spines in rat cortical neurons, highlighting the interesting possibility that ZNF804A may possess additional functions at this site. Assessment of Zfp804A expression in crude synaptosomal fractions confirmed enrichment of the full length protein at synapses, though it should be noted that these fractions also contain membranes and thus the possibility remains that this protein may also be tightly integrated within the membrane. A subportion of Zfp804A was also found to be expressed at the base of dendritic spines via superresolution imaging. Previous research has found this site to be a critical area in which the local translation of mRNAs occurs (Martin and Zukin, 2006). C2H2 zinc finger proteins are also known to act as RNA binding partners (Brown, 2005), thus this intriguing extranuclear localisation may be indicative of an additional role in local RNA processing, both at the base of spines and within the spine head itself. ZNF804A/Zfp804A may bind to specific sequences on mRNAs for proteins involved in synaptic formation, maintenance or function, thereby influencing these processes by mediating mRNA transport, degradation or translation. Indeed, several RNA-binding proteins localised to the synapse have

previously been found to contribute to disease-related processes. For example, the RNA-binding protein FMRP is known to mediate both mRNA transport in dendrites and local translation at synapses; mutations in the gene coding for this protein (*FMR1*) result in one of the most common heritable forms of autism, Fragile X syndrome. *FMR1* mutations have also previously been found to result in synaptic dysfunction and reductions in neurite outgrowth in human stem cell models, mouse models and post-mortem tissue (Dictenberg et al., 2008; Irwin et al., 2000; Liu et al., 2012). In light of the novel synaptic localisation and potential RNA-binding functions of ZNF804A and Zfp804A seen in this chapter, the impact of these proteins on dendritic spine morphology and function will similarly be explored in **Chapter 6**.

Interestingly, expression of the ZNF804A protein appears to be malleable as hNPCs terminally differentiate, switching from a predominately nuclear localisation in NPCs to a more cytoplasmic/neuritic distribution in mature neurons. In addition to reflecting the pattern of localisation seen rat NPCs and human cortical neurons in previous research (Bernstein et al., 2014; Girgenti et al., 2012; Tao et al., 2014), this phenomenon has also been noted in rat primary cortical neurons as they differentiate (Hinna et al., 2015). In these cells a shift in Zfp804A localisation has been observed, from perinuclear regions to a more universal (both cytoplasmic and dendritic) distribution with particularly high expression being seen in the growth cones of the more mature neurons. However, it should be noted that the Hinna study utilised the Santa Cruz D-14 ZNF804A antibody without any control experiments; based on the validation experiments performed in this chapter any results obtained using this antibody must be interpreted with caution. Despite this, the shift in ZNF804A distribution seen in CTX0E16 NPCs and neurons offers an intriguing insight into the different roles this protein may play at different stages of development. Based on the putative role of ZNF804A as a transcription factor, and the potential role this protein may play in local translation at synapses, this shift may represent an alteration in the primary function of the full length protein: early in differentiation ZNF804A localises primarily to the nucleus and regulates expression of several genes including those involved in neurite outgrowth, while later on this protein is redistributed to local sites to regulate synaptic formation, function or maintenance through the regulation of processes relevant to local mRNA translation. This redistribution may arise as a consequence of alterations in trafficking or degradation of the full length protein at various time points in development. The potential cellular functions of ZNF804A and Zfp804A will be further explored in **Chapter 6**.

An alternative explanation for the alterations in the pattern of ZNF804A expression seen in CTX0E16 cells may that these changes reflect fluctuations in the expression profile of various ZNF804A isoforms throughout differentiation. *ZNF804A*^{exon4} was previously shown to be downregulated in neurons relative to NPCs, while no significant differences were seen in *ZNF804A*^{E3E4} and *ZNF804A*$^{exon2.2}$ expression. The full length variant may act primarily within the nucleus as a transcription factor, with other variants being preferentially upregulated following differentiation which adopt extranuclear distributions and functions. For example, the disease-linked E3/E4 variant lacks the C2H2 ZNF domain present within the full length protein and thus possesses no obvious ability to bind to DNA or act as a transcription factor (Tao et al., 2014).

The fascinating discovery of two subsets of primary rat cortical neurons expressing Zfp804A in a highly distinct manner raises critical questions about the regional and functional identity of these cells. The present investigation focused primarily on the subcellular localisation of the ZNF804a/Zfp804A protein, and the consequences of manipulation of expression of these proteins. However, a key experiment to conduct in future investigations would be to determine whether each of these patterns of expression is associated with markers of specific neuronal subtypes or cortical layers, and further whether the brightly stained Zfp804A-positive “logs” along the putative dendrites of type III neurons co-localise with different proteins to those for type II neurons. Given the morphology of these individual domains it is of interest to note that immunostaining of excitatory synapses typically adopts a punctate pattern, while immunostaining of inhibitory synaptic proteins such as GAD65 and GAD67 typically occurs in an elongated fashion (Schwab et al., 2013) very similar to the “logs” seen in some of the intensely stained Zfp804A-positve neurons. Additionally, inhibitory synapses are commonly expressed on the cell soma of the post-synaptic neuron similarly to the Zfp804A staining seen in type III neurons (Fritschy et al., 2006). Thus, these two subgroups of cells may differentially express Zfp804A at excitatory or inhibitory synapses respectively. Such a binarised pattern of expression appears highly unusual in neurons possessing both excitatory and inhibitory synapses; thus further investigation must be conducted to determine whether this pattern of staining is truly reflective of synaptic localisation as seen in type I Zfp804A-positive neurons.

Interestingly, no other variants of the Zfp804A protein could be detected in whole cell lysates or in synaptosomal fractions, raising the possibility that a rodent homologue of the disease-associated

E3/E4 variant may not exist, though notably another predicted isoform for this gene is listed on ACEVIEW, consisting of exon 2, exon 3 and a truncated exon 4 (http://www.ncbi.nlm.nih.gov/IEB/Research/Acembly/av.cgi?db=mouse&q=Zfp804a). This finding also suggests that the protein expressed at post-synaptic sites in human neurons may indeed be the full length protein, possessing the ZNF domain. Thus, if ZNF804A does indeed act locally at the synapse via RNA-binding mediated by this ZNF domain, it is likely that this function would be conserved in the dendritic spines of rodent neurons.

This chapter has presented considerable data on the mRNA and protein expression of several variants of ZNF804A and Zfp804A in a number of *in vitro* models, providing a valuable insight into potential novel functions of this protein. However, further work is required before an extranuclear function of this protein can be definitively established, particularly in the context of expression at dendritic spines. The manipulation of expression of a given protein can provide key information about its prospective functions. Overexpression, knockdown or even knockout of ZNF804A and Zfp804A can indicate whether ZNF804A's putative role as a transcription factor has functional relevance, while subsequently indicating alternative functions outside of the nucleus. These techniques can also provide valuable tools to aid in the validation of antibodies targeted to a given protein. The next chapter will discuss several experiments attempting the manipulation of ZNF804A and Zfp804A expression in human and rodent cell lines. It will further discuss how these techniques can aid in the validation of antibodies described in the present chapter, and discuss how the findings of these experiments integrate into the pre-existing body of literature.

CHAPTER 6: THE ROLE OF ZNF804A IN NEURITE OUTGROWTH AND DENDRITIC SPINE MAINTENANCE AND PLASTICITY

6.1 SUMMARY

This chapter describes investigations into the cellular functions of *ZNF804A* via several techniques aimed at altering the expression of this gene by knockout, knockdown or overexpression. An initial effort to excise exon 3 of the full length ZNF804A gene from the genome of the previously described CTX0E16 hNPC line proved unsuccessful, as did attempts to overexpress two tagged ZNF804A constructs in several cell lines. This chapter also outlines several experiments attempting to knockdown ZNF804A and Zfp804A in human and rodent neuronal cells using two independent siRNAs, and describes how treatment with these siRNAs impacted early neurite outgrowth and maintenance of dendritic spines in mature neurons. The impact of inducing chemical-LTP on the subcellular localisation of Zfp804A in rat primary cortical neurons is also shown. Finally, these findings are discussed in the context of previous studies assessing the function of these proteins using knockdown and overexpression techniques.

6.2 INTRODUCTION

In **Chapter 5** the detailed characterisation of the subcellular localisation of ZNF804A and its rodent homologue, Zfp804A, provided a valuable insight into their potential extranuclear and non-transcriptional functions. This highlighted interesting avenues of experimental inquiry into these roles, as well as the predicted actions of these proteins as transcription factors. However, further investigation is required to determine whether this extranuclear localisation is reflective of additional functions within the cell cytoplasm or even at the synapse. Several previous studies have attempted to assess the functions of ZNF804A and Zfp804A through techniques altering the expression of these proteins. Specifically, a large number of studies have now strongly implicated ZNF804A and Zfp804A as regulators of gene transcription (Hill et al., 2012; Girgenti et al., 2012; Chen et al., 2015; Umeda-Yano et al., 2013; Colak et al., 2008; Pereira, Delany, & Canalis, 2004; Jia, Wang, Meltzer, & Zhao, 2010;

Miller, Buckley, Seabolt, Mellor, & Kirkpatrick, 2011). However, no studies have yet attempted to determine whether these alterations in gene expression have downstream effects on neuronal characteristics. As the expression of genes involved in neurite outgrowth and cell adhesion has previously been found to be altered in hNPCs following ZNF804A knockdown (Hill et al., 2012), a subsequent investigation into whether alterations in ZNF804A expression also impact early neurite outgrowth may provide a valuable insight into the links between this protein and the disease mechanisms underlying psychiatric disorders. In addition to this, as cell adhesion proteins play a key role in the formation of synapses (McAllister, 2007), the alterations in expression of several cell adhesion genes seen in hNPCs following ZNF804A knockdown in this study may also indicate that this protein mediates synapse development via regulation of transcription. Furthermore, as Zfp804A and ZNF804A were found to be expressed at putative synapses in the previous chapter, these proteins may possess a role in the formation, maturation or maintenance of dendritic spines in a similar manner to other synaptic proteins.

In light of the lack of information of the downstream consequences of the manipulation of ZNF804A/Zfp804A expression on functional characteristics of neurons, the current investigation utilised siRNA-mediated knockdown of ZNF804A and Zfp804A, commonly used in *in vitro* studies as a means of assessing the potential functions of a given protein (Hannon, 2002; Ma et al., 2007; Prelich, 2012; Santiago et al., 2008). Specifically, this study describes the impact of siRNA treatment on early neurite outgrowth in multiple human neural stem cell models, as well as the impact of ZNF804A knockdown on expression of adhesion proteins. It further outlines the impact of Zfp804A knockdown on dendritic spine maintenance and LTP-dependent spine plasticity as well as the effect of LTP induction on the subcellular expression of Zfp804A in mature rat primary cortical neurons. Taken together, these data provide a further understanding of both the upstream and downstream pathways involved in ZNF804A and Zfp804A function, and thus how these proteins may integrate into the pathophysiological mechanisms underlying psychiatric disease.

6.3 RESULTS

6.3.1 ZNF804A MEDIATES EARLY NEURITE OUTGROWTH IN CTX0E16 CELLS

siRNA (Small Interfering RNA)-mediated knockdown of ZNF804A expression has been previously used in a sister cell line of CTX0E16 hNPCs, CTX0E03, to study its influence on the

expression of other genes (Hill et al., 2012). In this study two independent siRNAs targeting exon 4 (siRNA 1) and exon 2 (siRNA 2) of the full length *ZNF804A* transcript were validated using a microarray and by q-PCR. Given the high degree of similarity between the cell line used in the previous study and the CTX0E16 line, as well as the high efficiency of transfection and efficacy in reducing ZNF804A transcript expression, this siRNA protocol would be ideal for the current line of inquiry with only minor modifications.

siRNA-mediated knockdown of ZNF804A was previously validated in CTX0E16 cells in **Section 5.3.2, 5.3.3** and **5.3.4** using q-PCR as well as western blotting and ICC with the Genetex C2C3 antibody. The immunostained cultures from these experiments were re-examined to determine the morphological characteristics of the differentiating cells: number and length of neurites; cell soma size. Interestingly, a modest reduction in total neurite length per cell was observed in the two ZNF804A-knockdown conditions relative to the blank and scramble siRNA controls. A one way ANOVA with a posthoc Bonferroni multiple comparisons test revealed both a main effect of treatment on total neurite length ($p<0.05$) and that the reduction in neurite length seen in siRNA 1 and 2-treated conditions relative to the scramble siRNA control was significant at the $p=0.05$ level (see **Figure 6.3.1**, **A** & **B**). However, no significant differences could be observed between conditions for cell soma size or the number of neurites per cell, indicating that this relative reduction in neurite length was not related to other morphological changes associated with poor cell culture health and apoptosis. Furthermore, the number of neurite branch points per cell was not found to be affected by treatment condition in these cultures (data not shown). Taken together, these results indicate that ZNF804A plays a role in mediating early neurite outgrowth during human neuronal differentiation, although whether this is due to actions on transcription of specific genes or alternative extranuclear functions remains to be determined.

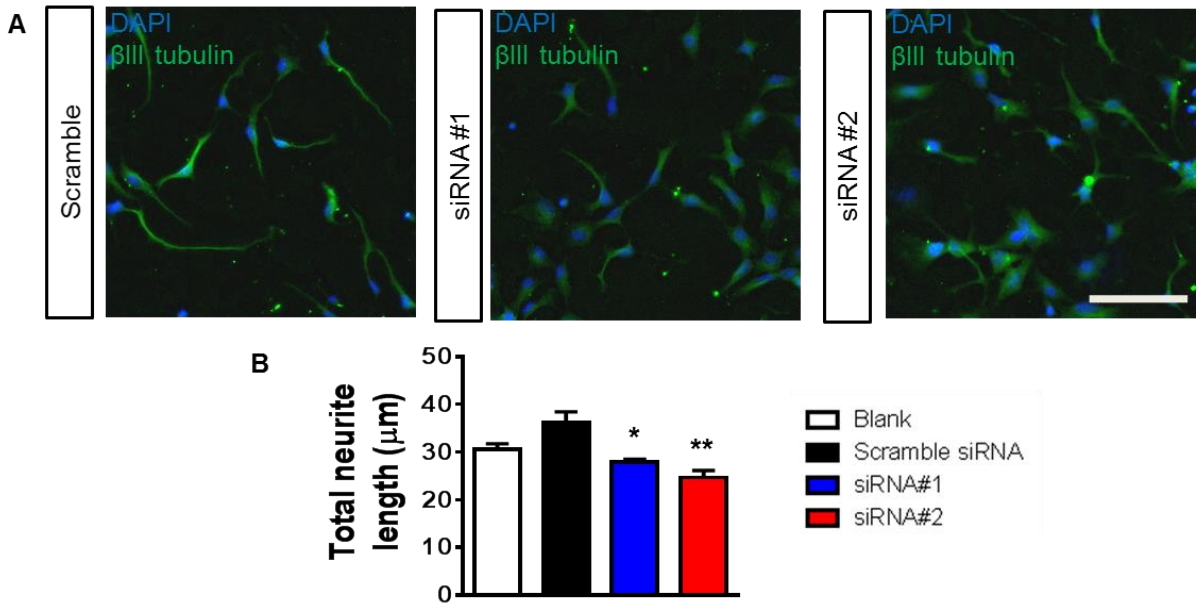

Figure 6.3.1: siRNA-mediated knockdown of ZNF804A in CTX0E16 neurons. **A**: Representative images of neurite length in early stage (DD7) CTX0E16 neurons following a 7 day treatment with control (scramble) or ZNF804A-targeting siRNAs. **B**: Total neurite length was significantly reduced in neurons treated with both siRNAs relative to the scramble siRNA control (n = 3 independent experiments; *p<0.05; **p<0.01). Scale bar = 50 μm (**A**).

6.3.2 NEUROLIGIN 4X RESCUES DEFICITS IN NEURITE OUTGROWTH FOLLOWING ZNF804A KNOCKDOWN IN CTX0E16 CELLS

ZNF804A has been suggested to control the expression of neuroligin 4X (Chen et al., 2015), a member of the neuroligin-neurexin family of adhesion proteins. This protein is associated with autism spectrum disorders, and it localises to synapses and regulates synapse density (Chih et al., 2004; Zhang et al., 2009). To confirm this finding in the CTX0E16 cell line, the siRNA-treated CTX0E16 lysates probed for ZNF804A protein expression in **Section 5.3.2** were reprobed using an antibody for neuroligin 4x, as well as the adhesion protein N-cadherin and the AMPA receptor subunit GluA2. As with ZNF804A, staining intensity values for protein bands were normalised to a β-Actin control, and values for all treatment conditions were normalised to the scramble control condition within each replicate. One way ANOVA were conducted on the normalised expression data for each protein, with posthoc Tukey multiple comparisons tests. Neuroligin 4x was found to be significantly reduced in cell lysates from ZNF804A siRNA CTX0E16 neurons ($p<0.05$ and $p<0.01$ for siRNA 1 and siRNA 2 vs scramble control respectively); the adhesion protein N-cadherin and the GluA2 AMPA receptor subunit were unaffected ($p>0.05$), suggesting that this result was not due to a nonspecific reduction in adhesion protein

expression or synapse number (see **Figure 6.3.2, A** & **B**). Neuroligin 4x has previously been suggested to be involved in neurite outgrowth (Shi et al., 2013); however, this has not yet been validated. If neuroligin 4x was indeed important for neurite outgrowth then exogenous expression of this protein may rescue deficits in neurite length in siRNA-treated cells. To investigate this, CTX0E16 cultures treated with the ZNF804A-targetting siRNAs were additionally transfected with a NLGN4 construct tagged with an HA reporter then immunostained as in the other siRNA experiment conditions (**Figure 6.3.2, C**). Average neurite length values for the siRNA 1/HA-NLGN4 and siRNA 2/HA-NLGN4 conditions were then compared to their respective siRNA-alone treatment conditions using a 1 way ANOVA with a posthoc Bonferonni multiple comparisons test. Total neurite length in siRNA 1- or 2-treated cells, overexpressing HA-NLGN4, was significantly increased compared with siRNA-alone conditions ($p<0.01$) but did not differ from control conditions ($p>0.05$) (**Figure 6.3.2, D**). Collectively, these data demonstrate that ZNF804A plays a role in early neuritogenesis in human neurons, an effect that may be mediated via the control of neuroligin 4x expression.

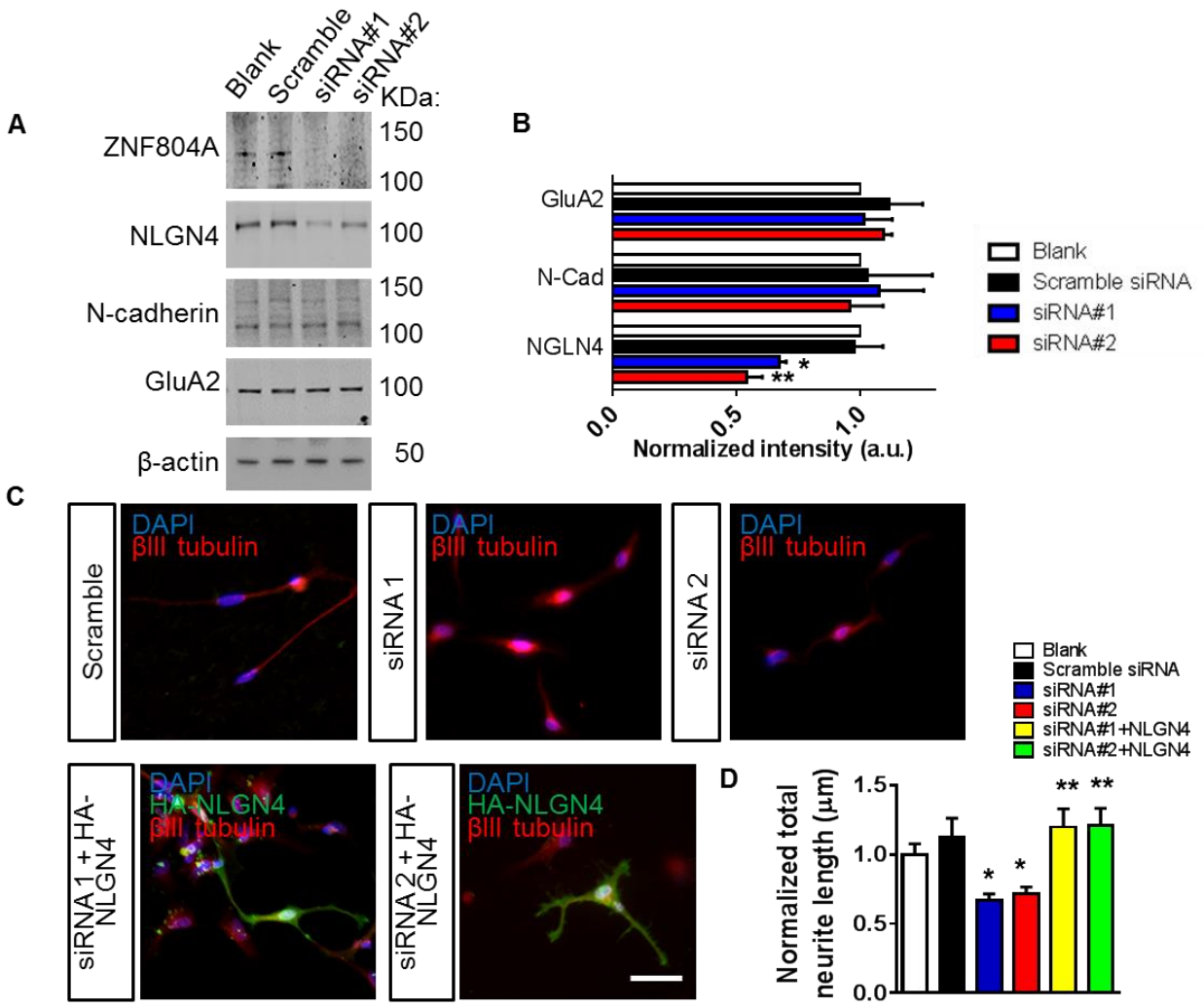

Figure 6.3.2: Neuroligin 4x overexpression ameliorates deficits in neurite outgrowth mediated by ZNF804A knockdown in CTX0E16 neurons. (**A** & **B**): Western blot analysis of synaptic and adhesion protein expression in control and siRNA expressing CTX0E16 neurons. In ZNF804A knockdown cells, neuroligin 4x (NLGN4) is significantly reduced; N-cadherin and AMPA receptor subunit 2 (GluA2) are unaffected (n = 3 independent experiments; *p<0.05; **p<0.01). **C**: Representative images of early stage (DD7) CTX0E16 neurons after a 7-day treatment with no transfection (blank), control (scramble), or ZNF804A-targeting siRNAs, with or without exogenous expression of HA-NLGN4 for 2 days. **D**: Quantification of neurite outgrowth of cells in **E**. siRNA-treated cells had significantly reduced outgrowth compared with blank or scramble conditions. Neurons treated with ZNF804A-siRNA and HA-NLGN4 had significantly longer neurites than siRNA alone conditions, but they did not differ from control conditions (n = 3-4 independent experiments; *p<0.05; **p<0.01). Scale bar = 20 μm (**C**).

6.3.3 ZNF804A MEDIATES EARLY NEURITE OUTGROWTH IN HIPSC-DERIVED NEURONS

In light of this fascinating early finding, a follow-up experiment was carried out by applying the same experimental protocol to immature neurons generated from the same hiPSC lines utilised in **Section 5.3.10**, in order to confirm the findings observed in the CTX0E16 cell line and further establish whether any morphological phenotypes seen hiPSC-neurons can be further studied in patient and risk-allele-carrier lines. To this end, NPCs derived from the hiPSC lines generated from keratinocytes of three apparently healthy individuals were treated with siRNA 1, siRNA 2 or the scramble control siRNA for 7 days until DD30, a stage of rapid neurite outgrowth during terminal differentiation of hiPSC-neurons that approximates neuronal development in the second trimester fetal cortex (Brennand et al., 2014). Furthermore, transfection efficiency in the hiPSC lines was assessed via transfection with the additional fluorescent olignucleotide control described in the previous section. Cell counts of epifluorescence images taken of these cultures one day post-transfection revealed that uptake of the fluorescent oligonucleotide occurred in around 63.79±6.73% of cells (**Figure 6.3.3**, **A**).

Cells transfected with the ZNF804A siRNAs were terminally differentiated for 7 days and immunostained for MAP2, DAPI and ZNF804A with the Genetex C2C3 ZNF804A antibody. Interestingly, ZNF804A staining intensity using the C2C3 antibody was again found to be modestly reduced by 20-30% in neuronal cultures treated with the anti-ZNF804A siRNAs relative to the scramble siRNA control condition (see **Figure 6.3.3**, **C**). A one way ANOVA of the C2C3 data revealed a significant effect of treatment condition, while a posthoc Dunn's multiple comparisons test found the reductions in neuronal staining intensity in the siRNA 1 and 2 conditions relative to the scramble siRNA to be significant or approaching significance ($p=0.012$ and $p=0.053$ for scramble vs siRNA 2 and scramble vs siRNA 1 respectively). This further lends support to the validity of the C2C3 antibody as a specific probe for ZNF804A via immunocytochemistry, and additionally indicates that both anti-ZNF804A siRNAs are also efficacious in reducing expression of the ZNF804A proteins in immature hiPSC-derived neurons.

Following on from this validation of ZNF804A knockdown in these cells, the cultures were assessed for morphological characteristics: cell soma size, average number of neurites per cell, number of neurite branch points per cell and total neurite length per cell were all recorded as before, and then compared across experimental conditions. Although reductions in total neurite length per cell were seen

in the two ZNF804A knockdown conditions relative to the scramble siRNA control, the large degree of variability in values within each condition appeared to obscure the true magnitude of the effect of ZNF804A knockdown on neurite length. To further assess this variation, values for each condition were separated for each hiPSC line to determine whether inter-cell line differences accounted for this variability (see **Figure 6.3.3**, **E**). Interestingly, neurite length values were found to vary across cell lines as well as across experimental conditions, though both siRNA 1 and siRNA 2 were found to consistently reduce total neurite length per cell in comparison to scramble siRNA treated controls within each individual line. When data was normalised to the scramble siRNA control condition within each hiPSC cell line and normalised values were averaged across cell lines instead, the reduction in neurite length seen in the two ZNF804A knockdown conditions was retained, but with less variation within the individual conditions (**Figure 6.3.3**, **D**). A Kruskall-Wallis test of this normalised data revealed a significant effect of experimental condition on total neurite length, while a posthoc Dunn's multiple comparisons test found that the reductions in neurite length seen in siRNA 1 and siRNA 2 treated cultures in comparison to the scramble control condition were both significant. In addition to this, no significant differences could be seen for cell soma size or the number of neurites per cell between conditions in hiPSC-derived neurons, suggesting that the differences in neurite length did not occur as a function of morphological changes associated with apoptosis. Furthermore, the number of neurite branch points per cell did not differ significantly between conditions. A Kruskall Wallis test of normalised data for these parameters confirmed the absence of any differences between treatment conditions. Overall, these data provide further support of a role of ZNF804A in regulating early neurite outgrowth during terminal differentiation of human neurons, and additionally highlight a phenotype that may be assessed in future investigations of hiPSC lines derived from samples taken from carriers of risk SNPs which reduce expression of the ZNF804A gene, in both psychosis patients and healthy controls.

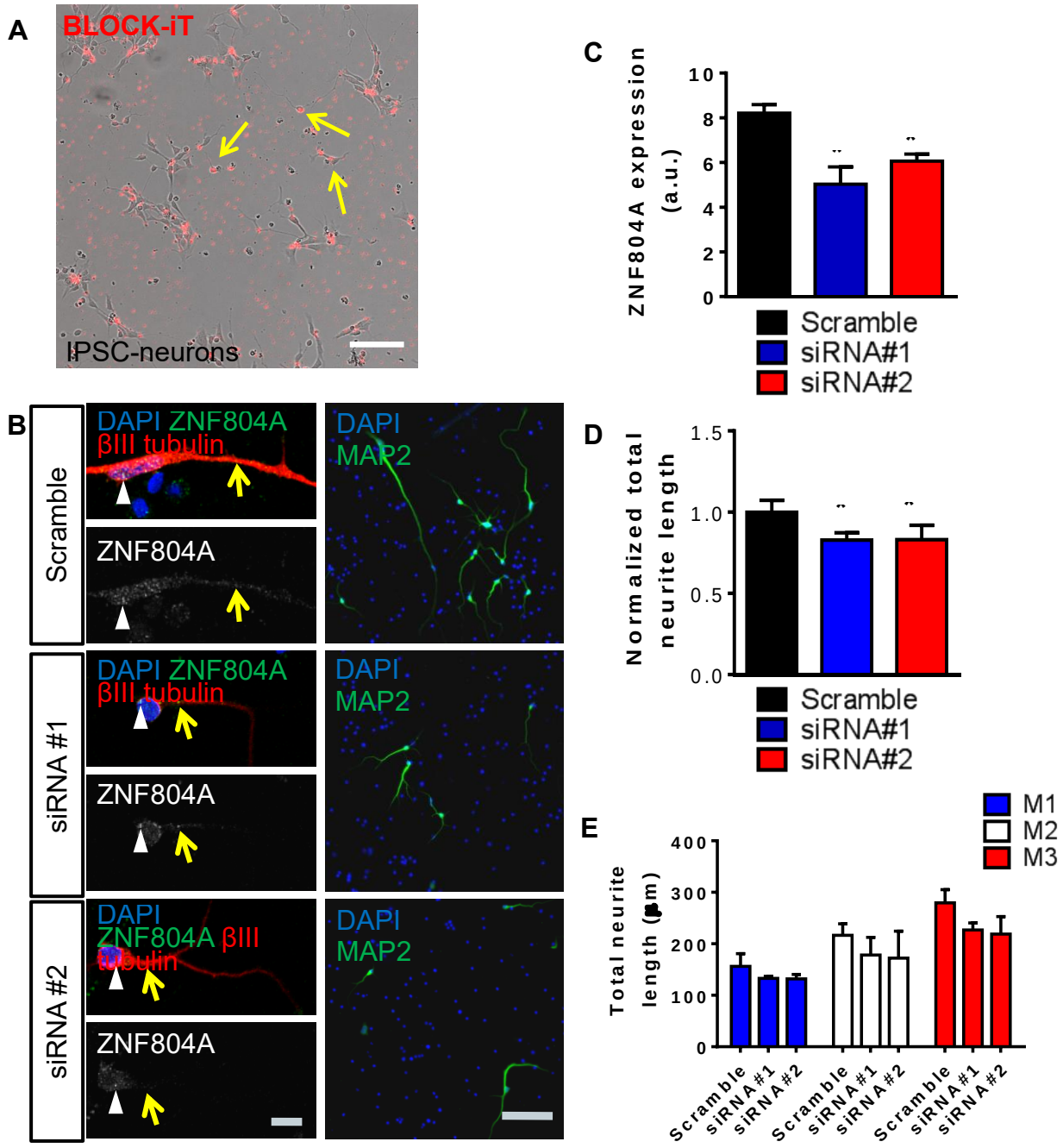

Figure 6.3.3: siRNA-mediated knockdown of ZNF804A in young hiPSC-derived neurons. **A**: Representative image of fluorescent oligonucleotide control condition assessing efficiency of N-Ter siRNA transfection. 63.79±6.73% of immature hiPSC-derived neurons were transfected with BLOCK-iT red fluorescent oligo 1 day post transfection. Yellow arrows indicate transfected cells. **B**: Representative images of ZNF804A staining and neurite length in early stage (DD30) hiPSC-derived neurons following a 7 day treatment with control (scramble) or ZNF804A-targeting siRNAs. **C**: Quantification of staining intensity seen in **B**. ZNF804A expression was significantly reduced in both siRNA treatment conditions relative to the scramble siRNA control (n = 3 independent cell lines, carried out in duplicate for each line; *p<0.05). **D**: Normalised total neurite length was significantly reduced in neurons treated with both siRNAs relative to the scramble siRNA control (n = 3 independent cell lines,

Figure 6.3.3, continued: carried out in duplicate for each line; *p<0.05). **E**: Raw total neurite length data for siRNA-treated neurons from each hiPSC line. Scale bars = 20 µm (**A**), 10 µm (**B1**) and 50 µm (**B2**).

6.3.4 ZFP804A REGULATES DENDRITIC SPINE MAINTENANCE AND PLASTICITY IN MATURE CORTICAL NEURONS

As previously described in **Chapter 5**, the ZNF804A protein and its rodent homologue, Zfp804A, have been found to be enriched in perisynaptic regions in human and rat neurons respectively, with strong evidence indicating that Zfp804A is highly integrated within the dendritic spines of mature rat primary cortical neurons. A number of endogenous proteins located at the post-synaptic density in a similar manner play crucial roles in the formation, maturation and maintenance of dendritic spines; thus, it is possible that ZNF804A and Zfp804A may possess one or more of these functions. Although ZNF804A was previously seen to be expressed at the putative dendritic spines of CTX0E16 neurons (see **Section 5.3.7**), an assessment of the impact of ZNF804A knockdown on spine density and morphology in this line would be problematic due to the long differentiation required for the appearance of spines as well as the relatively low number of spines observed previously in differentiated cultures. To bypass this potential difficulty, siRNA-mediated knockdown of Zfp804A was attempted in rat primary cortical neuron cultures, which robustly produce dendritic spines in a comparatively shorter timespan *in vitro*. Based on bioinformatical analysis of the two previously used siRNAs using BLAST, only siRNA 2 is predicted to specifically target the full length *Zfp804A* mRNA transcript due to dissimilarities between the equivalent human and rat sequences. Taking this into account, DIV18 primary rat cortical neuron cultures were transfected with a blank control condition, the scramble control siRNA or siRNA 2 as described previously. A subset of these cultures was subsequently transfected with GFP under control of the Synapsin1 promoter at DIV23 for later assessment of dendritic spine density and morphology. At DIV25, cultures were lysed for western blotting or immunostained for GFP and Genetex ZNF804A/Zfp804A. Western blotting of the siRNA-treated rat primary cortical lysates using the C2C3 ZNF804A/Zfp804A antibody revealed that siRNA 2 reduced expression of the Zfp804A protein by around 35% relative to the blank or scramble siRNA-treated control conditions, as assessed by normalising intensity values of a band corresponding with the predicted size of the full length protein to a loading control (see **Figure 6.3.4**, **A** & **B**). A Kruskall-Wallis test of this data revealed a significant effect of treatment condition ($p<0.05$), with a posthoc Dunn's multiple comparisons test revealing a significant reduction in Zfp804A expression in the siRNA 2 treatment condition relative to the two control

conditions ($p<0.05$). Further assessment of Zfp804A expression in immunostained, GFP-transfected rat cortical neurons revealed a comparable reduction in Zfp804A staining intensity in the siRNA 2-treated condition relative to the two control conditions (**Figure 6.3.4**, **C** & **D**); a one way ANOVA of this data with a posthoc Bonferroni multiple comparisons test found a significant effect of condition and a significant reduction in the siRNA 2 treatment condition relative to the controls ($p<0.05$). Taken together, these findings indicate that siRNA 2 successfully reduced expression of Zfp804A in the rat primary cortical neurons.

Following on from the validation of siRNA 2 in rat primary cortical neurons, these cells were further evaluated to determine whether this reduction in Zfp804A expression had impacted dendritic spine density or morphology. Interestingly, neurons treated with siRNA 2 were found to exhibit a reduced density of dendritic spines relative to neurons treated with either of the two control conditions (dendritic spine density per 10 µm of linear dendrite: blank, 4.6±0.37; scramble siRNA, 3.99±0.32; siRNA 2, 3.02±0.2; n = 3 independent experiments) (see **Figure 6.3.4**, **C** & **E**). A one way ANOVA of this data revealed a significant effect of experimental condition ($p<0.05$); a posthoc Tukey's multiple comparisons test found significance in the differences between the siRNA 2-treated neurons and those of the two control conditions. However, no significant differences could be seen in the morphological attributes – length, breadth and area – of the spines between the three conditions, indicating that the elimination of spines caused by Zfp804A knockdown was not restricted to a particular morphological subtype (**Figure 6.3.4**, **F**). As no significant differences were previously observed between the morphologies of Zfp804A-positive and Zfp804A-negative spines in **Section 5.3.11**, this finding may be consistent with a specific elimination of the Zfp804A-positive spines seen in untreated cortical neurons. Collectively, these data suggest that Zfp804A influences spine maintenance in cortical neurons, but also that this mediation of spine density is not limited to spines of a specific morphology.

Because loss of ZNF804A in young human neurons correlated with a reduced neuroligin 4x expression, a protein known to regulate synapse density (Shi et al., 2013; Zhang et al., 2009), this protein was further assessed in the siRNA-treated rat cortical neuron cultures. DIV20 rat primary cortical neuron cultures were treated with siRNA 2 for five days as before, then lysed for subsequent probing for neuroligin 4x, N-cadherin and SNAP-25 as in the previous experiment in the CTX0E16 line. Western blotting of siRNA treated rat primary cortical neuron lysates revealed that neuroligin 4x was reduced in

Zfp804A knockdown neurons (**Figure 6.3.4**, **G** & **H**); subsequent significance testing using a one way ANOVA with a posthoc Tukey multiple comparisons test revealed this reduction to be significant ($p<0.05$). In contrast to this, no significant changes in expression of the adhesion protein N-cadherin or the synaptic protein SNAP-25 were observed (**Figure 6.3.4**, **G** & **H**), suggesting that the decrease in neuroligin 4x expression was not due to a general reduction in synaptic or adhesion proteins.

As altering Zfp804A expression influenced spine density, loss of Zfp804A may additionally affect activity-dependent spine plasticity. To investigate this possibility, DIV25 rat primary cortical neurons were pre-treated with the siRNA conditions for five days as before, then treated with ACSF supplemented with APV or ACSF supplemented with 10 µM glycine, 100mM picrotoxin and 1 µM strychnine (inducing chemical LTP (cLTP)) (Xie et al., 2007) 30 minutes prior to fixation. Application of cLTP on control cells or neurons expressing scramble siRNA resulted in an increase in density (~33%) and spine area (~24%) (**Figure 6.3.4**, **I-K**). Two way ANOVA testing with posthoc Tukey's multiple comparisons tests revealed that these increases in spine density and area were statistically significant ($p<0.001$). However, in Zfp804A knockdown neurons, no increase in spine area was observed after cLTP treatment, although spine density increased (~35%) to a level similar to unstimulated (basal) control levels (Two way ANOVA, posthoc Tukey's multiple comparisons test; $p<0.05$) (**Figure 6.3.4**, **I-K**). In addition to this, cLTP did not appear to significantly increase spine area in Zfp804A knockdown neurons as occurred in the control or scramble siRNA-treated neurons (Two way ANOVA, posthoc Tukey's multiple comparisons test; $p>0.05$). Taken with the previous data on the impact of Zfp804A knockdown on dendritic spine density, these experiments demonstrate that Zfp804a is required for spine maintenance and that loss of the protein impairs the ability of neurons to respond fully to activity-dependent stimulations.

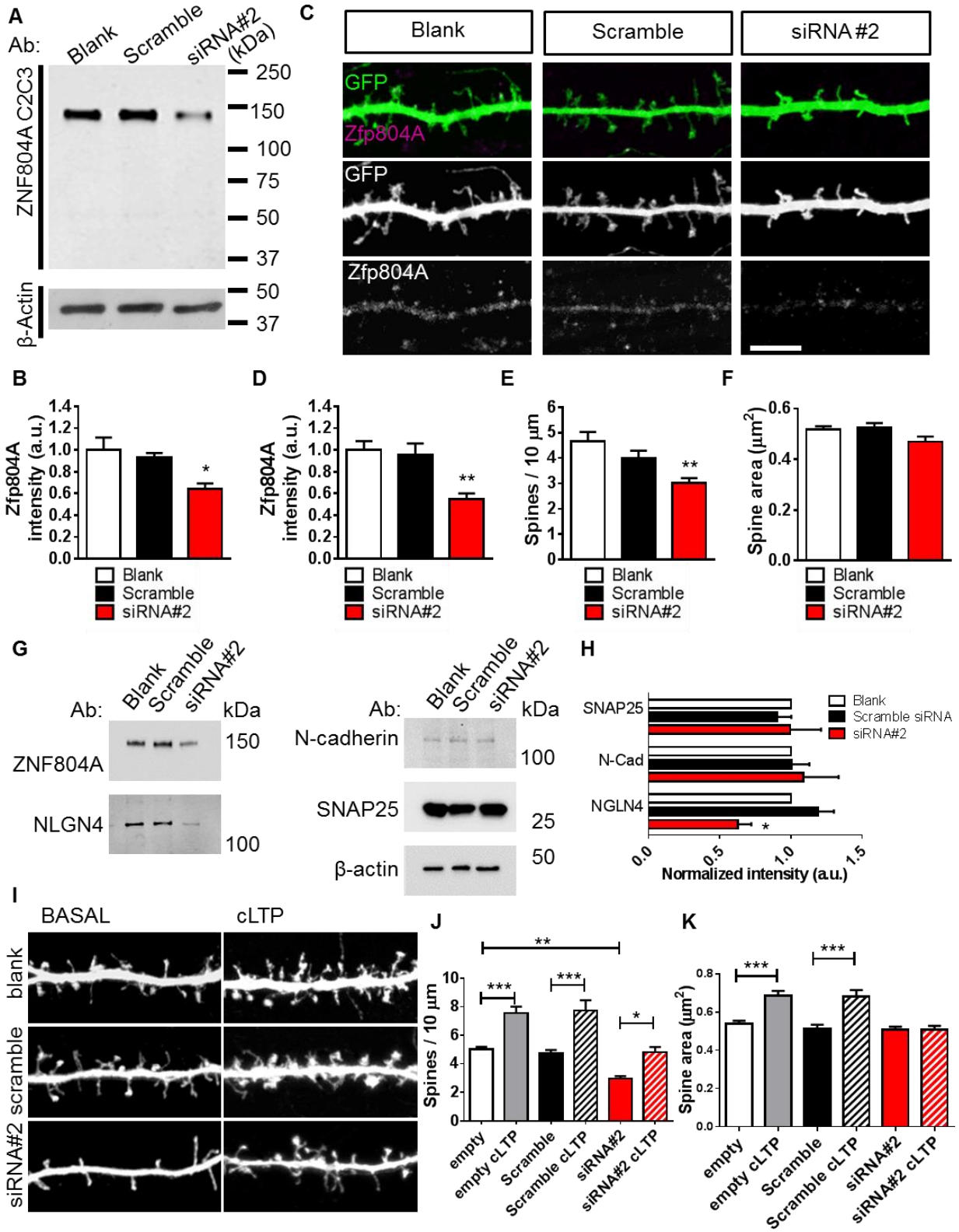

Figure 6.3.4. siRNA-mediated knockdown of zinc finger binding protein 804A (Zfp804A) in rat primary cortical neurons. **A**: Representative western blot of Zfp804A in 26-day in vitro (DIV26) primary rat cortical neurons after a 5-day treatment with no transfection (blank), control (scramble), or ZNF804A-targeting siRNA. **B**: Quantification of the major protein band found at ~135 kDa, roughly equal to the

Figure 6.3.4, continued: predicted molecular mass of Zfp804A, revealed a significant reduction in staining intensity compared with blank and control conditions (n = 3 independent experiments). **C**: Representative confocal images of dendrites and dendritic spines after siRNA treatment of neurons as in **A**. **D**: Quantification of Zfp804A staining intensity after 5-day siRNA treatment. Zfp804A was significantly reduced in neurons treated with siRNA 2 in comparison with blank and control conditions (n = 3 independent experiments). **E**: Quantification of spine density after siRNA treatment (n = 3 independent experiments). **F**: Spine area was not found to be significantly altered in neurons treated with siRNA 2 relative to the two control conditions (n = 3 independent experiments). **G**: Western blot analysis of cell lysates of blank, control, and siRNA-treated neurons. **H**: Quantification of **F** reveals that neuroligin-4 (NLGN4), but not N-cadherin or synaptosomal-associated protein 25 (SNAP25), is significantly reduced in Zfp804A knockdown cells (n = 3 independent experiments). **I**: Representative confocal images of dendritic spines from neurons treated as in A and after chemical long-term potentiation (cLTP) stimulation (n = 3 independent experiments). **J**: Quantification of spine density in siRNA-treated cells after cLTP revealed that linear density was increased in all conditions; in Zfp804A cells, cLTP increased spine density back to basal levels. **K**: Quantification of spine size (area) after cLTP revealed that loss of Zfp804A impaired the ability of cells to undergo structural plasticity (n = 3 independent experiments). Scale bar for **C** & **I** = 5 µm. Scale bar for **A** = 5 µm. This work was carried out by Pooja Raval.

6.3.5 NEURONAL ACTIVITY-INDUCING STIMULI INDUCE ALTERATIONS IN THE SUBCELLULAR PATTERNING OF ZFP804A EXPRESSION

This chapter has thus far detailed attempts to manipulate ZNF804A and Zfp804A expression in several neuronal lines, and the downstream effects these manipulations have had on cellular phenotypes in immature and mature neurons. However, little is currently known about the upstream regulators of these proteins. Previous research has found expression of the Zfp804A transcript to be upregulated in cultured rat primary cortical neurons following 3 hour treatment with glutamate; this upregulation was blocked by addition of the NMDA receptor antagonist, MK-801 (Chang et al., 2015). It is currently unknown however whether this upregulation is also reflected at the protein level. Additionally, in **Chapter 5** extranuclear expression of ZNF804A and Zfp804a was found in both human and rodent neuronal cells, and differential localisation of ZNF804A was seen in human NPCs and neurons. An investigation into whether the relative expression of these proteins in nuclear and extranuclear neuronal compartments is altered following exposure to activity-inducing stimuli may therefore also indicate whether the upregulation in expression of the Zfp804A transcript seen in the research by Chang et al. (2015) corresponds to a specific cellular region. An initial test of the regulation of subcellular expression of the ZNF804A protein in immature human neurons in response to activity-

inducing stimuli was carried out in the experiment detailed in **Section 4.3.5**. As described previously, DD13 CTX0E16 neurons were transfected with pEGFP under the control of a CMV promoter and treated with either control NDM, NDM supplemented with 30 mM NaCl as an osmotic control or NDM supplemented with 30 mM KCl as a depolarising stimulus 7 hours prior to fixation on DD15. Cultures were immunostained for DAPI and GFP as described in the prior section, but were additionally stained with the Genetex anti-ZNF804A antibody to assess subcellular expression of this protein in each experimental condition. A one way ANOVA was performed on the data for each subcellular compartment and whole-cell expression for each of the three conditions; treatment of the CTX0E16 cultures with 30 mM KCl was not found to significantly alter expression of ZNF804A in any single subcellular compartment nor within the cell as a whole relative to control conditions ($p>0.05$; 3-5 independent experiments) (**Figure 6.3.5**, **B-E**). However, a closer evaluation of the images taken of the cells from these experiments revealed the ZNF804A immunostaining to be poor quality and not exhibiting the pattern of localisation seen in previous experiments (**Figure 6.3.5**, **A**). This may be an artifact of transfection with the GFP construct used in this experiment, a result of Z-projections eliminating differences in staining between the nuclei and cytoplasm of each cell, variations in the efficacy of the staining protocol used and non-neuronal cells potentially being included in the analysis.

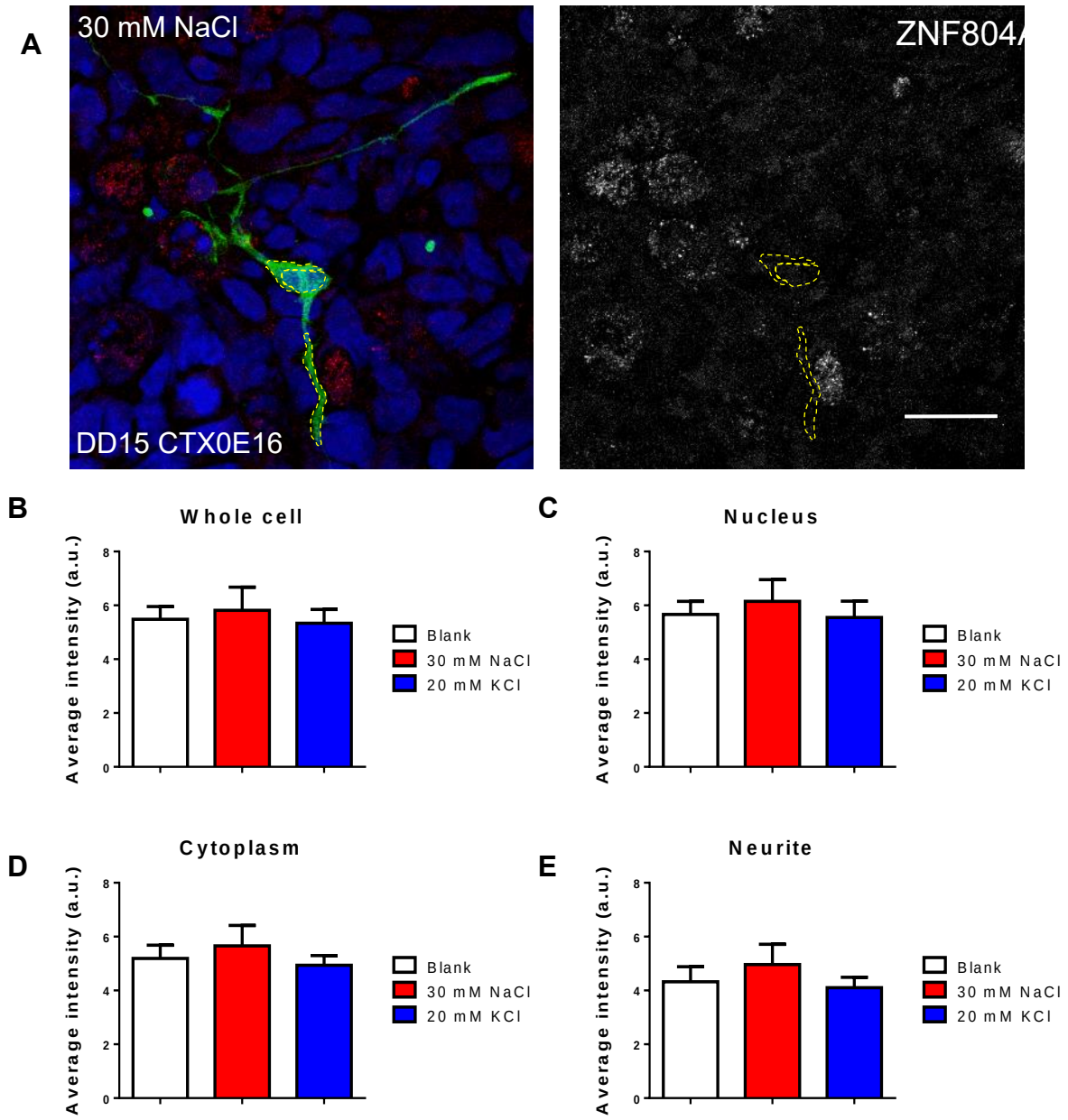

Figure 6.3.5: Initial test of impact of chemically-induced neuronal depolarisation on ZNF804A localisation in DD15 CTX0E16 neurons. **A**: Representative images of GFP-expressing CTX0E16 neuron (DD 15) following 7 hour treatment with vehicle control condition; yellow dotted lines delineate areas where ZNF804A staining intensity was measured. **B**-**E**: Measurement of average ZNF804A staining intensity in whole cell (**B**), nuclear (**C**), cytoplasmic (**D**) and neurite (**E**) regions did not demonstrate any effect of activity-dependent stimulation (30 mM KCl) on ZNF804A expression or localisation; n = 14–22 neurons from 3–5 independent experiments. Scale bar for **A** = 20 µm.

To address these issues, another investigation was carried out in primary rat cortical neurons to more closely match the experimental paradigm used in the Chang et al. (2015) paper. Briefly, untransfected rat cortical neurons were cultured in media containing 200 µM APV (an NMDA receptor blocker which reduces excitotoxicity in neuronal cultures *in vitro*) and differentiated up to DIV25, a stage

by which they typically have developed mature dendritic spines and functional synapses. These neurons were then treated with ACSF supplemented with APV or ACSF supplemented with 10 µM glycine, 100mM picrotoxin and 1 µM strychnine (inducing chemical LTP (cLTP)) (Xie et al., 2007) 30 minutes prior to fixation. Cultures were immunostained for DAPI, Genetex ZNF804A/Zfp804A and PSD-95 as a marker of mature neuronal cells. Interestingly, treatment of rat neurons with the cLTP condition was found to modestly reduce Zfp804A expression in nuclei, but not cytoplasmic regions, relative to neurons treated with the control condition (see **Figure 6.3.6**, **A-C**). A one way ANOVA revealed a significant effect of experimental condition and of the assessed region on the data ($p<0.05$; 3 independent experiments); a posthoc Tukey's pairwise comparisons test revealed the reduction in nuclear Zfp804A in cLTP-treated neurons relative to control neurons to be significant ($p<0.05$). Taken together, these data suggest that Zfp804A expression is reduced in neuronal nuclei following induction of cLTP.

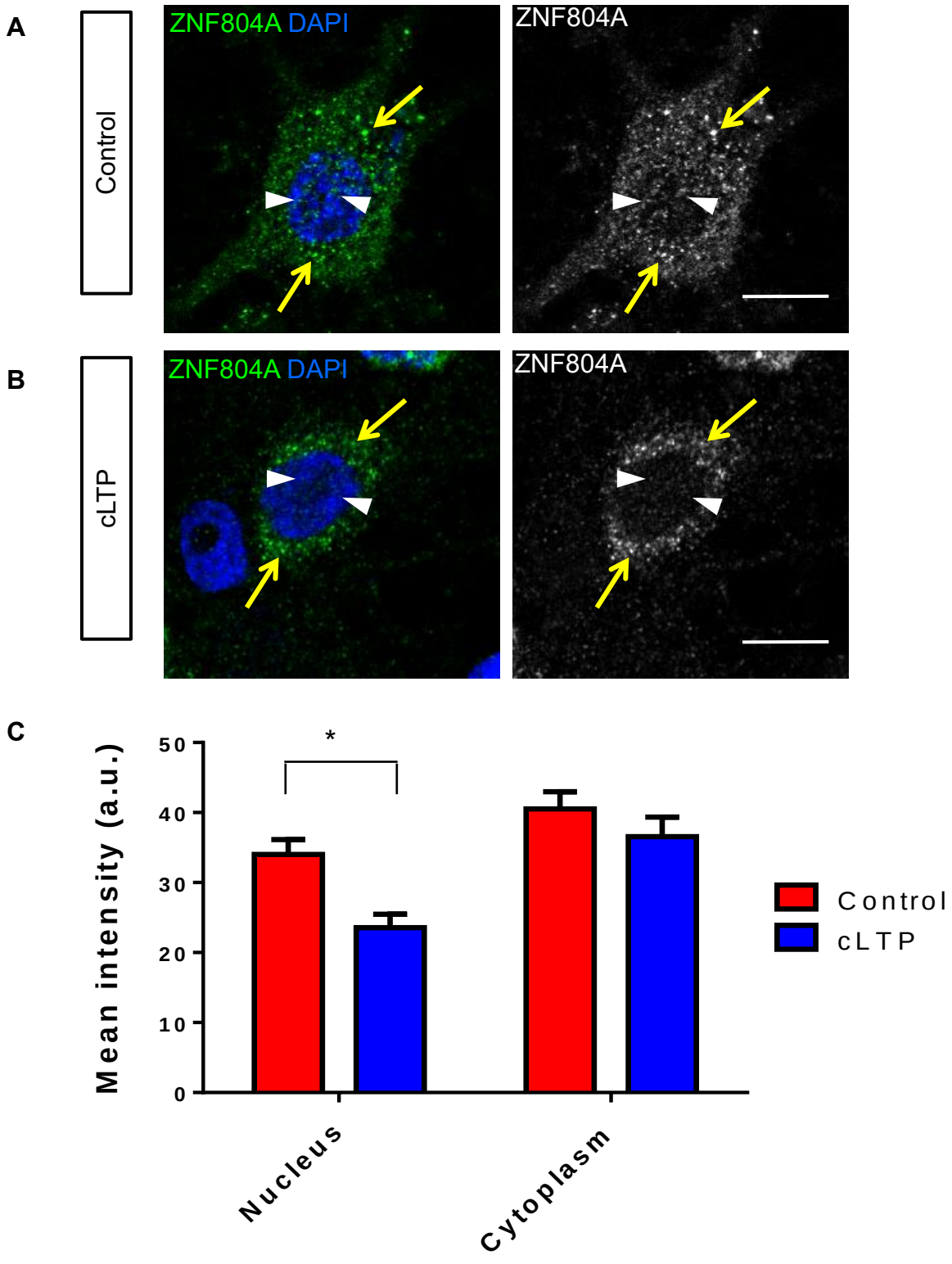

Figure 6.3.6: Chemically-induced LTP reduces nuclear Zfp804A expression in rat primary cortical neurons. **A** & **B**: Representative confocal images of Zfp804A-stained DIV25 rat primary cortical neurons treated with a vehicle control (**A**) or a cLTP treatment condition (**B**). Note the reduction in nuclear Zfp804A staining in the cLTP condition. **B**: Measurement of nuclear and cytoplasmic Zfp804A expression in response to cLTP stimulation demonstrates that induction of cLTP results in a decrease in average nuclear Zfp804A staining intensity; n = 21–28 neurons from 3 independent experiments;

Figure 6.3.6, continued: *p <0.05 (two way analysis of variance with Bonferroni post hoc analysis). Scale bars for **A** & **B** = 10 µm. The experiment for this work was carried out by Pooja Raval, with imaging and analysis conducted by P.J. Michael Deans.

6.4 DISCUSSION

This chapter has detailed numerous attempts at the manipulation of expression of ZNF804A and Zfp804A in human and rodent neuronal cells *in vitro*, including overexpression of tagged ZNF804A constructs and knockdown via RNAi techniques. It has described how knockdown of these proteins via siRNA transfection resulted in alterations in neurite outgrowth in immature neurons, while also impacting dendritic spine maintenance and plasticity in mature neurons. Finally, it has provided data indicating that induction of LTP via chemical stimuli produces subtle alterations in the pattern of Zfp804A expression.

siRNA treatment of developing neurons derived from the CTX0E16 hNPC line was found to attenuate early neurite outgrowth; this was later confirmed in neurons generated from three separate hiPSC lines. This finding was particularly intriguing when taken into account with the previous findings of the study by Hill et al. (2012), who found that a similar knockdown of ZNF804A expression using the same siRNAs also altered expression of *STMN3*, a gene involved in neurite outgrowth, as well as several genes involved in cell adhesion. Here, knockdown of ZNF804A and Zfp804A resulted in a significant reduction in neuroligin 4x expression in immature human cortical neurons and rat primary cortical neurons. A rescue of neuroligin 4x expression using overexpression of a tagged construct in the CTX0E16 cell line was found to ameliorate the neurite outgrowth phenotype found in ZNF804A-knockdown cells. In light of the previous research and the findings of the present investigation it may therefore be possible that the reduction in early neurite outgrowth following ZNF804A knockdown occurs via mediation of the expression of *STMN3* and/or one or more cell adhesion genes, including *NLGN4*. However, the possibility remains that these effects occur outside any putative role as a transcription factor - as previously mentioned, the presence of ZNF804A and Zfp804A within the cytoplasm, dendrites and axons of human and rat neurons may be consistent with an extranuclear function. Moreover, the work presented in this chapter does not rule out the possibility that any effect of neuroligin 4x overexpression on neurite outgrowth occurs independently of pathways mediated by ZNF804A.

The finding of a significant reduction in dendritic spine density in primary rat cortical neurons treated with siRNA 2 is particularly interesting in context of previous work establishing that ZNF804A regulates expression of genes involved in cell adhesion (Hill et al., 2012) as well as the discovery in the previous chapter of ZNF804A and Zfp804A expression at putative human and rodent synapses respectively. As mature dendritic spines are typically well established by DIV20 in rat neuronal cultures (the time point at which siRNA treatment is initiated)(Boyer et al., 1998), this elimination of spines is likely to occur via effects on dendritic spine maintenance rather than spinogenesis. Two explanations may therefore account for this effect on spine maintenance in these cortical neurons: it may indirectly influence synapse number through mediating the expression of genes involved in cell adhesion or, as discussed in **Chapter 5**, ZNF804A/Zfp804A may act directly at the synapse to promote spine maintenance by binding directly to specific RNA molecules via its zinc finger domain. Distinguishing between these two possibilities is therefore a key avenue for further experimentation in future research into these proteins.

In contrast to the expression of neuroligin-4, the presynaptic protein SNAP-25 was not found to be significantly altered in ZNF804A/Zfp804A knockdown conditions, both in early CTX0E16 neurons and mature primary rat cortical neurons. This is perhaps surprising in light of previous research conducted by Anitha et al (2014), who found that knockdown of ZNF804A in SH-SY5Y neuroblastoma cells resulted in a significant reduction in SNAP-25 protein expression. This anomalous result may have arisen due to differences in neuroblastoma cells relative to the two cellular systems used in the current investigation, or may be due to the greater knockdown of ZNF804A achieved via electroporation with the SH-SY5Y cells relative to the transfection method of the present chapter. This interesting previous finding may therefore still merit investigation if a knockout line is generated from a neuronal cell line in future research.

Interestingly, knockdown of Zfp804A was additionally found to impact LTP-dependent alterations in spine density and size: Zfp804A-knockdown neurons exhibited an increase spine density following induction of LTP (though not to the extent of control neurons), while an LTP-dependent increase in spine size was not seen in knockdown neurons. These data suggest that Zfp804A actions at the synapse may be modulated in part by neuronal activity. Synaptic RNA-binding proteins such as FMRP (Fragile X syndrome) have previously been demonstrated to exhibit rapid, activity-dependent

transport of mRNAs important for synaptogenesis and plasticity (Dictenberg et al., 2008), and FMRP-containing RNA granules translocate from dendritic spines to the dendritic shaft after depolarisation (Antar et al., 2004, 2005). As Zfp804A was found within both dendritic spines and the dendritic shaft of rat primary cortical neurons in **Chapter 5**, this possibility may be worth additionally exploring for ZNF804A in future research. The potential parallels between ZNF804A and FMRP function are particularly worth noting given that, like ZNF804A, FMRP isoforms have been previously found to be expressed within the nuclei of cortical neurons in a distinct punctate pattern; these nuclear isoforms are also known to bind a C2H2 zinc finger domain-containing protein, NUFIP (Bardoni et al., 1999). Such similarities highlight intriguing avenues for future research into the potential RNA-binding roles of ZNF804A.

Previous research in rat primary cortical neurons has found that treatment with glutamate increases Zfp804A mRNA in an NMDA receptor-dependent manner (Chang et al., 2015). As LTP requires NMDA receptor activation (Lüscher and Malenka, 2012), it would be reasonable to assume that the induction of NMDA receptor-dependent LTP would also increase Zfp804A mRNA in a similar manner. This increase in Zfp804A mRNA following glutamate treatment may be consistent with it contributing to mechanisms involved in LTP-dependent increases in dendritic spine size and density; upregulation of Zfp804A in response to NMDA receptor activation may further be reflective of participation in a feedback mechanism linked to LTP-mediated RNA transport, translation or metabolism.

Zfp804A was additionally shown to demonstrate alterations in distribution in rat primary cortical neurons following induction of cLTP in this chapter, specifically a reduction in nuclear Zfp804A. It is interesting that the shift in subcellular localisation following induction of LTP appears to represent a more polarised form of the predominately cytoplasmic expression seen for both ZNF804A and Zfp804A in human and rat neurons respectively in the previous chapter. Given that data presented in the previous chapter indicated that relative nuclear expression of ZNF804A is reduced during differentiation in a similar manner while cytoplasmic ZNF804A increases, early neuronal activity may be a factor in the reduction in nuclear expression seen in differentiated neurons. A reduction in nuclear Zfp804A expression may be indicative of transport of this protein out of the nucleus. Although the full length Zfp804A sequence lacks a nuclear export signal, analysis of this sequence using the online Eukaryotic

Linear Motif (ELM) resource, an online database which provides information on predicted modification, binding and cleavage sites of a given protein based on its amino acid sequence, revealed the presence of a predicted sumotylation site. Sumotylation is a protein modification which has previously been found to promote cytonuclear transport of several other proteins (Pichler and Melchior, 2002) and thus may provide a mechanism through which nuclear expression is altered during differentiation and following LTP. Chaperone proteins are also a common mediator of nuclear import and export and thus may represent another method of Zfp804A and ZNF804A transportation (Echeverría et al., 2009; Galigniana et al., 2010; Pemberton and Paschal, 2005). ZNF804A has also been predicted to bind NUP35, a core component of the nuclear membrane transport complex in a recent study of the schizophrenia interactome; this may be one such mechanism through which ZNF804A exits the nucleus during development and after LTP (Ganapathiraju et al., 2016). However, the possibility remains that the reduction in nuclear Zfp804A may reflect a degradation of existing protein within this compartment - when coupled with increased mRNA expression this may indicate an increased turnover of the protein following NMDA receptor activation.

In addition to the techniques outlined in the results section of this chapter, genome editing of the CTX0E16 line was explored as a potential model to study ZNF804A function. However, efforts to establish a ZNF804A knockout line from CTX0E16 cultures using a zinc finger nuclease system ultimately proved unsuccessful due to problems with culture viability, an inefficient selection method, the considerable time required to expand cultures and wild type cells outcompeting knockout cell proliferation in mixed cultures. Future investigations attempting to generate a similar knockout from human neuronal lines would benefit from a simultaneous insertion of a reporter gene to detect knockout cells in mixed cultures, an alternative means of selection of the knockout cell line (for example, insertion of an antibiotic resistance gene) or the use of a more efficient protocol for genome editing such as CRISPR/Cas9 (Hsu et al., 2014). In addition to this, attempts to overexpress ZNF804A using transfection of tagged constructs ultimately proved unsuccessful in the present investigation, partially due to the time requirements necessary for the establishment of a working protocol and a thorough characterisation of either plasmid. Future investigations may benefit from exploration of alternate transfection reagents and the use of subcloning to insert the full length ZNF804A gene into other vectors containing alternative promoters or reporters. Subcloning may also be used in future to generate

constructs corresponding to multiple isoforms of ZNF804A to determine whether these isoforms exhibit differential patterns of expression and functional roles.

In conclusion, this chapter has shown that ZNF804A and Zfp804A play a role in the regulation of early neurite outgrowth as well as maintenance and plasticity of dendritic spines in mature neurons. Furthermore, data presented in this chapter demonstrated that expression of Zfp804A is modulated by the induction of cLTP in rat primary cortical neurons. These findings, taken together with the work presented in the previous chapter on the subcellular localisation of these proteins, have provided a more thorough understanding of the location of ZNF804A at the junction of multiple signalling pathways. The following discussion chapter will describe these findings in the greater context of the pre-existing literature on ZNF804A's effects on cognitive and structural phenotypes, and will describe how the data presented in the current chapter integrates into previously established disease mechanisms underlying schizophrenia and bipolar disorder. It will also discuss how the characterisation of the CTX0E16 cell line in chapters 3 and 4 has provided a valuable tool to add to the growing number of *in vitro* stem cell models used to investigate cellular mechanisms in development and disease.

CHAPTER 7: DISCUSSION

7.1 AIMS OF INVESTIGATION AND SUMMARY OF MAIN FINDINGS

In this thesis a human neural progenitor line was characterised for future use in studies of human neural development and disease. This line was employed alongside several other cellular models in a study of the biological functions of the psychosis-linked gene *ZNF804A.* The first aim of this thesis was to determine whether the CTX0E16 hNPC line was capable of generating cultures of glutamatergic cortical neurons. This was addressed in **Chapter 3**, where the CTX0E16 line was subject to an assessment of markers of cellular identity and an evaluation of the development of neuronal morphology. Here, CTX0E16 cultures were shown to downregulate markers of stem cell identity and upregulate markers of neuronal identity in the majority of cells after 4 weeks of differentiation. Furthermore, these neurons were found to predominately express markers of glutamatergic identity, with markers of cortical neurons and synaptic proteins also being present in these cultures. A subset of these neurons also expressed markers of GABAergic interneurons, indicating a heterogeneous population. Neurons from these cultures were additionally found to progressively develop key morphological features of cortical pyramidal neurons, including a triangular cell soma, polarised axonal and dendritic processes, neurite arborisation and even putative dendritic spines. Overall these findings are consistent with the generation of cultures predominately consisting of excitatory cortical neurons, as expected.

The second aim of the current research was to determine whether these CTX0E16 neuronal cultures also were capable of producing functional synapses and responses to a range of physiologically-relevant stimuli. This was examined in **Chapter 4**, where CTX0E16 neurons were shown to express a wide variety of key synaptic proteins in a pattern consistent with developing synapses. These neurons also demonstrate Ca^{2+} oscillations and responses to treatment with key neurotransmitters as well as displaying morphological plasticity after prolonged depolarisation. Furthermore, these cells also demonstrate a number of electrophysiological hallmarks of functional neurons, including action potentials. Collectively, these experiments have shown that CTX0E16 neurons are capable of producing functional synapses and the physiological responses consistent with those of mature glutamatergic neurons. Taken together, **Chapters 3** and **4** have demonstrated clearly

that the CTX0E16 cell line is an ideal platform for studying early neural development and disease in human neurons.

The third major aim of this study was to elucidate the precise pattern of ZNF804A/Zfp804A expression and subcellular localisation in NPCs and neurons. In **Chapter 5** the expression of ZNF804A isoforms was demonstrated at the mRNA level in NPCs and neurons from the CTX0E16 line as well as hiPSCs and hiPSC-neurons from several control lines. This expression was further demonstrated at the protein level in CTX0E16 cells using a thoroughly validated anti-ZNF804A antibody; the pattern of subcellular localisation of ZNF804A was found to alter as cultures of these cells terminally differentiated. The pattern of expression of ZNF804A/Zfp804A was found to be conserved across neuronal models, with a predominately punctate, cytoplasmic expression being seen in CTX0E16 neurons, hiPSC-neurons and rat primary cortical neurons. Additionally, in this chapter expression of ZNF804A/Zfp804A was seen at putative synapses in both human and rat cortical neurons. In **Chapter 6**, the pattern of expression of Zfp804A in rat cortical neurons was also found to be modulated by treatment with an LTP-inducing stimulus. These findings offer a more detailed overview of the pattern of expression of ZNF804A/Zfp804A and moreover, demonstrate how this pattern alters during differentiation and after LTP induction in a manner that amalgamates the findings of previous studies in both NPCs and neurons.

The final aim of this investigation was to determine whether ZNF804A/Zfp804a plays a role in the development and maintenance of neuronal morphology. This was explored in **Chapter 6** using siRNA-mediated knockdown techniques in each of the three previously described neuronal models. Knockdown of ZNF804A was found to reduce expression of the adhesion protein neuroligin 4x and early neurite outgrowth in CTX0E16 and hiPSC-derived neurons during differentiation; overexpression of neuroligin 4x in ZNF804A-knockdown cells was found to rescue this phenotype. Knockdown of the ZNF804A rodent homologue Zfp804A also resulted in reductions in dendritic spine maintenance and deficits in the morphological changes of these spines following LTP induction in mature primary rat cortical neurons. Overall, these findings demonstrate that ZNF804A influences the development of early neuronal morphology by mediating neurite outgrowth, and the rodent homologue of this protein influences the maintenance and plasticity of dendritic spines in mature cortical neurons.

7.2 THE CTX0E16 CELL LINE AS A TOOL FOR INVESTIGATING MECHANISMS OF CORTICAL DEVELOPMENT, FUNCTION AND DISEASE

The data presented throughout this investigation has provided strong evidence that cultures of neurons differentiated from the CTX0E16 cell line can adopt the hallmarks of functional pyramidal neurons derived from the human cortex. Furthermore, the findings presented in **Chapters 3** and **4** highlight a number of baseline characteristics of this cell line which may be further investigated in the context of development and disease. CTX0E16 cells offer a number of advantages over other *in vitro* models of cortical neurons. The CTX0E16 cell line offers greater resilience, requires less culture time and provides greater experimental flexibility than hiPSC-based experimental platforms and related stem cell technologies. The CTX0E16 line also provides a platform with a greater focus on cortical glutamatergic neurons than was previously available with comparable human NSC and NPC lines (Carpenter et al., 1999b; De Filippis et al., 2007), thus being a more effective model for the study of cortical development and disease. Finally, it offers a distinct advantage over non-human cellular models such as rat primary neuron cultures due to the inherent differences in neuronal phenotypes across species.

However, there are several caveats regarding the use of the CTX0E16 cell line instead of alternative cellular models. The use of a single immortalised hNPC line from a single individual fetus may limit application of certain findings to the population as a whole due to the homogeneity of cultures derived from only one such line; thus hiPSC cultures and similar models may provide a better representation of the diversity of cortical neuron phenotypes. Moreover, human cellular models like the CTX0E16 line are at a disadvantage relative to rodent cell cultures in that the culture time required before they produce key hallmarks of neuronal maturity such as action potentials and dendritic spines is much greater than that for rodent neurons (Papa et al., 1995). Finally, the CTX0E16 cell line is limited by two further properties: it does not produce the same neuronal populations as dorsal telencephalon progenitors *in vivo*, and it does not generate any structures analogous to those seen in early cortical development (such as neural rosettes in hiPSC cultures during neuralisation).

A combinatorial approach integrating experiments using neurons derived from multiple sources (as shown in **Chapters 5** and **6**) can provide a great deal of experimental flexibility and may therefore prove to be an effective way of addressing these weaknesses. For example, rodent neurons appear best suited for experiments requiring rapid assessment of mechanisms occurring in mature neurons

(particularly synaptic function), CTX0E16 neurons appear to be particularly useful in assessing phenomena specific to human glutamatergic neurons in the cortex and disease-related mechanisms within this structure, while hiPSC lines can be of use in assessing the impact of genetic variants known to cause psychiatric diseases on neuronal function or cortical structure *in vitro*. In addition to this, fate specification protocols could be employed to increase the proportion of glutamatergic neurons in differentiated CTX0E16 cultures; similar fate-specification protocols have been previously developed in hiPSC lines. Finally, the lack of structures analogous to the developing cortex in CTX0E16 cultures may be ameliorated by instead focusing studies on the expression of specific markers of cortical identity, such as layer-specific markers, to investigate developmental processes in the cortex.

In addition to studies of human cortical development and disease, CTX0E16 cells may also be of use in high-throughput screening of novel drug treatments and other therapeutic molecules by assessing how disease phenotypes (induced by genetic manipulation) can be rescued through pharmacological intervention. Moreover, genome editing could be used to induce specific disease-associated mutations or knockout disease-linked genes to determine their functional relevance to cortical development and physiology. Indeed, the exploration of ZNF804A function using the CTX0E16 NPCs in **Chapters 5** and **6** may double as pilot work to highlight potential experimental techniques and designs for larger scale studies of gene function in future with this cell line.

7.3 THE CTX0E16 CELL LINE AS A TOOL FOR INVESTIGATING ZNF804A

In addition to the initial exploration of the functional characteristics of CTX0E16 cultures, this line has also been employed as a tool to study the expression and localisation of ZNF804A in human neurons, further demonstrating the validity of these cells as a model for studying disease mechanisms within the cortex. Critically, CTX0E16 neurons demonstrated similar ZNF804A localisation to that seen in hiPSC-derived neurons and rat primary cortical neuron cultures in **Chapter 5** as well as in post-mortem human cortex (Tao et al, 2014). Moreover, siRNA-mediated knockdown of ZNF804A was shown to result in a comparable reduction in neurite outgrowth in CTX0E16 and hiPSC-derived neurons. Moreover, this effect is in line with previous genetic studies which found that siRNA-mediated knockdown of *ZNF804A* in a sister cell line of CTX0E16, CTX0E03, resulted in altered expression of genes involved in neurite outgrowth and cell adhesion. This demonstrates that CTX0E16 cellular

phenotypes are consistent with several other *in vitro* and *in vivo* findings, thus showing that this cell line is an effective platform for studying at the cellular level.

Genome editing has provided a powerful approach to produce models of human genetic lesions and mutations, overexpress genes of interest, and knockout genes entirely in a range of human stem cell lines. Knockout (KO) cell lines are a commonly used method of determining the potential functions of a given gene (Santiago et al., 2008). Recent advances in genome-editing technology have given rise to Zinc finger nucleases (ZFNs) which offer a versatile method through which genes can be specifically targeted for removal from the genome of a particular cell line (Urnov et al., 2005). As well as providing a valuable tool for investigating the functions of a gene, knockout lines also remain the gold standard for negative controls in antibody validation experiments. One of the main difficulties encountered during the investigation of ZNF804A function in CTX0E16 cells was the lack of success in generating a *ZNF804A* knockout line using zinc finger nuclease-mediated genome editing, due to a combination of a low editing efficiency and difficulties in producing clonal populations. However, since this work was halted, advances in new genome-editing technologies such as CRISPR have provided a much more effective means of inducing gene knockouts in specific cell lines. Future studies into ZNF804A function would greatly benefit from the establishment of such a knockout line, particularly in the study of the function of individual *ZNF804A* isoforms and mechanistic pathways downstream of the full length protein.

Throughout the course of the research presented in this thesis, CTX0E16 NPC and neuronal cultures have been successfully subject to a wide variety of experimental techniques, demonstrating that these cellular systems are an ideal platform for large screening projects. Indeed, the combination of these techniques with high throughput, automated methods for cell culture, assessments of pharmacological responses and evaluation of cellular morphology will mark this line as a useful tool for screening of novel treatments for psychiatric disease relevant mechanisms in future research.

7.4 EXPRESSION AND SUBCELLULAR LOCALISATION OF ZNF804A /ZFP804A

Previous research into the functions of ZNF804A has predominately adopted neuroimaging, neuropsychological, or genetic approaches, with the few studies assessing this protein using cellular models primarily focusing on a putative role as a transcription factor and in particular determining the

specific genes regulated by ZNF804A's transcriptional effects. The current investigation describes several findings regarding the expression and localisation of ZNF804A and Zfp804A as neurons differentiate and are exposed to physiological stimuli. Based on the findings of western blotting and q-PCR experiments in human cells and what is known about the rodent protein Zfp804A, the pattern of protein localisation seen in **Chapter 5** is most likely to reflect that of the full length protein. Thus, a key area of ambiguity to be explored in future research would be to further determine the pattern of localisation for other ZNF804A isoforms, especially the disease-relevant E3E4 and 2.2 variants described in the introduction chapter. As mentioned above, the establishment of a ZNF804A knockout line would be invaluable in such studies, as a rescue with tagged ZNF804A constructs for each of these isoforms would provide an accurate method of determining their subcellular distribution.

One key aspect of the full length ZNF804A transcript is the presence of two nuclear localisation signals, raising the possibility that this protein may be trafficked into the nucleus. ZNF804A also contains a predicted binding site for NUP35, a key component of the nuclear membrane transport apparatus (Ganapathiraju et al., 2016; Strambio-De-Castillia et al., 2010); this protein may therefore be a mediator of the shifts in nuclear expression seen during differentiation and LTP in the current research. Fluorescently tagged ZNF804A constructs could in future be a highly useful method to explore the potential redistribution of this protein in live cells over time and in response to physiological stimuli.

Collectively, the data presented on the expression and subcellular localisation of ZNF804A isoforms and homologues in this thesis has provided a significant contribution to the overall knowledge of this protein and has thus partially addressed the second aim of this study. The following section of this discussion will now detail how these findings, and the subsequent finding of a role for ZNF804A/Zfp804A in influencing neuronal morphology and plastic responses, integrate into the previous body of work on ZNF804A and how this protein relates to the literature at large on schizophrenia and bipolar disorder.

7.5 ZNF804A AND NEURONAL MORPHOLOGY: IMPLICATIONS FOR GROSS NEUROANATOMICAL CHANGES IN NEUROPSYCHIATRIC DISEASE

7.5.1 APPROACHES OF THE CURRENT STUDY

In addition to a thorough characterisation of ZNF804A/Zfp804A localisation in cortical neurons, the present investigation further determined the impact of ZNF804A knockdown on early and mature neuronal morphology, including responses to plasticity-inducing stimuli. In differentiating neurons from both CTX0E16 and hiPSC sources, neurite outgrowth was reduced following ZNF804A knockdown while in mature primary rat cortical neurons knockdown of the rat ZNF804A homologue, Zfp804A, resulted in a decrease in dendritic spine density and impaired plasticity in response to induction of LTP. These findings in particular build on previous research by adding a potential link between studies assessing the impact of ZNF804A on gene expression and those examining the effects of ZNF804A on gross neuroanatomical features, functional connectivity and cognitive and behavioural phenotypes. Moreover, these findings further address the second main hypothesis of the investigation by showing that ZNF804A and Zfp804A act as a regulator of early neurite outgrowth and maintenance of dendritic spines in cortical neurons, demonstrating a previously unknown role for these proteins in determining key aspects of neuronal morphology.

7.5.2 RELEVANCE OF FINDINGS TO PREVIOUS LITERATURE

The reduction in neurite outgrowth seen in ZNF804A knockdown neurons is consistent with previous research indicating that disease linked variant at rs1344706 in the *ZNF804A* locus exert their effect during the second trimester of foetal development (Hill and Bray, 2012). This developmental stage is concurrent with a period of cortical neuron maturation including outgrowth of neurites (Huang et al., 2006); previously early developmental timepoints have been hypothesised as being crucial periods during which early genetic and environmental insults can later impact the development of schizophrenia during adulthood, a theory known as the ‘neurodevelopmental hypothesis’ of schizophrenia. A potential mechanistic link has previously been described via ZNF804A-mediated effects on expression of *STMN3*, a gene previously reported to be involved in neurite outgrowth (Hill et al., 2011). One alternate mechanism through which ZNF804A may impact early neurite outgrowth is via regulation of *NLGN4* expression. In **Chapter 6**, siRNA-mediated knockdown of ZNF804A/Zfp804A expression was found to simultaneously reduce neurite outgrowth and expression of neuroligin 4x; subsequent overexpression

of exogenous neuroligin 4x attenuated this neurite outgrowth phenotype. Either one or both of these genes may be responsible for ZNF804A-mediated neurite outgrowth phenotypes. However, it should be noted that neurite outgrowth is impacted by a vast repertoire of genes, therefore any impact of ZNF804A knockdown may not be primarily mediated by *NLGN4* and/or *STMN3*. Moreover, this mediation of neurite outgrowth may not be the primary function of this protein or indeed the ultimate biological mechanism through which SNPs at the *ZNF804A* locus convey an impact on neuronal function and disease risk, given that the reduction in neurite outgrowth seen following ZNF804A knockdown in the current investigation is relatively modest. It is also worth noting that in light of the extranuclear localisation of ZNF804A found in **Chapter 5**, this protein may alternatively influence neurite outgrowth via mechanisms within the neurites themselves such as binding to mRNA molecules via the C2H2 zinc finger domain and mediating local translation of proteins relevant involved in cytoskeletal remodelling; indeed, local translation has previously been found to influence neurite outgrowth in cultured neurons (van Kesteren et al., 2006).

Despite these caveats, the neurite outgrowth phenotype observed in the current investigation may be an influence on the alterations in structural and functional connectivity seen in carriers of the risk allele of the psychosis associated rs1344706 SNP. In addition to being associated with altered expression of ZNF804A isoforms, the risk allele has also been found to be linked to white matter abnormalities, including divergent alterations in white matter integrity in the left prefrontal lobe of schizophrenics and healthy controls as well as reductions in a proxy measure of white matter integrity within the left cingulate gyrus and both parietal lobes in schizophrenic and healthy cohorts (Kuswanto et al., 2012; Wei et al., 2012; Zhang et al., 2016). Rs1344706 genotype is further associated with alterations in the corpus callosum and left forceps major (white matter tracts connecting the two cerebral hemispheres) in healthy controls, as well as abnormalities in a wide ranging white matter network in schizophrenics, bipolar patients and healthy individuals (Ikuta et al., 2014; Mallas et al., 2016). These broad alterations in white matter microstructure are accompanied with changes in the functional connectivity between several regions including the dorsolateral prefrontal cortex, the cingulate cortex and the hippocampus, within and across hemispheres (Esslinger et al., 2009, 2011; Paulus et al., 2013; Rasetti et al., 2011; Thurin et al., 2013; Zhang et al., 2016). However, the impact of alterations in neurite outgrowth brought about by may not be limited to white matter tracts.

Based on the findings described in **Chapter 6**, abnormalities in neurite outgrowth arising from altered expression of *ZNF804A* may additionally contribute to the alterations in dendritic arborisation seen in several regions of the schizophrenic brain. Previous studies have found a reduction in dendritic arbor complexity in layer III and layer V pyramidal neurons of the frontal cortex, as well as alterations in dendritic morphology in CA3 of the hippocampus in schizophrenic brains (Broadbelt et al., 2002; Kolomeets et al., 2005). Although no studies have yet attempted to characterise the effect of disease-associated *ZNF804A* genotypes on the morphological characteristics of cortical neurons *in vivo*, it is possible that ZNF804A-mediated alterations in early neurite outgrowth may be a contributory factor underlying the morphological changes seen in cortical neuron dendrites within the regions affected in the schizophrenic brain.

Zfp804A was found to further mediate dendritic spine maintenance in mature cortical neurons, a further potential mechanism through which this protein may impact the etiology of schizophrenia and other psychiatric disorders. Dendritic spines are the primary site of glutamatergic neurotransmission within the mammalian neocortex (Penzes et al., 2011). Glutamate is the most prevalent excitatory neurotransmitter within the brain, and dysfunctional glutamatergic signalling and connectivity has long been hypothesised to be a significant component of the underlying pathophysiology of schizophrenia, bipolar disorder and autism (Choudhury et al., 2012; Eastwood and Harrison, 2010; Howes et al., 2015). In particular, NMDA receptor hypofunction has been proposed as a key feature of schizophrenic pathology, specifically being thought to underlie the cognitive and negative symptoms of this disease (Stone et al., 2007). Alterations in dendritic spine density are also a common feature in these neuropsychiatric diseases: reductions in dendritic spine density have previously been demonstrated in layer III of the dorsolateral prefrontal cortex (Glantz and Lewis, 2000), the superior temporal gyrus (Sweet et al., 2009b) and CA3 of the hippocampus (Kolomeets et al., 2005) in schizophrenic brains as well as in layer III of the dorsolateral prefrontal cortex of bipolar brains (Konopaske et al., 2014). Thus, alterations in dendritic spine density within specific regions of the neocortex may be a common cellular substrate in the pathophysiology of psychotic disorders.

In schizophrenic brains loss of dendritic spines has previously been found to correlate with increases in neuronal density and reductions in grey matter volume in several brain regions, indicating that reductions in dendritic spines are the driving force behind the grey matter alterations seen in

schizophrenia rather than loss of neurons (otherwise known as 'the neuropil hypothesis' of schizophrenia (Selemon and Goldman-Rakic, 1999)). Alterations in grey matter volume in several regions have also been observed in individuals possessing the risk allele of the rs1344706 SNP: in healthy controls several studies have demonstrated reductions of grey matter in a number of regions including the prefrontal cortex, temporal cortex and cingulate cortex (Lencz et al., 2010; Nenadic et al., 2015). Conversely, in schizophrenic patients possession of the risk allele is associated with an attenuation of the pathological changes in grey matter commonly seen in schizophrenia, notably in prefrontal, temporal and hippocampal regions (Donohoe et al., 2011; Schultz et al., 2013). ZNF804A-mediated changes in dendritic spine density may therefore account for some of these alterations in healthy controls, and moreover may be a contributing factor in the (albeit attenuated) grey matter changes seen in the risk allele carrier schizophrenia subgroup. One potential mechanism which may mediate the effects of ZNF804A on cortical spine density is via altering expression of genes involved in cell adhesion (Hill et al., 2011). Cell adhesion proteins are involved in a wide variety of cellular processes but notably are key regulators of the early formation and subsequent maintenance of synapses (Gerrow et al., 2006). Thus, dysregulation of these genes may result in the reduction in dendritic spines seen in the current investigation. In addition to this, as ZNF804A and Zfp804a were both found to localise to putative synapses in human and rat cortical neurons these proteins may also possess novel, extra-nuclear functions directly at the synapse and thereby influence dendritic spine maintenance through interactions with proteins within the post-synaptic density.

In addition to being involved in dendritic spine maintenance in mature cortical neurons, Zfp804A was also found to influence LTP-mediated plasticity at these spines, specifically impacting spine enlargement following LTP induction and indicating that Zfp804A impacts LTP-induced mechanistic pathways involved in spine enlargement but not spine formation. Although impaired LTP-mediated spine plasticity cannot currently be investigated directly in patients with schizophrenia or bipolar disorder, there is some evidence to suggest that schizophrenic patients exhibit altered plasticity (Stephan et al., 2006), and altered synaptic plasticity has also been posited as a contributory factor in the pathophysiology of bipolar disorder (Duman, 2002). Proxy measures of cortical plasticity in studies of transcranial magnetic stimulation, fMRI imaging and EEG recordings have previously been found to be disrupted in schizophrenic cohorts relative to healthy controls (Stephan et al., 2006; Voineskos et al., 2013). Moreover, animal models of schizophrenia have also demonstrated abnormal induction of

LTP, particularly in rodent brain regions analogous to the prefrontal cortex in humans (Goto and Grace, 2006; Tseng et al., 2007). Local translation of mRNAs has previously been demonstrated to be a crucial step in LTP-dependent spine enlargement (Lai and Ip, 2013). This protein synthesis is thought to be driven by pathways mediated by BDNF signalling, metabotropic glutamate receptor activation and mTOR phosphorylation (Lai and Ip, 2013); disruption of these signalling pathways has previously been demonstrated to prevent spine enlargement following LTP induction. Zfp804A possesses a C2H2 zinc finger domain; as mentioned previously some members of the zinc finger protein family demonstrate RNA binding activity via this domain, thus Zfp804A may influence LTP-dependent spine enlargement by binding to RNAs and regulating their translation within the spine head. If this is indeed found to be the case then future research would benefit from identifying whether ZNF804A and Zfp804A specifically mediate LTP-dependent spine enlargement through BDNF and mGluR signalling pathways.

It is also worth noting that LTP at glutamatergic synapses on dendritic spines is dependent on activation of NMDA receptors (Lüscher and Malenka, 2012); spine formation and enlargement following LTP induction are also NMDA receptor dependent processes. In the current study both ZNF804A and Zfp804A were found to co-localise with the NMDA receptor subunit GluN1, and in rat primary cortical neurons Zfp804A was revealed to be tightly integrated within the post-synaptic density of dendritic spines, directly adjacent to GluN1. One potential alternative to the hypothesised RNA-binding properties of Zfp804A and ZNF804A may be that these proteins instead regulate spine maintenance and structural plasticity via direct interaction with members of the postsynaptic density, including GluN1. Members of the zinc finger family have previously been demonstrated to mediate protein-protein and protein-RNA interactions (Brayer and Segal, 2008), so the possibility remains that the zinc finger domain of ZNF804A possesses similar attributes within the postsynaptic density.

Aberrant synaptic plasticity may potentially be an additional pathway through which ZNF804A impacts psychosis-relevant pathology in the brain. Synaptic plasticity ultimately influences connectivity of cortical neurons, and may therefore be a contributory factor in the aberrant cortical connectivity seen in carriers of *ZNF804A* risk alleles and in psychosis patients in general. Furthermore, deficits in spine plasticity may also directly impact glutamatergic neurotransmission in the cortex: alterations in spine morphology have previously been found to be linked to functional deficits in transmission (Penzes et

al., 2011). Thus, altered expression of *ZNF804A* may induce alterations in glutamatergic neurotransmission, a feature common to both schizophrenia and bipolar disorder.

When taken together, the evidence provided by the previous literature and the findings of the current body of work indicates that ZNF804A contributes to the risk of developing psychiatric disorders via acting on the expression of a wide range of genes involved in neuronal development and immune function, as well as mediating the development, maintenance and plasticity of key aspects of neuronal morphology and connectivity. The morphological changes resulting from alterations in the expression of ZNF804A in turn impact gross neuroanatomy across a wide range of cortical regions, particularly in the prefrontal cortex, cingulate cortex and temporal cortex as well as in several white matter tracts interconnecting these regions and both hemispheres. Subsequently, these alterations affect functional connectivity between these regions and ultimately, this disruption results in the behavioural and cognitive deficits seen in schizophrenia and bipolar disorder. It should be noted however, that the alterations in *ZNF804A* expression associated with SNPs and CNVs at this locus may result in differential impacts on neuronal morphology, gross neuroanatomy, functional connectivity, behavioural phenotypes and ultimately clinical syndromes. Variants at the *ZNF804A* locus are also associated with a category of psychosis patients consisting of both bipolar and schizophrenia diagnoses, yet characterised clinically by more severe and treatment-resistant positive symptoms as well as an attenuation of the cognitive deficits typically seen in schizophrenia. This is accompanied by a similar attenuation of the neuroanatomical abnormalities typically seen in schizophrenia and is associated with an increase in $ZNF804A^{FL}$ expression in the adult prefrontal and temporal cortex but a decrease in fetal $ZNF804A^{E3E4}$ expression in the second trimester.

7.6 LIMITATIONS OF THE CURRENT WORK AND FUTURE RESEARCH

Based on the findings of the current investigation and previous studies of ZNF804A and Zfp804A, a clear area of ambiguity in urgent need of future research is regarding the functions of the known ZNF804A isoforms. The current demonstration clearly demonstrated the subcellular pattern of ZNF804A expression in NPCs and cortical neurons from multiple sources, and moreover found that reducing the expression of the *ZNF804A and ZFP804A* genes resulted in alterations in early and mature neuronal morphology. However, the study focused primarily on the function of the full length *ZNF804A* transcript and its rodent homologue, *ZFP804A*. Thus, it did not demonstrate whether the distributions

of the full length and disease-associated (*ZNF804A*^{E3E4} and *ZNF804A*$^{2.2}$) isoforms differed in their relative expression within each subcellular compartment. As the impact on neuronal morphology seen in ZNF804A-knockdown neurons was not specific to either of the siRNAs used (targeting exon 2 and exon 4 of *ZNF804A* respectively), this effect is unlikely to be mediated by ZNF804A isoforms lacking either of these exons such as *ZNF804A*^{E3E4}. In addition to this, the western blotting data presented in **Chapter 6** indicates that a homologue of *ZNF804A*^{E3E4} is not expressed in rat primary cortical neurons alongside the rodent homologue of the full length variant, Zfp804A. Thus, the impact of Zfp804A knockdown on dendritic spine maintenance and plasticity is likely to be mediated by the full length Zfp804A protein, indicating that the full length ZNF804A isoform (possessing the C2H2 zinc finger domain) may mediate the same synaptic functions. A subsequent investigation assessing the influence of the disease-associated *ZNF804A* isoforms on neuronal structure and connectivity would provide valuable clues as to whether these isoforms possess different functions, particularly given that the *ZNF804A*^{E3E4} isoform lacks any obvious DNA or RNA binding domain and thus may not act as a transcription factor or impact RNA translation, transport or metabolism (as posited in this chapter) (Tao et al., 2014). It is therefore possible that this isoform is expressed entirely outwith the nucleus. Although a western blot band consistent with the predicted size of the *ZNF804A*^{E3E4} variant could be detected in CTX0E16 cell lysates probed with the C2C3 anti-ZNF804A antibody, a knockout of the *ZNF804A* gene followed by rescue via exogenous expression of the *ZNF804A*^{E3E4} isoform using a tagged construct would be ultimately required to fully verify whether this band truly represents the disease associated isoform.

In addition to this, a similar assessment of whether individual ZNF804A isoforms convey different effects on similar aspects of neuronal morphology and function would be highly useful given the altered expression of *ZNF804A*^{E3E4} isoform seen in carriers of the risk allele of the psychosis-associated rs1344706 SNP. This would help identify more accurately the ZNF804A-mediated functions which are most relevant to the pathophysiology underlying psychosis, and eventually may highlight potential targets for therapeutic treatments.

One potential mechanism suggested in this chapter for the local actions of ZNF804A and Zfp804A at the synapse and within dendrites is the direct interaction of these proteins with mRNA molecules via the C2H2 zinc finger domain, thus regulating translation of key RNAs involved in spine

maintenance and plasticity. Although this hypothesised mechanism has not yet been confirmed, future investigations may explore this possibility via several key experiments. Primarily, the impact of ZNF804A/Zfp804A knockdown on local translation at the synapse could be studied via a combination of transcriptional inhibition with assessments of local protein production in knockdown and control cortical neurons, either via puromycin-based assays for translation in synaptosomal preparations such as SUnSET (Schmidt et al., 2009) or using direct visualisation of photoconvertible fluorescent protein translational reporters (Wang et al., 2009). The specific proteins being translationally regulated by ZNF804A/Zfp804A could be further determined using FUNCAT, a technique which uses a proximity ligation assay-based strategy to directly visualise newly synthesised target proteins (tom Dieck et al., 2015). The subsynaptic localisation of ZNF804A could further be assessed to determine whether it colocalises with key components of local translation machinery such as RNA granules or ribosomes. Moreover, the participation of ZNF804A in mechanisms specific to LTP-dependent spine enlargement may be further studied in future experiments utilising exogenous expression of tagged ZNF804A/Zfp804A constructs. For example, a combination of overexpression of exogenous Zfp804A with inhibition of specific components of the translational pathways involved in LTP-dependent spine remodelling (rapamycin to blocks mTOR phosphorylation; MCPG to block metabotropic glutamate receptors; or K252a to inhibit BDNF-TrkB signalling) can identify the potential position of Zfp804A in mechanistic pathways regulating local translation. Given that the most likely mechanism of action of full length ZNF804A/Zfp804A would occur via direct binding to RNA sequences via their zinc finger domain to regulate local translation of mRNAs, these proteins are likely to be involved in these mechanistic pathways downstream of mTOR phosphorylation. To confirm whether Zfp804A/ZNF804A binds directly to RNA, a direct assessment of the RNA binding properties of these proteins could additionally be conducted via previously described RNA binding assays (Bardoni et al., 1999); specific RNA sequences bound by these proteins could be further assessed using the yeast three-hybrid system (Martin, 2012). Taken together, these experiments would determine whether the local actions of ZNF804A are indeed mediated by direct binding of RNA molecules, and moreover, whether this mechanism occurs as part of local translational machinery involved in the regulation of dendritic spine maintenance and plasticity.

The use of hiPSC-derived neurons in the current study not only provided a valuable confirmation of the findings seen in CTX0E16 neurons, it also indicated the utility of these lines in future research regarding ZNF804A. hiPSC studies are particularly well suited for assessing the impact of

genetic variants of disease-relevant genes on very specific cellular phenotypes (Brennand et al., 2014). An intriguing future experiment would be to assess the impact of psychosis-associated SNPs and CNVs on multiple parameters including the expression of multiple ZNF804A isoforms during various stages of neuronal differentiation, whether these variants impact the morphological attributes measured in the current study, and whether there is a “genetic variant x diagnostic condition” interaction impacting any effects conveyed by the mutations on these attributes. As discussed in **Chapter 1**, recent advances in genome editing have provided a relatively simple means of inducing these mutations in control lines, and inversely, reverting these mutations in lines derived from carriers of risk alleles. Thus, isogenic lines offer a useful means of assessing the biological significance of these disease associated genetic variants, both in psychosis patients and healthy controls.

7.7 FINAL CONCLUSIONS

This thesis has presented a large body of work demonstrating the suitability of the CTX0E16 cell line for future cellular studies of human cortical development and disease, showing in particular that the neurons differentiated from this line adopt a predominately glutamatergic, deep cortical layer identity and exhibit the hallmarks of immature, yet functional neurons. These cells progressively adopt the morphological features of pyramidal neurons during differentiation, they exhibit a wide range of synaptic and disease-associated proteins, they demonstrate morphological plasticity and functional responses to physiologically-relevant stimuli and they display the electrophysiological attributes of functional neurons including action potentials. Thus, the CTX0E16 line will provide a highly useful tool for investigating the mechanisms of cortical glutamatergic neuron function and dysfunction in future research.

This study has also employed the CTX0E16 cell line, in conjunction with hiPSC lines, rat primary cortical neuron cultures and several other immortalised cell lines, to investigate the expression, subcellular localisation and function of ZNF804A throughout cortical neuron differentiation. It has shown how the expression of ZNF804A alters during neuronal development, explored the shifts in the subcellular localisation of this protein as neurons are terminally differentiated and exposed to LTP-inducing stimuli and demonstrated a novel distribution of this protein within the dendritic spines of cortical neurons. Furthermore, this investigation has shown that ZNF804A plays a role in the

development and maintenance of cortical neuron morphology, mediating early neurite outgrowth as well as dendritic spine maintenance and plasticity in mature neurons.

Finally, this thesis has integrated the findings of the current research with that of the previous literature, showing how the data presented here provides a crucial conceptual link between prior studies investigating ZNF804A's influence on gene expression and those studying the link to neuroanatomy, cognition, behaviour and clinical syndromes.

8 BIBLIOGRAPHY

Aasen, T., Raya, A., Barrero, M.J., Garreta, E., Consiglio, A., Gonzalez, F., Vassena, R., Bilić, J., Pekarik, V., Tiscornia, G., et al. (2008). Efficient and rapid generation of induced pluripotent stem cells from human keratinocytes. Nat. Biotechnol. *26*, 1276–1284.

Ageta, H., Murayama, A., Migishima, R., Kida, S., Tsuchida, K., Yokoyama, M., and Inokuchi, K. (2008). Activin in the brain modulates anxiety-related behavior and adult neurogenesis. PLoS One *3*.

Akiyama, Y., Honmou, O., Kato, T., Uede, T., Hashi, K., and Kocsis, J.D. (2001). Transplantation of clonal neural precursor cells derived from adult human brain establishes functional peripheral myelin in the rat spinal cord. Exp. Neurol. *167*, 27–39.

Albert, K. a, Hemmings, H.C., Adamo, A.I.B., Potkin, S.G., Akbarian, S., Sandman, C. a, Cotman, C.W., Bunney, W.E., and Greengard, P. (2002). Evidence for decreased DARPP-32 in the prefrontal cortex of patients with schizophrenia. Arch. Gen. Psychiatry *59*, 705–712.

Anderson, G.W., Deans, P.J.M., Taylor, R.D.T., Raval, P., Chen, D., Lowder, H., Murkerji, S., Andreae, L.C., Williams, B.P., and Srivastava, D.P. (2015). Characterisation of neurons derived from a cortical human neural stem cell line CTX0E16. Stem Cell Res. Ther. *6*, 149.

Angst, J. (2013). Bipolar disorders in DSM-5 : strengths , problems and perspectives. 5–7.

Angst, J., Gamma, A., and Lewinsohn, P. (2002). The evolving epidemiology of bipolar disorder. World Psychiatry 2–4.

Anitha, A., Thanseem, I., and Nakamura, K. (2014). Zinc finger protein 804A (ZNF804A) and verbal deficits in individuals with autism. J. Psychiatry Neurosci. *39*, 294–303.

Antar, L.N., Afroz, R., Dictenberg, J.B., Carroll, R.C., and Bassell, G.J. (2004). Metabotropic Glutamate Receptor Activation Regulates Fragile X Mental Retardation Protein and FMR1 mRNA Localization Differentially in Dendrites and at Synapses. J. Neurosci. *24*, 2648–2655.

Antar, L.N., Dictenberg, J.B., Plociniak, M., Afroz, R., and Bassell, G.J. (2005). Localization of FMRP-associated mRNA granules and requirement of microtubules for activity-dependent trafficking in hippocampal neurons. Genes, Brain Behav. *4*, 350–359.

Antonucci, F., Corradini, I., Morini, R., Fossati, G., Menna, E., Pozzi, D., Pacioni, S., Verderio, C., Bacci, A., and Matteoli, M. (2013). Reduced SNAP-25 alters short-term plasticity at developing glutamatergic synapses. EMBO Rep. *14*, 645–651.

Arlotta, P., Molyneaux, B.J., Jabaudon, D., Yoshida, Y., and Macklis, J.D. (2008). Ctip2 Controls the Differentiation of Medium Spiny Neurons Striatum. *28*, 622–632.

Aruga, J., Yokota, N., Hashimoto, M., Furuichi, T., Fukuda, M., and Mikoshiba, K. (1994). A novel zinc finger protein, zic, is involved in neurogenesis, especially in the cell lineage of cerebellar granule cells. J. Neurochem. *63*, 1880–1890.

Arun, P., Madhavarao, C.N., Moffett, J.R., and Namboodiri, A.M. a (2008). Antipsychotic drugs increase N-acetylaspartate and N-acetylaspartylglutamate in SH-SY5Y human neuroblastoma cells. J. Neurochem. *106*, 1669–1680.

Balog, Z., Kiss, I., and Kéri, S. (2011). ZNF804A may be associated with executive control of attention. Genes. Brain. Behav. *10*, 223–227.

Bardoni, B., Schenck, A., and Mandel, J.L. (1999). A novel RNA-binding nuclear protein that interacts with the fragile X mental retardation (FMR1) protein. *8*, 2557–2566.

Bardy, C., van den Hurk, M., Eames, T., Marchand, C., Hernandez, R. V, Kellogg, M., Gorris, M., Galet, B., Palomares, V., Brown, J., et al. (2015). Neuronal medium that supports basic synaptic functions and activity of human neurons in vitro. Proc. Natl. Acad. Sci. U. S. A. *112*, E2725-34.

Barnes, A.P., and Polleux, F. (2009). Establishment of axon-dendrite polarity in developing neurons. Annu. Rev. Neurosci. *32*, 347–381.

Bayer, S.A., Altman, J., and Raymond, J. (1993). Timetables of Neurogenesis in the Human Brain Based on Experimentally Determined Patterns in the Rat. Neurotoxicology *14*, 83–144.

Beaulieu, J.-M., and Gainetdinov, R.R. (2011). The physiology, signaling, and pharmacology of dopamine receptors. Pharmacol. Rev. *63*, 182–217.

Beneyto, M., and Meador-Woodruff, J.H. (2008). Lamina-specific abnormalities of NMDA receptor-associated postsynaptic protein transcripts in the prefrontal cortex in schizophrenia and bipolar disorder. Neuropsychopharmacology *33*, 2175–2186.

Bergmann, O., Haukvik, U.K., Brown, A. a, Rimol, L.M., Hartberg, C.B., Athanasiu, L., Melle, I., Djurovic, S., Andreassen, O. a, Dale, A.M., et al. (2013). ZNF804A and cortical thickness in schizophrenia and bipolar disorder. Psychiatry Res. *212*, 154–157.

Bernstein, H.-G., Steiner, J., Dobrowolny, H., and Bogerts, B. (2014). ZNF804A protein is widely expressed in human brain neurons: possible implications on normal brain structure and pathomorphologic changes in schizophrenia. Schizophr. Bull. *40*, 499–500.

Betizeau, M., Cortay, V., Patti, D., Pfister, S., Gautier, E., Bellemin-Ménard, A., Afanassieff, M., Huissoud, C., Douglas, R.J., Kennedy, H., et al. (2013). Precursor diversity and complexity of lineage relationships in the outer subventricular zone of the primate. Neuron *80*, 442–457.

Bi, C., Wu, J., Jiang, T., Liu, Q., Cai, W., Yu, P., Cai, T., Zhao, M., Jiang, Y.H., and Sun, Z.S. (2012). Mutations of ANK3 identified by exome sequencing are associated with Autism susceptibility. Hum. Mutat. *33*, 1635–1638.

Biedler, J.L., Roffler-tarlov, S., Schachner, M., and Freedman, L.S. (1978). Multiple Neurotransmitter Synthesis by Human Neuroblastoma Cell Lines and Clones. 3751–3757.

Black, M.D. (2005). Therapeutic potential of positive AMPA modulators and their relationship to AMPA receptor subunits. A review of preclinical data. Psychopharmacology (Berl). *179*, 154–163.

Blom, H., Rönnlund, D., Scott, L., Westin, L., Widengren, J., Aperia, A., and Brismar, H. (2013). Spatial distribution of DARPP-32 in dendritic spines. PLoS One *8*, e75155.

Borgmann-Winter, K.E., Rawson, N.E., Wang, H.-Y., Wang, H., Macdonald, M.L., Ozdener, M.H., Yee, K.K., Gomez, G., Xu, J., Bryant, B., et al. (2009). Human olfactory epithelial cells generated in vitro express diverse neuronal characteristics. Neuroscience *158*, 642–653.

Bourgeron, T. (2009). A synaptic trek to autism. Curr. Opin. Neurobiol. *19*, 231–234.

Boyer, C., Schikorski, T., and Stevens, C.F. (1998). Comparison of Hippocampal Dendritic Spines in Culture and in Brain. *18*, 5294–5300.

Bray, N.J., Kapur, S., and Price, J. (2012). Investigating schizophrenia in a “dish”: possibilities, potential and limitations. World Psychiatry *11*, 153–155.

Brayer, K.J., and Segal, D.J. (2008). Keep your fingers off my DNA: protein-protein interactions mediated by C2H2 zinc finger domains. Cell Biochem. Biophys. *50*, 111–131.

Brennand, K.J., Simone, A., Jou, J., Gelboin-Burkhart, C., Tran, N., Sangar, S., Li, Y., Mu, Y., Chen, G., Yu, D., et al. (2011a). Modelling schizophrenia using human induced pluripotent stem cells. Nature *473*, 221–225.

Brennand, K.J., Simone, A., Jou, J., Gelboin-Burkhart, C., Tran, N., Sangar, S., Li, Y., Mu, Y., Chen, G., Yu, D., et al. (2011b). Modelling schizophrenia using human induced pluripotent stem cells. Nature *473*, 221–225.

Brennand, K.J., Landek-Salgado, M. a, and Sawa, A. (2014). Modeling heterogeneous patients with a clinical diagnosis of schizophrenia with induced pluripotent stem cells. Biol. Psychiatry *75*, 936–944.

Broadbelt, K., Byne, W., and Jones, L.B. (2002). Evidence for a decrease in basilar dendrites of pyramidal cells in schizophrenic medial prefrontal cortex. Schizophr. Res. *58*, 75–81.

Brown, R.S. (2005). Zinc finger proteins: getting a grip on RNA. Curr. Opin. Struct. Biol. *15*, 94–98.

Budreck, E.C., and Scheiffele, P. (2007). Neuroligin-3 is a neuronal adhesion protein at GABAergic and glutamatergic synapses. Eur. J. Neurosci. *26*, 1738–1748.

Burbach, J.P., and Van Der Zwaag, B. (2009). Contact in the genetics of autism and schizophrenia. Trends Neurosci. *32*, 69–72.

Cacci, E., Villa, a, Parmar, M., Cavallaro, M., Mandahl, N., Lindvall, O., Martinez-Serrano, a, and Kokaia, Z. (2007). Generation of human cortical neurons from a new immortal fetal neural stem cell line. Exp. Cell Res. *313*, 588–601.

Callicott, J.H., Straub, R.E., Pezawas, L., Egan, M.F., Mattay, V.S., Hariri, A.R., Verchinski, B.A., Meyer-Lindenberg, A., Balkissoon, R., Kolachana, B., et al. (2005). Variation in DISC1 affects hippocampal structure and function and increases risk for schizophrenia. Proc. Natl. Acad. Sci. U. S. A. *102*, 8627–8632.

Canuso, B.C.M., and Pandina, G. (2007). Gender and Schizophrenia. Schizophr. Bull. *40*, 178–190.

Cardno, a G., and Gottesman, I.I. (2000). Twin studies of schizophrenia: from bow-and-arrow concordances to star wars Mx and functional genomics. Am. J. Med. Genet. *97*, 12–17.

Cardno, a G., Marshall, E.J., Coid, B., Macdonald, a M., Ribchester, T.R., Davies, N.J., Venturi, P., Jones, L. a, Lewis, S.W., Sham, P.C., et al. (1999). Heritability estimates for psychotic disorders: the Maudsley twin psychosis series. Arch. Gen. Psychiatry *56*, 162–168.

Carpenter, M.K., Cui, X., Hu, Z.Y., Jackson, J., Sherman, S., Seiger, a, and Wahlberg, L.U. (1999a). In vitro expansion of a multipotent population of human neural progenitor cells. Exp. Neurol. *158*, 265–278.

Carpenter, M.K., Cui, X., Hu, Z., Jackson, J., Sherman, S., and Wahlberg, L.U. (1999b). In Vitro Expansion of a Multipotent Population of Human Neural Progenitor Cells. Exp. Neurol. *278*, 265–278.

Carpenter, M.K., Inokuma, M.S., Denham, J., Mujtaba, T., Chiu, C.P., and Rao, M.S. (2001). Enrichment of neurons and neural precursors from human embryonic stem cells. Exp. Neurol. *172*, 383–397.

Carroll, L.S., and Owen, M.J. (2009). Genetic overlap between autism , schizophrenia and bipolar disorder. Genome Med. *1*, 1–7.

Chamberlain, S.J., Chen, P.F., Ng, K.Y., Bourgois-Rocha, F., Lemtiri-Chlieh, F., Levine, E.S., and Lalande, M. (2010). Induced pluripotent stem cell models of the genomic imprinting disorders Angelman and Prader-Willi syndromes. Proc Natl Acad Sci U S A *107*, 17668–17673.

Chang, E.H., Kirtley, A., Chandon, T.-S.S., Borger, P., Husain-Krautter, S., Vingtdeux, V., and Malhotra, A.K. (2015). Postnatal neurodevelopmental expression and glutamate-dependent regulation of the ZNF804A rodent homologue. Schizophr. Res. *168*, 402–410.

Chen, Y.A., and Scheller, R.H. (2001). SNARE-mediated membrane fusion. Nat. Rev. Mol. Cell Biol. *2*, 98–106.

Chen, J., Lin, M., Hrabovsky, A., Pedrosa, E., Dean, J., Jain, S., Zheng, D., and Lachman, H.M. (2015). ZNF804A Transcriptional Networks in Differentiating Neurons Derived from Induced Pluripotent Stem Cells of Human Origin. PLoS One *10*, e0124597.

Chen, M., Xu, Z., Zhai, J., Bao, X., Zhang, Q., Gu, H., Shen, Q., Cheng, L., Chen, X., Wang, K., et al. (2012). Evidence of IQ-modulated association between ZNF804A gene polymorphism and cognitive function in schizophrenia patients. Neuropsychopharmacology *37*, 1572–1578.

Cherlyn, S.Y.T., Woon, P.S., Liu, J.J., Ong, W.Y., Tsai, G.C., and Sim, K. (2010). Genetic association

studies of glutamate, GABA and related genes in schizophrenia and bipolar disorder: a decade of advance. Neurosci. Biobehav. Rev. *34*, 958–977.

Cherubini, E., Gaiarsa, J.L., and Ben-aft, Y. (1991). GABA: an excitatory transmitter in early postnatal life. Trends Neurosci. *14*, 515–519.

Chih, B., Afridi, S.K., Clark, L., and Scheiffele, P. (2004). Disorder-associated mutations lead to functional inactivation of neuroligins. Hum. Mol. Genet. *13*, 1471–1477.

Choudhury, P.R., Lahiri, S., and Rajamma, U. (2012). Glutamate mediated signaling in the pathophysiology of autism spectrum disorders. Pharmacol. Biochem. Behav. *100*, 841–849.

Cichon, S., Craddock, N., Daly, M., Faraone, S. V, Gejman, P. V, Kelsoe, J., Lehner, T., Levinson, D.F., Moran, A., Sklar, P., et al. (2009). Genomewide association studies: history, rationale, and prospects for psychiatric disorders. Am. J. Psychiatry *166*, 540–556.

Clancy, B., Finlay, B.L., Darlington, R., and Anand, K.J.S. (2008). Extrapolating Brain Development from Experimental Species to Humans. Neurotoxicology *28*, 1–15.

Cocks, G., Romanyuk, N., Amemori, T., Jendelova, P., Forostyak, O., Jeffries, A.R., Perfect, L., Thuret, S., Dayanithi, G., Sykova, E., et al. (2013). Conditionally immortalized stem cell lines from human spinal cord retain regional identity and generate functional V2a interneurons and motorneurons. Stem Cell Res. Ther. *4*, 69.

Cocks, G., Curran, S., Gami, P., Uwanogho, D., Jeffries, A.R., Kathuria, A., Lucchesi, W., Wood, V., Dixon, R., Ogilvie, C., et al. (2014). The utility of patient specific induced pluripotent stem cells for the modelling of Autistic Spectrum Disorders. Psychopharmacology (Berl). *231*, 1079–1088.

Cohan, C.S., and Kater, S.B. (1970). Suppression of Neurite Elongation and Growth Cone Motility by Electrical Activity. Science (80-.). *232*, 1638–1640.

Colak, D., Mori, T., Brill, M.S., Pfeifer, A., Falk, S., Deng, C., Monteiro, R., Mummery, C., Sommer, L., and Götz, M. (2008). Adult neurogenesis requires Smad4-mediated bone morphogenic protein signaling in stem cells. J. Neurosci. *28*, 434–446.

Cornblatt, B. a, Lencz, T., Smith, C.W., Correll, C.U., Auther, A.M., and Nakayama, E. (2003). The schizophrenia prodrome revisited: a neurodevelopmental perspective. Schizophr. Bull. *29*, 633–651.

Cousijn, H., Tunbridge, E.M., Rolinski, M., Wallis, G., Colclough, G.L., Woolrich, M.W., Nobre, A.C., and Harrison, P.J. (2015). Modulation of hippocampal theta and hippocampal-prefrontal cortex function by a schizophrenia risk gene. Hum. Brain Mapp. *36*, 2387–2395.

Cousins, D., Butts, K., and Young, A. (2009). The role of dopamine in bipolar disorder. Bipolar Disord. *11*, 787–806.

Craddock, N., and Owen, M.J. (2005). The beginning of the end for the Kraepelinian dichotomy. Br. J. Psychiatry *186*, 364–366.

Craddock, N., O'Donovan, M.C., and Owen, M.J. (2005). The genetics of schizophrenia and bipolar disorder: dissecting psychosis. J. Med. Genet. *42*, 193–204.

Cross-Disorder Group of the Psychiatric Genomics Consortium (2013). Identification of risk loci with shared effects on five major psychiatric disorders: a genome-wide analysis. Lancet *381*, 1371–1379.

Crow, T.J. (1986). The continuum of psychosis and its implication for the structure of the gene. Br. J. Psychiatry *149*, 419–429.

DeFelipe, J. (1997). Types of neurons, synaptic connections and chemical characteristics of cells immunoreactive for calbindin-D28K, parvalbumin and calretinin in the neocortex. J. Chem. Neuroanat. *14*, 1–19.

Dhara, S.K., and Stice, S.L. (2008). Neural differentiation of human embryonic stem cells. J. Cell. Biochem. *105*, 633–640.

Dichter, M. a. (1978). Rat cortical neurons in cell culture: Culture methods, cell morphology, electrophysiology, and synapse formation. Brain Res. *149*, 279–293.

Dictenberg, J.B., Swanger, S. a, Antar, L.N., Singer, R.H., and Bassell, G.J. (2008). A direct role for FMRP in activity-dependent dendritic mRNA transport links filopodial-spine morphogenesis to fragile X syndrome. Dev. Cell *14*, 926–939.

Diflorio, A., and Jones, I. (2010). Is sex important? Gender differences in bipolar disorder. Int. Rev. Psychiatry *22*, 437–452.

Donato, R., Miljan, E. a, Hines, S.J., Aouabdi, S., Pollock, K., Patel, S., Edwards, F. a, and Sinden, J.D. (2007). Differential development of neuronal physiological responsiveness in two human neural stem cell lines. BMC Neurosci. *8*, 36.

Donohoe, G., Rose, E., Frodl, T., Morris, D., Spoletini, I., Adriano, F., Bernardini, S., Caltagirone, C., Bossù, P., Gill, M., et al. (2011). ZNF804A risk allele is associated with relatively intact gray matter volume in patients with schizophrenia. Neuroimage *54*, 2132–2137.

Dotti, C.G., Sullivan, C. a, and Banker, G. a (1988). The establishment of polarity by hippocampal neurons in culture. J. Neurosci. *8*, 1454–1468.

Doyon, Y., Choi, V.M., Xia, D.F., Vo, T.D., Gregory, P.D., and Holmes, M.C. (2010). Transient cold shock enhances zinc-finger nuclease-mediated gene disruption. Nat. Methods *7*, 459–460.

Duman, R.S. (2002). Synaptic plasticity and mood disorders. Mol. Psychiatry *7 Suppl 1*, S29-34.

Durand, C.M., Betancur, C., Boeckers, T.M., Bockmann, J., Chaste, P., Fauchereau, F., Nygren, G., Rastam, M., Gillberg, I.C., Anckarsäter, H., et al. (2007). Mutations in the gene encoding the synaptic scaffolding protein SHANK3 are associated with autism spectrum disorders. Nat. Genet. *39*, 25–27.

Durand, C.M., Perroy, J., Loll, F., Perrais, D., Fagni, L., Bourgeron, T., Montcouquiol, M., and Sans, N. (2012). SHANK3 mutations identified in autism lead to modification of dendritic spine morphology via an actin-dependent mechanism. Mol. Psychiatry *17*, 71–84.

Eastwood, S.L., and Harrison, P.J. (2001). Synaptic pathology in the anterior cingulate cortex in schizophrenia and mood disorders. A review and a western blot study of synaptophysin, GAP-43 and the complexins. Brain Res. Bull. *55*, 569–578.

Eastwood, S.L., and Harrison, P.J. (2010). Markers of Glutamate Synaptic Transmission and Plasticity Are Increased in the Anterior Cingulate Cortex in Bipolar Disorder. Biol. Psychiatry *67*, 1010–1016.

Echeverría, P.C., Mazaira, G., Erlejman, A., Gomez-Sanchez, C., Piwien Pilipuk, G., and Galigniana, M.D. (2009). Nuclear import of the glucocorticoid receptor-hsp90 complex through the nuclear pore complex is mediated by its interaction with Nup62 and importin beta. Mol. Cell. Biol. *29*, 4788–4797.

Ellison-Wright, I., and Bullmore, E. (2010). Anatomy of bipolar disorder and schizophrenia: a meta-analysis. Schizophr. Res. *117*, 1–12.

Encinas, M., Iglesias, M., Liu, Y., Wang, H., Muhaisen, A., Cen, V., Gallego, C., Comella, J.X., and Herna, U.M. (2000). Sequential Treatment of SH-SY5Y Cells with Retinoic Acid and Brain-Derived Neurotrophic Factor Gives Rise to Fully Differentiated, Neurotrophic Factor-Dependent, Human Neuron-Like Cells. J. Neurochem. *75*, 991–1002.

Englund, C., Fink, A., Lau, C., Pham, D., Daza, R. a M., Bulfone, A., Kowalczyk, T., and Hevner, R.F. (2005). Pax6, Tbr2, and Tbr1 are expressed sequentially by radial glia, intermediate progenitor cells, and postmitotic neurons in developing neocortex. J. Neurosci. *25*, 247–251.

Espuny-Camacho, I., Michelsen, K. a, Gall, D., Linaro, D., Hasche, A., Bonnefont, J., Bali, C., Orduz, D., Bilheu, A., Herpoel, A., et al. (2013). Pyramidal neurons derived from human pluripotent stem cells integrate efficiently into mouse brain circuits in vivo. Neuron *77*, 440–456.

Esslinger, C., Walter, H., Kirsch, P., Erk, S., Schnell, K., Arnold, C., Haddad, L., Mier, D., Boberfeld,

C.O. Von, Raab, K., et al. (2009). Neural Mechanisms of a Genome-Wide Supported Psychosis Variant. Science (80-.). *324*, 605.

Esslinger, C., Kirsch, P., Haddad, L., Mier, D., Sauer, C., Erk, S., Schnell, K., Arnold, C., Witt, S.H., Rietschel, M., et al. (2011). Cognitive state and connectivity effects of the genome-wide significant psychosis variant in ZNF804A. Neuroimage *54*, 2514–2523.

Faissner, A., Pyka, M., Geissler, M., Sobik, T., Frischknecht, R., Gundelfinger, E.D., and Seidenbecher, C. (2010). Contributions of astrocytes to synapse formation and maturation - Potential functions of the perisynaptic extracellular matrix. Brain Res. Rev. *63*, 26–38.

Fan, Y., Abrahamsen, G., McGrath, J.J., and Mackay-Sim, A. (2012). Altered cell cycle dynamics in schizophrenia. Biol. Psychiatry *71*, 129–135.

Fattorini, G., Verderio, C., Melone, M., Gioved??, S., Benfenati, F., Matteoli, M., and Conti, F. (2009). VGLUT1 and VGAT are sorted to the same population of synaptic vesicles in subsets of cortical axon terminals. J. Neurochem. *110*, 1538–1546.

Fenster, S.D., Chung, W.J., Zhai, R., Cases-langhoff, C., Voss, B., Garner, A.M., Kaempf, U., Kindler, S., Gundelfinger, E.D., and Garner, C.C. (2000). Piccolo , a Presynaptic Zinc Finger Protein Structurally Related to Bassoon. *25*, 203–214.

Ferreira, M.A.R., O'Donovan, M.C., Meng, Y.A., Jones, I.R., Ruderfer, D.M., Jones, L., Fan, J., Kirov, G., Perlis, R.H., Green, E.K., et al. (2008). Collaborative genome-wide association analysis supports a role for ANK3 and CACNA1C in bipolar disorder. Nat. Genet. *40*, 1056–1058.

Fields, D.R., Neale, E.A., and Nelson, P.G. (1990). Effects of Patterned Electrical Mouse Sensory Neurons Activity on Neurite Outgrowth from Mouse Sensory Neurons. J. Neurosci. *10*, 2950–2964.

De Filippis, L., Lamorte, G., Snyder, E.Y., Malgaroli, A., and Vescovi, A.L. (2007). A novel, immortal, and multipotent human neural stem cell line generating functional neurons and oligodendrocytes. Stem Cells *25*, 2312–2321.

Flax, J.D., Aurora, S., Yang, C., Simonin, C., Wills, a M., Billinghurst, L.L., Jendoubi, M., Sidman, R.L., Wolfe, J.H., Kim, S.U., et al. (1998). Engraftable human neural stem cells respond to developmental cues, replace neurons, and express foreign genes. Nat. Biotechnol. *16*, 1033–1039.

Fossati, G., Morini, R., Corradini, I., Antonucci, F., Trepte, P., Edry, E., Sharma, V., Papale, a, Pozzi, D., Defilippi, P., et al. (2015). Reduced SNAP-25 increases PSD-95 mobility and impairs spine morphogenesis. Cell Death Differ. *22*, 1425–1436.

Fritschy, J.-M., Panzanelli, P., Kralic, J.E., Vogt, K.E., and Sassoè-Pognetto, M. (2006). Differential dependence of axo-dendritic and axo-somatic GABAergic synapses on GABAA receptors containing the alpha1 subunit in Purkinje cells. J. Neurosci. *26*, 3245–3255.

Frydecka, D., Misiak, B., Beszlej, J.A., Karabon, L., Pawlak-Adamska, E., Tomkiewicz, A., Partyka, A., Jonkisz, A., and Kiejna, A. (2013). Genetic variants in transforming growth factor-b gene (TGFB1) affect susceptibility to schizophrenia. Mol. Biol. Rep. *40*, 5607–5614.

Fuentealba, L.C., Obernier, K., and Alvarez-Buylla, A. (2012). Adult neural stem cells bridge their niche. Cell Stem Cell *10*, 698–708.

Fukata, Y., Kimura, T., and Kaibuchi, K. (2002). Axon specification in hippocampal neurons. Neurosci. Res. *43*, 305–315.

Galigniana, M.D., Echeverría, P.C., Erlejman, A.G., and Piwien-Pilipuk, G. (2010). Role of molecular chaperones and TPR-domain proteins in the cytoplasmic transport of steroid receptors and their passage through the nuclear pore. Nucleus *1*, 299–308.

Ganapathiraju, M.K., Thahir, M., Handen, A., Sarkar, S.N., Sweet, R. a, Nimgaonkar, V.L., Loscher, C.E., Bauer, E.M., and Chaparala, S. (2016). Schizophrenia interactome with 504 novel protein–protein interactions. Npj Schizophr. *2*, 16012.

Gandal, M.J., Leppa, V., Won, H., Parikshak, N.N., and Geschwind, D.H. (2016). The road to precision psychiatry: translating genetics into disease mechanisms. Nat. Neurosci. *19*, 1397–1407.

García-López, P., García-Marín, V., and Freire, M. (2010). Dendritic spines and development: towards a unifying model of spinogenesis--a present day review of Cajal's histological slides and drawings. Neural Plast. *2010*, 769207.

Gaspar, P., Berger, B., Febvret, A., Vigny, A., Krieger-Poulet, M., and Borri-Voltattorni, C. (1987). Tyrosine hydroxylase-immunoreactive neurons in the human cerebral cortex: a novel catecholaminergic group? Neurosci. Lett. *80*, 257–262.

Gaspard, N., Bouschet, T., Hourez, R., Dimidschstein, J., Naeije, G., van den Ameele, J., Espuny-Camacho, I., Herpoel, A., Passante, L., Schiffmann, S.N., et al. (2008). An intrinsic mechanism of corticogenesis from embryonic stem cells. Nature *455*, 351–357.

Gauthier, J., Champagne, N., Lafrenière, R.G., Xiong, L., Spiegelman, D., Brustein, E., Lapointe, M., Peng, H., Côté, M., Noreau, A., et al. (2010). De novo mutations in the gene encoding the synaptic scaffolding protein SHANK3 in patients ascertained for schizophrenia. Proc. Natl. Acad. Sci. U. S. A. *107*, 7863–7868.

Georgieva, L., Dimitrova, A., Ivanov, D., Nikolov, I., Williams, N.M., Grozeva, D., Zaharieva, I., Toncheva, D., Owen, M.J., Kirov, G., et al. (2008). Support for Neuregulin 1 as a Susceptibility Gene for Bipolar Disorder and Schizophrenia. Biol. Psychiatry *64*, 419–427.

Gerrow, K., Romorini, S., Nabi, S.M., Colicos, M. a, Sala, C., and El-Husseini, A. (2006). A preformed complex of postsynaptic proteins is involved in excitatory synapse development. Neuron *49*, 547–562.

Ghasemi-Dehkordi, P., Allahbakhshian-Farsani, M., Abdian, N., Mirzaeian, A., Saffari-Chaleshtori, J., Heybati, F., Mardani, G., Karimi-Taghanaki, A., Doosti, A., Jami, M.-S., et al. (2015). Comparison between the cultures of human induced pluripotent stem cells (hiPSCs) on feeder-and serum-free system (Matrigel matrix), MEF and HDF feeder cell lines. J. Cell Commun. Signal. *9*, 233–246.

Gibbons, H.M., and Dragunow, M. (2010). Adult human brain cell culture for neuroscience research. Int. J. Biochem. Cell Biol. *42*, 844–856.

Di Giorgio, F.P., Carrasco, M.A., Siao, M.C., Maniatis, T., and Eggan, K. (2007). Non-cell autonomous effect of glia on motor neurons in an embryonic stem cell-based ALS model. Nat. Neurosci. *10*, 608–614.

Girgenti, M.J., Loturco, J.J., and Maher, B.J. (2012). ZNF804a Regulates Expression of the Schizophrenia-Associated Genes PRSS16, COMT, PDE4B, and DRD2. PLoS One *7*, e32404.

Glantz, L.A., and Lewis, D.A. (2000). Decreased dendritic spine density on prefrontal cortical pyramidal neurons in schizophrenia. Arch. Gen. Psychiatry *57*, 65–73.

Glynn, M.W., and McAllister, a K. (2006). Immunocytochemistry and quantification of protein colocalization in cultured neurons. Nat. Protoc. *1*, 1287–1296.

Goldstein, G., Minshew, N.J., Allen, D.N., and Seaton, B.E. (2002). High-functioning autism and schizophrenia A comparison of an early and late onset neurodevelopmental disorder. *17*, 461–475.

González, F., Zhu, Z., Shi, Z.-D., Lelli, K., Verma, N., Li, Q. V, and Huangfu, D. (2014). An iCRISPR platform for rapid, multiplexable, and inducible genome editing in human pluripotent stem cells. Cell Stem Cell *15*, 215–226.

Goto, Y., and Grace, A.A. (2006). Alterations in Medial Prefrontal Cortical Activity and Plasticity in Rats with Disruption of Cortical Development. Biol. Psychiatry *60*, 1259–1267.

Gould, T.D., and Einat, H. (2007). Animal models of bipolar disorder and mood stabilizer efficacy: a critical need for improvement. Neurosci. Biobehav. Rev. *31*, 825–831.

Green, M.F. (2006). Cognitive impairment and functional outcome in schizophrenia and bipolar

disorder. J. Clin. Psychiatry *67*, e12.

Green, E.K., Grozeva, D., Jones, I., Jones, L., Kirov, G., Caesar, S., Gordon-Smith, K., Fraser, C., Forty, L., Russell, E., et al. (2010). The bipolar disorder risk allele at CACNA1C also confers risk of recurrent major depression and of schizophrenia. Mol. Psychiatry *15*, 1016–1022.

Green, E.K., Hamshere, M., Forty, L., Gordon-Smith, K., Fraser, C., Russell, E., Grozeva, D., Kirov, G., Holmans, P., Moran, J.L., et al. (2013). Replication of bipolar disorder susceptibility alleles and identification of two novel genome-wide significant associations in a new bipolar disorder case-control sample. Mol. Psychiatry *18*, 1302–1307.

Grosse, G., Grosse, J., Tapp, R., Gorsleben, M., Fetter, I., Ho, B., Gratzl, M., and Bergmann, M. (1999). SNAP-25 Requirement for Dendritic Growth of Hippocampal Neurons. *546*, 539–546.

Gustafsson, M.G.L. (2000). Surpassing the lateral resolution limit by a factor of two using structured illumination microscopy. J. Microsc. *198*, 82–87.

Hannon, G.J. (2002). RNA interference. Nature *418*, 24–26.

Hansen, D. V, Lui, J.H., Parker, P.R.L., and Kriegstein, A.R. (2010). Neurogenic radial glia in the outer subventricular zone of human neocortex. Nature *464*, 554–561.

Hansen, D. V, Lui, J.H., Flandin, P., Yoshikawa, K., Rubenstein, J.L., Alvarez-Buylla, A., and Kriegstein, A.R. (2013). Non-epithelial stem cells and cortical interneuron production in the human ganglionic eminences. Nat. Neurosci. *16*, 1576–1587.

Harrison, P.J. (1999). The neuropathology of schizophrenia. A critical review of the data and their interpretation. Brain *122 (Pt 4*, 593–624.

Hashimoto, R., Ohi, K., Yasuda, Y., Fukumoto, M., Iwase, M., Iike, N., Azechi, M., Ikezawa, K., Takaya, M., Takahashi, H., et al. (2010). The impact of a genome-wide supported psychosis variant in the ZNF804A gene on memory function in schizophrenia. Am. J. Med. Genet. B. Neuropsychiatr. Genet. *153B*, 1459–1464.

Hattori, T., Baba, K., Matsuzaki, S., Honda, A., Miyoshi, K., Inoue, K., Taniguchi, M., Hashimoto, H., Shintani, N., Baba, A., et al. (2007). A novel DISC1-interacting partner DISC1-Binding Zinc-finger protein: implication in the modulation of DISC1-dependent neurite outgrowth. Mol. Psychiatry *12*, 398–407.

Hattori, T., Shimizu, S., Koyama, Y., Yamada, K., Kuwahara, R., Kumamoto, N., Matsuzaki, S., Ito, a, Katayama, T., and Tohyama, M. (2010). DISC1 regulates cell-cell adhesion, cell-matrix adhesion and neurite outgrowth. Mol. Psychiatry *15*, 778, 798–809.

Hayashi-Takagi, A., Takaki, M., Graziane, N., Seshadri, S., Murdoch, H., Dunlop, A.J., Makino, Y., Seshadri, A.J., Ishizuka, K., Srivastava, D.P., et al. (2010). Disrupted-in-Schizophrenia 1 (DISC1) regulates spines of the glutamate synapse via Rac1. Nat. Neurosci. *13*, 327–332.

Herzog, E., Takamori, S., Jahn, R., Brose, N., and Wojcik, S.M. (2006). Synaptic and vesicular co-localization of the glutamate transporters VGLUT1 and VGLUT2 in the mouse hippocampus. J. Neurochem. *99*, 1011–1018.

Hess, J.L., and Glatt, S.J. (2013). How might ZNF804A variants influence risk for schizophrenia and bipolar disorder? A literature review, synthesis, and bioinformatic analysis. Am. J. Med. Genet. B. Neuropsychiatr. Genet.

Hess, J.L., Quinn, T.P., Akbarian, S., and Glatt, S.J. (2015). Bioinformatic analyses and conceptual synthesis of evidence linking ZNF804A to risk for schizophrenia and bipolar disorder. Am. J. Med. Genet. B. Neuropsychiatr. Genet. *168B*, 14–35.

Hill, M.J., and Bray, N.J. (2012). Evidence that schizophrenia risk variation in the ZNF804A gene exerts its effects during fetal brain development. Am. J. Psychiatry *169*, 1301–1308.

Hill, M.J., Jeffries, A.R., Dobson, R.J.B., Price, J., and Bray, N.J. (2011). Knockdown of the psychosis susceptibility gene ZNF804A alters expression of genes involved in cell adhesion. Hum. Mol. Genet. *21*, 1–27.

Hill, M.J., Jeffries, A.R., Dobson, R.J.B., Price, J., and Bray, N.J. (2012). Knockdown of the psychosis susceptibility gene ZNF804A alters expression of genes involved in cell adhesion. Hum. Mol. Genet. *21*, 1018–1024.

Hinna, K.H., Rich, K., Fex-Svenningsen, Å., and Benedikz, E. (2015). The Rat Homolog of the Schizophrenia Susceptibility Gene ZNF804A Is Highly Expressed during Brain Development, Particularly in Growth Cones. PLoS One *10*, e0132456.

Hook, L., Vives, J., Fulton, N., Leveridge, M., Lingard, S., Bootman, M.D., Falk, A., Pollard, S.M., Allsopp, T.E., Dalma-Weiszhausz, D., et al. (2011). Non-immortalized human neural stem (NS) cells as a scalable platform for cellular assays. Neurochem. Int. *59*, 432–444.

Horowitz, M. a., Wertz, J., Zhu, D., Cattaneo, a., Musaelyan, K., Nikkheslat, N., Thuret, S., Pariante, C.M., and Zunszain, P. a. (2015). Antidepressant Compounds Can Be Both Pro- and Anti-Inflammatory in Human Hippocampal Cells. Int. J. Neuropsychopharmacol. *18*, pyu076-pyu076.

Horton, A.C., Rácz, B., Monson, E.E., Lin, A.L., Weinberg, R.J., and Ehlers, M.D. (2005). Polarized secretory trafficking directs cargo for asymmetric dendrite growth and morphogenesis. Neuron *48*, 757–771.

Horton, A.C., Yi, J.J., and Ehlers, M.D. (2006). Cell type-specific dendritic polarity in the absence of spatially organized external cues. Brain Cell Biol. *35*, 29–38.

Howes, O.D., and Kapur, S. (2009). The dopamine hypothesis of schizophrenia: version III--the final common pathway. Schizophr. Bull. *35*, 549–562.

Howes, O., McCutcheon, R., and Stone, J. (2015). Glutamate and dopamine in schizophrenia: An update for the 21st century. J. Psychopharmacol.

Hsu, P.D., Lander, E.S., and Zhang, F. (2014). Development and applications of CRISPR-Cas9 for genome engineering. Cell *157*, 1262–1278.

Huang, H., Zhang, J., Wakana, S., Zhang, W., Ren, T., Richards, L.J., Yarowsky, P., Donohue, P., Graham, E., van Zijl, P.C.M., et al. (2006). White and gray matter development in human fetal, newborn and pediatric brains. Neuroimage *33*, 27–38.

Huang, L., Ohi, K., Chang, H., Yu, H., Wu, L., Yue, W., Zhang, D., Gao, L., and Li, M. (2016). A comprehensive meta-analysis of ZNF804A SNPs in the risk of schizophrenia among Asian populations. Am. J. Med. Genet. B. Neuropsychiatr. Genet.

Huettner, J.E. (2003). Kainate receptors and synaptic transmission. Prog. Neurobiol. *70*, 387–407.

Hume, R.I., Dingledine, R., and Heinemann, S.F. (1991). Identification of a site in glutamate receptor subunits that controls calcium permeability. Science *253*, 1028–1031.

Hutsler, J.J., and Zhang, H. (2010). Increased dendritic spine densities on cortical projection neurons in autism spectrum disorders. Brain Res. *1309*, 83–94.

Huttenlocher, P.R., and Dabholkar, a S. (1997). Regional differences in synaptogenesis in human cerebral cortex. J. Comp. Neurol. *387*, 167–178.

Ikuta, T., Peters, B.D., Guha, S., John, M., Karlsgodt, K.H., Lencz, T., Szeszko, P.R., and Malhotra, a K. (2014). A schizophrenia risk gene, ZNF804A, is associated with brain white matter microstructure. Schizophr. Res. *155*, 15–20.

Illes, S., Theiss, S., Hartung, H.-P., Siebler, M., and Dihné, M. (2009). Niche-dependent development of functional neuronal networks from embryonic stem cell-derived neural populations. BMC Neurosci. *10*, 93.

Ippolito, D.M., and Eroglu, C. (2010). Quantifying synapses: an immunocytochemistry-based assay to quantify synapse number. J. Vis. Exp. 2–9.

Irwin, S.A., Galvez, R., and William, T. (2000). Dendritic Spine Structural Anomalies in Fragile-X Mental Retardation Syndrome. 1038–1044.

Irwin, S.A., Patel, B., Idupulapati, M., Harris, J.B., Crisostomo, R.A., Larsen, B.P., Kooy, F., Willems, P.J., Cras, P., Kozlowski, P.B., et al. (2001). Abnormal dendritic spine characteristics in the temporal and visual cortices of patients with fragile-X syndrome: a quantitative examination. Am. J. Med. Genet. *98*, 161–167.

Ivorra, J.L., Rivero, O., Costas, J., Iniesta, R., Arrojo, M., Ramos-Ríos, R., Carracedo, A., Palomo, T., Rodriguez-Jimenez, R., Cervilla, J., et al. (2014). Replication of previous genome-wide association studies of psychiatric diseases in a large schizophrenia case-control sample from Spain. Schizophr. Res. *159*, 107–113.

Jacobs, D.I., Qin, Q., Lerro, M.C., Fu, A., Dubrow, R., Claus, E.B., DeWan, A.T., Wang, G., Lin, H., and Zhu, Y. (2016). PIWI-Interacting RNAs in Gliomagenesis: Evidence from Post-GWAS and Functional Analyses. Cancer Epidemiol. Biomarkers Prev. *25*, 1073–1080.

Jakel, R.J., Schneider, B.L., and Svendsen, C.N. (2004). Using human neural stem cells to model neurological disease. Nat. Rev. Genet. *5*, 136–144.

Jakobsen, K.D., Frederiksen, J.N., Hansen, T., Jansson, L.B., Parnas, J., and Werge, T. (2005). Reliability of clinical ICD-10 schizophrenia diagnoses. Nord. J. Psychiatry *59*, 209–212.

Jamain, S., Quach, H., Betancur, C., Råstam, M., Colineaux, C., Gillberg, I.C., Soderstrom, H., Giros, B., Leboyer, M., Gillberg, C., et al. (2003). Mutations of the X-linked genes encoding neuroligins NLGN3 and NLGN4 are associated with autism. Nat. Genet. *34*, 27–29.

Jia, P., Wang, L., Meltzer, H.Y., and Zhao, Z. (2010). Common variants conferring risk of schizophrenia: A pathway analysis of GWAS data. Schizophr. Res. *122*, 38–42.

Johansson, S. (1994). Graded action potentials generated by differentiated human neuroblastoma cells. Acta Physiol. Scand. *151*, 331–341.

Johnson, M.A., Weick, J.P., Pearce, R. a, and Zhang, S.-C. (2007). Functional neural development from human embryonic stem cells: accelerated synaptic activity via astrocyte coculture. J. Neurosci. *27*, 3069–3077.

Jones, K.A., Eng, A.G., Raval, P., Srivastava, D.P., and Penzes, P. (2014). Scaffold Protein X11 Interacts with Kalirin-7 in Dendrites and Recruits It to Golgi Outposts. J. Biol. Chem.

Kamiya, A., Kubo, K., Tomoda, T., Takaki, M., Youn, R., Ozeki, Y., Sawamura, N., Park, U., Kudo, C., Okawa, M., et al. (2005). A schizophrenia-associated mutation of DISC1 perturbs cerebral cortex development. Nat. Cell Biol. *7*, 1167–1178.

van Kesteren, R.E., Carter, C., Dissel, H.M.G., van Minnen, J., Gouwenberg, Y., Syed, N.I., Spencer, G.E., and Smit, A.B. (2006). Local synthesis of actin-binding protein beta-thymosin regulates neurite outgrowth. J. Neurosci. *26*, 152–157.

Khazipov, R., and Luhmann, H.J. (2006). Early patterns of electrical activity in the developing cerebral cortex of humans and rodents. Trends Neurosci. *29*, 414–418.

Kim, E., and Sheng, M. (2004). PDZ domain proteins of synapses. Nat. Rev. Neurosci. *5*, 771–781.

Kim, A.H., Parker, E.K., Williamson, V., McMichael, G.O., Fanous, A.H., and Vladimirov, V.I. (2012). Experimental validation of candidate schizophrenia gene ZNF804A as target for hsa-miR-137. Schizophr. Res. *141*, 60–64.

Klein, R.J., Zeiss, C., Chew, E.Y., Tsai, J., Sackler, R.S., Haynes, C., Henning, A.K., Sangiovanni, J.P., Mane, S.M., Susan, T., et al. (2005). Complement Factor H Polymorphism in Age-Related

Macular Degeneration. Science (80-.). *308*, 385–389.

Kolomeets, N.S., Orlovskaya, D.D., Rachmanova, V.I., and Uranova, N.A. (2005). Ultrastructural alterations in hippocampal mossy fiber synapses in schizophrenia: a postmortem morphometric study. Synap. New York Ny *57*, 47–55.

König, H.G., Kögel, D., Rami, A., and Prehn, J.H.M. (2005). TGF-β1 activates two distinct type I receptors in neurons: Implications for neuronal NF-κB signaling. J. Cell Biol. *168*, 1077–1086.

Konopaske, G.T., Lange, N., Coyle, J.T., and Benes, F.M. (2014). Prefrontal cortical dendritic spine pathology in schizophrenia and bipolar disorder. JAMA Psychiatry *71*, 1323–1331.

Kraguljac, N.V., Reid, M., White, D., Jones, R., den Hollander, J., Lowman, D., and Lahti, A.C. (2012). Neurometabolites in schizophrenia and bipolar disorder - a systematic review and meta-analysis. Psychiatry Res. *203*, 111–125.

Krey, J.F., Paşca, S.P., Shcheglovitov, A., Yazawa, M., Schwemberger, R., Rasmusson, R., and Dolmetsch, R.E. (2013). Timothy syndrome is associated with activity-dependent dendritic retraction in rodent and human neurons. Nat. Neurosci. *16*, 201–209.

Kriegstein, a R., and Dichter, M. a (1983). Morphological classification of rat cortical neurons in cell culture. J. Neurosci. *3*, 1634–1647.

Krishna, S.S. (2003). Structural classification of zinc fingers: SURVEY AND SUMMARY. Nucleic Acids Res. *31*, 532–550.

Kukreti, R., Tripathi, S., Bhatnagar, P., Gupta, S., Chauhan, C., Kubendran, S., Janardhan Reddy, Y.C., Jain, S., and Brahmachari, S.K. (2006). Association of DRD2 gene variant with schizophrenia. Neurosci. Lett. *392*, 68–71.

Kuswanto, C.N., Woon, P.-S., Zheng, X. Bin, Qiu, A., Sitoh, Y.-Y., Chan, Y.H., Liu, J., Williams, H., Ong, W.Y., and Sim, K. (2012). Genome-wide supported psychosis risk variant in ZNF804A gene and impact on cortico-limbic WM integrity in schizophrenia. Am. J. Med. Genet. B. Neuropsychiatr. Genet. *159B*, 255–262.

Ladran, I., Tran, N., Topol, A., and Brennand, K.J. (2013). Neural stem and progenitor cells in health and disease. Wiley Interdiscip. Rev. Syst. Biol. Med. *5*, 701–715.

Lai, K.O., and Ip, N.Y. (2013). Structural plasticity of dendritic spines: The underlying mechanisms and its dysregulation in brain disorders. Biochim. Biophys. Acta - Mol. Basis Dis. *1832*, 2257–2263.

Laity, J.H., Lee, B.M., and Wright, P.E. (2001). Zinc finger proteins: New insights into structural and functional diversity. Curr. Opin. Struct. Biol. *11*, 39–46.

Lake, C.R., and Hurwitz, N. (2007). Schizoaffective disorder merges schizophrenia and bipolar disorders as one disease--there is no schizoaffective disorder. Curr. Opin. Psychiatry *20*, 365–379.

Lee, F.H.F., Fadel, M.P., Preston-Maher, K., Cordes, S.P., Clapcote, S.J., Price, D.J., Roder, J.C., and Wong, A.H.C. (2011). Disc1 point mutations in mice affect development of the cerebral cortex. J. Neurosci. *31*, 3197–3206.

Lencz, T., Szeszko, P.R., DeRosse, P., Burdick, K.E., Bromet, E.J., Bilder, R.M., and Malhotra, A.K. (2010). A schizophrenia risk gene, ZNF804A, influences neuroanatomical and neurocognitive phenotypes. Neuropsychopharmacology *35*, 2284–2291.

Lezcano, N., and Bergson, C. (2002). D1/D5 dopamine receptors stimulate intracellular calcium release in primary cultures of neocortical and hippocampal neurons. J. Neurophysiol. *87*, 2167–2175.

Li, C., Zhou, J., Shi, G., Ma, Y., Yang, Y., Gu, J., Yu, H., Jin, S., Wei, Z., Chen, F., et al. (2009). Pluripotency can be rapidly and efficiently induced in human amniotic fluid-derived cells. Hum. Mol. Genet. *18*, 4340–4349.

Li, J., Zhao, L., You, Y., Lu, T., Jia, M., Yu, H., Ruan, Y., Yue, W., Liu, J., Lu, L., et al. (2015).

Schizophrenia Related Variants in CACNA1C also Confer Risk of Autism. PLoS One *10*, e0133247.

Li, M., Luo, X.-J., Xiao, X., Shi, L., Liu, X.-Y., Yin, L., Diao, H.-B., and Su, B. (2011). Allelic Differences Between Han Chinese and Europeans for Functional Variants in ZNF804A and Their Association With Schizophrenia. Am. J. Psychiatry *2011*, 1–8.

Li, M., Zhang, H., Luo, X. jian, Gao, L., Qi, X. bin, Gourraud, P.A., and Su, B. (2013). Meta-Analysis Indicates That the European GWAS-Identified Risk SNP rs1344706 within ZNF804A Is Not Associated with Schizophrenia in Han Chinese Population. PLoS One *8*.

Li, X.-J., Du, Z.-W., Zarnowska, E.D., Pankratz, M., Hansen, L.O., Pearce, R. a, and Zhang, S.-C. (2005). Specification of motoneurons from human embryonic stem cells. Nat. Biotechnol. *23*, 215–221.

Lichtenstein, P., Yip, B.H., Björk, C., Pawitan, Y., Cannon, T.D., Sullivan, P.F., and Hultman, C.M. (2009). Common genetic determinants of schizophrenia and bipolar disorder in Swedish families: a population-based study. Lancet (London, England) *373*, 234–239.

Lim, M.-S., Chang, M.-Y., Kim, S.-M., Yi, S.-H., Suh-Kim, H., Jung, S.J., Kim, M.J., Kim, J.H., Lee, Y.-S., Lee, S.Y., et al. (2015). Generation of Dopamine Neurons from Rodent Fibroblasts through the Expandable Neural Precursor Cell Stage. J. Biol. Chem. *290*, 17401–17414.

Lin, L., Yuan, J., Sander, B., and Golas, M.M. (2015). In Vitro Differentiation of Human Neural Progenitor Cells Into Striatal GABAergic Neurons. Stem Cells Transl. Med. *4*, 1–14.

Lin, M., Zhao, D., Hrabovsky, A., Pedrosa, E., Zheng, D., and Lachman, H.M. (2014). Heat shock alters the expression of schizophrenia and autism candidate genes in an induced pluripotent stem cell model of the human telencephalon. PLoS One *9*, e94968.

Linden, D.E.J., Lancaster, T.M., Wolf, C., Baird, A., Jackson, M.C., Johnston, S.J., Donev, R., and Thome, J. (2013). ZNF804A genotype modulates neural activity during working memory for faces. Neuropsychobiology *67*, 84–92.

Liu, A., and Niswander, L.A. (2005). Bone morphogenetic protein signalling and vertebrate nervous system development. Nat. Rev. Neurosci. *6*, 945–954.

Liu, J., Kocielska, K.A., Cao, Z., Hulsizer, S., Grace, N., Mitchell, G., Nacey, C., Githinji, J., McGee, J., Garcia-Arocena, D., et al. (2012). Signaling defects in iPSC-derived fragile X premutation neurons. Hum. Mol. Genet. *21*, 3795–3805.

Liu, Y., Liu, H.S., Sauvey, C., Yao, L., Zarnowska, E.D., and Zhang, S.-C.C. (2013). Directed differentiation of forebrain GABA interneurons from human pluripotent stem cells. Nat Protoc *8*, 1670–1679.

Livak, K.J., and Schmittgen, T.D. (2001). Analysis of relative gene expression data using real-time quantitative PCR and the 2(-Delta Delta C(T)) Method. Methods *25*, 402–408.

Loh, Y.-H., Agarwal, S., Park, I.-H., Urbach, A., Huo, H., Heffner, G.C., Kim, K., Miller, J.D., Ng, K., and Daley, G.Q. (2009). Generation of induced pluripotent stem cells from human blood. Blood *113*, 5476–5479.

Luhmann, H.J., Reiprich, R.A., Hanganu, I., and Kilb, W. (2000). Cellular Physiology of the Neonatal Rat Cerebral Cortex : Intrinsic Membrane Properties , Sodium and Calcium Currents. *584*, 574–584.

Lüscher, C., and Malenka, R.C. (2012). NMDA receptor-dependent long-term potentiation and long-term depression (LTP/LTD). Cold Spring Harb. Perspect. Biol. *4*, 1–15.

Ma, H.T., On, K.F., Tsang, Y.H., and Poon, R.Y.C. (2007). An inducible system for expression and validation of the specificity of short hairpin RNA in mammalian cells. Nucleic Acids Res. *35*, e22.

Ma, L., Hu, B., Liu, Y., Vermilyea, S.C., Liu, H., Gao, L., Sun, Y., Zhang, X., and Zhang, S.C. (2012). Human embryonic stem cell-derived GABA neurons correct locomotion deficits in quinolinic acid-

lesioned mice. Cell Stem Cell *10*, 455–464.

Ma, T., Wang, C., Wang, L., Zhou, X., Tian, M., Zhang, Q., Zhang, Y., Li, J., Liu, Z., Cai, Y., et al. (2013). Subcortical origins of human and monkey neocortical interneurons. Nat. Neurosci. *16*, 1588–1597.

Madison, J.M., Zhou, F., Nigam, a, Hussain, a, Barker, D.D., Nehme, R., van der Ven, K., Hsu, J., Wolf, P., Fleishman, M., et al. (2015). Characterization of bipolar disorder patient-specific induced pluripotent stem cells from a family reveals neurodevelopmental and mRNA expression abnormalities. Mol. Psychiatry *20*, 703–717.

Magnuson, D.S.K., Morassutti, D.J., Staines, W.A., McBumey, M.W., and Marshall, K. (1995). In vivo electrophysiological maturation of neurons derived from a multipotent precursor (embryonal carcinoma) cell line. Dev. Brain Res. *84*, 130–141.

Mallas, E.-J., Carletti, F., Chaddock, C. a, Woolley, J., Picchioni, M.M., Shergill, S.S., Kane, F., Allin, M.P.G., Barker, G.J., and Prata, D.P. (2016). Genome-wide discovered psychosis-risk gene ZNF804A impacts on white matter microstructure in health, schizophrenia and bipolar disorder. PeerJ *4*, e1570.

Mao, Y., Ge, X., Frank, C.L., Madison, J.M., Koehler, A.N., Doud, M.K., Tassa, C., Berry, E.M., Soda, T., Singh, K.K., et al. (2009). Disrupted in schizophrenia 1 regulates neuronal progenitor proliferation via modulation of GSK3beta/beta-catenin signaling. Cell *136*, 1017–1031.

Marchetto, M.C.N., Carromeu, C., Acab, A., Yu, D., Yeo, G.W., Mu, Y., Chen, G., Gage, F.H., and Muotri, A.R. (2010a). A model for neural development and treatment of Rett syndrome using human induced pluripotent stem cells. Cell *143*, 527–539.

Marchetto, M.C.N., Carromeu, C., Acab, A., Yu, D., Yeo, G.W., Mu, Y., Chen, G., Gage, F.H., and Muotri, A.R. (2010b). A model for neural development and treatment of Rett syndrome using human induced pluripotent stem cells. Cell *143*, 527–539.

Maroof, A.M., Keros, S., Tyson, J.A., Ying, S.-W., Ganat, Y.M., Merkle, F.T., Liu, B., Goulburn, A., Stanley, E.G., Elefanty, A.G., et al. (2013). Directed differentiation and functional maturation of cortical interneurons from human embryonic stem cells. Cell Stem Cell *12*, 559–572.

Martin, F. (2012). Fifteen years of the yeast three-hybrid system: RNA-protein interactions under investigation. Methods *58*, 367–375.

Martin, K.C., and Zukin, R.S. (2006). RNA Trafficking and Local Protein Synthesis in Dendrites: An Overview. J. Neurosci. *26*, 7131–7134.

Matigian, N., Abrahamsen, G., Sutharsan, R., Cook, A.L., Vitale, A.M., Nouwens, A., Bellette, B., An, J., Anderson, M., Beckhouse, A.G., et al. (2010). Disease-specific, neurosphere-derived cells as models for brain disorders. Dis. Model. Mech. *3*, 785–798.

McAllister, a K. (2000). Cellular and molecular mechanisms of dendrite growth. Cereb. Cortex *10*, 963–973.

McAllister, K.A. (2007). Dynamic aspects of CNS synapse formation. Annu. Rev. Neurosci. *30*, 425–450.

McElroy, S.L., Keck, P.E., and Strakowski, S.M. (1996). Mania, psychosis, and antipsychotics. J. Clin. Psychiatry *57 Suppl 3*, 14-26-49.

McGrath, J., Saha, S., Chant, D., and Welham, J. (2008). Schizophrenia: A concise overview of incidence, prevalence, and mortality. Epidemiol. Rev. *30*, 67–76.

Merikangas, K.R., and Lamers, F. (2012). The “true” prevalence of bipolar II disorder. Curr. Opin. Psychiatry *25*, 19–23.

Merkle, F.T., and Eggan, K. (2013). Modeling human disease with pluripotent stem cells: From genome association to function. Cell Stem Cell *12*, 656–668.

Mertens, J., Marchetto, M.C., Bardy, C., and Gage, F.H. (2016). Evaluating cell reprogramming, differentiation and conversion technologies in neuroscience. Nat. Rev. Neurosci. *17*, 424–437.

Millar, J.K., Wilson-Annan, J.C., Anderson, S., Christie, S., Taylor, M.S., Semple, C.A., Devon, R.S., St Clair, D.M., Muir, W.J., Blackwood, D.H., et al. (2000). Disruption of two novel genes by a translocation co-segregating with schizophrenia. Hum. Mol. Genet. *9*, 1415–1423.

Millar, J.K., Pickard, B.S., Mackie, S., James, R., Christie, S., Buchanan, S.R., Malloy, M.P., Chubb, J.E., Huston, E., Baillie, G.S., et al. (2005). DISC1 and PDE4B are interacting genetic factors in schizophrenia that regulate cAMP signaling. Science (80-.). *310*, 1187–1191.

Miller, B.J., Buckley, P., Seabolt, W., Mellor, A., and Kirkpatrick, B. (2011). Meta-analysis of cytokine alterations in schizophrenia: Clinical status and antipsychotic effects. Biol. Psychiatry *70*, 663–671.

Miroci, H., Schob, C., Kindler, S., Ölschläger-Schütt, J., Fehr, S., Jungenitz, T., Schwarzacher, S.W., Bagni, C., and Mohr, E. (2012). Makorin ring zinc finger protein 1 (MKRN1), a novel poly(A)-binding protein-interacting protein, stimulates translation in nerve cells. J. Biol. Chem. *287*, 1322–1334.

Mittelstaedt, T., Alvaréz-Baron, E., and Schoch, S. (2010). RIM proteins and their role in synapse function. Biol. Chem. *391*, 599–606.

Molyneaux, B.J., Arlotta, P., Menezes, J.R.L., and Macklis, J.D. (2007). Neuronal subtype specification in the cerebral cortex. Nat. Rev. Neurosci. *8*, 427–437.

Mössner, R., Schuhmacher, A., Wagner, M., Lennertz, L., Steinbrecher, A., Quednow, B.B., Rujescu, D., Rietschel, M., and Maier, W. (2012). The schizophrenia risk gene ZNF804A influences the antipsychotic response of positive schizophrenia symptoms. Eur. Arch. Psychiatry Clin. Neurosci. *262*, 193–197.

Mühleisen, T.W., Mattheisen, M., Strohmaier, J., Degenhardt, F., Priebe, L., Schultz, C.C., Breuer, R., Meier, S., Hoffmann, P., Rivandeneira, F., et al. (2012). Association between schizophrenia and common variation in neurocan (NCAN), a genetic risk factor for bipolar disorder. Schizophr. Res. *138*, 69–73.

Müller, N., Riedel, M., Ackenheil, M., and Schwarz, M.J. (1999). The role of immune function in schizophrenia : an overview. 62–68.

Murphy, T.H., Blatter, L.A., Wier, W.G., and Barabanls, J.M. (1992). Spontaneous Synchronous Cortical Neurons Synaptic Calcium Transients in Cultured. *2*.

Murray, R.M., Sham, P., Van Os, J., Zanelli, J., Cannon, M., and McDonald, C. (2004). A developmental model for similarities and dissimilarities between schizophrenia and bipolar disorder. Schizophr. Res. *71*, 405–416.

Nagai, M., Re, D.B., Nagata, T., Chalazonitis, A., Jessell, T.M., Wichterle, H., and Przedborski, S. (2007). Astrocytes expressing ALS-linked mutated SOD1 release factors selectively toxic to motor neurons. Nat. Neurosci. *10*, 615–622.

Najafabadi, H.S., Mnaimneh, S., Schmitges, F.W., Garton, M., Lam, K.N., Yang, A., Albu, M., Weirauch, M.T., Radovani, E., Kim, P.M., et al. (2015). C2H2 zinc finger proteins greatly expand the human regulatory lexicon. Nat. Biotechnol. *33*, 555–562.

Need, A.C., Ge, D., Weale, M.E., Maia, J., Feng, S., Heinzen, E.L., Shianna, K. V, Yoon, W., Kasperaviciūte, D., Gennarelli, M., et al. (2009). A genome-wide investigation of SNPs and CNVs in schizophrenia. PLoS Genet. *5*, e1000373.

Nenadic, I., Maitra, R., Basmanav, F.B., Schultz, C.C., Lorenz, C., Schachtzabel, C., Smesny, S., Nöthen, M.M., Cichon, S., Reichenbach, J.R., et al. (2015). ZNF804A genetic variation (rs1344706) affects brain grey but not white matter in schizophrenia and healthy subjects. Psychol. Med. *45*, 143–152.

Nestler, E.J., and Hyman, S.E. (2010). Animal models of neuropsychiatric disorders. Nat. Neurosci.

13, 1161–1169.

Nicholas, C.R., Chen, J., Tang, Y., Southwell, D.G., Chalmers, N., Vogt, D., Arnold, C.M., Chen, Y.J.J., Stanley, E.G., Elefanty, A.G., et al. (2013). Functional maturation of hPSC-derived forebrain interneurons requires an extended timeline and mimics human neural development. Cell Stem Cell *12*, 573–586.

Nunes, M.C., Roy, N.S., Keyoung, H.M., Goodman, R.R., McKhann, G., and Jiang, L. (2003). Identification and isolation of multipotential neural progenitor cells from the subcortical white matter of the adult human brain. *3*, 3–11.

O'Donovan, M.C., Craddock, N., Norton, N., Williams, H., Peirce, T., Moskvina, V., Nikolov, I., Hamshere, M., Carroll, L., Georgieva, L., et al. (2008). Identification of loci associated with schizophrenia by genome-wide association and follow-up. Nat. Genet. *40*, 1053–1055.

O'Donovan, M.C., Craddock, N.J., and Owen, M.J. (2009). Genetics of psychosis; insights from views across the genome. Hum. Genet. *126*, 3–12.

Ogawa, S., Tokumoto, Y., Miyake, J., and Nagamune, T. (2011). Induction of oligodendrocyte differentiation from adult human fibroblast-derived induced pluripotent stem cells. In Vitro Cell. Dev. Biol. Anim. *47*, 464–469.

Okada, T., Hashimoto, R., Yamamori, H., Umeda-Yano, S., Yasuda, Y., Ohi, K., Fukumoto, M., Ikemoto, K., Kunii, Y., Tomita, H., et al. (2012). Expression analysis of a novel mRNA variant of the schizophrenia risk gene ZNF804A. Schizophr. Res. *141*, 277–278.

Olvet, D.M., Stearns, W.H., Mclaughlin, D., Auther, A.M., Correll, C.U., and Cornblatt, B.A. (2010). Comparing clinical and neurocognitive features of the schizophrenia prodrome to the bipolar prodrome. Schizophr. Res. *123*, 59–63.

van Os, J., and Kapur, S. (2009). Schizophrenia. Lancet *374*, 635–645.

Osen-Sand, A., Catsicas, M., Staple, J.K., Jones, K.A., Ayala, G., Knowles, J., Grenningloh, G., and Catsicas, S. (1993). Inhibition of axonal growth by SNAP-25 antisense oligonucleotides in vitro and in vivo. Nature *364*, 445–448.

Otani, T., Marchetto, M.C., Gage, F.H., Simons, B.D., and Livesey, F.J. (2016). 2D and 3D Stem Cell Models of Primate Cortical Development Identify Species-Specific Differences in Progenitor Behavior Contributing to Brain Size. Cell Stem Cell *18*, 467–480.

Pang, Z.P., Yang, N., Vierbuchen, T., Ostermeier, A., Fuentes, D.R., Yang, T.Q., Citri, A., Sebastiano, V., Marro, S., Südhof, T.C., et al. (2011). Induction of human neuronal cells by defined transcription factors. Nature *476*, 220–223.

Papa, M., Bundman, M.C., Greenberger, V., and Segal, M. (1995). Morphological Analysis of Dendritic Spine Development Cultures of Hippocampal Neurons. J. Neurosci. *15*, 1–11.

Park, S.W., Seo, M.K., Cho, H.Y., Lee, J.G., Lee, B.J., Seol, W., and Kim, Y.H. (2011). Differential effects of amisulpride and haloperidol on dopamine D2 receptor-mediated signaling in SH-SY5Y cells. Neuropharmacology *61*, 761–769.

Paşca, S.P., Portmann, T., Voineagu, I., Yazawa, M., Shcheglovitov, A., Paşca, A.M., Cord, B., Palmer, T.D., Chikahisa, S., Nishino, S., et al. (2011). Using iPSC-derived neurons to uncover cellular phenotypes associated with Timothy syndrome. Nat. Med. *17*, 1657–1662.

Paulsen, B.D.S., Cardoso, S.C., Stelling, M.P., Cadilhe, D.V., and Rehen, S.K. (2014). Valproate reverts zinc and potassium imbalance in schizophrenia-derived reprogrammed cells. Schizophr. Res. *154*, 30–35.

Paulus, F.M., Krach, S., Bedenbender, J., Pyka, M., Sommer, J., Krug, A., Knake, S., Nöthen, M.M., Witt, S.H., Rietschel, M., et al. (2013). Partial support for ZNF804A genotype-dependent alterations in prefrontal connectivity. Hum. Brain Mapp. *34*, 304–313.

Pedrosa, E., Sandler, V., Shah, A., Carroll, R., Chang, C., Rockowitz, S., Guo, X., Zheng, D., and Lachman, H.M. (2011). Development of patient-specific neurons in schizophrenia using induced pluripotent stem cells. J. Neurogenet. *25*, 88–103.

Pemberton, L.F., and Paschal, B.M. (2005). Mechanisms of receptor-mediated nuclear import and nuclear export. Traffic *6*, 187–198.

Pennington, K., Beasley, C.L., Dicker, P., Fagan, a, English, J., Pariante, C.M., Wait, R., Dunn, M.J., and Cotter, D.R. (2008). Prominent synaptic and metabolic abnormalities revealed by proteomic analysis of the dorsolateral prefrontal cortex in schizophrenia and bipolar disorder. Mol. Psychiatry *13*, 1102–1117.

Penzes, P., Cahill, M.E., Jones, K. a, VanLeeuwen, J.-E., and Woolfrey, K.M. (2011). Dendritic spine pathology in neuropsychiatric disorders. Nat. Neurosci. *14*, 285–293.

Pereira, R.C., Delany, A.M., and Canalis, E. (2004). CCAAT/enhancer binding protein homologous protein (DDIT3) induces osteoblastic cell differentiation. Endocrinology *145*, 1952–1960.

Peri, L. De, Crescini, A., Deste, G., Fusar-poli, P., and Sacchetti, E. (2012). Brain Structural Abnormalities at the Onset of Schizophrenia and Bipolar Disorder : A Meta-analysis of Controlled Magnetic Resonance Imaging Studies. 486–494.

Petrie, R.X., Reid, I.C., and Stewart, C. a (2000). The N-methyl-D-aspartate receptor, synaptic plasticity, and depressive disorder. A critical review. Pharmacol. Ther. *87*, 11–25.

Pfaffl, M. (2001). A new mathematical model for relative quantification in real-time RT-PCR. Nucleic Acids Res. *29*, e45.

Pfisterer, U., Kirkeby, A., Torper, O., Wood, J., Nelander, J., Dufour, A., Björklund, A., Lindvall, O., Jakobsson, J., and Parmar, M. (2011). Direct conversion of human fibroblasts to dopaminergic neurons. Proc. Natl. Acad. Sci. U. S. A. *108*, 10343–10348.

Phillips, M.L., and Kupfer, D.J. (2013). Bipolar disorder diagnosis: challenges and future directions. Lancet *381*, 1663–1671.

Pichler, A., and Melchior, F. (2002). Ubiquitin-Related Modifier SUMO1 and Nucleocytoplasmic Transport. 381–387.

Pin, J.P., and Duvoisin, R. (1995). Neurotransmitter receptors I: The Metabotropic Glutamate Receptors : Structure and Functions. Neuropharmacology *34*, 1–26.

Pinches, E.M., and Cline, H.T. (1998). Distribution of synaptic vesicle proteins within single retinotectal axons of Xenopus tadpoles. J. Neurobiol. *35*, 426–434.

Pini, S., De Queiroz, V., Pagnin, D., Pezawas, L., Angst, J., Cassano, G.B., and Wittchen, H.U. (2005). Prevalence and burden of bipolar disorders in European countries. Eur. Neuropsychopharmacol. *15*, 425–434.

Pollock, K., Stroemer, P., Patel, S., Stevanato, L., Hope, A., Miljan, E., Dong, Z., Hodges, H., Price, J., and Sinden, J.D. (2006). A conditionally immortal clonal stem cell line from human cortical neuroepithelium for the treatment of ischemic stroke. Exp. Neurol. *199*, 143–155.

Porter, A.C., Bymaster, F.P., DeLapp, N.W., Yamada, M., Wess, J., Hamilton, S.E., Nathanson, N.M., and Felder, C.C. (2002). M1 muscarinic receptor signaling in mouse hippocampus and cortex. Brain Res. *944*, 82–89.

Post, R.M. (1999). Comparative pharmacology of bipolar disorder and schizophrenia. In Schizophrenia Research, pp. 153–158.

Powell, C.M., and Miyakawa, T. (2006). Schizophrenia-Relevant Behavioral Testing in Rodent Models: A Uniquely Human Disorder? Biol. Psychiatry *59*, 1198–1207.

Prelich, G. (2012). Gene overexpression: Uses, mechanisms, and interpretation. Genetics *190*, 841–

854.

Price, J., and Williams, B.P. (2001). Neural stem cells. Curr. Opin. Neurobiol. *11*, 564–567.

Psychiatric GWAS Consortium Bipolar Disorder Working Group (2011). Large-scale genome-wide association analysis of bipolar disorder identifies a new susceptibility locus near ODZ4. Nat. Genet. *43*, 977–983.

Puri, M.C., and Nagy, A. (2012). Concise review: Embryonic stem cells versus induced pluripotent stem cells: The game is on. Stem Cells *30*, 10–14.

Radonjić, N. V, Ayoub, A.E., Memi, F., Yu, X., Maroof, A., Jakovcevski, I., Anderson, S. a, Rakic, P., and Zecevic, N. (2014). Diversity of cortical interneurons in primates: the role of the dorsal proliferative niche. Cell Rep. *9*, 2139–2151.

Raichle, M.E., MacLeod, a M., Snyder, a Z., Powers, W.J., Gusnard, D. a, and Shulman, G.L. (2001). A default mode of brain function. Proc. Natl. Acad. Sci. U. S. A. *98*, 676–682.

Rajkowska, G., Halaris, a, and Selemon, L.D. (2001). Reductions in neuronal and glial density characterize the dorsolateral prefrontal cortex in bipolar disorder. Biol. Psychiatry *49*, 741–752.

Rao, D.D., Vorhies, J.S., Senzer, N., and Nemunaitis, J. (2009). siRNA vs. shRNA: similarities and differences. Adv. Drug Deliv. Rev. *61*, 746–759.

Rao, J.S., Kellom, M., Reese, E.A., Rapoport, S.I., and Kim, H.-W. (2012). Dysregulated glutamate and dopamine transporters in postmortem frontal cortex from bipolar and schizophrenic patients. J. Affect. Disord. *136*, 63–71.

Rasetti, R., Sambataro, F., Chen, Q., Callicott, J.H., Mattay, V.S., and Weinberger, D.R. (2011). Altered Cortical Network Dynamics: A Potential Intermediate Phenotype for Schizophrenia and Association With ZNF804A. Arch. Gen. Psychiatry *68*, 1207–1217.

Rathouz, M.M., Vijayaraghavan, S., and Berg, D.K. (1995). Acetylcholine differentially affects intracellular calcium via nicotinic and muscarinic receptors on the same population of neurons. J. Biol. Chem. *270*, 14366–14375.

Raya, A., Rodríguez-Pizà, I., Guenechea, G., Vassena, R., Navarro, S., Barrero, M.J., Consiglio, A., Castellà, M., Río, P., Sleep, E., et al. (2009). Disease-corrected haematopoietic progenitors from Fanconi anaemia induced pluripotent stem cells. Nature *460*, 53–59.

Real, M.A., Dávila, J.C., and Guirado, S. (2006). Immunohistochemical localization of the vesicular glutamate transporter VGLUT2 in the developing and adult mouse claustrum. J. Chem. Neuroanat. *31*, 169–177.

Reinhardt, P., Schmid, B., Burbulla, L.F., Schöndorf, D.C., Wagner, L., Glatza, M., Höing, S., Hargus, G., Heck, S.A., Dhingra, A., et al. (2013). Genetic correction of a lrrk2 mutation in human iPSCs links parkinsonian neurodegeneration to ERK-dependent changes in gene expression. Cell Stem Cell *12*, 354–367.

Ricciardi, S., Ungaro, F., Hambrock, M., Rademacher, N., Stefanelli, G., Brambilla, D., Sessa, A., Magagnotti, C., Bachi, A., Giarda, E., et al. (2012). CDKL5 ensures excitatory synapse stability by reinforcing NGL-1-PSD95 interaction in the postsynaptic compartment and is impaired in patient iPSC-derived neurons. Nat. Cell Biol. *14*, 911–923.

Riley, B., Thiselton, D., Maher, B.S., Bigdeli, T., Mcmichael, G.O., Fanous, A.H., Vladimirov, V., Neill, A.O., Walsh, D., and Kendler, K.S. (2010a). Replication of association between schizophrenia and ZNF804A in the Irish Case-Control Study of Schizophrenia sample. Mol. Psychiatry *15*, 29–37.

Riley, B., Thiselton, D., Maher, B.S., Bigdeli, T., Wormley, B., McMichael, G.O., Fanous, A.H., Vladimirov, V., O'Neill, F.A., Walsh, D., et al. (2010b). Replication of association between schizophrenia and ZNF804A in the Irish Case-Control Study of Schizophrenia sample. Mol. Psychiatry *15*, 29–37.

Rimol, L.M., Nesvåg, R., Hagler, D.J., Bergmann, O., Fennema-Notestine, C., Hartberg, C.B., Haukvik, U.K., Lange, E., Pung, C.J., Server, A., et al. (2012). Cortical volume, surface area, and thickness in schizophrenia and bipolar disorder. Biol. Psychiatry *71*, 552–560.

Ring, K.L., Tong, L.M., Balestra, M.E., Javier, R., Andrews-Zwilling, Y., Li, G., Walker, D., Zhang, W.R., Kreitzer, A.C., and Huang, Y. (2012). Direct reprogramming of mouse and human fibroblasts into multipotent neural stem cells with a single factor. Cell Stem Cell *11*, 100–109.

Ripke, S., Sanders, A.R., Kendler, K.S., Levinson, D.F., Sklar, P., Holmans, P. a, Lin, D.-Y., Duan, J., Ophoff, R. a, Andreassen, O. a, et al. (2011). Genome-wide association study identifies five new schizophrenia loci. Nat. Genet. *1*, 1–91.

Ripke, S., O'Dushlaine, C., Chambert, K., Moran, J.L., Kähler, A.K., Akterin, S., Bergen, S.E., Collins, A.L., Crowley, J.J., Fromer, M., et al. (2013). Genome-wide association analysis identifies 13 new risk loci for schizophrenia. Nat. Genet. *45*, 1150–1159.

Robicsek, O., Karry, R., Petit, I., Salman-Kesner, N., Müller, F.-J., Klein, E., Aberdam, D., and Ben-Shachar, D. (2013). Abnormal neuronal differentiation and mitochondrial dysfunction in hair follicle-derived induced pluripotent stem cells of schizophrenia patients. Mol. Psychiatry *18*, 1067–1076.

Robinson, M.B. (1998). The family of sodium-dependent glutamate transporters: a focus on the GLT-1/EAAT2 subtype. Neurochem. Int. *33*, 479–491.

Rogers, J.H. (1992). Immunohistochemical markers in rat cortex: Co-localization of calretinin and calbindin-D28k with neuropeptides and GABA. Brain Res. *587*, 147–157.

Roisen, F.J., Klueber, K.M., Lu, C.L., Hatcher, L.M., Dozier, A., and Shields, C.B. (2001). Adult human olfactory stem cells. *890*, 11–22.

Rouhani, F., Kumasaka, N., de Brito, M.C., Bradley, A., Vallier, L., and Gaffney, D. (2014). Genetic Background Drives Transcriptional Variation in Human Induced Pluripotent Stem Cells. PLoS Genet. *10*.

Roussignol, G., Ango, F., Romorini, S., Tu, J.C., Sala, C., Worley, P.F., Bockaert, J., and Fagni, L. (2005). Shank expression is sufficient to induce functional dendritic spine synapses in aspiny neurons. J. Neurosci. *25*, 3560–3570.

Saetre, P., Agartz, I., De Franciscis, A., Lundmark, P., Djurovic, S., Kähler, A., Andreassen, O.A., Jakobsen, K.D., Rasmussen, H.B., Werge, T., et al. (2008). Association between a disrupted-in-schizophrenia 1 (DISC1) single nucleotide polymorphism and schizophrenia in a combined Scandinavian case-control sample. Schizophr. Res. *106*, 237–241.

Sah, D., Ray, J., and Gage, F. (1997). Bipotent progenitor cell lines from the human CNS. Nat. Biotechnol. *15*, 574–580.

Saint-André, V., Batsché, E., Rachez, C., and Muchardt, C. (2011). Histone H3 lysine 9 trimethylation and HP1γ favor inclusion of alternative exons. Nat. Struct. Mol. Biol. *18*, 337–344.

Sanchez-Wandelmer, J., Hernandez-Pinto, A.M., Cano, S., Davalos, A., de la Pena, G., Puebla-Jimenez, L., Arilla-Ferreiro, E., Lasuncion, M.A., and Busto, R. (2009). Effects of the antipsychotic drug haloperidol on the somastostatinergic system in SH-SY5Y neuroblastoma cells. J Neurochem *110*, 631–640.

Santiago, Y., Chan, E., Liu, P., Orlando, S., Zhang, L., Urnov, F.D., Holmes, M.C., Guschin, D., Waite, A., Miller, J.C., et al. (2008). Targeted gene knockout in mammalian cells by using engineered zinc-finger nucleases. *105*, 5809–5814.

Sareen, D., O'Rourke, J.G., Meera, P., Muhammad, A.K.M.G., Grant, S., Simpkinson, M., Bell, S., Carmona, S., Ornelas, L., Sahabian, A., et al. (2013). Targeting RNA foci in iPSC-derived motor neurons from ALS patients with a C9ORF72 repeat expansion. Sci. Transl. Med. *5*, 208ra149.

Saville, C.W.N., Lancaster, T.M., Davies, T.J., Toumaian, M., Pappa, E., Fish, S., Feige, B., Bender,

S., Mantripragada, K.K., Linden, D.E.J., et al. (2015). Elevated P3b latency variability in carriers of ZNF804A risk allele for psychosis. Neuroimage *116*, 207–213.

Schilling, K., Dickinson, M.H., Connor, J.A., and Morgan, J.I. (1991). Electrical Activity in Cerebellar Cultures Determines Purkinje Cell Dendritic Growth Patterns. Neuron *7*, 891–902.

Schmidt, E.K., Clavarino, G., Ceppi, M., and Pierre, P. (2009). SUnSET, a nonradioactive method to monitor protein synthesis. Nat. Methods *6*, 275–277.

Schöndorf, D.C., Aureli, M., McAllister, F.E., Hindley, C.J., Mayer, F., Schmid, B., Sardi, S.P., Valsecchi, M., Hoffmann, S., Schwarz, L.K., et al. (2014). iPSC-derived neurons from GBA1-associated Parkinson's disease patients show autophagic defects and impaired calcium homeostasis. Nat. Commun. *5*, 4028.

Schretlen, D.J., Cascella, N.G., Meyer, S.M., Kingery, L.R., Testa, S.M., Munro, C.A., Pulver, A.E., Rivkin, P., Rao, V.A., Diaz-Asper, C.M., et al. (2007). Neuropsychological Functioning in Bipolar Disorder and Schizophrenia. Biol. Psychiatry *62*, 179–186.

Schultz, C.C., Nenadic, I., Riley, B., Vladimirov, V.I., Wagner, G., Koch, K., Schachtzabel, C., Mühleisen, T.W., Basmanav, B., Nöthen, M.M., et al. (2013). ZNF804A and Cortical Structure in Schizophrenia: In Vivo and Postmortem Studies. Schizophr. Bull. 3–5.

Schwab, C., Yu, S., Wong, W., McGeer, E.G., and McGeer, P.L. (2013). GAD65, GAD67, and GABAT immunostaining in human brain and apparent GAD65 loss in Alzheimer's disease. J. Alzheimers. Dis. *33*, 1073–1088.

Schwartz, P.H., Bryant, P.J., Fuja, T.J., Su, H., O'Dowd, D.K., and Klassen, H. (2003). Isolation and characterization of neural progenitor cells from post-mortem human cortex. J. Neurosci. Res. *74*, 838–851.

Selemon, L.D., and Goldman-Rakic, P.S. (1999). The reduced neuropil hypothesis: a circuit based model of schizophrenia. Biol. Psychiatry *45*, 17–25.

Serretti, a, and Mandelli, L. (2008). The genetics of bipolar disorder: genome "hot regions," genes, new potential candidates and future directions. Mol. Psychiatry *13*, 742–771.

Shcheglovitov, A., Shcheglovitova, O., Yazawa, M., Portmann, T., Shu, R., Sebastiano, V., Krawisz, A., Froehlich, W., Bernstein, J. a, Hallmayer, J.F., et al. (2013). SHANK3 and IGF1 restore synaptic deficits in neurons from 22q13 deletion syndrome patients. Nature *503*, 267–271.

Shen, J., and Yakel, J.L. (2009). Nicotinic acetylcholine receptor-mediated calcium signaling in the nervous system. Acta Pharmacol. Sin. *30*, 673–680.

Sheng, M., and Kim, E. (2000). The Shank family of scaffold proteins. J. Cell Sci. *113 (Pt 1*, 1851–1856.

Shi, L., Chang, X., Zhang, P., Coba, M.P., Lu, W., and Wang, K. (2013). The functional genetic link of NLGN4X knockdown and neurodevelopment in neural stem cells. Hum. Mol. Genet. *22*, 3749–3760.

Shi, Y., Kirwan, P., Smith, J., Robinson, H.P.C., and Livesey, F.J. (2012a). Human cerebral cortex development from pluripotent stem cells to functional excitatory synapses. Nat. Neurosci. *15*, 477–486.

Shi, Y., Kirwan, P., and Livesey, F.J. (2012b). Directed differentiation of human pluripotent stem cells to cerebral cortex neurons and neural networks. Nat. Protoc. *7*, 1836–1846.

Shum, C., Macedo, S.C., Warre-Cornish, K., Cocks, G., Price, J., and Srivastava, D.P. (2015). Utilizing induced pluripotent stem cells (iPSCs) to understand the actions of estrogens in human neurons. Horm. Behav.

Silver, M. a, and Stryker, M.P. (1999). Synaptic density in geniculocortical afferents remains constant after monocular deprivation in the cat. J. Neurosci. *19*, 10829–10842.

Simms, B.A., and Zamponi, G.W. (2014). Neuronal voltage-gated calcium channels: Structure, function, and dysfunction. Neuron *82*, 24–45.

Singh, S., Narang, A.S., and Mahato, R.I. (2011). Subcellular fate and off-target effects of siRNA, shRNA, and miRNA. Pharm. Res. *28*, 2996–3015.

Singh Roy, N., Nakano, T., Xuing, L., Kang, J., Nedergaard, M., and Goldman, S.A. (2005). Enhancer-specified GFP-based FACS purification of human spinal motor neurons from embryonic stem cells. Exp Neurol *196*, 224–234.

Smith, E.J., Stroemer, R.P., Gorenkova, N., Nakajima, M., Crum, W.R., Tang, E., Stevanato, L., Sinden, J.D., and Modo, M. (2011). Implantation Site and Lesion Topology Determine Efficacy of a Human Neural Stem Cell Line in a Rat Model of Chronic Stroke. Stem Cells 785–796.

Smith, K.R., Kopeikina, K.J., Fawcett-Patel, J.M., Leaderbrand, K., Gao, R., Schürmann, B., Myczek, K., Radulovic, J., Swanson, G.T., and Penzes, P. (2014). Psychiatric Risk Factor ANK3/Ankyrin-G Nanodomains Regulate the Structure and Function of Glutamatergic Synapses. Neuron *84*, 399–415.

Spitzer, N.C. (2002). Activity-dependent neuronal differentiation prior to synapse formation : the functions of calcium transients. J. Physiol. *96*, 73–80.

Srivastava, D.P., Woolfrey, K.M., and Penzes, P. (2011). Analysis of dendritic spine morphology in cultured CNS neurons. J. Vis. Exp. JoVE e2794.

Srivastava, D.P., Woolfrey, K.M., Jones, K.A., Anderson, C.T., Smith, K.R., Russell, T.A., Lee, H., Yasvoina, M. V, Wokosin, D.L., Ozdinler, P.H., et al. (2012). An autism-associated variant of Epac2 reveals a role for Ras/Epac2 signaling in controlling basal dendrite maintenance in mice. Plos Biol. *10*, e1001350.

St Clair, D., Blackwood, D., Muir, W., Carothers, A., Walker, M., Spowart, G., Gosden, C., and Evans, H.J. (1990). Association within a family of a balanced autosomal translocation with major mental illness. Lance *336*, 13–16.

Stefanis, N.C., Hatzimanolis, A., Avramopoulos, D., Smyrnis, N., Evdokimidis, I., Stefanis, C.N., Weinberger, D.R., and Straub, R.E. (2012). Variation in Psychosis Gene ZNF804A Is Associated With a Refined Schizotypy Phenotype but Not Neurocognitive Performance in a Large Young Male Population. Schizophr. Bull. 1–9.

Stefansson, H., Sigurdsson, E., Steinthorsdottir, V., Bjornsdottir, S., Sigmundsson, T., Ghosh, S., Brynjolfsson, J., Gunnarsdottir, S., Ivarsson, O., Chou, T.T., et al. (2002). Neuregulin 1 and Susceptibility to Schizophrenia. Am. J. Hum. Genet. *71*, 877–892.

Stefansson, H., Ophoff, R. a, Steinberg, S., Andreassen, O. a, Cichon, S., Rujescu, D., Werge, T., Pietiläinen, O.P.H., Mors, O., Mortensen, P.B., et al. (2009). Common variants conferring risk of schizophrenia. Nature *460*, 744–747.

Steinberg, S., Mors, O., Børglum, A.D., Gustafsson, O., Werge, T., Mortensen, P.B., Andreassen, O.A., Sigurdsson, E., Thorgeirsson, T.E., Böttcher, Y., et al. (2011). Expanding the range of ZNF804A variants conferring risk of psychosis. Mol. Psychiatry *16*, 59–66.

Stenman, J., Toresson, H., and Campbell, K. (2003). Identification of Two Distinct Progenitor Populations in the Lateral Ganglionic Eminence : Implications for Striatal and Olfactory Bulb Neurogenesis. *23*, 167–174.

Stephan, K.E., Baldeweg, T., and Friston, K.J. (2006). Synaptic Plasticity and Dysconnection in Schizophrenia. Biol. Psychiatry *59*, 929–939.

Stevanato, L., Corteling, R.L., Stroemer, P., Hope, A., Heward, J., Miljan, E. a, and Sinden, J.D. (2009). c-MycERTAM transgene silencing in a genetically modified human neural stem cell line implanted into MCAo rodent brain. BMC Neurosci. *10*, 86.

Stiles, J., and Jernigan, T.L. (2010). The basics of brain development. Neuropsychol. Rev. *20*, 327–

348.

Stone, J.L., O'Donovan, M.C., Gurling, H., Kirov, G.K., Blackwood, D.H.R., Corvin, A., Craddock, N.J., Gill, M., Hultman, C.M., Lichtenstein, P., et al. (2008). Rare chromosomal deletions and duplications increase risk of schizophrenia. Nature *455*, 237–241.

Stone, J.M., Morrison, P.D., and Pilowsky, L.S. (2007). Review: Glutamate and dopamine dysregulation in schizophrenia a synthesis and selective review. J. Psychopharmacol. *21*, 440–452.

Stone, J.M., Morrison, P.D., and Pilowsky, L.S. (2016). Glutamate and dopamine dysregulation in schizophrenia – a synthesis and selective review.

Storch, a, Paul, G., Csete, M., Boehm, B.O., Carvey, P.M., Kupsch, a, and Schwarz, J. (2001). Long-term proliferation and dopaminergic differentiation of human mesencephalic neural precursor cells. Exp. Neurol. *170*, 317–325.

Strakowski, S.M., Delbello, M.P., and Adler, C.M. (2005). The functional neuroanatomy of bipolar disorder: a review of neuroimaging findings. Mol. Psychiatry *10*, 105–116.

Strambio-De-Castillia, C., Niepel, M., and Rout, M.P. (2010). The nuclear pore complex: bridging nuclear transport and gene regulation. Nat Rev Mol Cell Biol *11*, 490–501.

Stroemer, P., Patel, S., Hope, A., Oliveira, C., Pollock, K., and Sinden, J. (2009). The neural stem cell line CTX0E03 promotes behavioral recovery and endogenous neurogenesis after experimental stroke in a dose-dependent fashion. Neurorehabil. Neural Repair *23*, 895–909.

Südhof, T.C. (2008). Neuroligins and neurexins link synaptic function to cognitive disease. Nature *455*, 903–911.

Sun, Y., Pollard, S., Conti, L., Toselli, M., Biella, G., Parkin, G., Willatt, L., Falk, A., Cattaneo, E., and Smith, A. (2008). Long-term tripotent differentiation capacity of human neural stem (NS) cells in adherent culture. Mol. Cell. Neurosci. *38*, 245–258.

Sun, Y., Zhao, L.-Y., Wang, G.-B., Yue, W.-H., He, Y., Shu, N., Lin, Q.-X., Wang, F., Li, J.-L., Chen, N., et al. (2015). ZNF804A variants confer risk for heroin addiction and affect decision making and gray matter volume in heroin abusers. Addict. Biol.

Svenningsson, P., Nishi, A., Fisone, G., Girault, J.-A., Nairn, A.C., and Greengard, P. (2004). DARPP-32: an integrator of neurotransmission. Annu. Rev. Pharmacol. Toxicol. *44*, 269–296.

Swanson, L., Araque, A., Parpura, V., Sanzgiri, R.P., and Haydon, P.G. (1999). Tripartite synapses : glia , the unacknowledged partner. *22*.

Sweet, R.A., Henteleff, R.A., Zhang, W., Sampson, A.R., and Lewis, D.A. (2009a). Reduced dendritic spine density in auditory cortex of subjects with schizophrenia. Neuropsychopharmacology *34*, 374–389.

Sweet, R.A., Henteleff, R.A., Zhang, W., Sampson, A.R., and Lewis, D.A. (2009b). Reduced dendritic spine density in auditory cortex of subjects with schizophrenia. Neuropsychopharmacology *34*, 374–389.

Swistowski, A., Peng, J., Liu, Q., Mali, P., Rao, M.S., Cheng, L., and Zeng, X. (2010). Efficient generation of functional dopaminergic neurons from human induced pluripotent stem cells under defined conditions. Stem Cells *28*, 1893–1904.

Tada, T., and Sheng, M. (2006). Molecular mechanisms of dendritic spine morphogenesis. Curr. Opin. Neurobiol. *16*, 95–101.

Takahashi, K., and Yamanaka, S. (2006). Induction of Pluripotent Stem Cells from Mouse Embryonic and Adult Fibroblast Cultures by Defined Factors. Cell *126*, 663–676.

Takahashi, K., Tanabe, K., Ohnuki, M., Narita, M., Ichisaka, T., Tomoda, K., and Yamanaka, S. (2007). Induction of Pluripotent Stem Cells from Adult Human Fibroblasts by Defined Factors. Cell

131, 861–872.

Taketo, M., and Yoshioka, T. (2000). Developmental change of GABA A-mediated current in rat hippocampus. Neuroscience *96*, 507–514.

Tandon, R., Gaebel, W., Barch, D.M., Bustillo, J., Gur, R.E., Heckers, S., Malaspina, D., Owen, M.J., Schultz, S., Tsuang, M., et al. (2013). Definition and description of schizophrenia in the DSM-5. Schizophr. Res. *150*, 3–10.

Tao, R., Cousijn, H., Jaffe, A.E., Burnet, P.W.J., Edwards, F., Eastwood, S.L., Shin, J.H., Lane, T. a, Walker, M. a, Maher, B.J., et al. (2014). Expression of ZNF804A in Human Brain and Alterations in Schizophrenia, Bipolar Disorder, and Major Depressive Disorder: A Novel Transcript Fetally Regulated by the Psychosis Risk Variant rs1344706. JAMA Psychiatry *21205*, 1–9.

Teffer, K., and Semendeferi, K. (2012). Human prefrontal cortex. Evolution, development, and pathology. (Elsevier B.V.).

Thomson, J.A., Itskovitz-eldor, J., Shapiro, S.S., Waknitz, M.A., Swiergiel, J.J., Marshall, V.S., and Jones, J.M. (1998). Embryonic Stem Cell Lines Derived from Human Blastocysts. Science (80-.). *282*, 1145–1148.

Threadgill, R., Bobb, K., and Ghosh, A. (1997). Regulation of dendritic growth and remodeling by Rho, Rac, and Cdc42. Neuron *19*, 625–624.

Thurin, K., Rasetti, R., Sambataro, F., Safrin, M., Chen, Q., Callicott, J.H., Mattay, V.S., and Weinberger, D.R. (2013). Effects of ZNF804A on neurophysiologic measures of cognitive control. Mol. Psychiatry *18*, 852–854.

Tian, C., Ambroz, R.J., Sun, L., Wang, Y., Ma, K., Chen, Q., Zhu, B., and Zheng, J.C. (2012). Direct conversion of dermal fibroblasts into neural progenitor cells by a novel cocktail of defined factors. Curr. Mol. Med. *12*, 126–137.

tom Dieck, S., Kochen, L., Hanus, C., Heumüller, M., Bartnik, I., Nassim-Assir, B., Merk, K., Mosler, T., Garg, S., Bunse, S., et al. (2015). Direct visualization of newly synthesized target proteins in situ. Nat. Methods *12*, 411–414.

Tomasoni, R., Repetto, D., Morini, R., Elia, C., Gardoni, F., Luca, M. Di, Turco, E., Defilippi, P., and Michela Matteoli (2013). SNAP-25 regulates spine formation through postsynaptic binding to p140Cap. Nat. Commun. *4*, 2156.

Torrey, E.F., Barci, B.M., Webster, M.J., Bartko, J.J., Meador-Woodruff, J.H., and Knable, M.B. (2005). Neurochemical markers for schizophrenia, bipolar disorder, and major depression in postmortem brains. Biol. Psychiatry *57*, 252–260.

Tseng, K.Y., Lewis, B.L., Lipska, B.K., and O'Donnell, P. (2007). Post-Pubertal Disruption of Medial Prefrontal Cortical Dopamine-Glutamate Interactions in a Developmental Animal Model of Schizophrenia. Biol. Psychiatry *62*, 730–738.

Uchino, S., and Waga, C. (2013). SHANK3 as an autism spectrum disorder-associated gene. Brain Dev. *35*, 106–110.

Umeda-Yano, S., Hashimoto, R., Yamamori, H., Okada, T., Yasuda, Y., Ohi, K., Fukumoto, M., Ito, A., and Takeda, M. (2013). The regulation of gene expression involved in TGF-β signaling by ZNF804A, a risk gene for schizophrenia. Schizophr. Res. *146*, 273–278.

Urnov, F.D., Miller, J.C., Lee, Y.-L., Beausejour, C.M., Rock, J.M., Augustus, S., Jamieson, A.C., Porteus, M.H., Gregory, P.D., and Holmes, M.C. (2005). Highly efficient endogenous human gene correction using designed zinc-finger nucleases. Nature *435*, 646–651.

Verpelli, C., Dvoretskova, E., Vicidomini, C., Rossi, F., Chiappalone, M., Schoen, M., Di Stefano, B., Mantegazza, R., Broccoli, V., Böckers, T.M., et al. (2011). Importance of Shank3 protein in regulating metabotropic glutamate receptor 5 (mGluR5) expression and signaling at synapses. J. Biol. Chem.

286, 34839–34850.

Verpelli, C., Carlessi, L., Bechi, G., Poli, E.F., Orellana, D., Heise, C., Franceschetti, S., Mantegazza, R., Mantegazza, M., Delia, D., et al. (2013). Comparative neuronal differentiation of self-renewing neural progenitor cell lines obtained from human induced pluripotent stem cells. Front. Cell. Neurosci. *7*, 175.

Vierbuchen, T., Ostermeier, A., Pang, Z.P., Kokubu, Y., Südhof, T.C., and Wernig, M. (2010). Direct conversion of fibroblasts to functional neurons by defined factors. Nature *463*, 1035–1041.

Villa, A., Navarro-Galve, B., Bueno, C., Franco, S., Blasco, M.A., and Martinez-Serrano, A. (2004). Long-term molecular and cellular stability of human neural stem cell lines. Exp. Cell Res. *294*, 559–570.

Voineskos, A.N., Lerch, J.P., Felsky, D., Tiwari, A., Rajji, T.K., Miranda, D., Lobaugh, N.J., Pollock, B.G., Mulsant, B.H., and Kennedy, J.L. (2011). The ZNF804A gene: characterization of a novel neural risk mechanism for the major psychoses. Neuropsychopharmacology *36*, 1871–1878.

Voineskos, D., Rogasch, N.C., Rajji, T.K., Fitzgerald, P.B., and Daskalakis, Z.J. (2013). A review of evidence linking disrupted neural plasticity to schizophrenia. Can. J. Psychiatry *58*, 86–92.

Waites, C.L., Leal-Ortiz, S. a, Okerlund, N., Dalke, H., Fejtova, A., Altrock, W.D., Gundelfinger, E.D., and Garner, C.C. (2013). Bassoon and Piccolo maintain synapse integrity by regulating protein ubiquitination and degradation. EMBO J. *32*, 954–969.

Wallace, T.L., and Bertrand, D. (2013). Importance of the nicotinic acetylcholine receptor system in the prefrontal cortex. Biochem. Pharmacol. *85*, 1713–1720.

Walsh, T., McClellan, J.M., McCarthy, S.E., Addington, A.M., Pierce, S.B., Cooper, G.M., Nord, A.S., Kusenda, M., Malhotra, D., Bhandari, A., et al. (2008). Rare structural variants disrupt multiple genes in neurodevelopmental pathways in schizophrenia. Science *320*, 539–543.

Walters, J.T.R., Corvin, A., Owen, M.J., Williams, H., Dragovic, M., Quinn, E.M., Judge, R., Smith, D.J., Norton, N., Giegling, I., et al. (2010). Psychosis susceptibility gene ZNF804A and cognitive performance in schizophrenia. Arch. Gen. Psychiatry *67*, 692–700.

Wang, D.O., Kim, S.M., Zhao, Y., Hwang, H., Miura, S.K., Sossin, W.S., and Martin, K.C. (2009). Synapse- and Stimulus-Specific Local Translation During Long-Term Neuronal Plasticity. Science (80-.). *324*, 1536–1540.

Wang, M., Lu, C., Li, H., Qiu, M., Winstead, W., and Roisen, F. (2011a). Lineage restriction of adult human olfactory-derived progenitors to dopaminergic neurons. Stem Cell Discov. *1*, 29–43.

Wang, Q., Charych, E.I., Pulito, V.L., Lee, J.B., Graziane, N.M., Crozier, R. a, Revilla-Sanchez, R., Kelly, M.P., Dunlop, a J., Murdoch, H., et al. (2011b). The psychiatric disease risk factors DISC1 and TNIK interact to regulate synapse composition and function. Mol. Psychiatry *16*, 1006–1023.

Wang, X., Li, X., Wang, K., Zhou, H., Xue, B., Li, L., and Wang, X. (2004). Forskolin cooperating with growth factor on generation of dopaminergic neurons from human fetal mesencephalic neural progenitor cells. Neurosci. Lett. *362*, 117–121.

Washbourne, P., Liu, X.-B., Jones, E.G., and McAllister, a K. (2004). Cycling of NMDA receptors during trafficking in neurons before synapse formation. J. Neurosci. *24*, 8253–8264.

Wassink, T.H., Epping, E.A., Rudd, D., Axelsen, M., and Ziebell, S. (2012). Influence of ZNF804a on Brain Structure Volumes and Symptom Severity in Individuals With Schizophrenia. Arch Gen Psychiatry *69*, 885–892.

Wei, Q., Kang, Z., Diao, F., Shan, B., Li, L., Zheng, L., Guo, X., Liu, C., Zhang, J., and Zhao, J. (2012). Association of the ZNF804A gene polymorphism rs1344706 with white matter density changes in Chinese schizophrenia. Prog. Neuropsychopharmacol. Biol. Psychiatry *36*, 122–127.

Wei, Q., Kang, Z., Diao, F., Guidon, A., Wu, X., Zheng, L., Li, L., Guo, X., Hu, M., Zhang, J., et al. (2013). No association of ZNF804A rs1344706 with white matter integrity in schizophrenia: a tract-based spatial statistics study. Neurosci. Lett. *532*, 64–69.

Wei, Q., Li, M., Kang, Z., Li, L., Diao, F., Zhang, R., Wang, J., Zheng, L., Wen, X., Zhang, J., et al. (2015). ZNF804A rs1344706 is Associated With Cortical Thickness , Surface Area , and Cortical Volume of the Unmedicated First Episode Schizophrenia and Healthy Controls.

Weiss, L. a, Escayg, a, Kearney, J. a, Trudeau, M., MacDonald, B.T., Mori, M., Reichert, J., Buxbaum, J.D., and Meisler, M.H. (2003). Sodium channels SCN1A, SCN2A and SCN3A in familial autism. Mol. Psychiatry *8*, 186–194.

Wen, Z., Christian, K.M., Song, H., and Ming, G. li (2016). Modeling psychiatric disorders with patient-derived iPSCs. Curr. Opin. Neurobiol. *36*, 118–127.

Williams, H.J., Owen, M.J., and O'Donovan, M.C. (2007). Is COMT a susceptibility gene for schizophrenia? Schizophr Bull *33*, 635–641.

Williams, H.J., Norton, N., Dwyer, S., Moskvina, V., Nikolov, I., Carroll, L., Georgieva, L., Williams, N.M., Morris, D.W., Quinn, E.M., et al. (2011). Fine mapping of ZNF804A and genome-wide significant evidence for its involvement in schizophrenia and bipolar disorder. Mol. Psychiatry *16*, 429–441.

Willig, K.I., and Barrantes, F.J. (2014). Recent applications of superresolution microscopy in neurobiology. Curr. Opin. Chem. Biol. *20C*, 16–21.

Wilson, P.G., and Stice, S.S. (2006). Development and Differentiation of Neural Rosettes Derived From Human Embryonic Stem Cells. Stem Cell Rev. *2*, 67–77.

Woolfrey, K.M., Srivastava, D.P., Photowala, H., Yamashita, M., Barbolina, M. V, Cahill, M.E., Xie, Z., Jones, K.A., Quilliam, L.A., Prakriya, M., et al. (2009). Epac2 induces synapse remodeling and depression and its disease-associated forms alter spines. Nat. Neurosci. *12*, 1275–1284.

Wright, C., Turner, J. a, Calhoun, V.D., and Perrone-Bizzozero, N. (2013). Potential Impact of miR-137 and Its Targets in Schizophrenia. Front. Genet. *4*, 58.

Xie, Z., Srivastava, D.P., Photowala, H., Kai, L., Cahill, M.E., Woolfrey, K.M., Shum, C.Y., Surmeier, D.J., and Penzes, P. (2007). Kalirin-7 controls activity-dependent structural and functional plasticity of dendritic spines. Neuron *56*, 640–656.

Xu, W., Cohen-Woods, S., Chen, Q., Noor, A., Knight, J., Hosang, G., Parikh, S. V, De Luca, V., Tozzi, F., Muglia, P., et al. (2014). Genome-wide association study of bipolar disorder in Canadian and UK populations corroborates disease loci including SYNE1 and CSMD1. BMC Med. Genet. *15*, 2.

Yan, Y., Yang, D., Zarnowska, E.D., Du, Z., Werbel, B., Valliere, C., Pearce, R. a, Thomson, J. a, and Zhang, S.-C. (2005). Directed differentiation of dopaminergic neuronal subtypes from human embryonic stem cells. Stem Cells *23*, 781–790.

Yang, Y., Li, W., Yang, G., Xiao, B., Wang, X., Ding, M., Zhao, J., Song, X., Yue, W., Zhang, D., et al. (2013). Evaluation of the relationship between the ZNF804A single nucleotide polymorphism rs1344706 A/C variant and schizophrenia subtype in Han Chinese patients. Int. J. Psychiatry Med. *45*, 269–278.

Yoshimizu, T., Pan, J.Q., Mungenast, a E., Madison, J.M., Su, S., Ketterman, J., Ongur, D., McPhie, D., Cohen, B., Perlis, R., et al. (2015). Functional implications of a psychiatric risk variant within CACNA1C in induced human neurons. Mol. Psychiatry *20*, 162–169.

Young, J.E., Boulanger-Weill, J., Williams, D. a, Woodruff, G., Buen, F., Revilla, A.C., Herrera, C., Israel, M. a, Yuan, S.H., Edland, S.D., et al. (2015). Elucidating molecular phenotypes caused by the SORL1 Alzheimer's disease genetic risk factor using human induced pluripotent stem cells. Cell Stem Cell *16*, 373–385.

Yuan, A., Yi, Z., Wang, Q., Sun, J., Li, Z., Du, Y., Zhang, C., Yu, T., Fan, J., Li, H., et al. (2012). ANK3 as a risk gene for schizophrenia: New data in han Chinese and meta analysis. Am. J. Med. Genet. Part B Neuropsychiatr. Genet. *159 B*, 997–1005.

Zaharie, A., Ergul, E., Ozel, M.D., Miclutia, I.V., Stanculete, M.F., and Sazci, A. (2012). ZNF804A rs1344706 Variant and Schizophrenia in a Romanian Population from Cluj Napoca. Genet. Test. Mol. Biomarkers *0*, 1–3.

Zander, J.-F., Münster-Wandowski, A., Brunk, I., Pahner, I., Gómez-Lira, G., Heinemann, U., Gutiérrez, R., Laube, G., and Ahnert-Hilger, G. (2010). Synaptic and vesicular coexistence of VGLUT and VGAT in selected excitatory and inhibitory synapses. J. Neurosci. *30*, 7634–7645.

Zhang, S.-C. (2006). Neural Subtype Specification from Embryonic Stem Cells. Brain Pathol. *16*, 132–142.

Zhang, C., Milunsky, J.M., Newton, S., Ko, J., Zhao, G., Maher, T. a, Tager-Flusberg, H., Bolliger, M.F., Carter, A.S., Boucard, A. a, et al. (2009). A neuroligin-4 missense mutation associated with autism impairs neuroligin-4 folding and endoplasmic reticulum export. J. Neurosci. *29*, 10843–10854.

Zhang, C., Wang, Z., Hong, W., Wu, Z., Peng, D., and Fang, Y. (2015). ZNF804A Genetic Variation Confers Risk to Bipolar Disorder. Mol. Neurobiol.

Zhang, F., Chen, Q., Ye, T., Lipska, B.K., Straub, R.E., Vakkalanka, R., Rujescu, D., St Clair, D., Hyde, T.M., Bigelow, L., et al. (2011). Evidence of sex-modulated association of ZNF804A with schizophrenia. Biol. Psychiatry *69*, 914–917.

Zhang, H., Wang, Y., Zhao, Y., Yin, Y., Xu, Q., and Xu, Q. (2008). Immortalized human neural progenitor cells from the ventral telencephalon with the potential to differentiate into GABAergic neurons. J. Neurosci. Res. *86*, 1217–1226.

Zhang, X., Bailey, S.D., and Lupien, M. (2014). Laying a solid foundation for Manhattan--'setting the functional basis for the post-GWAS era'. Trends Genet. *30*, 140–149.

Zhang, Z., Chen, X., Yu, P., Zhang, Q., Sun, X., Gu, H., Zhang, H., Zhai, J., Chen, M., Du, B., et al. (2016). Effect of rs1344706 in the ZNF804A gene on the connectivity between the hippocampal formation and posterior cingulate cortex. Schizophr. Res. *170*, 48–54.